

7-2010

Rhodium-Catalyzed Hydroboration: Directed Asymmetric Desymmetrization

Judy L. Miska

University of Nebraska at Lincoln, jmiska@unlserve.unl.edu

Follow this and additional works at: <http://digitalcommons.unl.edu/chemistrydiss>



Part of the [Organic Chemistry Commons](#)

Miska, Judy L., "Rhodium-Catalyzed Hydroboration: Directed Asymmetric Desymmetrization" (2010). *Student Research Projects, Dissertations, and Theses - Chemistry Department*. 10.
<http://digitalcommons.unl.edu/chemistrydiss/10>

This Article is brought to you for free and open access by the Chemistry, Department of at DigitalCommons@University of Nebraska - Lincoln. It has been accepted for inclusion in Student Research Projects, Dissertations, and Theses - Chemistry Department by an authorized administrator of DigitalCommons@University of Nebraska - Lincoln.

**RHODIUM-CATALYZED HYDROBORATION:
DIRECTED ASYMMETRIC DESYMMETRIZATION**

By

Judy Lynn Miska

A THESIS

**Presented to the Faculty of
The Graduate College at the University of Nebraska
In Partial Fulfillment of Requirements
For the Degree of Master of Science
Major: Chemistry**

Under the Supervision of Professor James M. Takacs

Lincoln, Nebraska

July, 2010

Rhodium-Catalyzed Hydroboration: Directed Asymmetric Desymmetrization

Judy Lynn Miska, M.S.

University of Nebraska, 2010

Adviser: James M. Takacs

Rhodium-catalyzed asymmetric hydroboration in conjunction with directing groups can be used control relative and absolute stereochemistry. Hydroboration has the potential to create new C–C, C–O, and C–N bonds from an intermediate C–B bond with retention of stereochemistry. Desymmetrization resulting in the loss of one or more symmetry elements can give rise to molecular chirality, *i.e.*, the conversion of a prochiral molecule to one that is chiral. Unsaturated amides and esters hold the potential for two-point binding to the rhodium catalyst and have been shown to direct the regiochemistry and impact stereochemistry in asymmetric hydroborations of acyclic β,γ -unsaturated substrates. In the present study, the pendant amide functionality directs the hydroboration *cis* in the cyclic substrates studied; the corresponding ester substrates do so to a lesser extent. The enantioselectivity is determined by regioselective addition to the *re* or *si* site of the rhodium-complexed alkene. The effect of catalyst, ligand and borane on the observed diastereoselectivity and enantioselectivity for a variety of cyclopentenyl ester and amide substrates is discussed.

For Charles

Table of Contents

i.	Acknowledgements	v
ii.	Index of Schemata	vi
iii.	Index of Tables	ix
iv.	Index of Figures	xiii
v.	List of Abbreviations	xiv
1.	Introduction	1
2.	Synthesis of Prochiral Cyclopentenyl Esters and Amides	14
3.	Model for Rhodium-Catalyzed Hydroboration	18
4.	Ligands and Boranes used in Rhodium-Catalyzed Hydroboration	21
5.	Rhodium-Catalyzed Asymmetric Hydroboration on Prochiral Cyclopentenyl Ester Substrates	24
6.	Rhodium-Catalyzed Asymmetric Hydroboration on <i>N</i>-Phenylcyclopent-3-enecarboxamide	29
7.	Rhodium-Catalyzed Asymmetric Hydroboration on 1-Methyl-<i>N</i>-phenylcyclopent-3-enecarboxamide	39
8.	Rhodium-Catalyzed Asymmetric Hydroboration on 1-Benzyl-<i>N</i>-phenylcyclopent-3-enecarboxamide	49
9.	Rhodium-Catalyzed Asymmetric Hydroboration on Weinreb Amides	52
10.	Summary for the Reactions of the Various Substrates, Ligands and Boranes	58

11. Absolute Configuration Determination of	
<i>N</i>-phenylcyclopent-3-enecarboxamide	62
12. Conversion of <i>N</i>-Phenylcyclopent-3-enecarboxamide	
to its Trifluoroborate salt	66
13. Conclusions	69
14. Experimental Procedures	74
15. Spectra Appendix	118
16. References	165

i. Acknowledgements

I would like to thank Professor Takacs for your advisement throughout my duration at UNL; to Professors Kozliak, Smoliakova, Rajca, Berkowitz, Powers and Redeppening: thank you for your helpful advice and insightful discussions. To my parents; to my brother and sister; to *Charlie*; to my parents-in-law; to my brother- and sister-in-law; to the rest of my family: thank you for the love and belief that you had and continue to have in me — I am eternally grateful. To my friends at UNL: Sara (DG), Judit, Leah, Jayson, Mattie, Monica, John, Mike, Bob, Trista, Sasha, Ross, Laura, Katie, Bridget, Lesya, Manuela, Deanna, Dodie, all of the WA ladies: thank you for the support, the ear, and the shoulder. To my friends who have supported me from afar: Cristin, Leah, Don, Katy, Rachel, Rachel, Seina, Kayla, Dana, Kari, Ben, Lisa, Angie, Carrie, Errin, Matt, Shirin, Jenny, Jess, Dave, Amy, Karen, the Kerstens (Rolly, Joan, Koko), Lori, Mo, PK, Ty, and Vanessa: thank you for the varied things you have provided and shown me. I will always remember the memories of Hamilton Hall and for the late nights in lab. All of you have contributed to the person I am today. The strength I have gained from this experience will carry with me for the rest of my career and I am grateful for the person I am today.

“For I know the plans I have for you,” declares the *LORD*, “plans to prosper you and not to harm you, plans to give you hope and a future...”

~Jeremiah 29:11~

IXΘΥΣ

ii. Index of Schemata

Scheme 1.1. Organoboronate esters as a valuable synthon in organic chem.	1
Scheme 1.2. The first reported example of rhodium-catalyzed hydroboration.	2
Scheme 1.3. Directed rhodium-catalyzed hydroboration of cyclohexenol derivatives.	3
Scheme 1.4. Amide-directed iridium-catalyzed hydroboration.	5
Scheme 1.5. <i>N</i> -Benzyl amide-directed iridium-catalyzed hydroboration.	5
Scheme 1.6. An example of a “reverse-amide”-directed hydroboration.	6
Scheme 1.7. Amide-directed rhodium-catalyzed asymmetric hydroboration of β,γ -unsaturated amides.	7
Scheme 1.8. Rhodium-catalyzed asymmetric hydroboration of trisubstituted alkene substrates.	8
Scheme 1.9. Rh-catalyzed asymmetric hydroboration of cyclopropenes.	10
Scheme 1.10. Rhodium-catalyzed asymmetric hydroboration of prochiral ester and amide cyclopentenyl substrates.	11
Scheme 2.1. Synthesis of methyl cyclopent-3-enecarboxylate.	14
Scheme 2.2. Synthesis of phenyl- and benzyl cyclopent-3-enecarboxylate.	15
Scheme 2.3. Synthesis of dibenzyl cyclopent-3-ene-1,1-dicarboxylate.	15
Scheme 2.4. Synthesis of <i>N</i> -phenylcyclopent-3-enecarboxamide.	16
Scheme 2.5. Synthesis of 1-methyl- and 1-benzyl- <i>N</i> -phenylcyclopent-3-enecarboxamide.	16
Scheme 2.6. Synthesis of <i>N</i> -methoxyl- <i>N</i> -methylcyclopent-3-enecarboxamide and its α -methyl and α -benzyl derivatives.	17

Scheme 3.1. Proposed mechanism of an alkene using CatBH.	19
Scheme 3.2. Model for rhodium-catalyzed hydroboration of prochiral cyclopentenyl substrates.	20
Scheme 4.1. TMDB undergoes oxidative addition with Wilkinson's catalyst.	23
Scheme 4.2. TMDB in the use of the stoichiometric hydroboration of olefins.	23
Scheme 4.3. Diols are easily converted to its corresponding borane.	23
Scheme 5.1. Rhodium-catalyzed hydroboration of phenyl cyclopent-3-enecarboxylate.	24
Scheme 5.2. Rhodium-catalyzed hydroboration of benzyl cyclopent-3-enecarboxylate.	25
Scheme 5.3. Rhodium-catalyzed hydroboration of dibenzyl cyclopent-3-ene-1,1-dicarboxylate.	27
Scheme 5.4. Rhodium-catalyzed hydroboration of methyl cyclopent-3-enecarboxylate.	28
Scheme 6.1. Rhodium-catalyzed hydroboration of <i>N</i> -phenylcyclopent-3-enecarboxamide.	30
Scheme 6.2. An enantioswitch example: asymmetric reduction of ketones with borane.	32
Scheme 7.1. The rhodium-catalyzed hydroboration of 1-methyl- <i>N</i> -phenylcyclopent-3-enecarboxamide.	40

Scheme 8.1. The rhodium-catalyzed hydroboration of 1-benzyl- <i>N</i> -phenylcyclopent-3-enecarboxamide.	49
Scheme 9.1. Rhodium-catalyzed asymmetric hydroboration of <i>N</i> -methoxy- <i>N</i> -methylcyclopent-3-enecarboxamide.	52
Scheme 9.2. Rhodium-catalyzed asymmetric hydroboration of <i>N</i> -methoxy- <i>N</i> ,1 -dimethylcyclopent-3-enecarboxamide.	54
Scheme 9.3. Rhodium-catalyzed asymmetric hydroboration of 1-benzyl- <i>N</i> -methoxy- <i>N</i> -methylcyclopent-3-enecarboxamide.	56
Scheme 11.1. Determination of the absolute configuration of 3-Hydroxy- <i>N</i> -phenylcyclopentanecarboxamide.	62
Scheme 11.2. The major enantiomer obtained for the rhodium-catalyzed hydroborations is the (1 <i>R</i> ,3 <i>S</i>)- <i>cis</i> -isomer.	64
Scheme 12.1. Suzuki cross-coupling of an aryl halide with a potassium cyclopentyltrifluoroborate salt.	66
Scheme 12.2. Suzuki cross-coupling of a six-membered disubstituted trifluoroborate salt.	67
Scheme 12.3. Conversion of <i>N</i> -phenylcyclopent-3-enecarboxamide to its trifluoroborate salt.	68

iii. Index of Tables

Table 1.1. Catalytic hydroboration using Wilkinson's catalyst with CatBH.	3
Table 1.2. Hydroboration of cyclohexenol derivatives.	4
Table 1.3. The rhodium-catalyzed asymmetric hydroboration of β,γ -unsaturated amides.	8
Table 1.4. Various trisubstituted alkene substrates used in rhodium-catalyzed hydroboration.	9
Table 1.5. Asymmetric hydroboration of 3,3-disubstituted cyclopropenes.	10
Table 5.1. The rhodium-catalyzed hydroboration of 67 using PinBH and the influence of a four ligand screening set on diastereo- and enantioselectivities.	25
Table 5.2. The rhodium-catalyzed hydroboration of 70 using PinBH and the influence of a six ligand screening set on diastereo- and enantioselectivities.	26
Table 5.3. The rhodium-catalyzed hydroboration of 73 using PinBH and the influence of a six ligand screening set on diastereo- and enantioselectivities.	27
Table 5.4. The rhodium-catalyzed hydroboration of 76 using PinBH and the influence of a three ligand screening set on diastereo- and enantioselectivities.	28
Table 6.1. The rhodium-catalyzed hydroboration of 79 using PinBH and the influence of an 11 ligand screening set on diastereo- and enantioselectivities.	31
Table 6.2. The rhodium-catalyzed hydroboration of 79 using TMDb and the influence of a six ligand screening set on diastereo- and enantioselectivities.	33
Table 6.3. The rhodium-catalyzed hydroboration of 79 using 3,5-VI and the influence of a four ligand screening set on diastereo- and enantioselectivities.	34
Table 6.4. The rhodium-catalyzed hydroboration of 79 using 3,3,4-V and the	

influence of a six ligand screening set on diastereo- and enantioselectivities.	35
Table 6.5. The rhodium-catalyzed hydroboration of 79 using 3-VI and the influence of a six ligand screening set on diastereo- and enantioselectivities.	36
Table 6.6. The rhodium-catalyzed hydroboration of 79 using 4-VI and the influence of a four ligand screening set on diastereo- and enantioselectivities.	36
Table 6.7. The iridium-catalyzed hydroboration of 79 using CatBH (2 eq.) and the influence of a five ligand screening set on diastereo- and enantioselectivities.	37
Table 6.8. The rhodium-catalyzed hydroboration of 79 using CatBH (2 eq.) and the influence of a five ligand screening set on diastereo- and enantioselectivities.	38
Table 7.1. The rhodium-catalyzed hydroboration of 87 using PinBH and the influence of a six ligand screening set on diastereo- and enantioselectivities.	40
Table 7.2. The rhodium-catalyzed hydroboration of 87 using TMDB and the influence of a nine ligand screening set on diastereo- and enantioselectivities.	41
Table 7.3. The rhodium-catalyzed hydroboration of 87 using 3,5-VI and the influence of a three ligand screening set on diastereo- and enantioselectivities.	42
Table 7.4. The rhodium-catalyzed hydroboration of 87 using 3-V and the influence of a six ligand screening set on diastereo- and enantioselectivities.	43
Table 7.5. The rhodium-catalyzed hydroboration of 87 using 3,4-V and the influence of a two ligand screening set on diastereo- and enantioselectivities.	44
Table 7.6. The rhodium-catalyzed hydroboration of 87 using 3-V and the influence of a five ligand screening set on diastereo- and enantioselectivities.	44

Table 7.7. The rhodium-catalyzed hydroboration of 87 using CatBH (2 eq.) and the influence of a seven ligand screening set on diastereo- and enantioselectivities.	45
Table 7.8. The rhodium-catalyzed hydroboration of 87 using CatBH (5 eq.) and the influence of a six ligand screening set on diastereo- and enantioselectivities.	46
Table 7.9. The iridium-catalyzed hydroboration of 87 using PinBH and the influence of a six ligand screening set on diastereo- and enantioselectivities.	47
Table 7.10. The iridium-catalyzed hydroboration of 87 using TMDB and the influence of a six ligand screening set on diastereo- and enantioselectivities.	47
Table 7.11. The iridium-catalyzed hydroboration of 87 using CatBH (2 eq.) and the influence of a 5 ligand screening set on diastereo- and enantioselectivities.	48
Table 8.1. The rhodium-catalyzed hydroboration of 90 using PinBH and the influence of a six ligand screening set on diastereo- and enantioselectivities.	50
Table 8.2. The rhodium-catalyzed hydroboration of 90 using TMDB and the influence of a six ligand screening set on diastereo- and enantioselectivities.	51
Table 9.1. The rhodium-catalyzed hydroboration of 93 using PinBH and the influence of a six ligand screening set on diastereoselectivities.	53
Table 9.2. The rhodium-catalyzed hydroboration of 93 using TMDB and the influence of a six ligand screening set on diastereoselectivities.	53
Table 9.3. The rhodium-catalyzed hydroboration of 96 using PinBH and the influence of a six ligand screening set on diastereoselectivities.	55

Table 9.4. The rhodium-catalyzed hydroboration of 96 using TMDB and the influence of a six ligand screening set on diastereoselectivities.	55
Table 9.5. The rhodium-catalyzed hydroboration of 99 using PinBH and the influence of a six ligand screening set on diastereoselectivities.	56
Table 9.6. The rhodium-catalyzed hydroboration of 99 using TMDB and the influence of a six ligand screening set on diastereoselectivities.	57
Table 10.1. A summary of the best results for rhodium-catalyzed hydroboration with various substrates, boranes, and ligands.	60
Table 13.1. A summary of the best results of rhodium-catalyzed hydroboration with various substrates, boranes, and ligands.	70

iv. Index of Figures

Figure 1.1. TADDOL- and BINOL-derived chiral ligands, respectively.	6
Figure 1.2. Various substrates, ligands and boranes studied.	13
Figure 4.1. TADDOL- and BINOL-derived phosphite and phosphoramidite ligands.	21
Figure 4.2. Boranes used in the rhodium-catalyzed hydroboration of prochiral substrates.	22
Figure 11.1. HPLC trace of the four possible ester products: (1 <i>S</i> ,3 <i>R</i>)- <i>cis</i> - isomer, (1 <i>R</i> ,3 <i>S</i>)- <i>cis</i> -isomer, (1 <i>R</i> ,3 <i>R</i>)- <i>trans</i> -isomer, and (1 <i>S</i> ,3 <i>S</i>)- <i>trans</i> -isomer.	63
Figure 11.2. HPLC traces of: a) amide derived from diester b) sample amide and a c) coinjection of the two.	65

v. **List of Abbreviations**

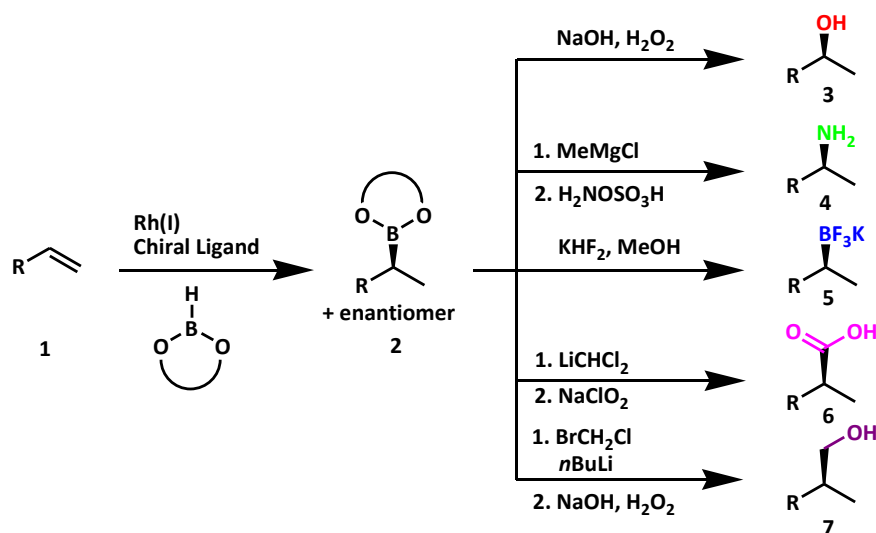
Ad	Adamantyl
9-BBN	9-Borabicyclo(3.3.1)nonane
BINAP	2,2'- <i>Bis</i> (diphenylphosphino)-1,1'-binaphthyl
Bn	Benzyl
Bu	Butyl
<i>ca.</i>	Circa
Calcd.	Calculated
CatBH	Catecholborane
CDI	1,1'-Carbonyldiimidazole
COD	Cyclooctadiene
Cy	Cyclohexyl
DCC	Dicyclohexylcarbodiimide
DCE	Dichloroethane
DCM	Dichloromethane
de	Diastereomeric excess
DMAP	4-Dimethylaminopyridine
DMF	<i>N,N</i> -Dimethylformamide
DMS	Dimethyl sulfide
EDCI	1-Ethyl-3-(dimethylaminopropyl)carbodiimide
ee	Enantiomeric excess
Et	Ethyl
EtOH	Ethanol

Eq.	Equivalents
FTIR	Fourier Transform Infrared
GC	Gas Chromatography
HPLC	High Pressure Liquid Chromatography
HRMS	High Resolution Mass Spectrometry
Hz	Hertz
IR	Infrared
<i>J</i>	Coupling Constant
LDA	Lithium diisopropylamide
<i>M</i>	Molarity
Me	Methyl
MeOH	Methanol
Min	Minute
Mp	Melting Point
MS	Mass Spectrometry
<i>N</i>	Normality
nbd	Norbornadienyl
NMR	Nuclear Magnetic Resonance
PinBH	Pinacolborane
PMA	Phosphomolybdic acid
Pr	Propyl
Py	Pyridine
Rac	Racemic

Rt	Room temperature
Satd.	Saturated
S.M.	Starting Material
THF	Tetrahydrofuran
TLC	Thin Layer Chromatography
TMDB	4,4,6-Trimethyl-1,3,2-dioxaborinane
TMS	Trimethylsilyl
Tol	Tolyl
UV	Ultraviolet
Wt %	Weight percent

Chapter 1: Introduction

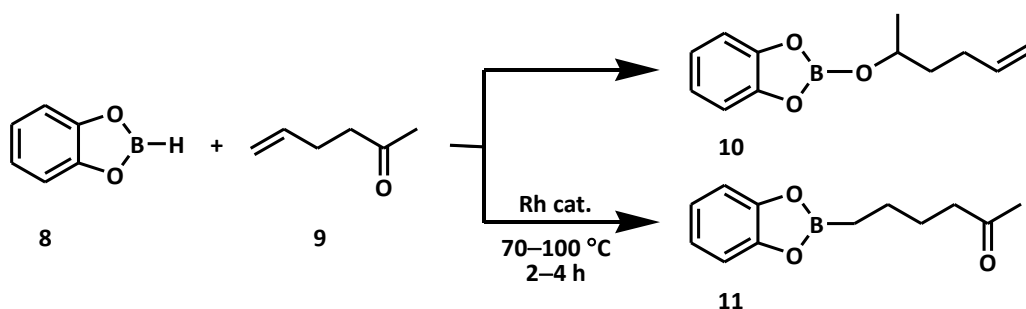
Over the last twenty-five years, the field of transition metal-catalyzed hydroboration has expanded dramatically and has increasingly become one of the relied upon methods for the transformations of carbon-carbon double and triple bonds.¹ The intermediate formed in the hydroboration of alkenes is an organoboronate ester which serves as a synthon for a variety of functional groups (Scheme 1.1). The organoboronate ester **2** can be converted to various functional groups including: secondary alcohols,² amines,^{3,a} potassium trifluoroborate salts,⁴ carboxylic acids,⁵ and primary alcohols.⁶ These functionalizations result in the retention of stereochemistry, which provides incentive for further development in the study of transition metal-catalyzed hydroboration.⁷ Moreover, transition metal-catalyzed hydroboration has an advantage over the uncatalyzed reaction, as the former proceeds with complementary regio- and diastereoselectivity in certain substrates.⁸



Scheme 1.1. Organoboronate esters as a valuable synthon in organic chemistry.²⁻⁶

- a. Where methylmagnesium chloride is used to convert the organoboronate ester to its corresponding trialkylborane. This intermediate is more easily aminated with hydroxylamine-*O*-sulfonic acid than the organoboronate.³

In 1985, Männig and Nöth reported the first example of rhodium-catalyzed hydroboration to carbon–carbon double bonds.⁹ At room temperature, catecholborane (CatBH) **8** reacts with hex-5-en-2-one **9** at the carbonyl double bond to form **10** (Scheme 1.2). However, in the presence of 5 mol% Wilkinson’s catalyst, $[\text{Rh}(\text{PPh}_3)\text{Cl}]$, the addition of the B–H bond occurs across the carbon–carbon double bond in an anti-Markovnikov fashion to form **11**.



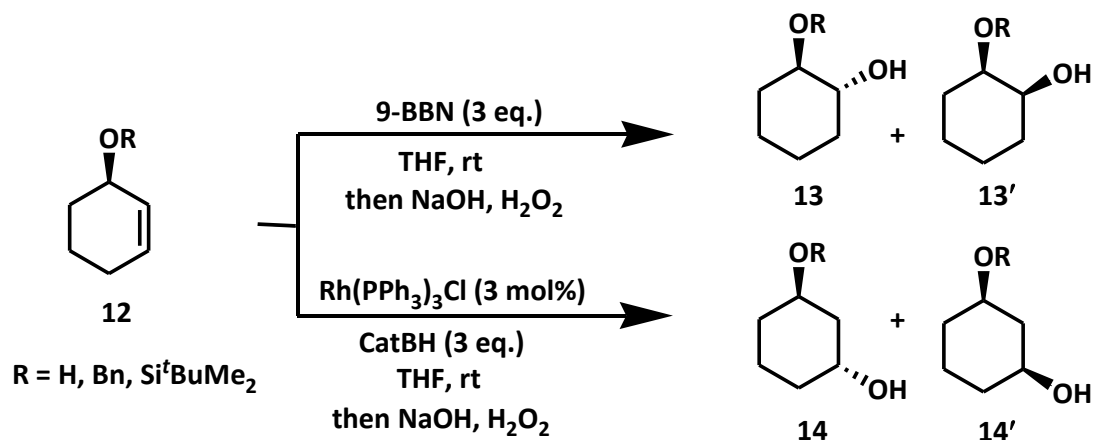
Scheme 1.2. The first reported example of rhodium-catalyzed hydroboration.⁹

Other rhodium complexes that provide good catalytic properties on this system include $[\text{Rh}(\text{PPh}_3)_2(\text{CO})\text{Cl}]$ and $[\text{Rh}(\text{COD})\text{Cl}_2]_2$. Metal complexes of platinum, palladium, iridium, and cobalt reportedly do not catalyze this reaction under similar conditions. Other substrates (Table 1.1) that are efficiently catalyzed by Wilkinson’s catalyst with CatBH include terminal (entries 1 and 4) and cyclic alkenes (entries 2–3), as well as an alkyne (entry 5).

Table 1.1. Catalytic hydroboration using Wilkinson's catalyst with CatBH at 20 °C (25 min).⁹

Entry	Substrate	Yield of hydroboration product (%)
1	1-Octene	77.7
2	Cyclopentene	83.3
3	Cyclohexene	21.5
4	3-Vinylcyclohexene	50.0 (Only of Vinyl group)
5	1-Hexyne	52.5

Following the initial findings of Männig and Nöth, Evans *et al.* document the first case of directed rhodium-catalyzed hydroboration on acyclic and cyclic systems that provide regio- and stereochemical control.¹⁰ The hydroboration of allylic alcohol derivatives **12** provide evidence of regioselectivity differences in the catalyzed versus uncatalyzed reactions, as shown in Scheme 1.3.



Scheme 1.3. Directed rhodium-catalyzed hydroboration of cyclohexenol derivatives.¹⁰

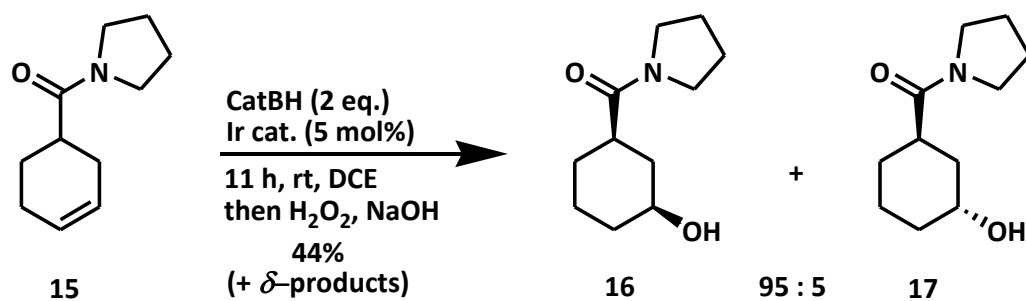
In the case of the allylic cyclohexenol, the uncatalyzed version forms predominately an *anti*-vicinal diol (entry 1, Table 1.2). When Wilkinson's catalyst is used, regiochemical

control is shown, *i.e.*, the major product formed is the *anti*-1,3-substituted diol **14**. The same general trend is found when R is either a benzyl group or a *tert*-butyldimethylsilyl ether.

Table 1.2. Hydroboration of cyclohexenol derivatives (from Scheme 1.3).¹⁰

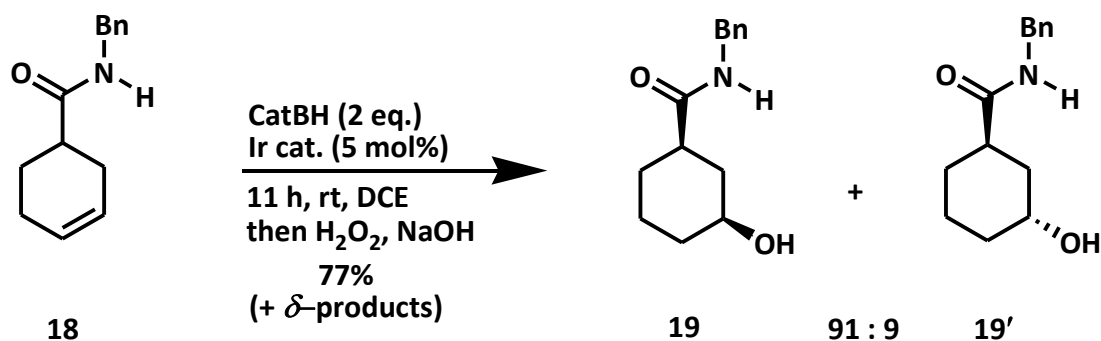
Entry	R	Conditions	Total Yield (%)	13	13'	14	14'
1	H	Uncatalyzed	86	83	2	5	10
2	H	Catalyzed	84	18	1	72	9
3	Bn	Uncatalyzed	73	68	0	13	19
4	Bn	Catalyzed	87	7	8	72	13
5	Si ^t BnMe ₂	Uncatalyzed	70	74	0	13	13
6	Si ^t BnMe ₂	Catalyzed	79	2	1	86	11

In 1991, Evans *et al.* provided the first example of amide-directed catalyzed hydroboration. Amides effectively direct the iridium-catalyzed hydroboration using [Ir(cod)(PCy₃)(py)]PF₆ and CatBH as the source of borane.¹¹ The catalyzed hydroboration of tertiary amide **15** provides a high diastereoselectivity preferring the *cis*-1,3-product **16** (Scheme 1.4). The δ -products (*i.e.* 1,4-substituted products) are also formed, but the amount formed is not stated in the communication. The authors state that the competitive reduction of the tertiary amide results in the reduced yield (44%) of the desired products **16** and **17**.



Scheme 1.4. Amide-directed iridium-catalyzed hydroboration.¹¹

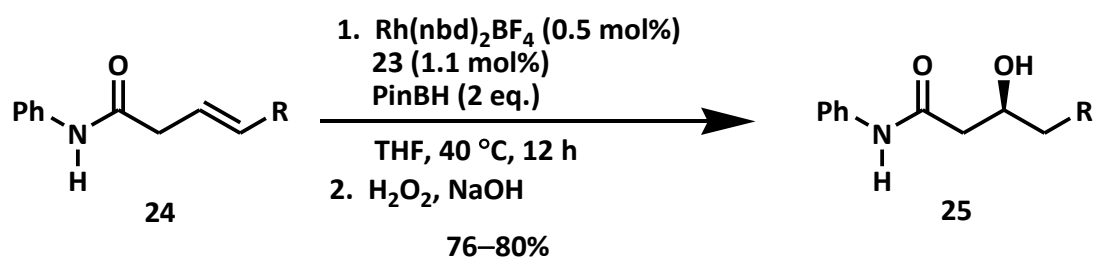
When a secondary amide **18** is substituted for the tertiary amide, the yield is substantially higher, most likely due to absence of the competitive reduction (Scheme 1.5). In the substituted cyclohexene cases, the methyl ester and the *tert*-butyldimethylsilyl ether are not shown to direct the hydroboration reaction; a statistical mixture of the four products is formed.¹¹



Scheme 1.5. *N*-Benzyl amide-directed iridium-catalyzed hydroboration.¹¹

Interestingly, the authors also study a “reverse-amide” **20** (Scheme 1.6). This example also shows a directing-effect where the diastereoselectivity is only narrowly decreased from the previous case shown in Scheme 1.5.

These TADDOL- and BINOL-derived monophosphites and phosphoramidite ligands are successfully used in the rhodium-catalyzed asymmetric hydroboration of *N*-phenyl amide **24**. This reaction results in excellent regiochemical control of the β -hydroxy carbonyl derivative **25** over the γ -isomer (Scheme 1.7). These findings are congruent with the findings of Evans *et al.*^{10,11} The regiochemistry obtained is controlled with the use of the amide group, as this directs the formation of the β -isomer. Two-point binding of the amide and alkene moieties to rhodium are attributed as an important factor for the observed regiocontrol.¹²



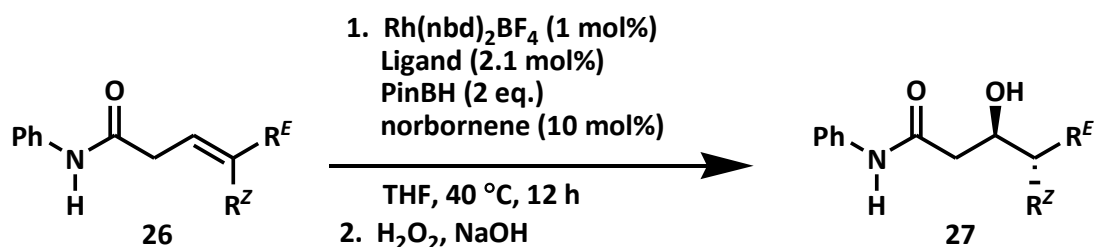
Scheme 1.7. Amide-directed rhodium-catalyzed asymmetric hydroboration of β,γ -unsaturated amides.¹²

Various alkyl chains are tolerated with the reaction (Table 1.3). The hydroboration of these substrates is efficient, providing high enantioselectivity (93–99%) with the chiral ligand (BINOL)N(Me)Ph **23** and pinacolborane (PinBH). The γ -isomer is only observed in less than 5% for entries 1–4. When one equivalent of PinBH is used, the conversion is only 30% on the same timescale, thus it appears an excess is required. In addition to this, low yields and poor enantioselectivities are achieved when PinBH is replaced with CatBH.¹²

Table 1.3. The rhodium-catalyzed asymmetric hydroboration of β,γ -unsaturated amides.¹²

Entry	R	ee (%)
1	^t Pr	93
2	^t Bu	95
3	CH ₂ CH ₂ Ph	99
4	ⁿ C ₄ H ₉	93

Earlier this year, the Takacs group published new studies on trisubstituted alkenes that contain different alkenyl substituents.¹³ Upon hydroboration, the trisubstituted alkene **26** results in product **27** with two new stereocenters (Scheme 1.8). Depending on whether the alkene is *E* or *Z*, both *syn*- and *anti*-products can be formed with high diastereoselectivity when Rh(nbd)₂BF₄ is used with a BINOL- or TADDOL-derived chiral ligand and PinBH; the reaction is therefore stereospecific and proceeds *via syn*-addition. Norbornene is used as an addend in this reaction. Its role is to be used as a sacrificial alkene addend reacting with an initially formed poorly selective catalyst allowing for higher enantioselectivity of the desired product.



Scheme 1.8. Rhodium-catalyzed asymmetric hydroboration of trisubstituted alkene substrates.¹³

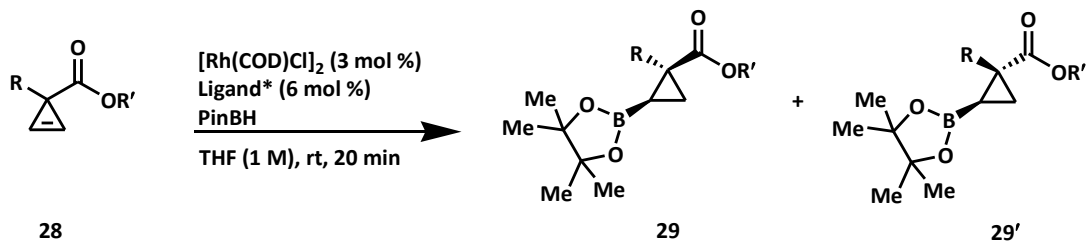
The rhodium-catalyzed hydroboration of various *E*- and *Z*-alkenes were studied, which allow pathways to both *syn*- and *anti*-products (Table 1.4). The hydroboration of *E*- and *Z*-isomers results in almost the same yield and enantioselectivity, yet, with the utilization of different ligands (*e.g.* entries 1 and 2 are *E*- and *Z*-isomers and the yields and ee's are nearly the same yet these results are achieved with the use of different ligands, *p*-Me(TADDOL)POPh and *x*(TADDOL)POPh, respectively).¹³

Table 1.4. Various trisubstituted alkene substrates used in rhodium-catalyzed hydroboration.¹³

Entry	Ligand	R ^E	R ^Z	Yield (%)	ee (%)
1	<i>p</i> -Me(TADDOL)POPh	(CH ₂) ₃ Ph	CH ₃	81	95
2	<i>x</i> (TADDOL)POPh	CH ₃	(CH ₂) ₃ Ph	83	95
3	<i>p</i> -Me(TADDOL)POPh	(CH ₂) ₄ Ph	CH ₃	79	93
4	^t Bu(TADDOL)POPh	(CH ₂) ₂ Me	CH ₃	80	96
5	<i>p</i> -Me(TADDOL)POPh	CH ₃	CH ₂ CH(CH ₃) ₂	81	91
6	^t Bu(TADDOL)POPh	CH ₃	CH(CH ₃) ₂	80	95
7	^t Bu(TADDOL)POPh	CH ₃	<i>c</i> -C ₆ H ₁₁	82	93

In addition to the directed transition-metal catalyzed asymmetric hydroboration of acyclic amides previously discussed, asymmetric desymmetrization of cyclopropenes was reported by Gevorgyan *et al.*¹⁴ Desymmetrization is the loss of one or more symmetry elements that can give rise to molecular chirality, *i.e.*, the conversion of a prochiral molecule to one that is chiral, as shown in Scheme 1.9. The rhodium-catalyzed

hydroboration of prochiral cyclic substrate **28** results in desymmetrization, forming *cis*- and *trans*-products, **29** and **29'**, respectively.



Scheme 1.9. Rhodium-catalyzed asymmetric hydroboration of cyclopropenes.¹⁴

The ester moiety provides a directing-effect in this reaction under optimized conditions. When the hydroboration occurs with Wilkinson's catalyst and CatBH, the reaction is not diastereoselective and also forms a significant amount of ring-opening products. However, when PinBH is substituted for CatBH, high levels of diastereoselectivity (99:1) and enantioselectivity (92–98%) are achieved in a variety of substituted esters (Table 1.5).¹⁴

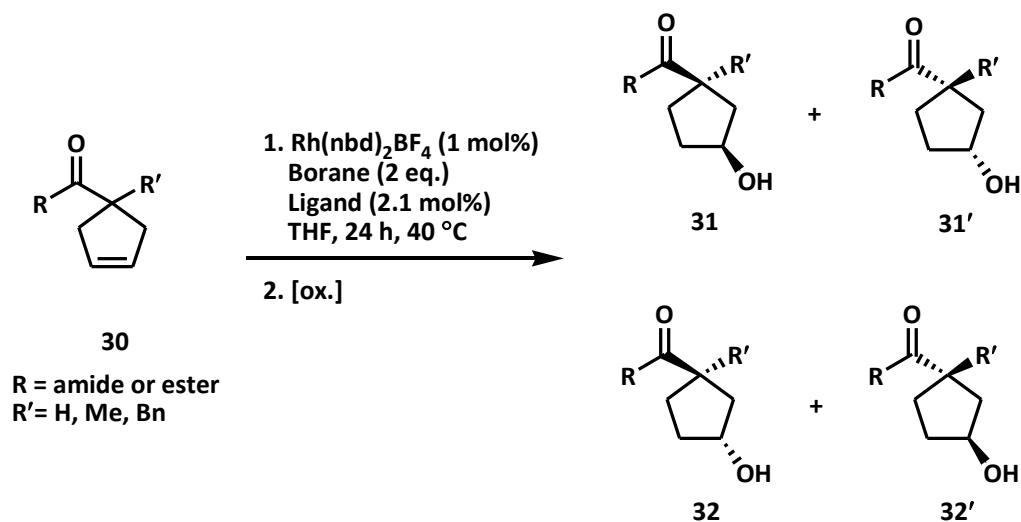
Table 1.5. Asymmetric Hydroboration of 3,3-disubstituted cyclopropenes.¹⁴

Entry	R	R'	Ligand	<i>cis</i> : <i>trans</i>	Yield (%)	ee (%)
1	Me	Me	(<i>R</i>)-BINAP	99 : 1	94	94
2	TMS	Et	(<i>R</i>)-BINAP	99 : 1	99	97
3	Ph	Me	(<i>R</i>)-BINAP	99 : 1	99	92
4	COOMe	Me	(<i>S</i>)-Tol-BINAP	–	99	98

It was hypothesized that γ,δ -unsaturated cyclic amide and ester substrates could efficiently achieve rhodium-catalyzed asymmetric hydroboration. This is based on the previous work of rhodium-catalyzed hydroboration on β,γ -unsaturated acyclic amides and

β,γ -unsaturated cyclic cyclopropenyl esters by Takacs *et al.* and Gevorgyan *et al.*, respectively.¹²⁻¹⁴ Even though these cases involve slightly different positioning of the directing-group to the olefin moiety, it was thought that these substrates would allow for the necessary two-point binding of the rhodium catalyst due to their fixed positioning, *i.e.* cyclic substrates.

Examples of efficient asymmetric desymmetrization *via* transition metal-mediated hydroboration of cyclopentenyl derivatives have not been previously studied. Similarly, to the work of Gevorgyan *et al.*, these γ,δ -unsaturated cyclic amide and ester substrates would allow for desymmetrization upon rhodium-catalyzed hydroboration. As shown in Scheme 1.10, this process results in the loss of one or more symmetry elements and gives rise to molecular chirality, which converts prochiral substrate **30** to potentially chiral γ -hydroxy products **31**, **31'**, **32** and **32'**.



Scheme 1.10. Rhodium-catalyzed asymmetric hydroboration of prochiral ester and amide cyclopentenyl substrates.

In this process, four possible products can be obtained: *cis*-isomer **31**, its enantiomer **31'**, *trans*-isomer **32**, and its enantiomer **32'**. Due to the directing-group and two-point binding of the rhodium-catalyst, it is hypothesized that predominately the *cis*-isomers **31** and **31'** will be formed. As a consequence of the possibility of the formation of four different products, it is necessary to take a combinatorial approach to this chemistry as different catalysts, substrates, ligands and boranes may result in different diastereo- and enantioselectivities of these products.

Rhodium-catalyzed hydroboration in conjunction with directing groups can be used to control relative and absolute stereochemistry. Multiple asymmetric centers can be formed in one step; these building blocks serve the potential to be incorporated in biologically relevant molecules. More importantly, these systems provide supplement mechanistic insight into previous work done with β,γ -unsaturated acyclic amides.

My work, and the subject of this dissertation, is the application of rhodium-catalyzed asymmetric hydroboration of prochiral ester and amide cyclopentenyl substrates studied under various conditions including catalysts, ligands and boranes, as shown in Figure 1.2.

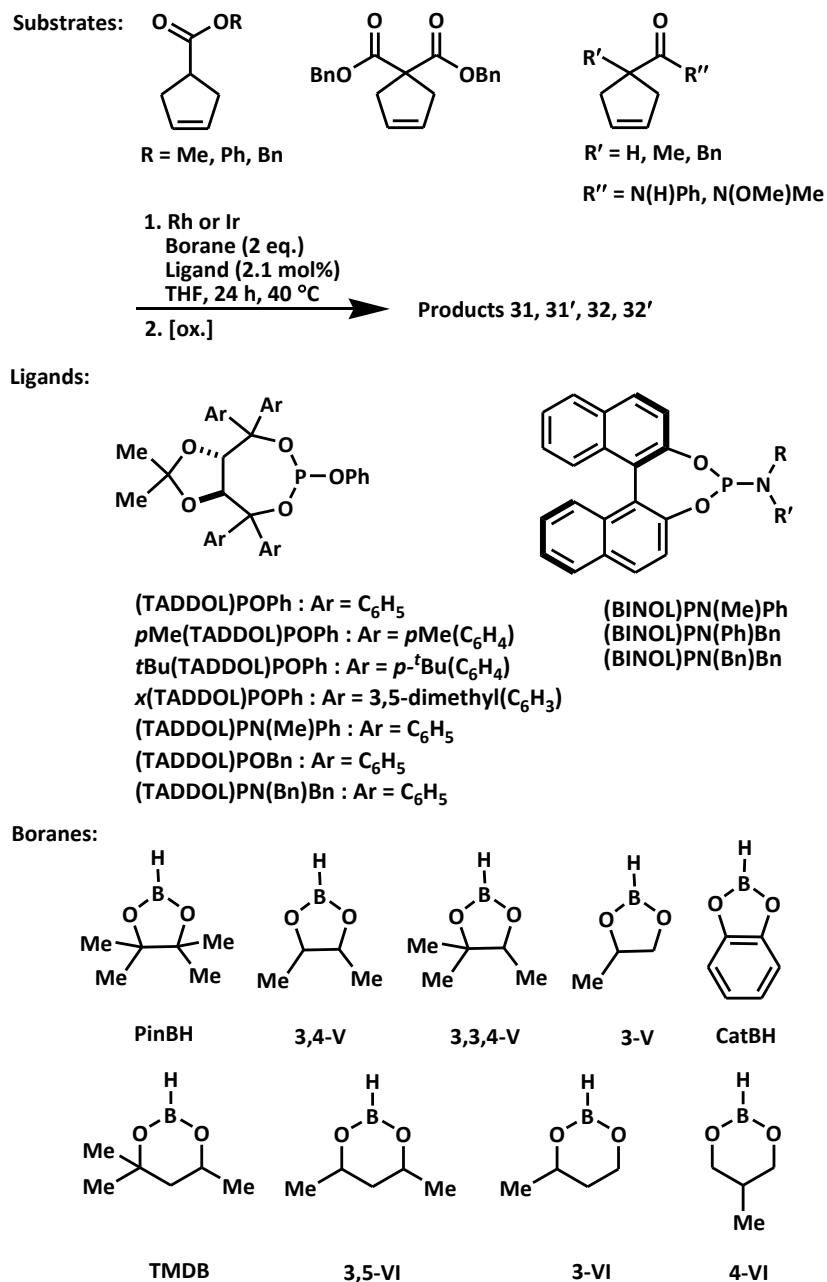
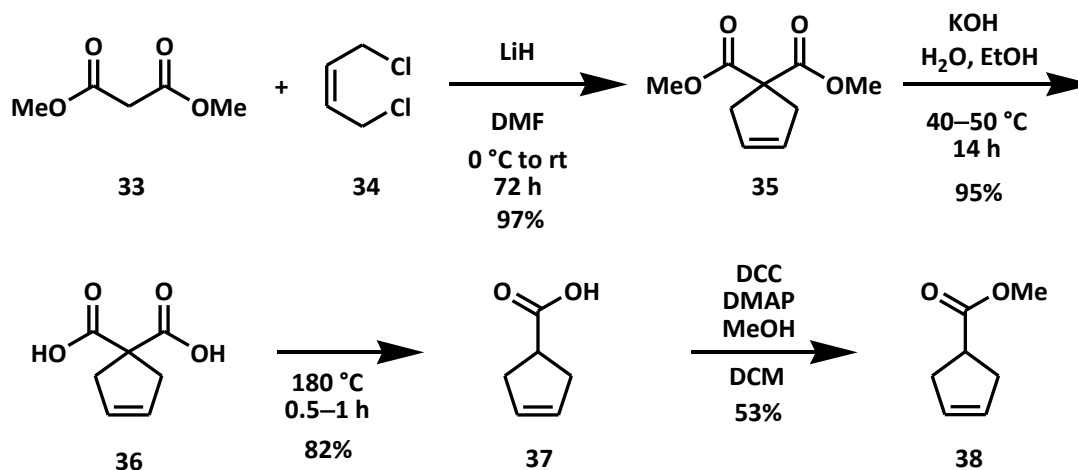


Figure 1.2. Various substrates, ligands and boranes studied.

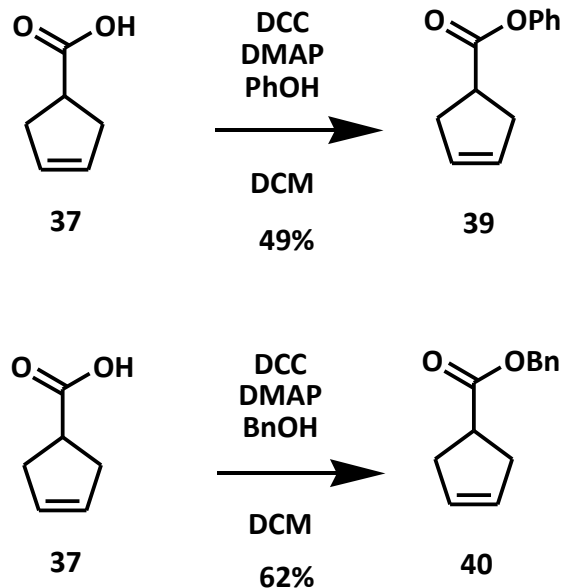
Chapter 2: Synthesis of Prochiral Cyclopentenyl Esters and Amides

To achieve asymmetric desymmetrization *via* rhodium-catalyzed hydroboration of cyclopentenyl prochiral substrates, the ester and amide derivatives were synthesized. Methyl cyclopent-3-enecarboxylate **38** was synthesized *via* the dicyclohexylcarbodiimide (DCC) coupling of methanol and cyclopent-3-enecarboxylic acid **37** (Scheme 2.1) with catalytic amounts of 4-dimethylaminopyridine (DMAP) to promote the reaction.¹⁵ The acid was formed by the decarboxylation of cyclopent-3-ene-1,1-dicarboxylic acid **36**; the reaction occurs upon heating the diacid. The diacid **36** was synthesized *via* saponification of **35**, which came from the double S_N2 displacement of *cis*-1,4-dichloro-2-butene **34** by dimethylmalonate **33**.¹⁶



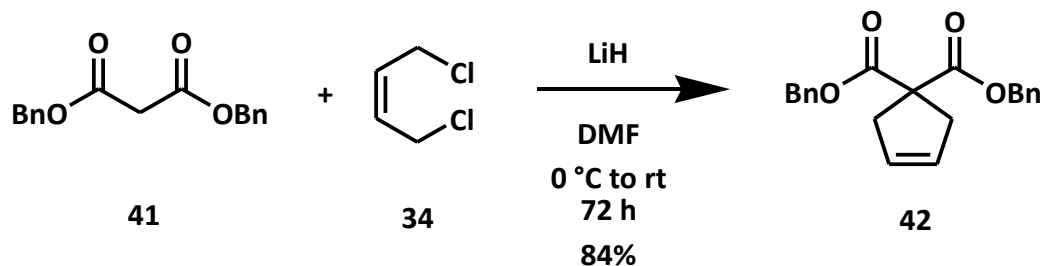
Scheme 2.1. Synthesis of methyl cyclopent-3-enecarboxylate.

In a similar fashion, phenyl- and benzyl cyclopent-3-ene (**39** and **40**, respectively) can be synthesized by the DCC-DMAP coupling of the appropriate alcohol or phenol to acid **37** (Scheme 2.2).



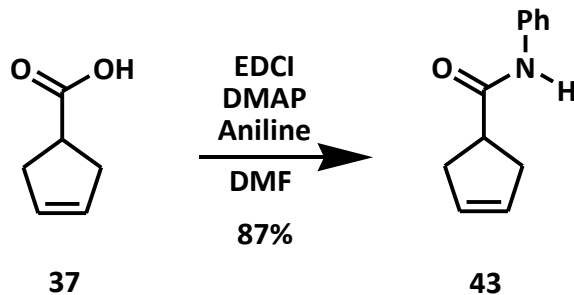
Scheme 2.2. Synthesis of phenyl- and benzyl cyclopent-3-enecarboxylate.

A double S_N2 displacement of *cis*-1,4-dichloro-2-butene **34** with dibenzylmalonate **41** gives the corresponding dibenzyl cyclopentene **42** (Scheme 2.3).



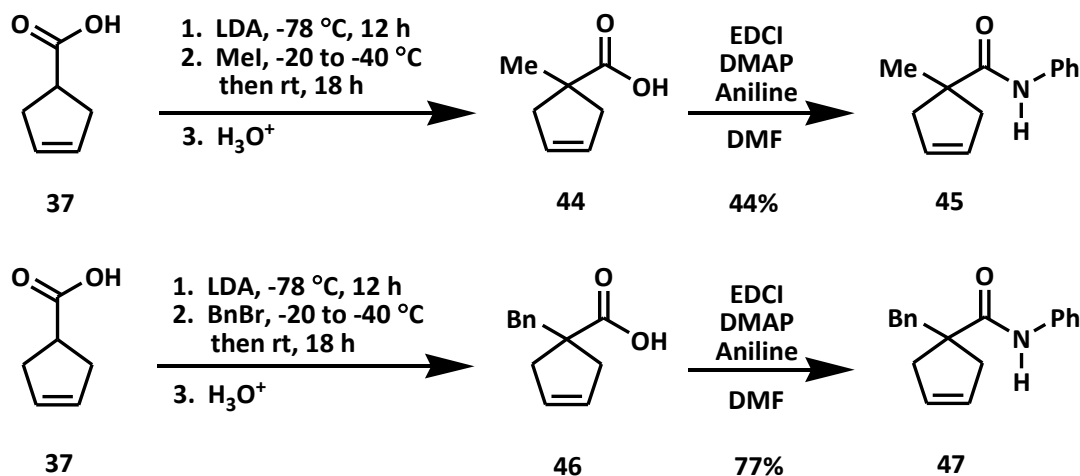
Scheme 2.3. Synthesis of dibenzyl cyclopent-3-ene-1,1-dicarboxylate.

The synthesis of the desired amides uses a comparable method to the esters. The coupling is done with EDCI (1-ethyl-3-(3-dimethylaminopropyl) carbodiimide) with catalytic amounts of DMAP. The acid **37** with aniline gives the corresponding amide **43** (Scheme 2.4).



Scheme 2.4. Synthesis of *N*-phenylcyclopent-3-enecarboxamide.

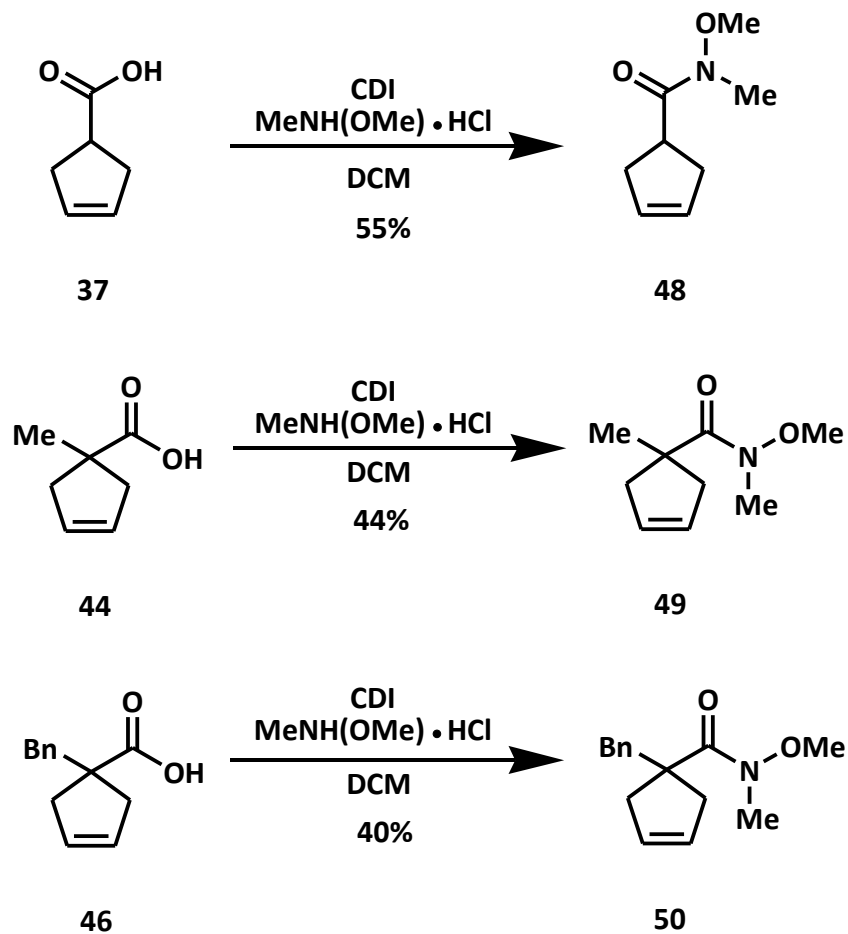
The desired α -substituted amides are prepared from the corresponding substituted acids. Acid **37** is doubly deprotonated with lithium diisopropylamide (LDA) giving an enolate dianion to which the electrophile (iodomethane or benzyl bromide) is added slowly. After an acid work up and extraction, the crude α -substituted acid is used in the EDCI coupling to form the consequent substituted amides, **45** and **47** (Scheme 2.5).



Scheme 2.5. Synthesis of 1-methyl- and 1-benzyl-*N*-phenylcyclopent-3-enecarboxamide.

The synthesis of the Weinreb amide derivatives applies a similar method to that employed for the *N*-phenyl amides, but uses a different coupling agent. The coupling is

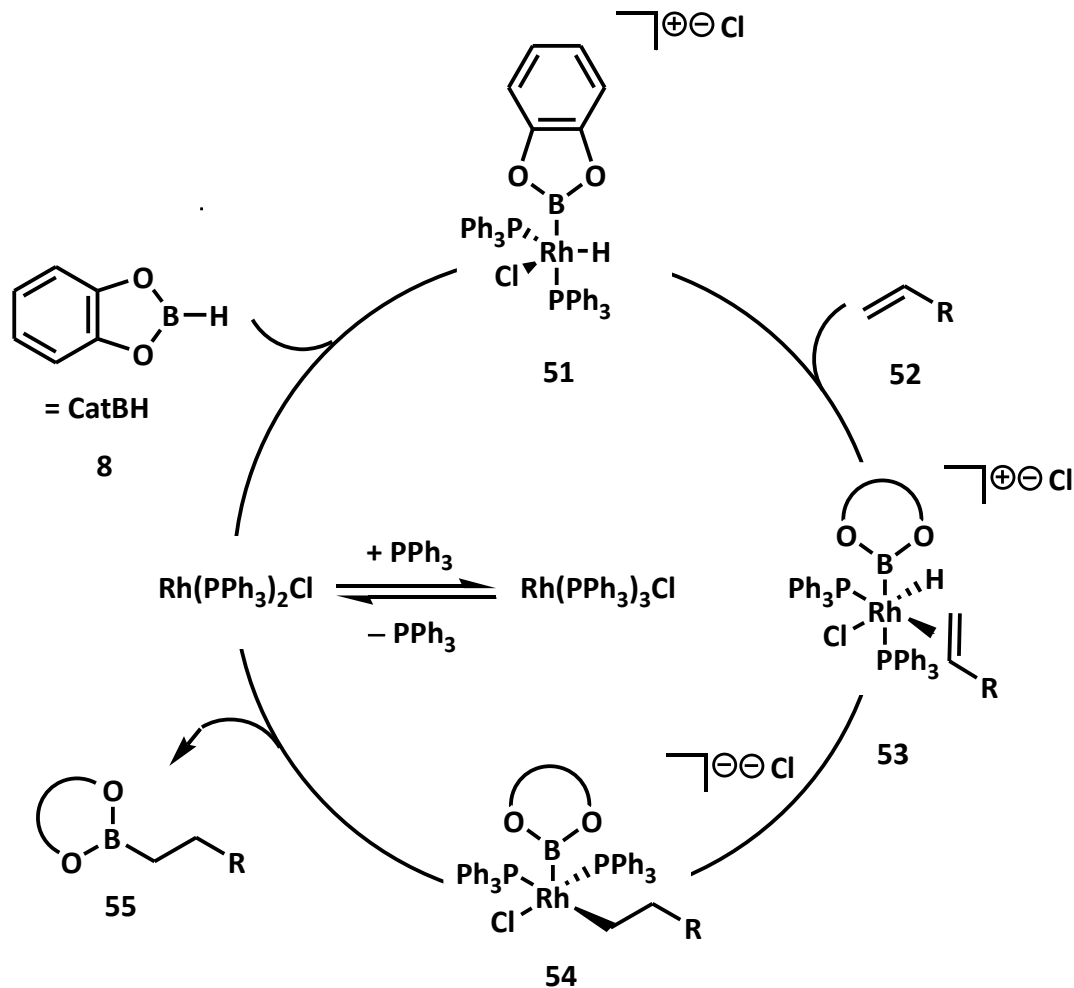
done with CDI (1,1'-carbonyldiimidazole) with a catalytic amount of DMAP, the acid and the amine to provide Weinreb amides **48**, **49**, and **50** (Scheme 2.6).



Scheme 2.6. Synthesis of *N*-methoxy-*N*-methylcyclopent-3-enecarboxamide, and its α -methyl and α -benzyl derivatives.

Chapter 3: Model for Rhodium-Catalyzed Hydroboration

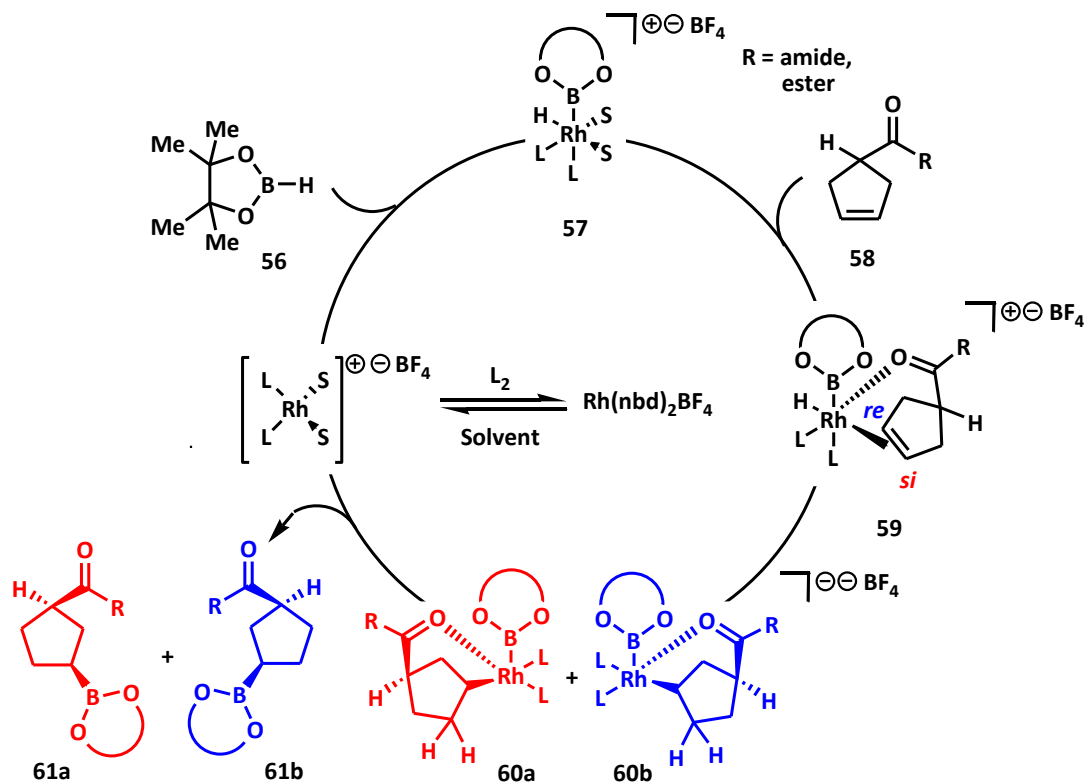
The mechanism of transition-metal catalyzed hydroboration of simple alkenes with Wilkinson's catalyst has been studied extensively, including deuterium-labeling studies with deuteriocatecholoborane (CatBD)¹⁷ and computational studies.¹⁸ The first step in the reaction mechanism with Wilkinson's catalyst is proposed to occur with the loss of a phosphine ligand to provide $\text{Rh}(\text{PPh}_3)_2\text{Cl}$ as the active catalyst species (Scheme 3.1). Oxidative addition of the B–H bond of CatBH **8** occurs to the unsaturated rhodium center to form intermediate **51**.¹⁹ The alkene **52** then coordinates to the rhodium center forming complex **53**. Insertion of the olefin into the rhodium–hydride bond occurs to make intermediate **54**. Reductive elimination of the B–C bond then produces the organoboronate ester **55** and regenerates the active catalyst species.²⁰



Scheme 3.1. Proposed mechanism of an alkene using CatBH.²⁰

The mechanistic pathway for the two-point binding of prochiral substrates used in this study has not been addressed directly. It is assumed that many features will mirror that of the simpler case of acyclic alkenes.¹³ It is essential to discuss additional factors for this mechanistic pathway. In the case of the prochiral olefin substrates **58**, the amide or ester group directs the diastereoselectivity in the hydroboration *cis*, that is, to the same side of the ring as the amide substituent (Scheme 3.2). The enantioselective catalyst must

differentiate between the sides of the bound π -system. The enantioselectivity is therefore determined by the regioselective addition to the *re* or *si* site of the olefin moiety, which depends on substrate, borane, and catalyst system (*vide infra*).



Scheme 3.2. Model for rhodium-catalyzed hydroboration of prochiral cyclopentenyl substrates.

Chapter 4: Ligands and Boranes used in Rhodium-Catalyzed Asymmetric Hydroboration

TADDOL- and BINOL-derived monophosphite and phosphoramidite ligands were screened in the rhodium-catalyzed asymmetric hydroboration of prochiral substrates to produce desymmetrized, substituted cyclopentanol products after oxidation of the carbon–boron bond. Both the TADDOL- and BINOL-scaffolds can be easily modified to obtain a series of different topographies of the chiral ligand (Figure 4.1).²¹ Even a slight change in the ligand scaffold can produce drastically different diastereo- and enantioselectivities, and therefore, it is expedient to use combinatorial methods for these hydroboration reactions.¹³

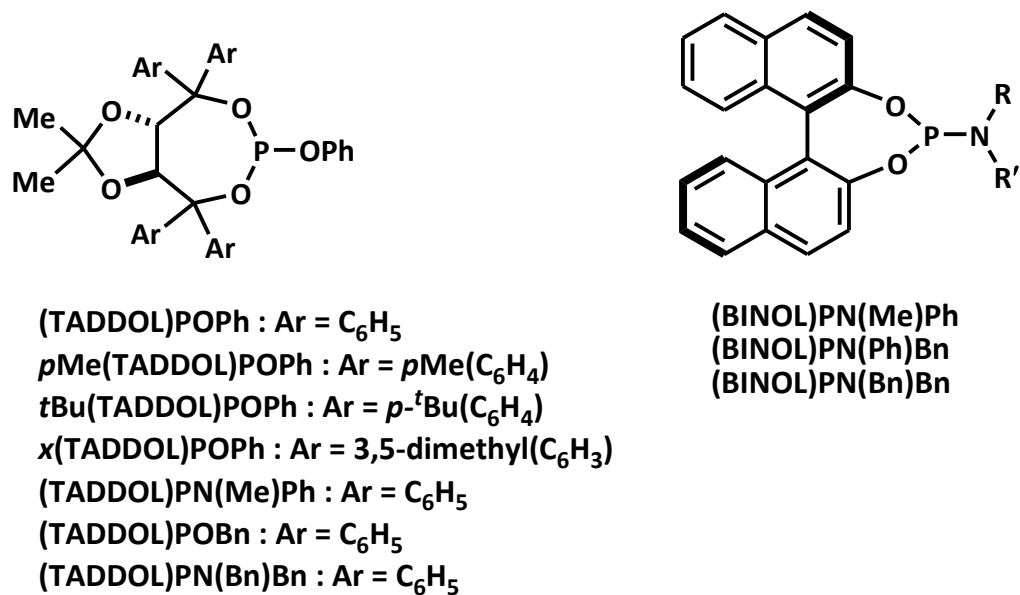


Figure 4.1. TADDOL- and BINOL-derived phosphite and phosphoramidite ligands.

Both PinBH and CatBH have been used extensively in the literature for transition-metal catalyzed hydroborations on various alkenes and alkynes.^{22–25} The Takacs group

has discovered that not only altering the ligand, but also the borane can radically change the outcome of the reaction. Therefore, a variety of boranes were also used in this study; these are shown in Figure 4.2.

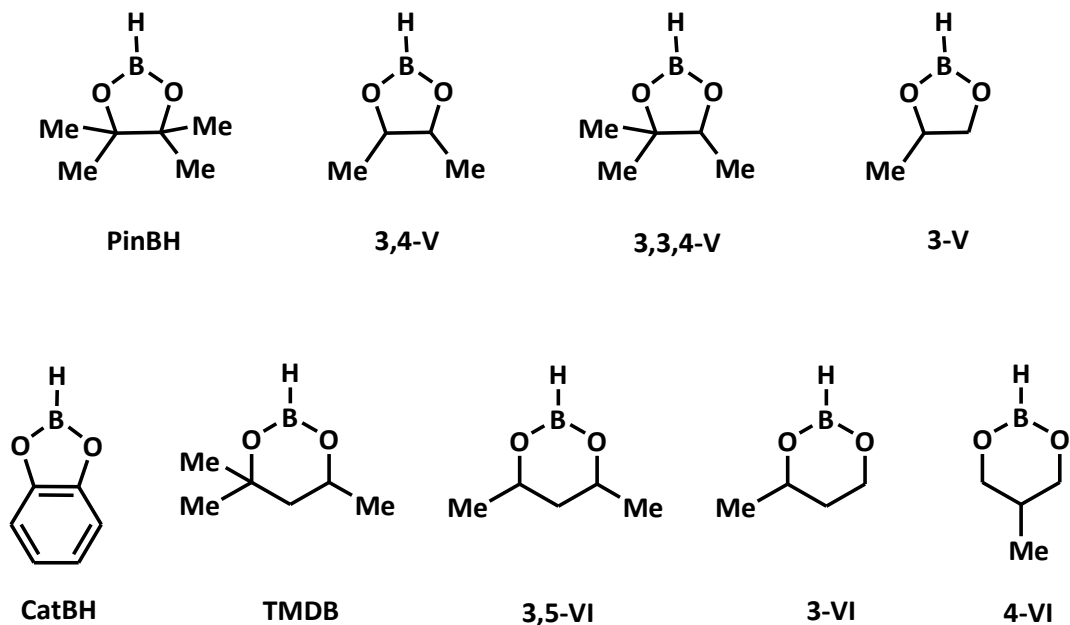
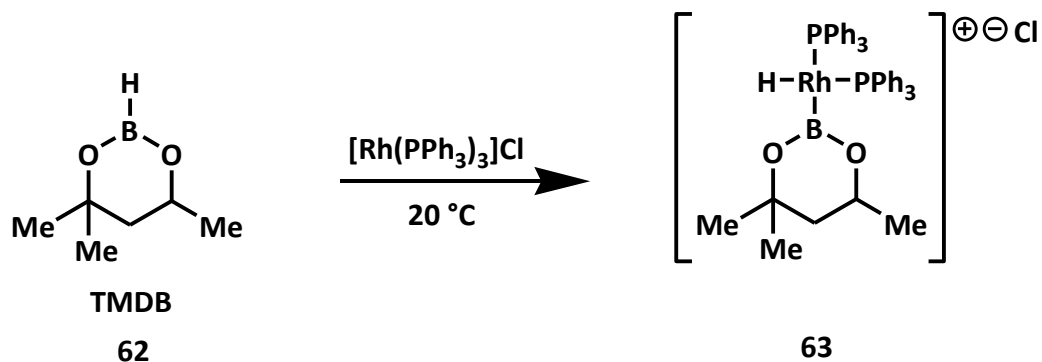
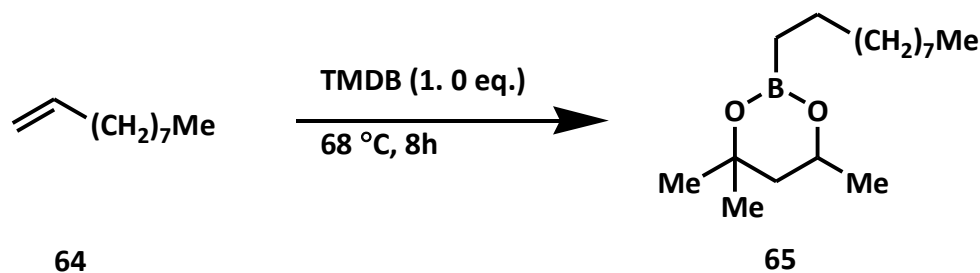


Figure 4.2. Boranes used in the rhodium-catalyzed hydroboration of prochiral cyclopentenyl substrates.

The borane 4,4,6-trimethyl-1,3,2-dioxaborinane (TMDB) was used over thirty years ago by Kono *et al.* and was found to undergo oxidative addition with Wilkinson's catalyst (Scheme 4.1).²⁶ In a different study, TMDB was used by Woods and Strong in the stoichiometric (*i.e.*, non-catalyzed) hydroboration of several alkenes (Scheme 4.2).²⁷ To this date, it is not found that other groups use TMDB, or any structurally similar borane, in transition-metal catalyzed hydroborations.

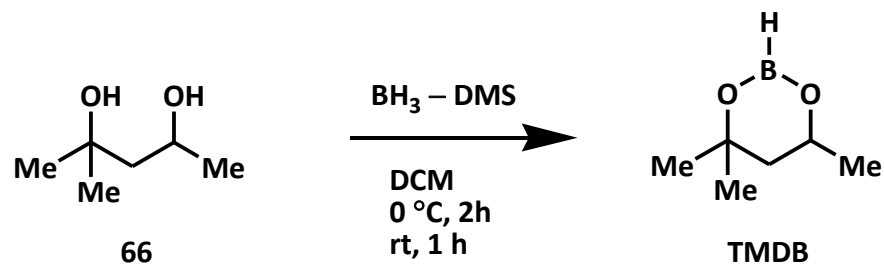


Scheme 4.1. TMDB undergoes oxidative addition with Wilkinson's catalyst.²⁶



Scheme 4.2 TMDB in the use of stoichiometric hydroboration of olefins.²⁷

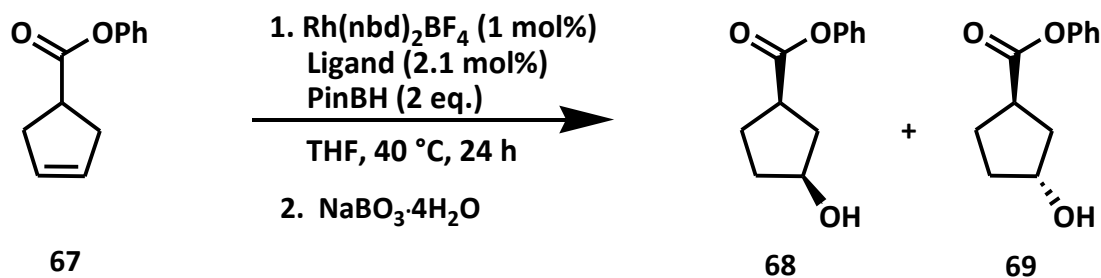
The boranes can be conveniently produced from the corresponding diol. The reaction is done in dry DCM with a concentrated solution of BH_3 in DMS (Scheme 4.3). After 3 h, the DMS is removed *in vacuo* and the borane is distilled and ready to be used in hydroboration reactions.



Scheme 4.3. Diols are easily converted to its corresponding borane.²⁷

Chapter 5: Rhodium-Catalyzed Asymmetric Hydroboration on Prochiral Cyclopentenyl Ester Substrates

Gevorgyan *et al.* successfully achieved high levels of diastereo- and enantioselectivity of cyclopropenyl prochiral substrates.¹⁴ The diastereoselectivity was controlled by exploiting the directing effect of the pendant ester moiety. This idea was applied to prochiral cyclopentenyl substrates, initially by Mr. Sean Smith, then continued using his protocol.¹³ Rhodium-catalyzed asymmetric hydroboration of phenyl cyclopent-3-enecarboxylate **67** formed a mixture of the *cis*- and *trans*-products **68** and **69**, respectively (Scheme 5.1). The results were initially disappointing. The diastereoselectivity is only 1.5:1 in the best case (entry 1, Table 5.1). In addition to poor diastereoselectivity, the enantioselectivity achieved is poor in all cases. The identification of the *trans*-products in these desymmetrization reactions was determined by comparison to the product obtained using BH_3 , a process which favors addition to the less sterically encumbered face of the cyclopentenyl ring.²⁸



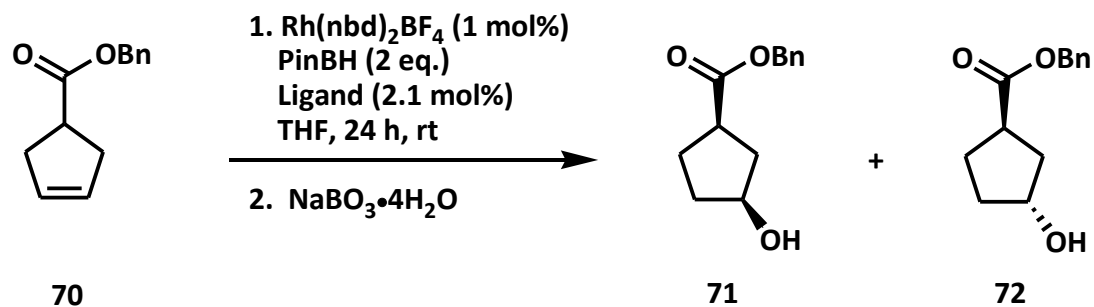
Scheme 5.1. Rhodium-catalyzed hydroboration of phenyl cyclopent-3-enecarboxylate.

Table 5.1. The rhodium-catalyzed hydroboration of **67** using PinBH and the influence of a four ligand screening set on diastereo- and enantioselectivities.

Entry	Ligand	Total Yield (%)	<i>cis</i> : <i>trans</i> (%)	ee (% <i>cis</i>)
1	(TADDOL)POPh	59	36 : 23	30
2	<i>p</i> -Me(TADDOL)POPh	62	32 : 30	29
3	<i>t</i> Bu(TADDOL)POPh	71	38 : 33	19
4	(TADDOL)PN(Me)Ph	73	41 : 32	48

Reaction conditions: 1 mol% Rh(nbd)₂BF₄, 2.1 mol% Ligand, 2 eq. PinBH, 40 °C, 24 h. Oxidation with NaBO₃·4H₂O. Yield determined by crude ¹H NMR with mesitylene as an internal standard; enantioselectivities determined by HPLC analysis.

Other work suggested that varying the ester substituent can alter the enantioselectivity and overall yield of the reaction.¹² Unfortunately, when the directing-group is changed from a phenyl ester to a benzyl ester (Scheme 5.2), the diastereo- and enantioselectivities remain roughly the same as shown in Table 5.2.



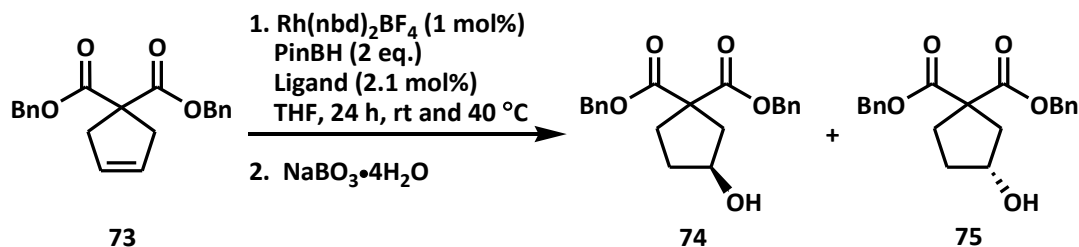
Scheme 5.2. Rhodium-catalyzed hydroboration of benzyl cyclopent-3-enecarboxylate.

Table 5.2. The rhodium-catalyzed hydroboration of **70** using PinBH and the influence of a six ligand screening set on diastereo- and enantioselectivities.

Entry	Ligand	Total Yield (%)	<i>cis</i> : <i>trans</i> (%)	ee (% <i>cis</i>)
1	(TADDOL)POPh	59	36 : 23	30
2	<i>p</i> -Me(TADDOL)POPh	62	32 : 30	29
3	^t Bu(TADDOL)POPh	71	38 : 33	19
4	<i>x</i> (TADDOL)POPh	74	40 : 34	-33
5	(BINOL)PN(Me)Ph	16	9 : 7	Rac
6	(TADDOL)PN(Me)Ph	74	42 : 32	48

Reaction conditions: 1 mol% Rh(nbd)₂BF₄, 2.1 mol% Ligand, 2 eq. PinBH, 40 °C, 24 h. Oxidation with NaBO₃·4H₂O. Yield determined by crude ¹H NMR with mesitylene as an internal standard; enantioselectivities determined by HPLC analysis.

Because the *cis/trans* diastereoselectivity was poor in the cases described above, we wanted to investigate a case which does not allow for diastereomers, only enantiomers. To circumvent the issue of diastereoselectivity, dibenzyl cyclopent-3-ene-1,1-dicarboxylate **73** was synthesized and screened with various ligands at room temperature for 24 h (Scheme 5.3). However, no conversion to form enantiomers **74** and **75** is observed. When heating these substrates to 40 °C, only 10% conversion to the products occurs after 24 h (Table 5.3). Due to the poor reactivity of this substrate, the enantioselectivity was not explored.



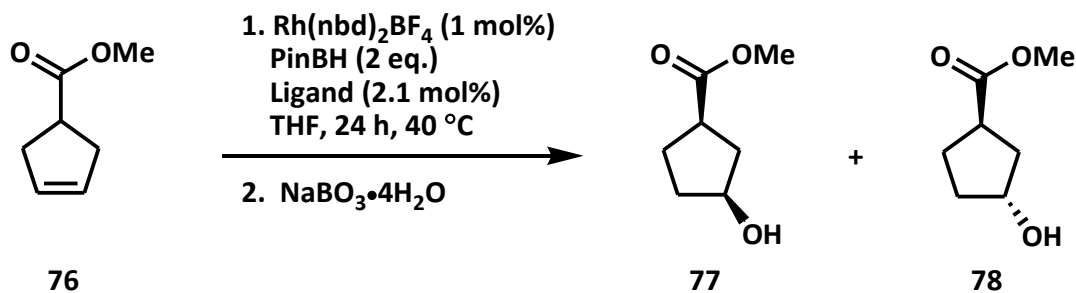
Scheme 5.3. Rhodium-catalyzed hydroboration of dibenzyl cyclopent-3-ene-1,1-dicarboxylate.

Table 5.3. The rhodium-catalyzed hydroboration of **73** using PinBH and the influence of a six ligand screening set on diastereo- and enantioselectivities.

Entry	Ligand	Yield (%)
1	(TADDOL)POPh	10
2	<i>p</i> -Me(TADDOL)POPh	0
3	^t Bu(TADDOL)POPh	11
4	<i>x</i> (TADDOL)POPh	9
5	(BINOL)PN(Me)Ph	0
6	(TADDOL)PN(Me)Ph	0

Reaction conditions: 1 mol% Rh(nbd)₂BF₄, 2.1 mol% Ligand, 2 eq. PinBH, rt and 40 °C, 24 h. Oxidation with NaBO₃·4H₂O. Yield determined by crude ¹H NMR with mesitylene as an internal standard.

It was hypothesized that perhaps the desired two-point binding of rhodium to the alkene and ester moieties was not efficiently achieved with the bulkier esters. Therefore, a methyl ester was synthesized and screened for rhodium-catalyzed asymmetric hydroboration. Nonetheless, when the methyl ester derivative **76** is hydroborated, an approximately 1:1 mixture of **77** and **78** is obtained. No diastereoselectivity is observed (Scheme 5.4). The enantioselectivity achieved is also meager (Table 5.4).



Scheme 5.4. Rhodium-catalyzed hydroboration of methyl cyclopent-3-enecarboxylate.

Table 5.4. The rhodium-catalyzed hydroboration of **76** using PinBH and the influence of a three ligand screening set on diastereo- and enantioselectivities.

Entry	Ligand	Total Yield (%)	<i>cis</i> : <i>trans</i> (%)	ee (% <i>cis</i>)
1	(TADDOL)POPh	72	38 : 34	22
2	^t Bu(TADDOL)POPh	69	35 : 34	Rac
3	<i>x</i> (TADDOL)POPh	66	35 : 31	8

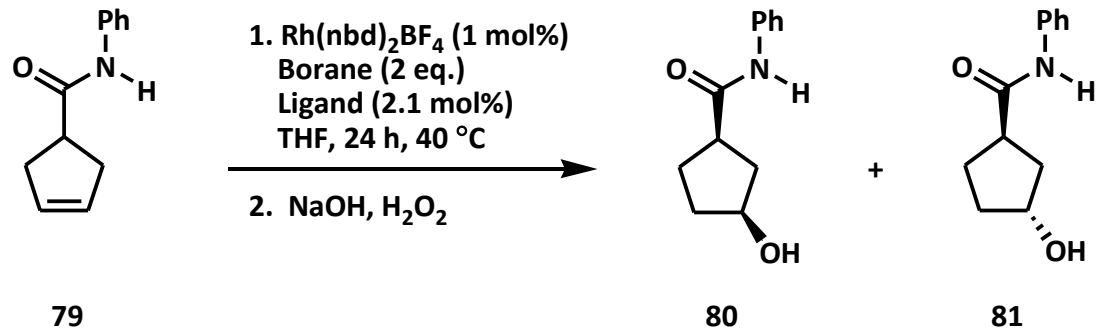
Reaction conditions: 1 mol% $\text{Rh}(\text{nbd})_2\text{BF}_4$, 2.1 mol% Ligand, 2 eq. PinBH, 40 °C, 24 h. Oxidation with $\text{NaBO}_3 \cdot 4\text{H}_2\text{O}$. Yield determined by crude ^1H NMR with mesitylene as an internal standard; enantioselectivities determined by HPLC analysis.

In the rhodium-catalyzed hydroboration of substituted cyclopentenyl substrates, the ester group does not provide an efficient mode to high levels of diastereoselectivity. With these substrates, the ester group is not enantioselective or effective in directing the reaction.

Chapter 6: Rhodium-Catalyzed Asymmetric Hydroboration on *N*-Phenylcyclopent-3-enecarboxamide

As discussed in Chapter 5, the ester moiety was shown not to be an efficient directing-group in rhodium-catalyzed hydroboration. The success of rhodium-catalyzed hydroboration on β,γ -unsaturated acyclic amide substrates by Takacs *et al.*,^{12,13} led to the examination of cyclopentenyl amide substrates. It was hypothesized that the amide moiety would serve as a better directing-group than the ester, presuming the rhodium binds at the carbonyl and not the nitrogen. More σ -donation into the carbonyl suggests more electron density on the carbonyl oxygen and therefore acting as a stronger σ -donor to the metal center. This theory is tested by examination of the diastereoselectivities.

The rhodium-catalyzed hydroboration of *N*-phenylcyclopent-3-enecarboxamide **79** provided a mixture of diastereomers **80** and **81** (Scheme 6.1). Initial results of the cyclic amide substrates showed that the amide provides a better directing group than the ester moiety as the diastereoselectivity is 1.5:1, *cis:trans*, respectively, for the ester moiety to 8:1, *cis:trans*, respectively, when the cyclic amide cyclopentenyl substrate was used in the rhodium-catalyzed hydroboration reaction (Table 6.1). By altering the directing-group, the level of enantiomeric excess (ee) also changed as it increased significantly. These preliminary results already showed promise when compared with analogous ester substrates, proving our hypothesis correct.



Scheme 6.1. Rhodium-catalyzed hydroboration of *N*-phenylcyclopent-3-enecarboxamide.

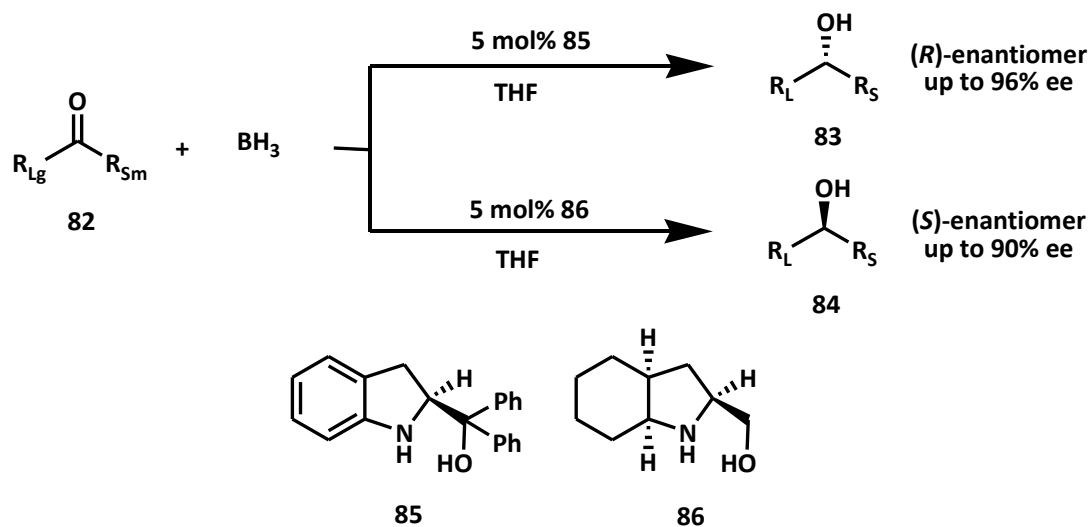
A small change in the scaffold alters the topography of the ligand. Therefore, it is of benefit to screen a variety of ligands whenever possible. When (BINOL)N(Me)Ph is used (entry 5, Table 6.1), the ee achieved is 84%. However, (TADDOL)PN(Me)Ph (entry 6) provides the opposite enantiomer in 70% ee (entry 6). The other TADDOL-derived phosphoramidite (TADDOL)PN(Bn)Bn also provides the opposite enantiomer, but to a much lesser degree (entry 8).

Table 6.1. The rhodium-catalyzed hydroboration of **79** using PinBH and the influence of an eleven ligand screening set on diastereo- and enantioselectivities.

Entry	Ligand	Total Yield (%)	<i>cis</i> : <i>trans</i> (%)	ee (% <i>cis</i>)
1	(TADDOL)POPh	72	60 : 12	60
2	<i>p</i> -Me(TADDOL)POPh	83	56 : 27	48
3	^t Bu(TADDOL)POPh	74	62 : 12	70
4	<i>x</i> (TADDOL)POPh	77	65 : 12	75
5	(BINOL)PN(Me)Ph	73	65 : 8	84
6	(TADDOL)PN(Me)Ph	74	60 : 14	-70
7	(TADDOL)POBn	26	16 : 10	10
8	(TADDOL)PN(Bn)Bn	48	18 : 30	-10
9	(BINOL)PN(Ph)Bn	63	51 : 12	56
10	(BINOL)PN(Bn)Bn	36	19 : 17	Rac
11	(BIPHEP)PN(Me)Ph	46	24 : 22	33

Reaction conditions: 1 mol% Rh(nbd)₂BF₄, 2.1 mol% Ligand, 2 eq. PinBH, 40 °C, 24 h. Oxidation with NaOH and H₂O₂. Yield determined by crude ¹H NMR with mesitylene as an internal standard; enantioselectivities determined by HPLC analysis.

It is often the case that opposite enantiomers exhibit different bioactivity. Therefore, it is a significant objective to obtain access to both enantiomers in high enantioselectivity; this is often a fastidious challenge.²⁹ If the ligand is synthesized from the chiral pool, it is possible that the antipode may not be available or that one is more expensive than the other.²⁹ However, it is shown by Kim *et al.* that both enantiomers of secondary alcohols can be obtained in high enantioselectivities in the asymmetric reduction of ketones with borane (Scheme 6.2). Access to both enantiomers is available with ligands derived from (*S*)-indoline-2-carboxylic acid.³⁰



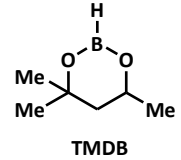
Scheme 6.2. An enantioswitch example: asymmetric reduction of ketones with borane.³⁰

Consequently, it is of importance to note the availability of enantioswitching in the above hydroboration of **79** with PinBH. Similar ligand scaffolds are used but the specific monophosphite or phosphoramidite is altered. Opposite enantiomers are formed from -70% to 84% ee in entries 6 and 5, respectively. However, this is not a true enantioswitch, because the ligand backbone is different (*i.e.* BINOL and TADDOL-derived ligands). Therefore, an enantioswitch occurs from -70% to 75% ee with (TADDOL)PN(Me)Ph and x (TADDOL)POPh (entries 6 and 4, respectively).

As it is shown that different ligands provide different diastereo- and enantioselectivities, it is hypothesized that also changing the source of borane will affect these results as well. It is then necessary to empirically test different borane sources as varied results are expected for both diastereo- and enantioselectivities.

When changing the borane from PinBH to TMDB, a structurally similar borane prepared in racemic form for these studies, the total yield remained effectively the same and the diastereoselectivity is slightly reduced to approximately 5:1 (Table 6.2). However, the enantioselectivities achieved are increased significantly in all cases except with (BINOL)PN(Me)Ph. When PinBH is used, the enantioswitch occurs with some TADDOL-derived phosphoramidites. However, an enantioswitch does not happen using the same ligands in combination with TMDB as the borane. These primary results confirm our hypothesis that altering the source of borane and ligand also varies the diastereo- and enantioselectivities. Given these results, it would benefit us to screen other boranes to examine their effect on yields and diastereo- and enantioselectivities.

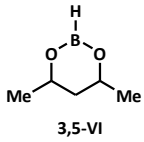
Table 6.2. The rhodium-catalyzed hydroboration of **79** using TMDB and the influence of a six ligand screening set on diastereo- and enantioselectivities.

Entry	Ligand	Total Yield (%)	<i>cis</i> : <i>trans</i> (%)	ee (% <i>cis</i>)	Borane
1	(TADDOL)POPh	54	42 : 12	87	 <p style="text-align: center;">TMDB</p>
2	<i>p</i> -Me(TADDOL)POPh	72	56 : 16	88	
3	^t Bu(TADDOL)POPh	78	62 : 16	88	
4	<i>x</i> (TADDOL)POPh	73	60 : 13	90	
5	(BINOL)PN(Me)Ph	78	62 : 16	81	
6	(TADDOL)PN(Me)Ph	86	66 : 20	44	

Reaction conditions: 1 mol% Rh(nbd)₂BF₄, 2.1 mol% Ligand, 2 eq. TMDB, 40 °C, 24 h. Oxidation with NaOH and H₂O₂. Yield determined by crude ¹H NMR with mesitylene as an internal standard; enantioselectivities determined by HPLC analysis.

Another borane that is structurally similar to TMDB is 3,5-VI. This borane has one less methyl group compared to TMDB. The removal of this methyl group decreases both the diastereo- and enantioselectivities drastically (Table 6.3).

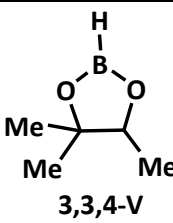
Table 6.3. The rhodium-catalyzed hydroboration of **79** using 3,5-VI and the influence of a four ligand screening set on diastereo- and enantioselectivities.

Entry	Ligand	Total Yield (%)	<i>cis</i> : <i>trans</i> (%)	ee (% <i>cis</i>)	Borane
1	^t Bu(TADDOL)POPh	45	27 : 18	17	 3,5-VI
2	<i>x</i> (TADDOL)POPh	53	30 : 23	33	
3	(BINOL)PN(Me)Ph	72	38 : 34	8	
4	(TADDOL)PN(Me)Ph	64	30 : 34	10	

Reaction conditions: 1 mol% Rh(nbd)₂BF₄, 2.1 mol% Ligand, 2 eq. 3,5-VI, 40 °C, 24 h. Oxidation with NaOH and H₂O₂. Yield determined by crude ¹H NMR with mesitylene as an internal standard; enantioselectivities determined by HPLC analysis.

The next logical step was to screen 3,3,4-V, the five-membered analog to TMDB. The rationale was that PinBH, a five-membered ring borane, provides moderate ee's with this substrate (84%), but TMDB, which contains the same methyl substitution as 3,3,4-V, achieves higher ee's (90%). It was thought that this borane would provide similar enantioselectivities to TMDB. However, the enantioselectivities obtained with it are very low, almost racemic in most cases. This told us that by simply changing the size of the ring from six to five, the difference in results can be significant. The ee's obtained are drastic, from 90% to 37% ee with TMDB and 3,3,4-V, respectively. Interestingly, the major diastereomer is now found to be the *trans*-product **81**, not the expected *cis*-product **80** (Table 6.4).

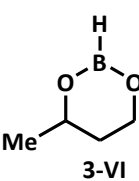
Table 6.4. The rhodium-catalyzed hydroboration of **79** using 3,3,4-V and the influence of a six ligand screening set on diastereo- and enantioselectivities.

Entry	Ligand	Total Yield (%)	<i>cis</i> : <i>trans</i> (%)	ee (% <i>cis</i>)	Borane
1	(TADDOL)POPh	65	17 : 48	20	
2	<i>p</i> -Me(TADDOL)POPh	59	14 : 45	12	
3	<i>t</i> Bu(TADDOL)POPh	65	15 : 50	Rac	
4	<i>x</i> (TADDOL)POPh	59	15 : 44	Rac	
5	(BINOL)PN(Me)Ph	66	17 : 49	24	
6	(TADDOL)PN(Me)Ph	75	20 : 55	37	

Reaction conditions: 1 mol% Rh(nbd)₂BF₄, 2.1 mol% Ligand, 2 eq. 3,3,4-V, 40 °C, 24 h. Oxidation with NaOH and H₂O₂. Yield determined by crude ¹H NMR with mesitylene as an internal standard; enantioselectivities determined by HPLC analysis.

Because TMDB does much better on this system than any other tested at this point (up to 90% ee), it was hypothesized that the six-membered rings with asymmetry would prove better than the five-membered ringed boranes. Due to this reasoning, borane 3-VI was screened. The diastereoselectivities increased from 4:1 for TMDB to 8:1 for borane 3-VI (Table 6.5). However, enantioselectivities are quite low; the best case is 20%, attained with (TADDOL)PN(Me)Ph (entry 6).

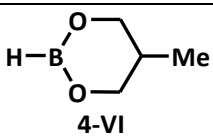
Table 6.5. The rhodium-catalyzed hydroboration of **79** using 3-VI and the influence of a six ligand screening set on diastereo- and enantioselectivities.

Entry	Ligand	Total Yield (%)	<i>cis</i> : <i>trans</i> (%)	ee (% <i>cis</i>)	Borane
1	(TADDOL)POPh	58	51 : 7	14	 3-VI
2	<i>p</i> -Me(TADDOL)POPh	59	52 : 7	10	
3	<i>t</i> Bu(TADDOL)POPh	67	57 : 10	10	
4	<i>x</i> (TADDOL)POPh	65	57 : 8	16	
5	(BINOL)PN(Me)Ph	72	63 : 8	4	
6	(TADDOL)PN(Me)Ph	64	58 : 8	20	

Reaction conditions: 1 mol% Rh(nbd)₂BF₄, 2.1 mol% Ligand, 2 eq. 3-VI, 40 °C, 24 h. Oxidation with NaOH and H₂O₂. Yield determined by crude ¹H NMR with mesitylene as an internal standard; enantioselectivities determined by HPLC analysis.

Borane 3,5-VI is a meso compound. Borane 4-VI does have an internal plane of symmetry but does not contain any stereocenters. When borane 4-VI was screened, the diastereoselectivities are low, *ca.* 1:1 to 2:1 (Table 6.6). The products formed with this borane were all racemic.

Table 6.6. The rhodium-catalyzed hydroboration of **79** using 4-VI and the influence of a four ligand screening set on diastereo- and enantioselectivities.

Entry	Ligand	Total Yield (%)	<i>cis</i> : <i>trans</i> (%)	ee (% <i>cis</i>)	Borane
1	<i>t</i> Bu(TADDOL)POPh	87	56 : 31	Rac	 4-VI
2	<i>x</i> (TADDOL)POPh	75	52 : 23	Rac	
3	(BINOL)PN(Me)Ph	59	38 : 21	Rac	
4	(TADDOL)PN(Me)Ph	66	44 : 22	Rac	

Reaction conditions: 1 mol% Rh(nbd)₂BF₄, 2.1 mol% Ligand, 2 eq. 4-VI, 40 °C, 24 h. Oxidation with NaOH and H₂O₂. Yield determined by crude ¹H NMR with mesitylene as an internal standard; enantioselectivities determined by HPLC analysis.

The boranes that provide us with the best results thus far are the ones that contain steric bulk (*e.g.* PinBH and TMDB). It was essential to next test CatBH, as this is a bulky borane that has been known to efficiently participate in transition-metal catalyzed hydroboration on various substrates.^{10–11,22–23,31–33} Both iridium and rhodium are known to catalyze hydroboration reactions using CatBH, although the use of iridium is much less common.¹¹ Unfortunately with our catalyst system, CatBH fails to proceed in the attempted transition-metal mediated hydroboration with either iridium and rhodium catalysts using the cyclopentenyl prochiral amide substrate **79** (Tables 6.7 and 6.8). A significant amount of starting material remains even after 24 h. Compared to PinBH, the enantioselectivity also suffers with the use of CatBH; only low levels are achieved. Table 6.8, entry 2 gives the most encouraging result.

Table 6.7. The iridium-catalyzed hydroboration of **79** using CatBH (2 eq.) and the influence of a five ligand screening set on diastereo- and enantioselectivities.

Entry	Ligand	Total Yield (%)	<i>cis</i> : <i>trans</i> (%)	ee (% <i>cis</i>)	Remaining S.M. (%)
1	(TADDOL)POPh	18	10 : 8	24	45
2	<i>p</i> -Me(TADDOL)POPh	12	8 : 4	10	50
3	^t Bu(TADDOL)POPh	41	25 : 16	20	55
4	<i>x</i> (TADDOL)POPh	14	10 : 4	16	50
5	(TADDOL)PN(Me)Ph	30	20 : 10	20	55

Reaction conditions: 1 mol% Ir(cod)₂BF₄, 2.1 mol% Ligand, 2 eq. CatBH, 40 °C, 24 h. Oxidation with NaOH and H₂O₂. Yield determined by crude ¹H NMR with mesitylene as an internal standard; enantioselectivities determined by HPLC analysis.

Table 6.8. The rhodium-catalyzed hydroboration of **79** using CatBH (2 eq.) and the influence of a five ligand screening set on diastereo- and enantioselectivities.

Entry	Ligand	Total Yield (%)	<i>cis</i> : <i>trans</i> (%)	ee (% <i>cis</i>)	Remaining S.M. (%)
1	(TADDOL)POPh	24	14 : 10	Rac	33
2	<i>p</i> -Me(TADDOL)POPh	36	15 : 21	60	36
3	<i>t</i> Bu(TADDOL)POPh	27	17 : 10	20	50
4	<i>x</i> (TADDOL)POPh	15	10 : 5	20	38
5	(TADDOL)PN(Me)Ph	30	20 : 10	27	43

Reaction conditions: 1 mol% Rh(nbd)₂BF₄, 2.1 mol% Ligand, 2 eq. CatBH, 40 °C, 24 h. Oxidation with NaOH and H₂O₂. Yield determined by crude ¹H NMR with mesitylene as an internal standard; enantioselectivities determined by HPLC analysis.

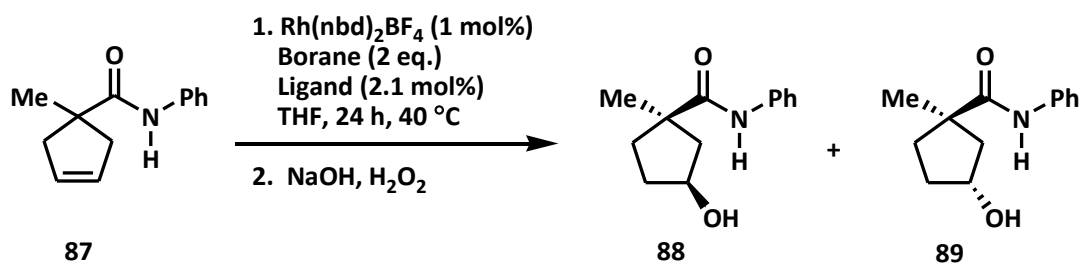
For the α -unsubstituted amide **79**, TMDB provides the highest level of enantioselectivity (90% with *x*(TADDOL)POPh; 73% total yield; 60:13 *cis:trans*) compared to the results of PinBH and all of the other synthesized boranes. When PinBH is used with (TADDOL)PN(Me)Ph, a significant enantioswitch occurs (-70% ee). However, when TMDB or any of the other synthesized boranes are screened with this ligand, no enantioswitch transpires. The data obtained supports the notion that it is beneficial to not only screen different TADDOL- and BINOL-derived chiral ligands, but also the borane. Relatively small changes in the structure of the borane can change the enantioselectivity significantly, as previously discussed. The best diastereoselectivity achieved is 8:1 for the ratio of *cis*- to *trans*-products, which is much improved when compared to 1.5:1 for the ratio of *cis*- to *trans*-products for the ester substrates.

Chapter 7: Rhodium-Catalyzed Asymmetric Hydroboration on 1-Methyl-*N*-phenylcyclopent-3-enecarboxamide

As discussed in Chapter 6, the level of diastereoselectivity achieved is at best 8:1 for the ratio of *cis*- to *trans*-products with *N*-phenylcyclopent-3-enecarboxylate **79**. As we had theorized, the nature of the directing-group influences the ratio of *cis*- to *trans*-isomers; amides are better directing-groups than esters. There is potentially another way to control the *cis/trans*-diastereoselectivity by blocking the face opposite of the directing group. It was hypothesized that substrates with steric bulk (larger than hydrogen) at the α -position of the carbonyl could make two-point binding with the carbonyl relatively more favorable. This would increase the likelihood of achieving better diastereomeric ratios, *i.e.* blocking the opposite face of the directing-group would allow for tighter two-point binding to the carbonyl throughout the rhodium-catalyzed hydroboration, therefore increasing the *cis:trans* product ratio.

To test our hypothesis, 1-Methyl-*N*-phenylcyclopent-3-enecarboxamide **87** was synthesized and was hydroborated to give the *cis*- and *trans*-products, **88** and **89**, respectively (Scheme 7.1). The diastereoselectivity is increased compared to the corresponding unsubstituted amide **79**; the diastereomeric ratio obtained is 12:1 (entry 4, Table 7.1). From a screening of the typical group of ligands, the highest ee is obtained with the chiral ligand (BINOL)N(Me)Ph (82%, entry 5). This is the same ligand that gives the highest level of enantioselectivity for the unsubstituted amide **79** with PinBH. As seen previously, enantioswitching is observed when the TADDOL-derived

phosphoramidite (TADDOL)PN(Me)Ph is used. The extent of the switch is however somewhat lower with this substrate — 42% ee for the opposite enantiomer rather than 70% ee in the prior case (entry 6). Overall, the enantioselectivities are comparable to those obtained in the rhodium-catalyzed hydroboration of **79**. The *trans*-product **89** was also isolated from the reaction of **87**. It is found to be formed with only low levels of enantiomeric excess as might be expected for a *meso*-alkene with no directing group.



Scheme 7.1. Rhodium-catalyzed hydroboration of 1-methyl-*N*-phenylcyclopent-3-enecarboxamide.

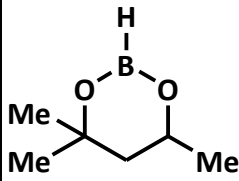
Table 7.1. The rhodium-catalyzed hydroboration of **87** using PinBH and the influence of a six ligand screening set on diastereo- and enantioselectivities.

Entry	Ligand	Total Yield (%)	<i>cis</i> : <i>trans</i> (%)	ee (% <i>cis</i>)	ee (% <i>trans</i>)
1	(TADDOL)POPh	72	65 : 7	52	28
2	<i>p</i> -Me(TADDOL)POPh	73	65 : 8	58	20
3	<i>t</i> Bu(TADDOL)POPh	73	65 : 8	74	42
4	<i>x</i> (TADDOL)POPh	64	59 : 5	65	28
5	(BINOL)PN(Me)Ph	77	70 : 7	82	6
6	(TADDOL)PN(Me)Ph	79	68 : 11	-42	34

Reaction conditions: 1 mol% Rh(nbd)₂BF₄, 2.1 mol% Ligand, 2 eq. PinBH, 40 °C, 24 h. Oxidation with NaOH and H₂O₂. Yield determined by crude ¹H NMR with mesitylene as an internal standard; enantioselectivities determined by HPLC analysis.

For the unsubstituted amide substrate **79**, TMDB increases the enantioselectivity in comparison to PinBH. TMDB was similarly screened with the α -methyl-substituted amide **87**. As anticipated, in each case, the enantioselectivity observed is higher than the corresponding reaction with PinBH. The lone exception is (BINOL)PN(Me)Ph for which the enantioselectivity remained nearly the same (Table 7.2). This is similar to the outcome with the rhodium-catalyzed hydroboration of the unsubstituted amide **79**. Enantioswitching is again absent in the TADDOL-derived phosphoramidites (entries 6 and 8). The highest ee achieved for the reaction of **87** was with (TADDOL)POPh (92%, entry 1). Recall, the reaction also proceeds with a high level of diastereoselectivity (*ca.* 12:1).

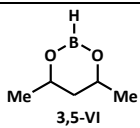
Table 7.2. The rhodium-catalyzed hydroboration of **87** using TMDB and the influence of a nine ligand screening set on diastereo- and enantioselectivities.

Entry	Ligand	Total Yield (%)	<i>cis</i> : <i>trans</i> (%)	ee (% <i>cis</i>)	Borane
1	(TADDOL)POPh	70	64 : 6	92	 <p style="text-align: center;">TMDB</p>
2	<i>p</i> -Me(TADDOL)POPh	46	38 : 8	90	
3	^t Bu(TADDOL)POPh	74	61 : 13	91	
4	<i>x</i> (TADDOL)POPh	66	57 : 9	90	
5	(BINOL)PN(Me)Ph	24	18 : 6	80	
6	(TADDOL)PN(Me)Ph	45	33 : 12	54	
7	(TADDOL)POBn	32	20 : 12	42	
8	(TADDOL)PN(Bn)Bn	16	9 : 7	20	
9	(BINOL)PN(Bn)Bn	17	11 : 6	32	

Reaction conditions: 1 mol% Rh(nbd)₂BF₄, 2.1 mol% Ligand, 2 eq. TMDB, 40 °C, 24 h. Oxidation with NaOH and H₂O₂. Yield determined by crude ¹H NMR with mesitylene as an internal standard; enantioselectivities determined by HPLC analysis.

As discovered previously in the unsubstituted amide case, altering the borane provides varying degrees of diastereo- and enantioselectivities. It is therefore beneficial to test different boranes with this particular substrate. Recall, borane 3,5-VI is structurally similar to TMDB, except it is missing one methyl group. Three ligands were screened against this substrate (Table 7.3). As predicted from the study of the unsubstituted substrate, the diastereoselectivity was much lower than with TMDB dropping from *ca.* 12:1 to 3:1, *i.e.* the same general trend occurs for Borane 3,5-VI. The enantioselectivity also suffered dramatically.

Table 7.3. The rhodium-catalyzed hydroboration of **87** using 3,5-VI and the influence of a three ligand screening set on diastereo- and enantioselectivities.

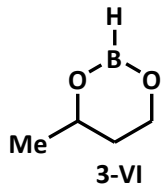
Entry	Ligand	Total Yield (%)	<i>cis</i> : <i>trans</i> (%)	ee (% <i>cis</i>)	Borane
1	<i>t</i> Bu(TADDOL)POPh	62	40 : 12	38	
2	<i>x</i> (TADDOL)POPh	72	56 : 16	57	
3	(TADDOL)PN(Me)Ph	44	35 : 9	26	

Reaction conditions: 1 mol% Rh(nbd)₂BF₄, 2.1 mol% Ligand, 2 eq. 3,5-VI, 40 °C, 24 h. Oxidation with NaOH and H₂O₂. Yield determined by crude ¹H NMR with mesitylene as an internal standard; enantioselectivities determined by HPLC analysis.

Empirical evidence suggests that the six-membered ring borane TMDB provides access to higher diastereo- and enantioselectivities. Recall, borane 3-VI is structurally similar to TMDB in that it does not have an internal plane of symmetry. It is not known if the asymmetry of these boranes is inherently favored by the rhodium-catalyzed asymmetric hydroboration reactions. Borane 3-VI lacks the overall steric bulk of TMDB and amide **87** was hypothesized to perform similarly to the unsubstituted amide. The

overall diastereoselectivities of the unsubstituted and α -methyl amides are consistent: 8:1 versus 7:1, respectively. It seems that the two extra methyl groups in TMDB are crucial in providing a high level of enantioselectivity from the results summarized in Table 7.4. The overall yields obtained with this borane are quite good, however, the diastereoselectivity is lower, about 7:1 compared to *ca.* 12:1 with TMDB and the ee's are modest. The best ee achieved is with (TADDOL)POPh (45%) with amide **87**; the highest ee achieved for the unsubstituted amide is 20% ee with (TADDOL)PN(Me)Ph.

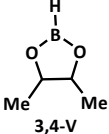
Table 7.4. The rhodium-catalyzed hydroboration of **87** using 3-V and the influence of a six ligand screening set on diastereo- and enantioselectivities.

Entry	Ligand	Total Yield (%)	<i>cis</i> : <i>trans</i> (%)	ee (% <i>cis</i>)	Borane
1	(TADDOL)POPh	75	66 : 9	45	
2	<i>p</i> -Me(TADDOL)POPh	64	58 : 8	Rac	
3	^t Bu(TADDOL)POPh	71	58 : 13	31	
4	<i>x</i> (TADDOL)POPh	72	63 : 9	32	
5	(BINOL)PN(Me)Ph	82	62 : 20	30	
6	(TADDOL)PN(Me)Ph	71	61 : 10	34	

Reaction conditions: 1 mol% Rh(nbd)₂BF₄, 2.1 mol% Ligand, 2 eq. 3-VI, 40 °C, 24 h. Oxidation with NaOH and H₂O₂. Yield determined by crude ¹H NMR with mesitylene as an internal standard; enantioselectivities determined by HPLC analysis.

The five-membered ring boranes were also explored. Borane 3,4-V is structurally similar to PinBH, *sans* two methyl groups. With this borane, the amide shows virtually no directing-effect; the *cis*- and *trans*-products are formed in roughly equal amounts (Table 7.5). After 24 h at 40 °C, a small amount of starting material remains. The enantioselectivities obtained are comparatively very low.

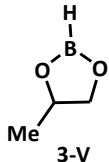
Table 7.5. The rhodium-catalyzed hydroboration of **87** using 3,4-V and the influence of a two ligand screening set on diastereo- and enantioselectivities.

Entry	Ligand	Total Yield (%)	<i>cis</i> : <i>trans</i> (%)	ee (% <i>cis</i>)	S.M. (%)	Borane
1	(TADDOL)POPh	62	33 : 29	34	11	
2	(TADDOL)PN(Me)Ph	43	20 : 23	25	18	

Reaction conditions: 1 mol% Rh(nbd)₂BF₄, 2.1 mol% Ligand, 2 eq. 3,4-V, 40 °C, 24 h. Oxidation with NaOH and H₂O₂. Yield determined by crude ¹H NMR with mesitylene as an internal standard; enantioselectivities determined by HPLC analysis. S.M. is remaining starting material.

Borane 3-V gives a ratio of *cis*- to *trans*-products of roughly 4:1 for the best ligand cases (entries 1 and 5, Table 7.6). However, the enantioselectivities are nearly racemic in all cases.

Table 7.6. The rhodium-catalyzed hydroboration of **87** using 3-V and the influence of a five ligand screening set on diastereo- and enantioselectivities.

Entry	Ligand	Total Yield (%)	<i>cis</i> : <i>trans</i> (%)	ee (% <i>cis</i>)	S.M. (%)	Borane
1	(TADDOL)POPh	50	40 : 10	18	20	
2	<i>p</i> -Me(TADDOL)POPh	45	34 : 11	18	25	
3	^t Bu(TADDOL)POPh	37	25 : 12	22	10	
4	<i>x</i> (TADDOL)POPh	25	20 : 5	16	10	
5	(TADDOL)PN(Me)Ph	51	40 : 11	18	5	

Reaction conditions: 1 mol% Rh(nbd)₂BF₄, 2.1 mol% Ligand, 2 eq. 3-V, 40 °C, 24 h. Oxidation with NaOH and H₂O₂. Yield determined by crude ¹H NMR with mesitylene as an internal standard; enantioselectivities determined by HPLC analysis. S.M. is remaining starting material.

CatBH has been known to provide a competent borane source in a variety of substrates, as stated previously. However, its use for the rhodium-catalyzed asymmetric hydroboration of α -methyl substituted amide **87** only gives a moderate yield (2 equiv. CatBH, Table 7.7). The highest ee observed is 35% when using (TADDOL)POPh (entry 1). Other work has shown that a larger excess of CatBH may be required for efficient transition-metal mediated hydroborations. Apparently, this is the result of the competing formation of diboronate compounds thus rendering the borane inactive.³⁴ Unfortunately, while the yield generally improves slightly, the diastereoselectivity and enantioselectivity remain very similar to when larger excess of CatBH is used (5 equiv. CatBH, Table 7.8).

Table 7.7. The rhodium-catalyzed hydroboration of **87** using CatBH (2 eq.) and the influence of a six ligand screening set on diastereo- and enantioselectivities.

Entry	Ligand	Total Yield (%)	<i>cis</i> : <i>trans</i> (%)	ee (% <i>cis</i>)
1	(TADDOL)POPh	78	60 : 18	35
2	<i>p</i> -Me(TADDOL)POPh	72	59 : 13	34
3	^t Bu(TADDOL)POPh	29	22 : 7	24
4	<i>x</i> (TADDOL)POPh	68	56 : 12	30
5	(BINOL)PN(Me)Ph	62	46 : 16	10
6	(TADDOL)PN(Me)Ph	55	45 : 10	17

Reaction conditions: 1 mol% Rh(nbd)₂BF₄, 2.1 mol% Ligand, 2 eq. CatBH, 40 °C, 24 h. Oxidation with NaOH and H₂O₂. Yield determined by crude ¹H NMR with mesitylene as an internal standard; enantioselectivities determined by HPLC analysis.

Table 7.8 The rhodium-catalyzed hydroboration of **87** using CatBH (5 eq.) and the influence of a six ligand screening set on diastereo- and enantioselectivities.

Entry	Ligand	Total Yield (%)	<i>cis</i> : <i>trans</i> (%)	ee (% <i>cis</i>)
1	(TADDOL)POPh	73	53 : 20	32
2	<i>p</i> -Me(TADDOL)POPh	87	64 : 23	28
3	^t Bu(TADDOL)POPh	90	65 : 25	26
4	<i>x</i> (TADDOL)POPh	74	55 : 19	32
5	(BINOL)PN(Me)Ph	81	60 : 21	10
6	(TADDOL)PN(Me)Ph	82	58 : 24	20

Reaction conditions: 1 mol% Rh(nbd)₂BF₄, 2.1 mol% Ligand, 5 eq. CatBH, 40 °C, 24 h. Oxidation with NaOH and H₂O₂. Yield determined by crude ¹H NMR with mesitylene as an internal standard; enantioselectivities determined by HPLC analysis.

When either PinBH or TMDB are used with iridium, rather than rhodium catalysts, the conversion to the product is very poor (Tables 7.9 and 7.10). In addition, isomerized alkene is also detected in the ¹H NMR of the crude product. The regioselectivity is poor with the catalyst systems examined. However, some promising levels of enantioselectivity are observed; the highest ee is attained with (TADDOL)PN(Me)Ph (50% ee). Further development is needed for this to be a practical method.

Table 7.9. The iridium-catalyzed hydroboration of **87** using PinBH and the influence of a six ligand screening set on diastereo- and enantioselectivities.

Entry	Ligand	Total Yield (%)	<i>cis</i> : <i>trans</i> (%)	ee (% <i>cis</i>)	S.M. (%)
1	(TADDOL)POPh	35	25 : 10	36	30
2	<i>p</i> -Me(TADDOL)POPh	5	5 : 0	Rac	70
3	^t Bu(TADDOL)POPh	7	7 : 0	Rac	70
4	<i>x</i> (TADDOL)POPh	9	9 : 0	Rac	30
5	(BINOL)PN(Me)Ph	10	10 : 0	Rac	75
6	(TADDOL)PN(Me)Ph	32	22 : 10	50	3

Reaction conditions: 1 mol% Ir(cod)₂BF₄, 2.1 mol% Ligand, 2 eq. PinBH, 40 °C, 24 h. Oxidation with NaOH and H₂O₂. Yield determined by crude ¹H NMR with mesitylene as an internal standard; enantioselectivities determined by HPLC analysis. S.M. is remaining starting material.

Table 7.10. The iridium-catalyzed hydroboration of **87** using TMDB and the influence of a six ligand screening set on diastereo- and enantioselectivities.

Entry	Ligand	Total Yield (%)	<i>cis</i> : <i>trans</i> (%)	ee (% <i>cis</i>)	S.M. (%)
1	(TADDOL)POPh	22	13 : 9	32	50
2	<i>p</i> -Me(TADDOL)POPh	22	12 : 10	32	70
3	^t Bu(TADDOL)POPh	31	19 : 12	32	65
4	<i>x</i> (TADDOL)POPh	21	13 : 8	30	50
5	(BINOL)PN(Me)Ph	17	11 : 6	30	46
6	(TADDOL)PN(Me)Ph	20	12 : 8	30	29

Reaction conditions: 1 mol% Ir(cod)₂BF₄, 2.1 mol% Ligand, 2 eq. TMDB, 40 °C, 24 h. Oxidation with NaOH and H₂O₂. Yield determined by crude ¹H NMR with mesitylene as an internal standard; enantioselectivities determined by HPLC analysis. S.M. is remaining starting material.

Using CatBH with the corresponding iridium catalysts gives very little conversion. This is a surprising result, since in the literature iridium-catalyzed hydroborations were shown to be an effective catalyst with CatBH.¹¹ Unfortunately, the conversion to the *cis*-

and *trans*-products is still very low (Table 7.11). A lot of starting material remains even after 24 h at 40 °C.

Table 7.11. The iridium-catalyzed hydroboration of **87** using CatBH (2 eq.) and the influence of a five ligand screening set on diastereo- and enantioselectivities.

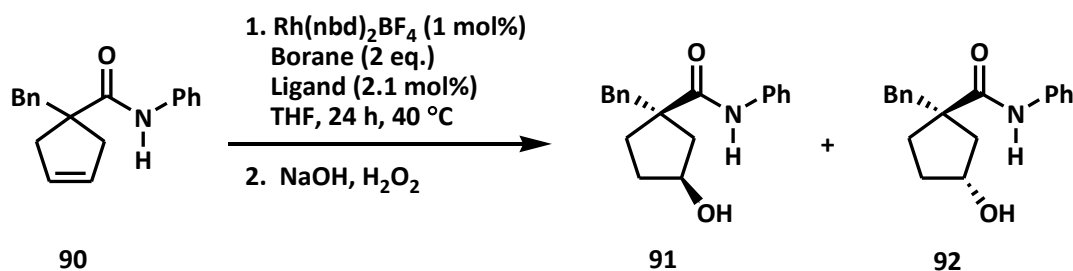
Entry	Ligand	Total Yield (%)	<i>cis</i> : <i>trans</i> (%)	ee (% <i>cis</i>)	S.M. (%)
1	(TADDOL)POPh	20	11 : 9	28	75
2	<i>p</i> -Me(TADDOL)POPh	39	22 : 17	24	60
3	^t Bu(TADDOL)POPh	40	22 : 18	25	60
4	<i>x</i> (TADDOL)POPh	40	25 : 15	30	60
5	(TADDOL)PN(Me)Ph	19	12 : 7	24	50

Reaction conditions: 1 mol% Ir(cod)₂BF₄, 2.1 mol% Ligand, 2 eq. CatBH, 40 °C, 24 h. Oxidation with NaOH and H₂O₂. Yield determined by crude ¹H NMR with mesitylene as an internal standard; enantioselectivities determined by HPLC analysis. S.M. is remaining starting material.

In summary, the iridium catalysts examined were less effective than the corresponding rhodium catalysts for the use of asymmetric desymmetrization of the prochiral cyclopentenyl amide substrates, both for the substituted and α -methyl derivatives. Rhodium provides much better turnover to the product on the same timescale at the same temperature (1 mol% catalyst, 40 °C, 24 h). In addition to the rhodium/iridium catalyst, the source of borane is also a very important factor. Even modest structural changes in the borane significantly affect diastereo- and enantioselectivity. The highest level of enantioselectivity is achieved when TMDB is used as the borane with the ligand (TADDOL)POPh to give 92% ee (70% total yield; 11:1 *cis:trans*-products). An enantioswitch still occurs with (TADDOL)POPh and PinBH, yet to a lesser degree than with the unsubstituted amide (-42% from -70% ee).

Chapter 8: Rhodium-Catalyzed Asymmetric Hydroboration on 1-Benzyl-*N*-phenylcyclopent-3-enecarboxamide

By increasing the sterics of the α -substituent from hydrogen to a methyl group, the ratio of *cis*- to *trans*-products increased from 8:1 to 12:1, respectively. It was our expectation that increasing the steric bulk of the α -substituent further would enhance the diastereoselectivity. Therefore, the 1-benzyl-*N*-phenylcyclopent-3-enecarboxamide **90** was prepared *via* alkylation of **46** with benzyl bromide and screened as above in the rhodium-catalyzed asymmetric hydroborations (Scheme 8.1).



Scheme 8.1. The rhodium-catalyzed hydroboration of 1-benzyl-*N*-phenylcyclopent-3-enecarboxamide.

The conversion and yield of products **91** and **92** are comparable to those obtained with the related substrates described above. The *cis* to *trans* ratio did increase but only marginally, 13:1 as opposed to 12:1 from the α -methyl substituted derivative. The best case for enantioselectivity is with the TADDOL-derived ligand (TADDOL)POPh, which gives an ee of 60% (entry 1, Table 8.1). With the unsubstituted and α -methyl substituted amides, this ligand does not provide the highest level of enantioselectivity (60% and 52% ee, respectively). It is also intriguing to note that a slight enantioswitch still occurs with

the TADDOL-derived phosphoramidite (TADDOL)PN(Me)Ph (−20%, entry 6) with PinBH. The enantioswitch occurs in a greater degree with this ligand on the unsubstituted and α -methyl substituted amides (−70% and −42% ee, respectively).

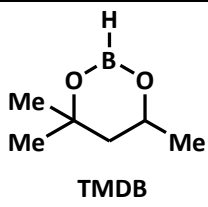
Table 8.1. The rhodium-catalyzed hydroboration of **90** using PinBH and the influence of a six ligand screening set on diastereo- and enantioselectivities.

Entry	Ligand	Total Yield (%)	<i>cis</i> : <i>trans</i> (%)	ee (% <i>cis</i>)
1	(TADDOL)POPh	81	75 : 6	60
2	<i>p</i> -Me(TADDOL)POPh	70	65 : 5	37
3	^t Bu(TADDOL)POPh	61	54 : 7	14
4	<i>x</i> (TADDOL)POPh	54	50 : 4	50
5	(BINOL)PN(Me)Ph	70	64 : 6	46
6	(TADDOL)PN(Me)Ph	65	60 : 5	−20

Reaction conditions: 1 mol% Rh(nbd)₂BF₄, 2.1 mol% Ligand, 2 eq. PinBH, 40 °C, 24 h. Oxidation with NaOH and H₂O₂. Yield determined by crude ¹H NMR with mesitylene as an internal standard; enantioselectivities determined by HPLC analysis.

It was expected that using TMDB as the borane would provide higher enantioselectivities than with PinBH based on prior observations described above. In fact, it is found that when TMDB is used with the α -benzyl substituted derivative, the same trend occurs. The enantioselectivity increases in each case; (TADDOL)POPh gives the highest enantiomeric excess (80%) among the group of ligands tested (Table 8.2). It is also again noteworthy that no enantioswitching is observed using (TADDOL)PN(Me)Ph. The best *cis* to *trans* ratio is obtained with (BINOL)N(Me)Ph as the ligand and provides a 20:1 ratio of *cis*- to *trans*-products, respectively (entry 5).

Table 8.2. The rhodium-catalyzed hydroboration of **90** using TMDB and the influence of a six ligand screening set on diastereo- and enantioselectivities.

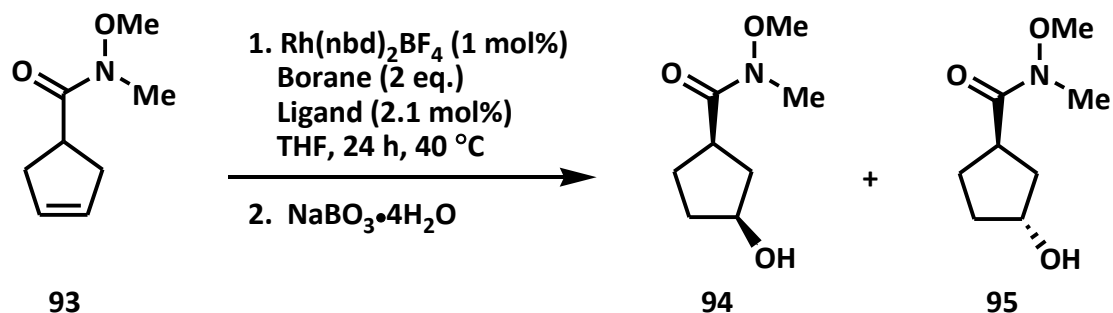
Entry	Ligand	Total Yield (%)	<i>cis</i> : <i>trans</i> (%)	ee (% <i>cis</i>)	Borane
1	(TADDOL)POPh	41	31 : 10	80	 <p style="text-align: center;">TMDB</p>
2	<i>p</i> -Me(TADDOL)POPh	61	55 : 6	72	
3	<i>t</i> Bu(TADDOL)POPh	53	50 : 3	66	
4	<i>x</i> (TADDOL)POPh	73	69 : 4	60	
5	(BINOL)PN(Me)Ph	64	61 : 3	74	
6	(TADDOL)PN(Me)Ph	49	42 : 7	30	

Reaction conditions: 1 mol% Rh(nbd)₂BF₄, 2.1 mol% Ligand, 2 eq. TMDB, 40 °C, 24 h. Oxidation with NaOH and H₂O₂. Yield determined by crude ¹H NMR with mesitylene as an internal standard; enantioselectivities determined by HPLC analysis.

The *cis:trans* ratio increases as the α -substitution increases: 8:1, 12:1, and 20:1 (unsubstituted amide, α -methyl substituted amide, α -benzyl substituted amide, respectively). The highest ee achieved is with the α -methyl substituted amide (92% ee with (TADDOL)POPh and TMDB)). An enantioswitch occurs only when PinBH is used as the borane with (TADDOL)PN(Me)Ph (-70%, -42%, and -20% ee for the unsubstituted amide, α -methyl substituted amide, α -benzyl substituted amide, respectively); as the size of the α -substituent increases, the level of enantioswitching decreases. It was found that for the rhodium-catalyzed hydroboration of these prochiral cyclopentenyl amides it is not only important to screen various BINOL- and TADDOL-derived ligands, but boranes also dramatically alter the outcome of both enantio- and diastereoselectivities.

Chapter 9: Rhodium-Catalyzed Asymmetric Hydroboration on Weinreb Amides

Weinreb amides are useful synthetic intermediates for organolithium and organomagnesium reactions. In addition to serving as an acylating agent, Weinreb amides act as a powerful analogue to aldehydes.³⁵ For these reasons, a series of Weinreb amides were synthesized, including *N*-methoxy-*N*-methylcyclopent-3-enecarboxamide **93**. This Weinreb amide was screened for rhodium-catalyzed asymmetric hydroboration to form *cis*- and *trans*-products **94** and **95**, respectively (Scheme 9.1). Unfortunately, the enantioselectivities were not examined as an efficient separation protocol was not found *via* HPLC. The highest level of diastereoselectivity is found to be 15:1 with (TADDOL)PN(Me)Ph as the ligand (entry 6, Table 9.1).



Scheme 9.1. Rhodium-catalyzed asymmetric hydroboration of *N*-methoxy-*N*-methylcyclopent-3-enecarboxamide.

Table 9.1. The rhodium-catalyzed hydroboration of **93** using PinBH and the influence of a six ligand screening set on diastereoselectivities.

Entry	Ligand	Total Yield (%)	<i>cis</i> : <i>trans</i> (%)
1	(TADDOL)POPh	70	60 : 10
2	<i>p</i> -Me(TADDOL)POPh	53	33 : 20
3	^t Bu(TADDOL)POPh	59	52 : 7
4	<i>x</i> (TADDOL)POPh	84	70 : 14
5	(BINOL)PN(Me)Ph	95	88 : 7
6	(TADDOL)PN(Me)Ph	97	91 : 6

Reaction conditions: 1 mol% Rh(nbd)₂BF₄, 2.1 mol% Ligand, 2 eq. PinBH, 40 °C, 24 h. Oxidation with NaBO₃·4H₂O. Yield determined by crude ¹H NMR with mesitylene as an internal standard.

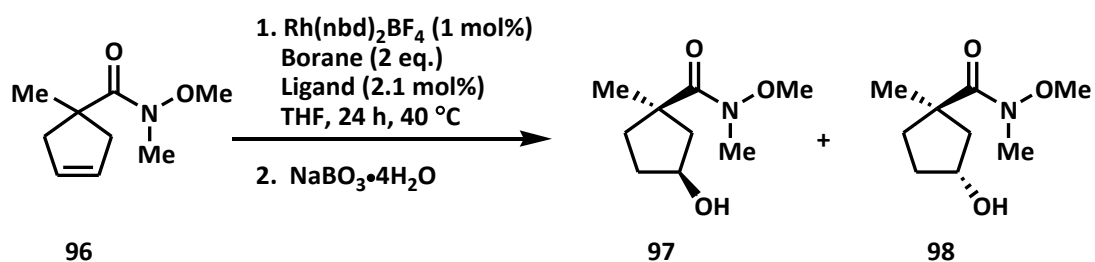
When TMDB was added to Weinreb **93**, *x*(TADDOL)POPh and (BINOL)PN(Me)Ph provide the highest levels of diastereoselectivities (entries 4 and 5, Table 9.2). However, the reactivity is variable and in two cases both starting material and isomerized alkene are detected by ¹H NMR analysis of the crude reaction mixture (entries 2 and 6).

Table 9.2. The rhodium-catalyzed hydroboration of **93** using TMDB and the influence of a six ligand screening set on diastereoselectivities.

Entry	Ligand	Total Yield (%)	<i>cis</i> : <i>trans</i> (%)	S.M. (%)	Isomerized Alkene (%)
1	(TADDOL)POPh	78	63 : 15	-	-
2	<i>p</i> -Me(TADDOL)POPh	18	13 : 5	29	15
3	^t Bu(TADDOL)POPh	49	39 : 10	-	-
4	<i>x</i> (TADDOL)POPh	93	81 : 12	-	-
5	(BINOL)PN(Me)Ph	55	48 : 7	-	-
6	(TADDOL)PN(Me)Ph	30	16 : 14	25	38

Reaction conditions: 1 mol% Rh(nbd)₂BF₄, 2.1 mol% Ligand, 2 eq. TMDB, 40 °C, 24 h. Oxidation with NaBO₃·4H₂O. Yield determined by crude ¹H NMR with mesitylene as an internal standard. S.M. is remaining starting material.

As discussed above, it was hypothesized that increasing the size of the α -substituent would also increase the level of diastereoselectivity in the Weinreb amide series of prochiral cyclopentenyl substrates. *N*-Methoxy-*N*,1-dimethylcyclopent-3-enecarboxamide **96** was synthesized and hydroborated to form *cis*- and *trans*-products **97** and **98**, respectively, after oxidative work-up (Scheme 9.2). Using PinBH for the borane, **96** reacts with only a modest level of diastereoselectivity. The formation of a small amount of isomerized alkene is detected as well as varying amounts of starting material remain (Table 9.3). The *cis* to *trans* ratio is 4:1 (entries 1, 3–4) at best.



Scheme 9.2. Rhodium-catalyzed asymmetric hydroboration of *N*-methoxy-*N*,1 - dimethylcyclopent-3-enecarboxamide.

Table 9.3. The rhodium-catalyzed hydroboration of **96** using PinBH and the influence of a six ligand screening set on diastereoselectivities.

Entry	Ligand	Total Yield (%)	<i>cis</i> : <i>trans</i> (%)	Remaining S.M. (%)	Isomerized Alkene (%)
1	(TADDOL)POPh	42	33 : 9	4	4
2	<i>p</i> -Me(TADDOL)POPh	14	6 : 8	79	6
3	^t Bu(TADDOL)POPh	40	32 : 8	2	3
4	<i>x</i> (TADDOL)POPh	44	35 : 9	10	7
5	(BINOL)PN(Me)Ph	29	22 : 7	17	8
6	(TADDOL)PN(Me)Ph	14	8 : 6	67	4

Reaction conditions: 1 mol% Rh(nbd)₂BF₄, 2.1 mol% Ligand, 2 eq. PinBH, 40 °C, 24 h. Oxidation with NaBO₃·4H₂O. Yield determined by crude ¹H NMR with mesitylene as an internal standard. S.M. is remaining starting material.

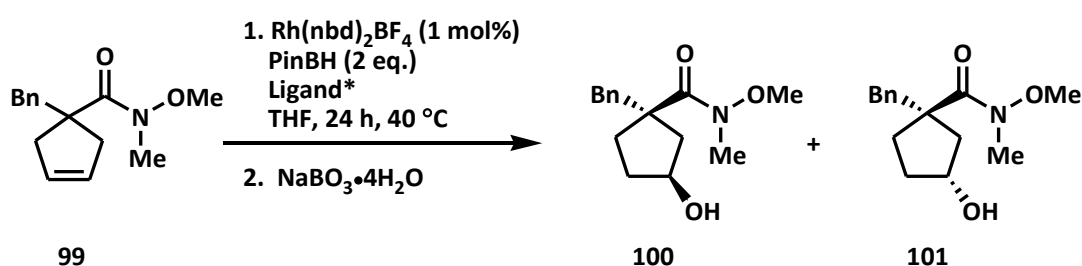
When TMDB is used as the borane source, the conversion to product is lower than with PinBH. With the *p*-Me(TADDOL)POPh ligand, only starting material is recovered (entry 2, Table 9.4).

Table 9.4. The rhodium-catalyzed hydroboration of **96** using TMDB and the influence of a six ligand screening set on diastereoselectivities.

Entry	Ligand	Total Yield (%)	<i>cis</i> : <i>trans</i> (%)	Remaining S.M. (%)	Isomerized Alkene (%)
1	(TADDOL)POPh	32	17 : 15	48	14
2	<i>p</i> -Me(TADDOL)POPh	-	-	100	-
3	^t Bu(TADDOL)POPh	20	12 : 8	45	16
4	<i>x</i> (TADDOL)POPh	28	14 : 4	41	15
5	(BINOL)PN(Me)Ph	21	21 : 0	60	10
6	(TADDOL)PN(Me)Ph	9	9 : 0	31	16

Reaction conditions: 1 mol% Rh(nbd)₂BF₄, 2.1 mol% Ligand, 2 eq. TMDB, 40 °C, 24 h. Oxidation with NaBO₃·4H₂O. Yield determined by crude ¹H NMR with mesitylene as an internal standard. S.M. is remaining starting material.

1-Benzyl-*N*-methoxy-*N*-methylcyclopent-3-enecarboxamide **99** undergoes rhodium-catalyzed asymmetric hydroboration to give the *cis*- and *trans*-products **100** and **101**, respectively (Scheme 9.3). Using PinBH, the diastereomeric ratio is on 3:1 in one instance (entry 5, Table 9.5) and 2:1 in all others (entries 1–4). When TMDB is used under the same conditions, the conversion is low (Table 9.6).



Scheme 9.3. Rhodium-catalyzed asymmetric hydroboration of 1-benzyl-*N*-methoxy-*N*-methylcyclopent-3-enecarboxamide.

Table 9.5. The rhodium-catalyzed hydroboration of **99** using PinBH and the influence of a six ligand screening set on diastereoselectivities.

Entry	Ligand	Total Yield (%)	<i>cis</i> : <i>trans</i> (%)	Remaining S.M. (%)
1	(TADDOL)POPh	54	37 : 17	-
2	^t Bu(TADDOL)POPh	48	33 : 15	-
3	<i>x</i> (TADDOL)POPh	51	36 : 15	11
4	(BINOL)PN(Me)Ph	70	45 : 25	-
5	(TADDOL)PN(Me)Ph	42	32 : 10	10

Reaction conditions: 1 mol% Rh(nbd)₂BF₄, 2.1 mol% Ligand, 2 eq. PinBH, 40 °C, 24 h. Oxidation with NaBO₃·4H₂O. Yield determined by crude ¹H NMR with mesitylene as an internal standard. S.M. is remaining starting material.

Table 9.6. The rhodium-catalyzed hydroboration of **99** using TMDB and the influence of a six ligand screening set on diastereoselectivities.

Entry	Ligand	Total Yield (%)	<i>cis</i> : <i>trans</i> (%)	Remaining S.M. (%)	Isomerized Alkene (%)
1	(TADDOL)POPh	7	7 : 0	14	27
2	^t Bu(TADDOL)POPh	14	14 : 0	16	27
3	<i>x</i> (TADDOL)POPh	6	6 : 0	13	27
4	(BINOL)PN(Me)Ph	10	10 : 0	37	22
5	(TADDOL)PN(Me)Ph	7	7 : 0	54	11

Reaction conditions: 1 mol% Rh(nbd)₂BF₄, 2.1 mol% Ligand, 2 eq. TMDB, 40 °C, 24 h. Oxidation with NaBO₃·4H₂O. Yield determined by crude ¹H NMR with mesitylene as an internal standard. S.M. is remaining starting material.

Initial results for the unsubstituted Weinreb amide were promising, as the diastereomeric ratio with (TADDOL)PN(Me)Ph and PinBH is 15:1. However, further optimization of both reaction conditions and HPLC separations are necessary. Specifically, optimized HPLC separation conditions for the Weinreb amide series are necessary to determine if these substrates are beneficial for future use. Also, optimization of the hydroboration conditions (solvent, temperature, time, catalyst, etc.) would be constructive to see if any of these changes would provide improved results.

Chapter 10: Summary for the Rhodium-Catalyzed Hydroboration of Prochiral Cyclopentenyl Substrates with Various Catalysts, Ligands and Boranes

Ester and amide prochiral cyclopentenyl substrates were tested in rhodium-catalyzed asymmetric hydroboration resulting in desymmetrized γ -hydroxy products. An assortment of ligands, boranes and catalyst systems were analyzed. It was found that small changes in these conditions allow for various outcomes in both diastereo- and enantioselectivities and therefore a combinatorial approach was performed.

The topography of chiral ligands can be modified by changing the scaffold slightly. Due to this, drastic differences in results are achieved from TADDOL- and BINOL-derived monophosphites and phosphoramidites. Modifying the borane also alters the outcome of the reaction.

The ester moiety does not provide a strong directing-effect in the case of the prochiral cyclopentenyl substrates. This is determined by investigating the ratio of the diastereomers. The highest level of *cis*- to *trans*-products was only 1.5:1 in the cases of benzyl- and phenyl cyclopent-3-enecarboxylate. The enantioselectivities were also very poor when the directing-group is an ester moiety (Table 10.1).

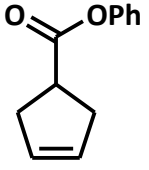
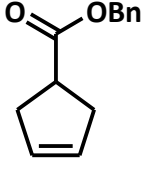
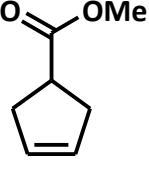
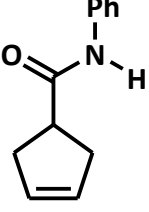
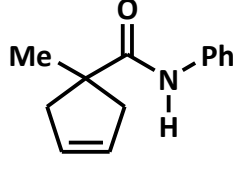
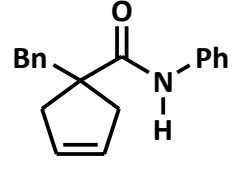
Because the ester group does not provide for an effective directing-effect, the amide moiety was expected to provide better results due to stronger two-point binding to the rhodium catalyst. Three different substituted amides were screened with BINOL- and

TADDOL-derived monophosphite and phosphoramidite ligands with a variety of catalyst systems and borane sources.

The α -unsubstituted amide is shown to provide enantioselectivity in the *cis*-product from -70 to 84% ee with PinBH ((TADDOL)PN(Me)Ph and (BINOL)PN(Me)Ph, respectively). When TMDB is used with *x*(TADDOL)POPh, a greater ee is achieved (90%). Enantioswitching only occurs when PinBH is used and does not occur with any of the other synthesized boranes. A combination of CatBH with both iridium and rhodium catalysts were inefficient in catalyzing the transition-metal catalyzed hydroboration reactions with the unsubstituted amide.

To achieve higher diastereoselectivities of *cis*- to *trans*-products, it was necessary to block one face of the molecule by synthesizing two different α -substituted amides. This is sufficient in increasing the ratio from the α -unsubstituted amide to the α -methyl substituted amide from 8:1 to 12:1, respectively. The most successful enantioselectivity achieved with the α -methyl substituted *N*-phenyl amide was obtained with TMDB and (TADDOL)POPh providing 92% ee. When the α -substitution is modified to a benzyl group, the diastereomeric ratio improves to 20:1 in the best case, but generally 13:1. The enantioselectivities obtained with this substrate are moderate; 80% ee is achieved with (TADDOL)POPh and TMDB in the best case.

Table 10.1. A summary of the best results for rhodium-catalyzed hydroboration with various substrates, boranes, and ligands.

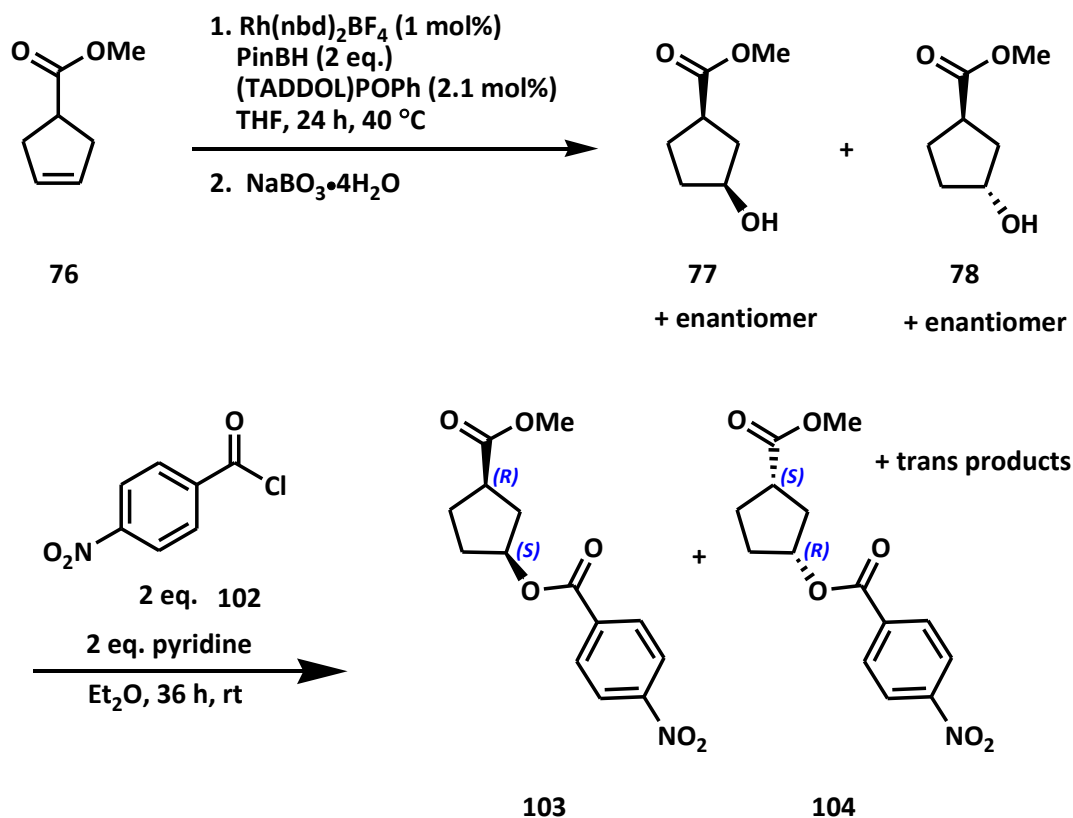
Substrate	Borane	Ligand	<i>cis:trans</i> (dr)	ee (%)
	PinBH	(TADDOL)POPh	2:1	30
	PinBH	(TADDOL)PN(Me)Ph	1:1	48
	PinBH	(TADDOL)POPh	2:1	30
	PinBH	(TADDOL)PN(Me)Ph	1:1	48
	PinBH	(TADDOL)POPh	1:1	22
	PinBH	(BINOL)PN(Me)Ph	8:1	84
	PinBH	(TADDOL)PN(Me)Ph	4:1	-70
	TMDB	α (TADDOL)POPh	5:1	90
	TMDB	(TADDOL)PN(Me)Ph	3:1	44
	PinBH	α (TADDOL)POPh	12:1	65
	PinBH	(BINOL)PN(Me)Ph	10:1	82
	PinBH	(TADDOL)PN(Me)Ph	6:1	-42
	TMDB	(TADDOL)POPh	11:1	92
	TMDB	(TADDOL)PN(Me)Ph	3:1	54
	PinBH	(TADDOL)POPh	13:1	60
	PinBH	(TADDOL)PN(Me)Ph	12:1	-20
	TMDB	(TADDOL)POPh	3:1	80
	TMDB	(BINOL)PN(Me)Ph	20:1	74
	TMDB	(TADDOL)PN(Me)Ph	6:1	30

An enantioswitch occurs when PinBH is used on all three amide substrates. However, this does not occur when TMDB is used as the source of borane. In all cases, TMDB provides higher levels of enantioselectivities along with varied diastereoselectivities. It is not understood why the enantioswitch only occurs with PinBH with the TADDOL-derived phosphoramidites, but does not happen when other structurally similar boranes are exploited. In addition, further optimization of the Weinreb amide series should be studied, as these substrates are beneficial synthetic intermediates.

Chapter 11: Determination of the Absolute Configuration of

3-Hydroxy-*N*-phenylcyclopentanecarboxamide

It was, of course, necessary to establish the absolute configuration of the major *cis*-product formed with catalytic asymmetric desymmetrization. The rhodium-catalyzed asymmetric hydroboration of methyl ester **76** provides a mixture of the *cis*- and *trans*-products **77** and **78**, respectively, after oxidation (Scheme 11.1). The mixture is treated with 4-nitrobenzoyl chloride **102** to give the corresponding mixture of diesters **103** and **104**, each partially enriched in one enantiomer.



Scheme 11.1. Determination of the absolute configuration of 3-Hydroxy-*N*-phenylcyclopentanecarboxamide.

Conditions for separating the four diesters (**99** and **100** and the trans products) via chiral HPLC have been reported in the literature (Chiralpak AD, 98:2 hexane:ethanol, 0.96 mL/min).³⁶ The retention times of the products are as follows: 25 min for (1*S*,3*R*)-*cis*-isomer, 29 min for (1*R*,3*S*)-*cis*-isomer, 37 min for (1*R*,3*R*)-*trans*-isomer, and 50 min for (1*S*,3*S*)-*trans*-isomer. The HPLC trace shown below is that obtained for the four products with retention times at 42, 44, 55, and 64 minutes (Figure 11.1). Shigematsu *et al.* use the Chiralpak AD column, which was also used for this particular separation. Therefore it can be assumed that the order of the products is the same. The authors confirm the absolute configurations of the products by comparing the retention times in HPLC to the authentic samples derived from known 3-oxocyclopentanecarboxylic acid.³³

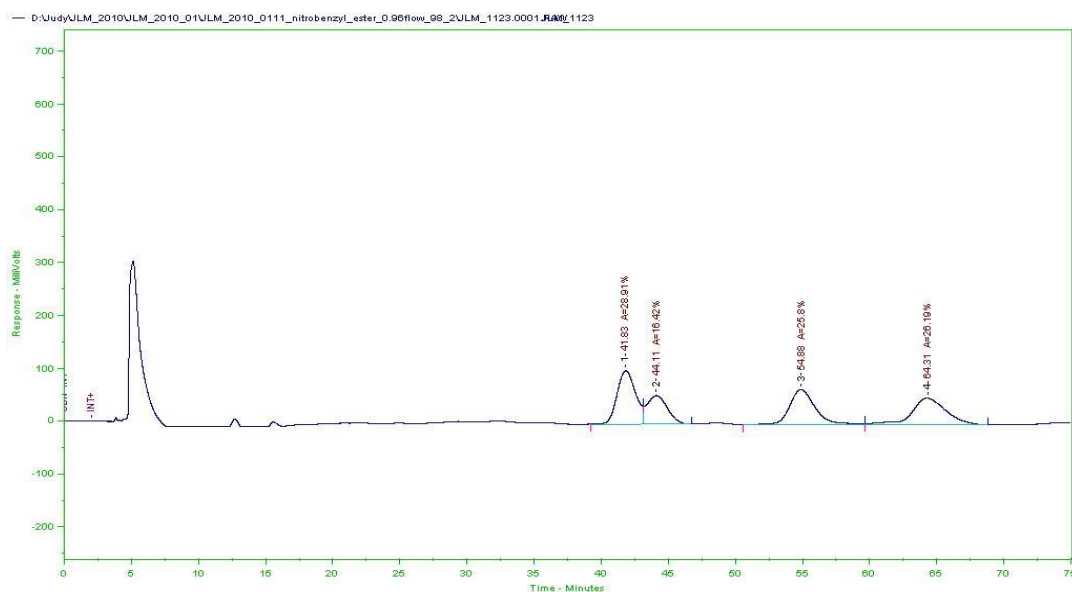
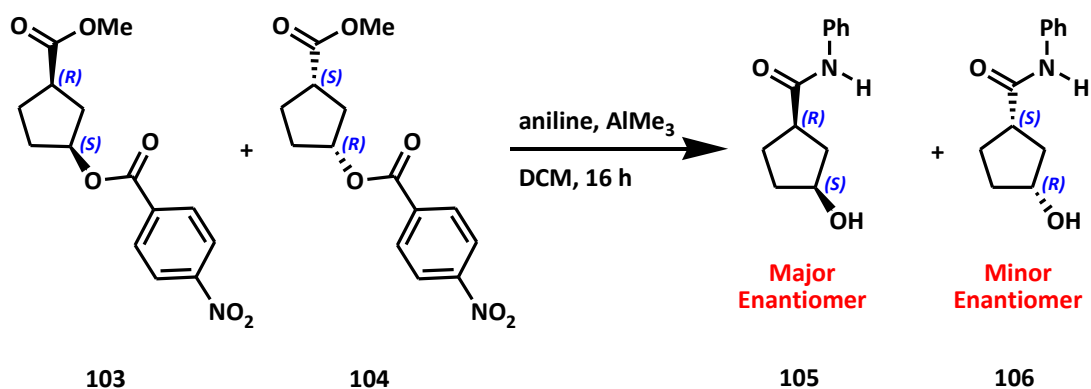


Figure 11.1. HPLC trace of the four possible ester products: (1*S*,3*R*)-*cis*-isomer, (1*R*,3*S*)-*cis*-isomer, (1*R*,3*R*)-*trans*-isomer, and (1*S*,3*S*)-*trans*-isomer.

Having assigned the stereochemistry of diesters **103** and **104**, they are easily converted to the corresponding *N*-phenylamides **105** and **106** using trimethylaluminum and aniline (Scheme 11.2). The *cis*- and *trans*- products are separated *via* column chromatography on silica (60:40 hexanes: ethyl acetate).



Scheme 11.2. The major enantiomer obtained for the rhodium-catalyzed hydroboration is the (1*R*,3*S*)-*cis*-isomer.

First, a sample amide of the *cis*-products was injected for reference. This was followed by the amide that was directly synthesized from diesters **103** and **104**. Lastly, a co-injection of the two samples was done, as shown below in Figure 11.2. In this way, it is concluded that the major enantiomer (of the *cis*-diastereomer) formed in the rhodium-catalyzed asymmetric hydroboration using (TADDOL)POPh with PinBH is of the (1*R*,3*S*)-3-hydroxy-*N*-phenylcyclopentanecarboxamide stereochemistry. Those ligands that exhibit enantioswitching give the (1*S*,3*R*) absolute stereochemistry. It is clear that the *cis*-diesters follow similar retention times than that of the amides, *i.e.*, the (1*R*,3*S*)-*cis*-isomer is followed by the (1*S*,3*R*)-*cis*-isomer in both cases.

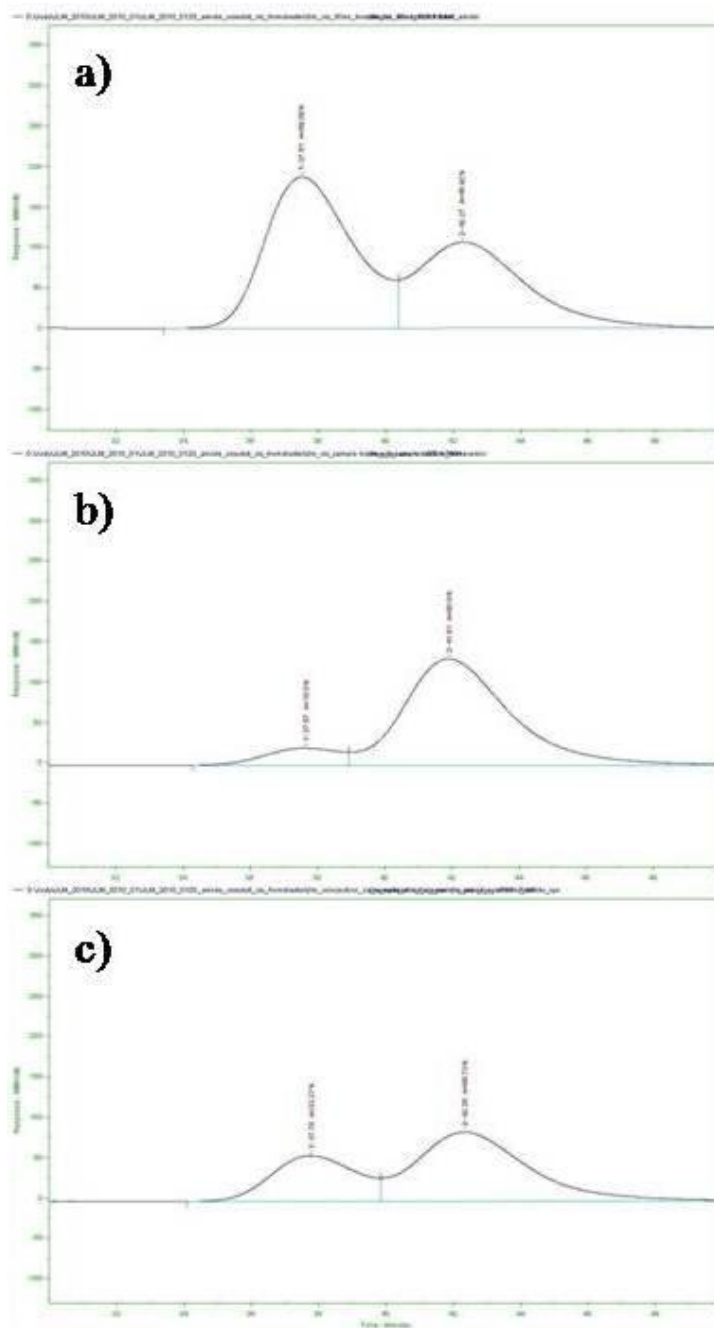
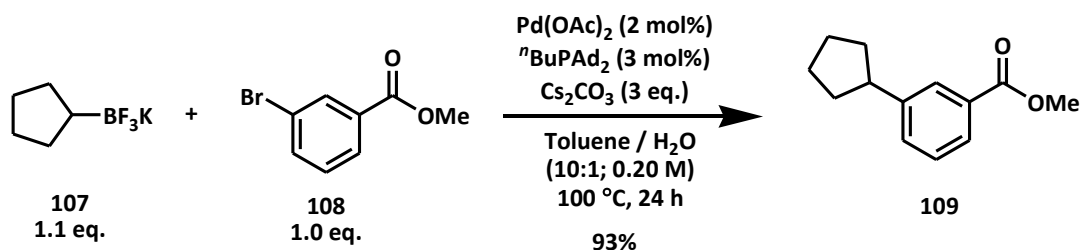


Figure 11.2. HPLC traces of: a) amide derived from diester b) sample amide and a c) co-injection of the two.

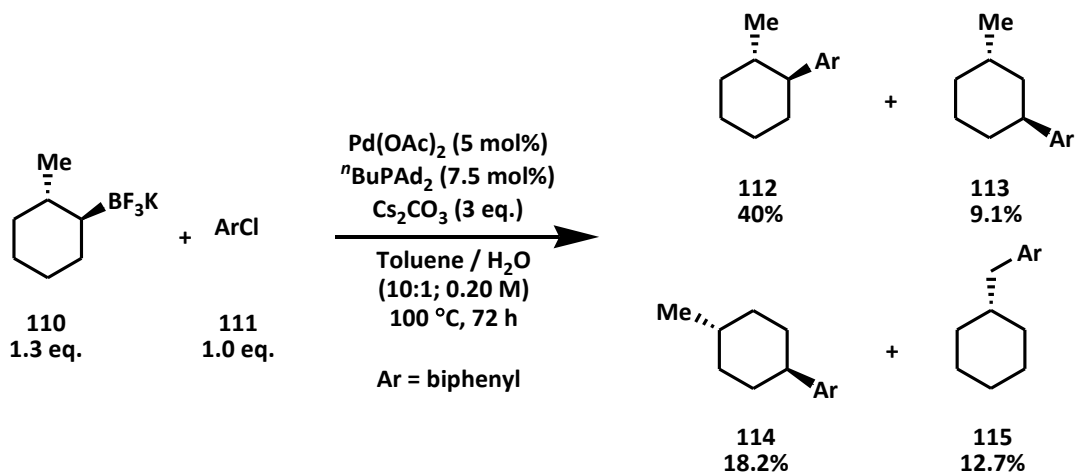
Chapter 12: Conversion of *N*-Phenylcyclopent-3-enecarboxamide to its Trifluoroborate salt

The enantiopure organoboronates discussed in the previous chapters have the potential to be functionalized into their corresponding trifluoroborate salts, which are employed in Suzuki cross-coupling reactions.^{37,38} For example, potassium cyclopentyltrifluoroborate **107** undergoes Suzuki cross-coupling with methyl 3-bromobenzoate **108** producing the cross-coupled product **109** in 93% yield (Scheme 12.1).



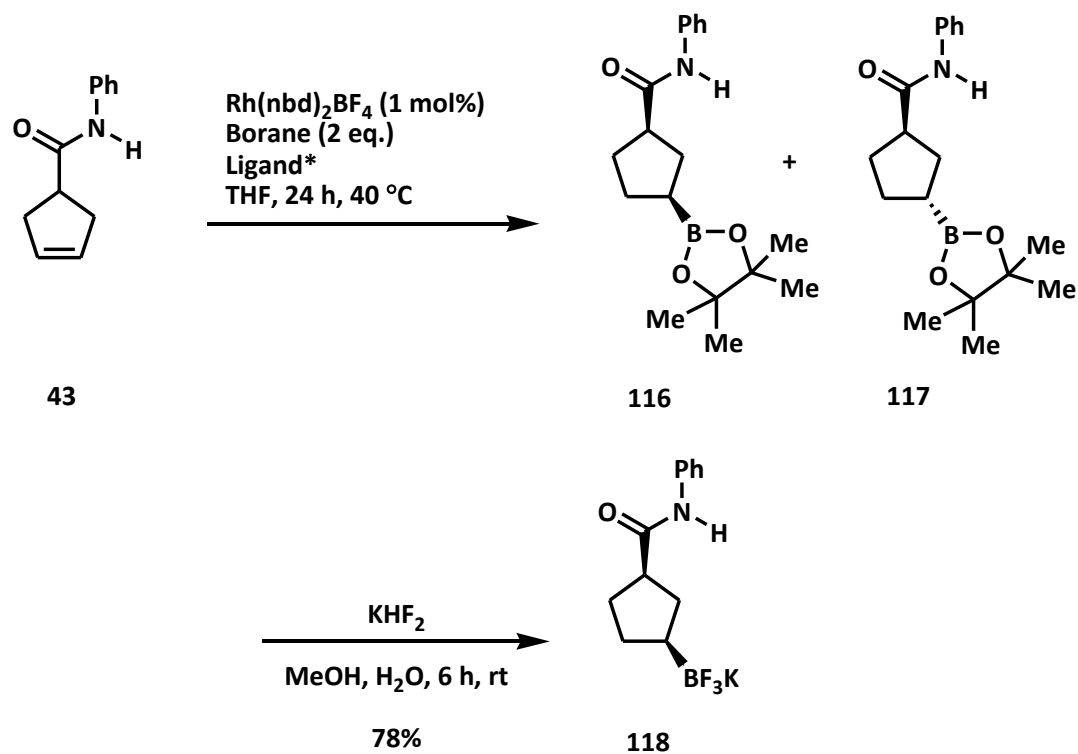
Scheme 12.1. Suzuki cross-coupling of an aryl halide with a potassium cyclopentyltrifluoroborate salt.³⁷

Under highly optimized conditions, cross-couplings of a six-membered disubstituted trifluoroborate salts have been achieved (Scheme 12.2).³⁷ However, β -hydride elimination / migration affects both regio- and stereocontrol in this reaction which results in various substituted products **112–115**.



Scheme 12.2. Suzuki cross-coupling of a six-membered disubstituted trifluoroborate salt.³⁷

This suggests that the chiral organoboron intermediates produced *via* catalytic asymmetric hydroboration might be useful partners in palladium-catalyzed cross-coupling reactions. The *cis*-organoboronate ester **116** is easily separated from the *trans*-products **117** (Scheme 12.3) using column chromatography on silica (70:30 hexanes:ethyl acetate). The substrate organoboronate ester can be treated with KHF_2 to generate its corresponding trifluoroborate salt **118**. This substrate has the potential for Suzuki cross-coupling which provides an opportunity for new C–C bonds. An attractive feature of further functionalizations is that these reactions occur with retention of stereochemistry.



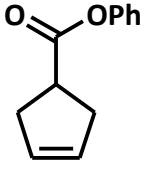
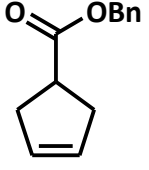
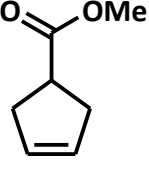
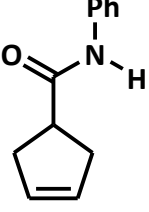
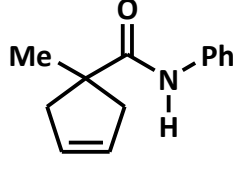
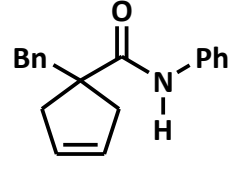
Scheme 12.3. Conversion of *N*-phenylcyclopent-3-enecarboxamide to its trifluoroborate salt.

Chapter 13: Conclusions

The rhodium-catalyzed asymmetric hydroboration of a variety of esters and amides were analyzed with various ligands, boranes and catalyst systems. It is necessary to use a combinatorial approach on this chemistry, because small changes in the system can provide varying outcomes. The topography of chiral ligands can be modified by changing the scaffold only slightly. Due to this, drastic differences in results can be achieved from using an assortment of TADDOL- and BINOL-derived monophosphites and phosphoramidites. In addition to catalyst/ligand systems, modifying the source of borane also alters the results. Screening structurally-similar boranes in this study has shown that not only the ratio of diastereomers can fluctuate, but also enantioselectivities. It is somewhat unpredictable to foresee the outcome of various boranes without empirical studies.

The ester moiety does not provide a strong directing-effect in the case of the prochiral cyclopentenyl substrates. This is determined by investigating the diastereomeric ratio; the highest level of *cis*- to *trans*-products was only 2:1 in the best case. The phenyl- and benzyl cyclopent-3-enecarboxylate substrates provide identical results where the highest diastereo- and enantioselectivities are achieved (2:1 *cis:trans* ratio, 30% ee and 1:1 *cis:trans* ratio, 48% ee with (TADDOL)POPh and (TADDOL)PN(Me)Ph, respectively; Table 13.1); both are poor.

Table 13.1. A summary of the best results for rhodium-catalyzed hydroboration with various substrates, boranes, and ligands.

Substrate	Borane	Ligand	<i>cis:trans</i> (dr)	ee (%)
	PinBH	(TADDOL)POPh	2:1	30
	PinBH	(TADDOL)PN(Me)Ph	1:1	48
	PinBH	(TADDOL)POPh	2:1	30
	PinBH	(TADDOL)PN(Me)Ph	1:1	48
	PinBH	(TADDOL)POPh	1:1	22
	PinBH	(BINOL)PN(Me)Ph	8:1	84
	PinBH	(TADDOL)PN(Me)Ph	4:1	-70
	TMDB	α (TADDOL)POPh	5:1	90
	TMDB	(TADDOL)PN(Me)Ph	3:1	44
	PinBH	α (TADDOL)POPh	12:1	65
	PinBH	(BINOL)PN(Me)Ph	10:1	82
	PinBH	(TADDOL)PN(Me)Ph	6:1	-42
	TMDB	(TADDOL)POPh	11:1	92
	TMDB	(TADDOL)PN(Me)Ph	3:1	54
	PinBH	(TADDOL)POPh	13:1	60
	PinBH	(TADDOL)PN(Me)Ph	12:1	-20
	TMDB	(TADDOL)POPh	3:1	80
	TMDB	(BINOL)PN(Me)Ph	20:1	74
	TMDB	(TADDOL)PN(Me)Ph	6:1	30

The low diastereoselectivity for the esters tells us that the ester moiety does not provide an effective directing-group to allow for two-point binding to the rhodium center. The amide moiety was hypothesized to provide better results due to stronger two-point binding to the rhodium catalyst. The diastereoselectivity increased from 2:1 to 8:1 for the ester and amide analogues, respectively. These results prove our hypothesis that the amide would serve as a better directing-group than an ester.

Three different substituted amides were screened with BINOL- and TADDOL-derived monophosphite and phosphoramidite ligands with a variety of catalyst systems and borane sources. The unsubstituted amide is shown to provide enantioselectivity in the *cis*-product from -70 to 84% ee with (TADDOL)PN(Me)Ph and (BINOL)PN(Me)Ph, respectively. When TMDB was used as the borane source and *x*(TADDOL)POPh as the ligand, the ee increased to 90%. It is of interest to note that the opposite enantiomer is not formed when (TADDOL)PN(Me)Ph is screened with TMDB or any other synthesized borane. CatBH failed to make efficient progress in the transition-metal catalyzed hydroboration with either iridium or rhodium as the catalyst source. Other synthesized boranes were screened with the unsubstituted amide with varying degrees of diastereo- and enantioselectivities, but TMDB is the most successful borane used with this substrate. It was of benefit to determine the absolute configuration of this substrate for better knowledge of these products. The absolute configuration was determined to be of the (1*R*,3*S*)-stereochemistry, namely (1*R*,3*S*)-3-hydroxy-*N*-phenylcyclopentanecarboxamide for the major enantiomer formed.

Two additional α -substituted amides were synthesized to allow for more efficient two-point binding to the rhodium center by blocking one face of the molecule. It was hypothesized this concept would provide higher levels of diastereoselectivity. This is sufficient in increasing the ratio from the α -unsubstituted amide to the α -methyl substituted amide from 8:1 to 12:1, respectively. When PinBH is used as the borane, a range of -42% to 82% ee is found with (TADDOL)POPh and (BINOL)N(Me)Ph, respectively. The most successful case with the α -methyl substituted *N*-phenyl amide was obtained with TMDB and (TADDOL)POPh provides 92% ee.

When the α -substitution is modified to a benzyl group, the diastereomeric ratio improves to 20:1 in the best case, 13:1 in most cases, which is a slight increase from 12:1 in the α -methyl substituted amide. The enantioselectivities obtained with this substrate are moderate (80% ee with (TADDOL)POPh).

An enantioswitch occurs when PinBH is used on all three amide substrates with (TADDOL)PN(Me)Ph, but the level of enantioswitching decreases with increasing size of the α -substituent. However, an enantioswitch does not occur with TMDB or other synthesized boranes. TMDB provides the highest level of enantioselectivity in all cases along with varied diastereoselectivities. It is not understood why the enantioswitch occurs only with PinBH/(TADDOL)PN(Me)Ph, but does not happen when other structurally similar boranes are used with the same ligand.

It is of relevance to find optimized chiral separation conditions for the Weinreb amide series. This would determine if investigating these Weinreb amides are beneficial for

further use. Also, optimization of the hydroboration conditions (solvent, temperature, time, catalyst, *etc.*) are necessary to see if these would alter the results.

Further functionalizations can be performed on the organoboronate esters. These compounds are air, water and chromatography stable. It is shown that the unsubstituted organoboronate ester can be converted to its corresponding trifluoroborate salt with retention of stereochemistry. This functionalization is beneficial as Suzuki cross-coupling reactions employ trifluoroborate salts to form new C–C bonds.

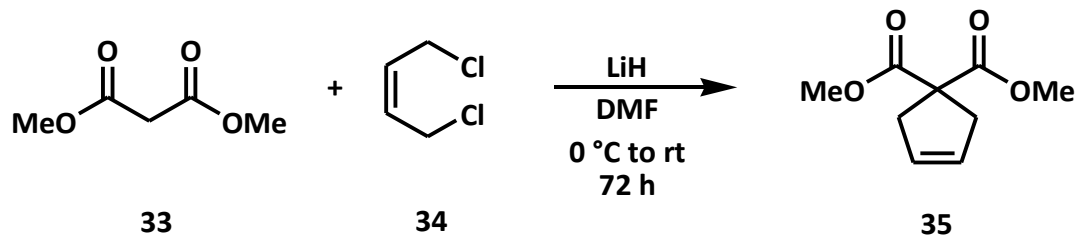
Additional cyclopentenyl prochiral substrates have further potential in rhodium-catalyzed hydroborations. As it is shown that the amide moiety is an efficient directing-group for rhodium-catalyzed hydroborations, different amide substrates can be explored (*e.g.* altering the amide itself, varying the α -substituent or using a “reverse-amide”). Furthermore, other prochiral substrates could be tested (*e.g.* an acyclic prochiral substrate, *etc.*). To date, TMDB is the borane of choice; however, additional structurally similar boranes can be synthesized and screened on these substrates to potentially increase levels of diastereo- and enantioselectivities.

Most importantly, these γ,δ -unsaturated cyclic amides provide mechanistic insight into the β,γ -unsaturated acyclic amides. It is clear that a directing-effect is shown in the case of the cyclic amides, as determined by the ratio of *cis*- to *trans*-isomers. This diastereoselectivity provides us with the information that two-point binding does, in fact, occur with the amides discussed. In conclusion, under identical ligand and catalyst systems, it is shown that two-point binding must also occur with the β,γ -unsaturated acyclic amides.

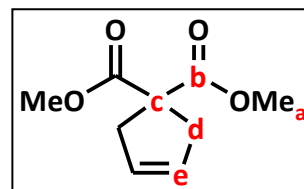
Chapter 14: Experimental Procedures

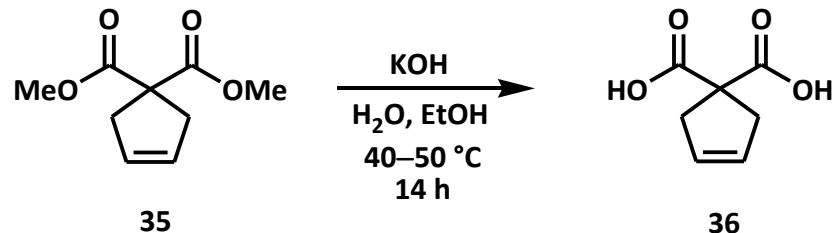
General Procedures: Air-sensitive reactions were run under an atmosphere of nitrogen. A nitrogen-filled glovebox was used to assemble catalytic reactions. Dichloromethane and tetrahydrofuran (THF) were freshly distilled under the following conditions: dichloromethane from calcium hydride, THF from sodium metal and benzophenone. When indicated, solvents were degassed by the freeze-pump-thaw method under a dry nitrogen atmosphere (4 times). Boranes were distilled immediately before use. Unless otherwise noted, all synthesized compounds were purified with flash chromatography (hexanes: ethyl acetate) using EMD Silica Gel 60 Geduran®. Chemicals were purchased from Aldrich, Alfa Aesar, Strem or TCI America and were used as received. Thin layer chromatography (TLC) analyses were performed on Analtech Silica Gel HLF (0.25 mm) precoated analytical plates and visualized with the use of a handheld short wavelength UV light, iodine stain (I_2 and EMD Silica Gel 60 Geduran®), vanillin stain (vanillin, 3 g; ethanol, 97 mL; H_2SO_4 , 3 mL), or PMA stain (phosphomolybdic acid, 10 wt. % in ethanol). NMR spectra were recorded on a 300, 400, or 600 MHz Bruker NMR spectrometer using residual $CHCl_3$ ($\delta 7.27$ for 1H) or $CDCl_3$ ($\delta 77.24$ for ^{13}C) as the reference standard. Peaks are expressed as s (singlet), d (doublet), t (triplet), q (quartet), m (unresolved multiplet), or combinations thereof. Coupling constants (J) are reported in Hertz (Hz). HPLC solvents were filtered through Millipore filter paper. HPLC analyses were performed with use of an ISCO model 2360 HPLC and Chiral Technologies, Inc. chiral HPLC column (Chiralpak AD and Chiralpak

OD: 250 x 4.6 mm). The data were recorded and analyzed with ChromPerfect chromatography software (version 5.1.0). IR spectra were recorded using an Avatar 360 FT-IR. HRMS analyses were performed by the Nebraska Center for Mass Spectrometry.

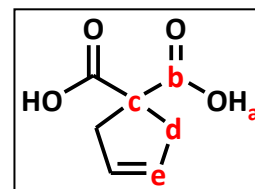


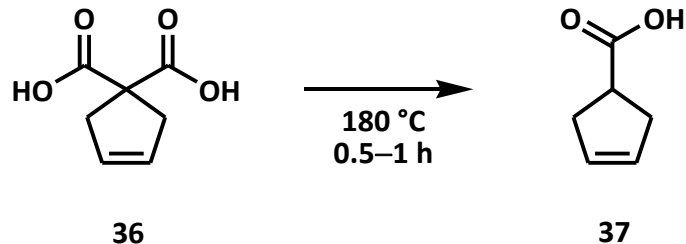
Preparation of dimethyl cyclopent-3-ene-1,1-dicarboxylate.¹⁶ To a stirred solution of dimethylmalonate (6.6 g, 49.95 mmol) in dry *N,N*-dimethylformamide (DMF, 75 mL) at 0 °C was added LiH in one portion (1.00 g, 125.79 mmol) under an atmosphere nitrogen. After 2 h, or when hydrogen gas ceases, *cis*-1,4-dichloro-2-butene (6.94 g, 55.5 mmol) was added dropwise and the mixture was allowed to warm to room temperature. After 72 h, the resulting mixture was diluted with 20% ether in hexanes (100 mL) and poured into cold water. The organic layer was washed with water (thrice) and brine. The organic layer was dried over magnesium sulfate followed by concentration under reduced pressure to afford an off-white solid (8.9151 g, 97%): mp 58.8–61.1 °C (published 58–59 °C)¹⁶; ¹H NMR (300 MHz, CDCl₃) δ 5.61 (2H, s, **e**), 3.73 (6H, s, **a**), 3.02 (4H, s, **d**); ¹³C NMR (75 MHz, CDCl₃) δ 172.84 (**b**), 127.98 (**e**), 58.97 (**c**), 53.00 (**a**), 41.13 (**d**); IR (neat, cm⁻¹) 2983 (CH sp² stretch), 2897 (CH sp³ stretch), 1720 (C=O stretch), 1430 (CH₂ deformation), 1258 (C-O-C antisymmetrical stretch), 752 (CH₂ rocking), 694 (O-C-O bend); HRMS (HREI) calcd. for C₉H₁₂O₄ (M⁺): 184.0736, found 184.0731 m/z. Please see page 119–120 for ¹H and ¹³C spectra, respectively.



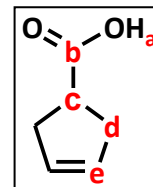


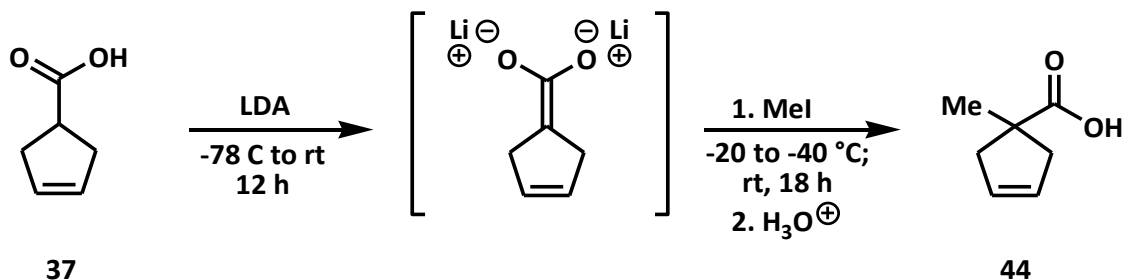
Preparation of cyclopent-3-ene-1,1-dicarboxylic acid.¹⁶ To dimethyl cyclopent-3-ene-1,1-dicarboxylate (1 g, 5.43 mmol) in 80% ethanol in water (10.8 mL total volume) was added KOH (0.9749 g, 17.38 mmol) and was stirred at 40–50 °C. After 14 h, the reaction mixture was concentrated under reduced pressure. 20% ether in hexane was added (7 mL) followed by 17 g ice. It was then carefully treated with 0.88 mL concentrated sulfuric acid. The aqueous phase was extracted thrice with 8 mL portions of ethyl acetate. The organic layers were combined and dried with magnesium sulfate followed by concentration under reduced pressure to afford a white solid (0.8049 g, 95%): mp 169.6–170.2 °C (published 162–165 °C)¹⁶; ¹H NMR (400 MHz, d-acetone) δ 10.58.74 (1H, br s, **a**), 5.60 (2H, s, **e**), 3.00 (4H, s, **d**); ¹³C NMR (400 MHz, d-acetone) δ 173.70 (**b**), 128.64 (**e**), 59.11 (**c**), 41.62 (**d**); IR (neat, cm⁻¹) 3391 (H-bonded OH stretch), 2987 (CH sp² stretch), 2966 (CH sp³ stretch), 1716 (C=O stretch), 1650 (C=C stretch), 1385 (CH₂ (sp³) deformation), 988 (C-OH deformation), 756 (O-C=O bend), 678 (C-C=O bend). Please see page 121–122 for ¹H and ¹³C spectra, respectively.



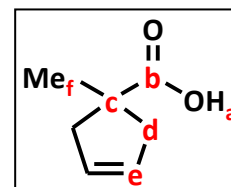


Preparation of cyclopent-3-ene carboxylic acid.¹⁶ Cyclopent-3-ene-1,1-dicarboxylic acid (18 g, 115.28 mmol) was heated in an oil bath at 180 °C for 0.5–1 h, or until gas evolution has ceased. The residual oil was distilled under reduced pressure (70 °C at 1 torr) yielding a pale yellow oil (10.5994 g, 82%): ¹H NMR (400 MHz, CDCl₃) δ 10.87 (1H, br s, **a**), 5.69 (2H, s, **e**), 3.22–3.14 (1H, dt, *J* = 8.1, **c**), 2.71–2.69 (4H, d, *J* = 8.1, **d**); ¹³C NMR (100 MHz, CDCl₃) 183.19 (**b**), 129.12 (**e**), 41.59 (**c**), 36.41 (**d**); IR (neat, cm⁻¹) 3265 (H-bonded OH stretch), 3064 (CH sp² stretch), 2929 (CH sp³ stretch), 1695 (C=O stretch), 1614 (C=C stretch), 1422 (CH₂ sp³ deformation), 931 (C-OH deformation), 678 (O-C=O bend); HRMS (HRFAB) calcd. for C₆H₉O₂ (M+H)⁺: 113.0603, found 113.0603 m/z. Please see page 123–124 for ¹H and ¹³C spectra, respectively.

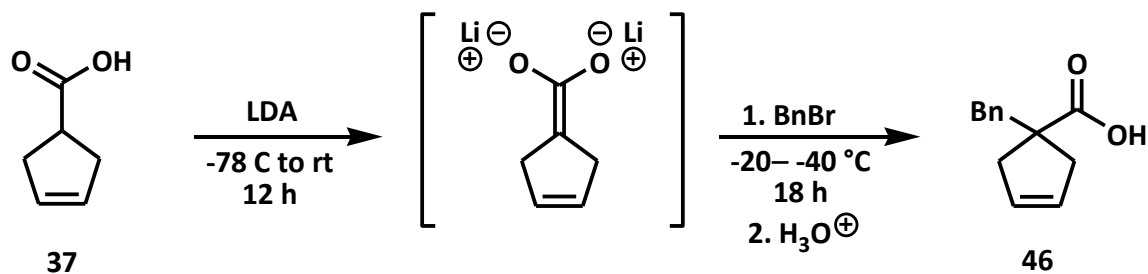




Preparation of 1-methylcyclopent-3-ene carboxylic acid. Under an atmosphere of nitrogen, diisopropylamine (5.8651 g, 57.96 mmol) in dry THF (228 mL) was cooled to -78°C . *n*Butyl lithium (20.51 mL, 2.5 M solution in hexanes) was slowly added to the solution and stirred for 1 h at this temperature, followed by 1 h at room temperature. At -20°C to -40°C , cyclopent-3-ene carboxylic acid (2.5353 g, 22.61 mmol) in THF (15 mL) was slowly added over 1 h. After 12 h, the solution was cooled to -20°C to -40°C and slowly added dropwise iodomethane (4.8541 g, 34.20 mmol). The alkylation was allowed to stir for 18 h. After the allotted time, the reaction was quenched with dilute HCl (3 M) then was extracted (thrice) with diethyl ether. The organic layers were combined and dried with magnesium sulfate, concentrated under reduced pressure and affording a brown liquid which was used without purification to the next step: TLC analysis R_f 0.36 (75:25 hexanes:ethyl acetate); ^1H NMR (400 MHz, CDCl_3) δ 11.56 (1H, br s, **a**), 5.63 (2H, s, **e**), 2.98–2.94 (2H, d, $J = 14.4$, **d**), 2.28–2.24 (2H, d, $J = 14.9$, **d**), 1.34 (3H, s, **f**); ^{13}C NMR (100 MHz, CDCl_3) δ 184.40 (**b**), 128.45 (**e**), 47.84 (**c**), 44.78 (**d**), 25.95 (**f**); IR (neat, cm^{-1}) 3195 (H-bonded OH stretch), 3064 (CH sp^2 stretch), 2970 (CH sp^3 stretch), 2917 (CH stretch in CH_3 compounds), 1695 (C=O stretch), 1467 (CH₂ deformation), 1405

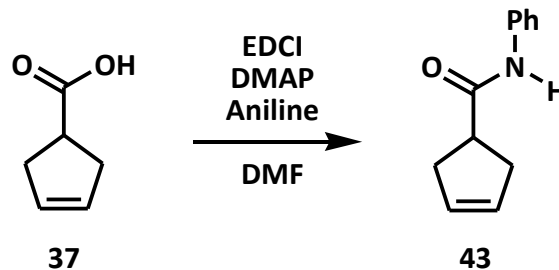


(CH₃ antisymmetrical deformation), 1287 (CH₃ symmetrical deformation), 944 (C-OH deformation), 670 (O-C=O bend); HRMS (HREI) calcd. for C₇H₁₀O₂ (M^{+•}): 126.0681, found 126.0676 m/z. Please see page 125–126 for ¹H and ¹³C spectra, respectively.

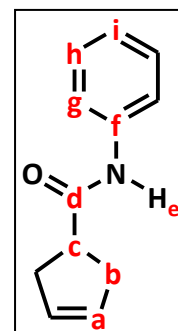


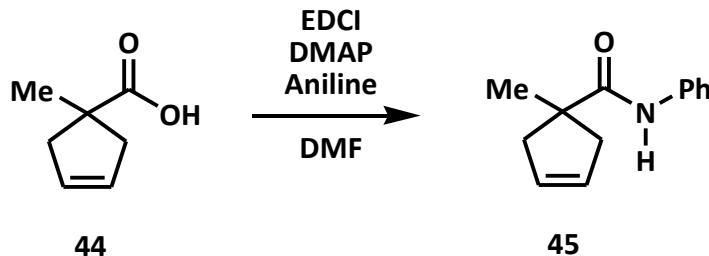
Preparation of 1-benzylcyclopent-3-ene carboxylic acid. Under an atmosphere of nitrogen, diisopropylamine (2.4020 g, 23.74 mmol) in dry THF (92 mL) was cooled to -78°C . *n*Butyl lithium (8.4 mL, 2.5 M solution in hexanes) was slowly added to the solution and stirred for 1 h at this temperature, followed by 1 h at room temperature. At -20°C to -40°C , cyclopent-3-ene carboxylic acid (1.0238 g, 9.13 mmol) in THF (15 mL) was slowly added over 1 h. After 12 h, the solution was cooled to -20°C to -40°C and benzyl bromide (2.3473 g, 13.72 mmol) was added slowly. The alkylation was allowed to stir for 18 h. After the allotted time, the reaction was quenched with dilute HCl (3 M) then was extracted (thrice) with diethyl ether. The organic layers were combined and dried with magnesium sulfate, concentrated under reduced pressure and used without purification to the next step affording a brown oil: ^1H NMR (400 MHz, CDCl_3) δ 8.86 (1H, br s, **a**), 7.30–7.20 (5H, m, **h–j**), 5.67 (2H, s, **e**), 3.07 (2H, s, **f**), 2.90–2.87 (2H, d, $J = 14.8$, **d**), 2.52–2.48 (2H, d, $J = 14.9$, **d**); ^{13}C NMR (100 MHz, CDCl_3) 183.24 (**b**), 138.05 (**g**), 129.95 (**i**), 128.64 (**h**), 128.42 (**j**), 126.86 (**e**), 54.01 (**c**), 44.11 (**f**), 41.92 (**d**); IR (neat, cm^{-1}) 3252 (H-bonded OH stretch), 3060 (CH aromatic stretch), 3032 (CH sp^2 stretch), 2917 (CH sp^3 stretch), 1699 (C=O stretch), 1491 (CH_2

deformation), 1458 (aromatic ring stretch), 952 (C-OH deformation), 764 (O-C=O bend), 694 (C-C=O bend); HRMS (HRFAB) calcd. for $C_{13}H_{14}LiO_2$ (M+Li)⁺: 209.1154, found 209.1149 m/z. Please see page 127–128 for 1H and ^{13}C spectra, respectively.



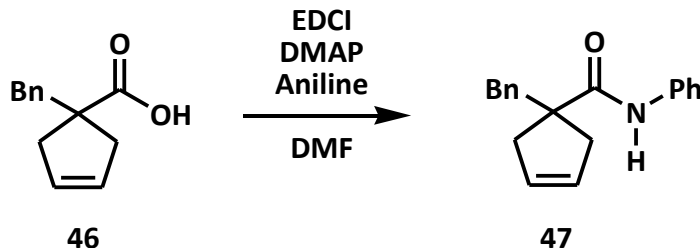
Preparation of *N*-phenylcyclopent-3-enecarboxamide. Cyclopent-3-ene carboxylic acid (0.9909 g, 8.84 mmol) was dissolved in DMF (40 mL) and was cooled to 0 °C. Aniline (0.89 mL, 9.72 mmol) was added and was stirred at this temperature for 0.5 h. After this allotted time, was added DMAP (0.5398 g, 4.42 mmol) and EDCI (1.8635 g, 9.72 mmol) and was stirred at room temperature overnight. The reaction was quenched with satd. NaHCO₃, and extracted with ether. The organic layers were combined, washed with 3N HCl, dried with magnesium sulfate, filtered and concentrated *in vacuo*. Flash chromatography on silica gel (75:25 hexanes:dichloromethane) afforded a white fluffy solid (1.4520 g, 87%): mp 155.6–156.5 °C; TLC analysis *R_f* 0.49 (75:25 hexanes:dichloromethane); ¹H NMR (400 MHz, CDCl₃) δ 7.509–7.507 (2H, d, *J* = 7.6, **h**), 7.37 (1H, br s, **e**), 7.34–7.30 (2H, t, *J* = 7.5, **g**), 7.12–7.08 (1H, dt, *J* = 1.1, 7.4, **i**), 5.74 (2H, s, **a**), 3.18–3.06 (1H, m, **c**), 2.78–2.69 (4H, m, **b**); ¹³C NMR (100 MHz, CDCl₃) 176.73 (**c**), 138.42 (**f**), 129.38 (**h**), 129.12 (**g**), 124.24 (**i**), 120.05 (**a**), 49.09 (**c**), 45.35 (**b**); IR (neat, cm⁻¹) 3288, 3253, 3142, 1655, 1544, 1439, 1310, 750; HRMS (HRFAB) calcd. for C₁₂H₁₄NO (M+H)⁺: 188.0997, found 188.1081 m/z. Please see page 129–130 for ¹H and ¹³C spectra, respectively.



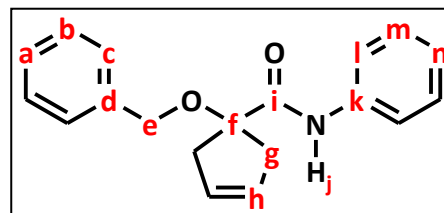


Preparation of 1-methyl-N-phenylcyclopent-3-enecarboxamide. Cyclopent-3-ene carboxylic acid (0.4776 g, 3.79 mmol) was dissolved in DMF (20 mL) and was cooled to 0 °C. Aniline (0.38 mL, 4.16 mmol) was added and stirred at this temperature for 0.5 h. After this allotted time, was added DMAP (0.2313 g, 1.90 mmol) and EDCI (0.7961 g, 4.16 mmol) and was stirred at room temperature overnight. The reaction was quenched with satd. NaHCO_3 , and was extracted with ether. The organic layers were combined, washed with 3N HCl, dried with magnesium sulfate, filtered and concentrated under reduced pressure. Flash chromatography on silica gel (75:25 hexanes:dichloromethane) afforded white needlelike crystals (0.3352 g, 44%): mp 120.0–121.6 °C; TLC analysis R_f 0.32 (75:25 hexanes:ethyl acetate); ^1H NMR (400 MHz, CDCl_3) δ 7.54–7.49 (2H, d, $J = 7.6$, **i**), 7.37 (1H, br s, **f**), 7.34–7.28 (2H, t, $J = 7.5$, **h**), 7.13–7.07 (1H, td, $J = 7.4$, 1.1, **j**), 5.74 (2H, s, **a**), 3.04–2.92 (2H, d, $J = 14.3$, **b**), 2.44–2.32 (2H, d, $J = 14.5$, **b**), 1.42 (3H, s, **d**); ^{13}C NMR (100 MHz, CDCl_3) 176.73 (**e**), 138.42 (**g**), 129.38 (**i**), 129.12 (**h**), 124.24 (**j**), 120.05 (**a**), 49.09 (**c**), 45.35 (**b**), 26.27 (**d**); IR (neat, cm^{-1}) 3657 (NH stretch), 2974 (CH sp^2 stretch), 2897 (CH sp^3 stretch), 1679 (C=O stretch), 1593 (C=C stretch), 1520 (NH bend), 1438 (CH_3 antisymmetrical deformation), 1303 (CH_3 symmetrical

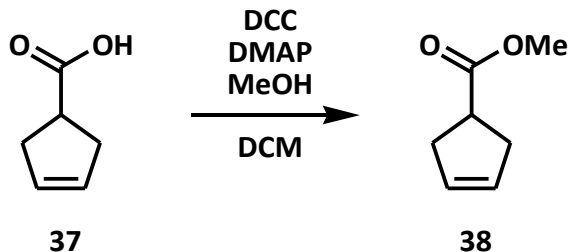
deformation), 727 (CH out-of-plane deformation); HRMS (HRFAB) calcd. for $C_{13}H_{16}NO$ ($M+H$)⁺: 202.1232, found 202.1228 m/z. Please see page 131–132 for 1H and ^{13}C spectra, respectively.



Preparation of 1-benzyl-N-phenylcyclopent-3-enecarboxamide. Cyclopent-3-ene carboxylic acid (0.6907 g, 3.41 mmol) was dissolved in DMF (34 mL) and was cooled to 0 °C. Aniline (0.38 mL, 4.09 mmol) was added and was stirred at this temperature. After 0.5 h, was added DMAP (0.2086 g, 1.71 mmol) and EDCI (0.7182 g, 3.76 mmol) and was allowed to warm to rt and stirred overnight. The reaction was quenched with satd. NaHCO₃, and was extracted with ether. The organic layers were combined, washed with 3N HCl, dried with magnesium sulfate, filtered and concentrated under reduced pressure. Flash chromatography on silica gel (85:15 hexanes:ethyl acetate) afforded a pale brown solid (0.5679 g, 77%): mp 142.4–142.7 °C; TLC analysis R_f 0.33 (85:15 hexanes:ethyl acetate); ¹H NMR (300 MHz, CDCl₃) δ 7.33–7.23 (10H, m, **a**, **h**), 6.76 (1H, br s, **b**), 5.77 (2H, s, **f**), 3.05 (2H, s, **g**), 2.83–2.78 (2H, d, *J* = 14.9, **e**), 2.60–2.55 (2H, d, *J* = 14.7, **e**); ¹³C NMR (75 MHz, CDCl₃) 175.15 (**i**), 137.99 (**d**), 137.92 (**k**), 130.47 (**b**), 129.29 (**m**), 129.10 (**c**), 128.40 (**l**), 126.94 (**d**), 124.44 (**k**), 120.36 (**h**), 55.44 (**f**), 44.79 (**e**), 41.92 (**g**); IR (neat, cm⁻¹) 3305 (NH stretch), 2991 (CH sp² stretch), 2970 (CH sp³ stretch), 1646 (C=O stretch), 1601 (C=C stretch), 1540 (NH bend), 1499 (CH₂ deformation), 1242 (C-N stretch), 1050 (R-C-O stretch, ether), 698 (CH out-

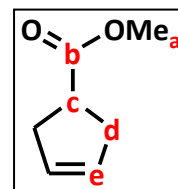


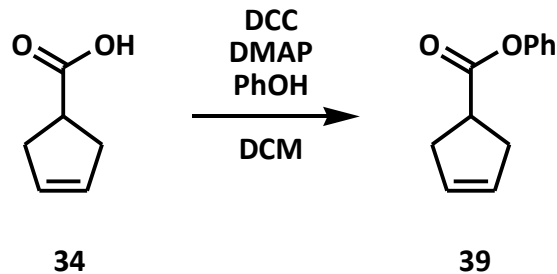
of-plane deformation); HRMS (HRFAB) calcd. for $C_{13}H_{16}NO$ (M+H)⁺: 278.1545, found 278.1543 m/z. Please see page 133–134 for 1H and ^{13}C spectra, respectively.



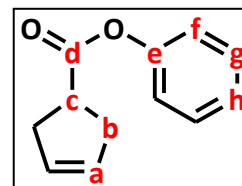
Preparation of methyl-3-enecarboxylate. Cyclopent-3-ene carboxylic acid (0.1114 g, 0.99 mmol) was dissolved in DCM (10 mL) and was cooled to 0 °C. Methanol (0.049 mL, 1.2 mmol) was added and was allowed to stir at this temperature. After 0.5 h, was added DCC (0.2050 g, 0.99 mmol) and DMAP (0.0607 g, 0.50 mmol). The reaction mixture was warmed to rt. After 14 h, the reaction was quenched with NaHCO₃ and extracted with ether. The organic layers were combined, dried over magnesium sulfate, and concentrated under reduced pressure. Flash chromatography on silica gel (75:25 hexanes:dichloromethane) affords the title compound as a light yellow oil (0.06639, 53% yield): TLC analysis *R_f* 0.64 (90:10 hexanes:acetone); ¹H NMR (400 MHz, CDCl₃) δ 5.67 (2H, s, **e**), 3.70 (3H, s, **a**), 3.17–3.09 (1H, dd, *J* = 8.5, 7.8, **c**), 2.67–2.65 (4H, d, *J* = 8.2, **d**); ¹³C NMR (100 MHz, CDCl₃) 176.88 (**b**), 129.18 (**e**), 52.01 (**a**), 41.64 (**c**), 36.52 (**d**); IR (neat, cm⁻¹) 2950 (CH sp² stretch), 2852 (CH sp³ stretch), 1724 (C=O stretch), 1434 (CH₃ antisymmetrical deformation), 1270 (C-O-C antisymmetrical stretch), 1201 (C-O-C stretch), 1172 (R-C-O stretch), 747 (O-C-O bend); HRMS (HREI) calcd. for C₇H₁₀O₂ (M⁺): 126.0681, found 126.0679 m/z.

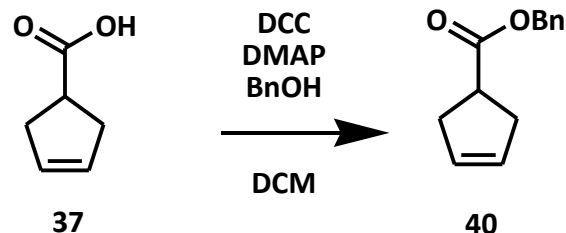
Please see page 135–136 for ¹H and ¹³C spectra, respectively.



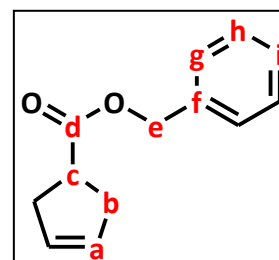


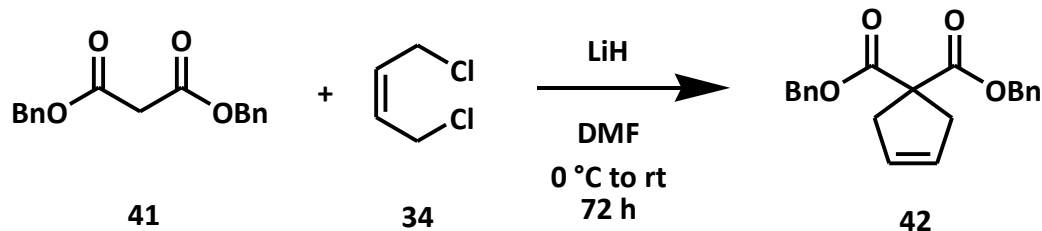
Preparation of phenyl cyclopent-3-ene-1-carboxylate. Cyclopent-3-ene carboxylic acid (0.0904 g, 0.81 mmol) was dissolved in DCM (8 mL) and was cooled to 0 °C. Phenol (0.09 mL, 0.97 mmol) was added and was allowed to stir at this temperature. After 0.5 h, was added DCC (0.1664 g, 0.81 mmol) and DMAP (0.0493 g, 0.40 mmol). The reaction mixture was warmed to rt. After 14 h, the reaction was quenched with NaHCO₃ and extracted with ether. The organic layers were combined, dried over magnesium sulfate, and concentrated under reduced pressure. Flash chromatography on silica gel (75:25 hexanes:dichloromethane) affords the title compound as an oil (0.0747, 49% yield): TLC analysis R_f 0.64 (90:10 hexanes:acetone); ¹H NMR (400 MHz, CDCl₃) δ 7.42–7.36, (2H, t, *J* = 8.0, **g**), 7.26–7.21 (1H, tt, *J* = 7.4, 1.6, 1.1, **h**), 7.12–7.07 (2H, dd, *J* = 7.5, 1.2, **f**), 5.73 (2H, s, **a**), 3.44–3.33 (1H, m, **c**), 2.87–2.77 (4H, m, **b**); ¹³C NMR (100 MHz, CDCl₃) δ 174.85 (**d**), 129.60 (**g**), 129.17 (**h**), 125.92 (**g**), 121.72 (**a**), 41.87 (**c**), 36.59 (**b**). Please see page 137–138 for ¹H and ¹³C spectra, respectively.



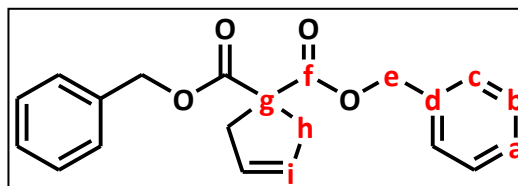


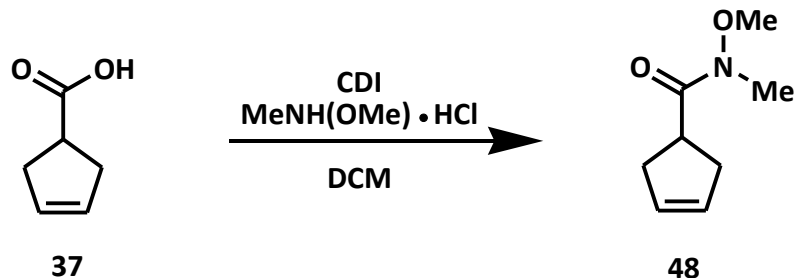
Preparation of benzyl cyclopent-3-ene-2-carboxylate. Cyclopent-3-ene carboxylic acid (0.5481 g, 4.89 mmol) was dissolved in DCM (11 mL) and was cooled to 0 °C. Benzyl alcohol (0.5 mL, 4.89 mmol) was added and was allowed to stir at this temperature. After 0.5 h, was added DCC (1.009 g, 4.89 mmol) and DMAP (0.2986 g, 2.45 mmol). The reaction mixture was warmed to rt. After 14 h, the reaction was quenched with NaHCO₃ and extracted with ether. The organic layers were combined, dried over magnesium sulfate, and concentrated under reduced pressure. Flash chromatography on silica gel (75:25 hexanes:dichloromethane) affords the title compound as an oil (0.5141 g, 52% yield): TLC analysis R_f 0.52 (90:10 hexanes:acetone); ¹H NMR (400 MHz, CDCl₃) δ 7.45–7.30, (5H, m, **g–i**), 5.68 (2H, s, **a**), 5.16 (2H, s, **e**), 3.24–3.14 (1H, dd, *J* = 9.0, 7.3, **c**), 2.74–2.64 (4H, d, *J* = 7.9, **b**); ¹³C NMR (100 MHz, CDCl₃) δ 176.24 (**d**), 136.38 (**f**), 129.18 (**h**), 128.17 (**g**), 128.37 (**i**), 128.30 (**a**), 66.51 (**e**), 41.75 (**c**), 36.52 (**b**). Please see page 139–140 for ¹H and ¹³C spectra, respectively.



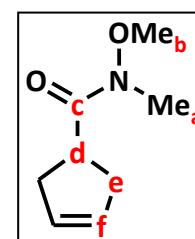


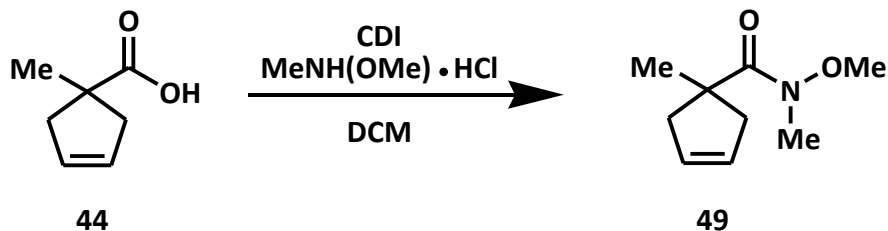
Preparation of dibenzyl cyclopent-3-ene-1,1-dicarboxylate. To a stirred solution of dibenzylmalonate (13.2 g, 46.43 mmol) in dry *N,N*-dimethylformamide (DMF, 150 mL) at 0 °C was added LiH (2.00 g, 251.57 mmol) in one portion under an atmosphere nitrogen. After 2 h, or when hydrogen gas ceases, *cis*-1,4-dichloro-2-butene (12 mL, 115.23 mmol) was added dropwise and the mixture was allowed to warm to room temperature. After 72 h, the resulting mixture was diluted with 20% ether in hexanes (100 mL) and poured into cold water. The organic layer was washed with water (thrice) and brine. The organic layer was dried over magnesium sulfate followed by concentration under reduced pressure to afford a white solid (13.1193 g, 84%): ^1H NMR (400 MHz, CDCl_3) δ 7.35–7.25, (10H, m, **a–c**), 5.63 (2H, s, **i**), 5.15 (4H, s, **e**), 3.07 (4H, s, **h**); ^{13}C NMR (100 MHz, CDCl_3) δ 172.02 (**f**), 135.70 (**d**), 128.70 (**b**), 128.42 (**c**), 128.18 (**a**), 127.98 (**i**), 67.41 (**e**), 59.14 (**g**), 41.10 (**h**). Please see page 141–142 for ^1H and ^{13}C spectra, respectively.





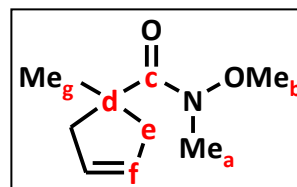
Preparation of *N*-phenylcyclopent-3-enecarboxamide. Cyclopent-3-enecarboxylic acid (1.0 g, 8.92 mmol) was dissolved in dichloromethane (45 mL) and cooled to 0 °C. At this temperature was added CDI (1.7354 g, 10.70 mmol) and stirred for 0.5 h. Afterwards, was added *N,O*-dimethylhydroxylamine hydrochloride (2.1748 g, 22.30 mmol). After 13 h, the salts were filtered through cotton and the filtrate was washed with aq. HCl (25 mL, twice) then brine (25 mL, twice) and extracted with dichloromethane. The organic layers were combined and dried over magnesium sulfate. Flash chromatography on silica gel (75:25 hexanes:ethyl acetate) afforded the title compound (0.9127 g, 55%). TLC analysis R_f 0.33 (75:25 hexanes:ethyl acetate); ^1H NMR (300 MHz, CDCl_3) δ 5.61 (2H, s, **f**), 3.69 (3H, s, **b**), 5.53–3.41 (1H, quintet, $J = 7.8$, **d**), 3.19 (3H, s, **a**), 2.69–2.55 (4H, m, **e**); ^{13}C NMR (75 MHz, CDCl_3) δ 177.31 (**c**), 129.05 (**f**), 61.47 (**b**), 60.68 (**d**), 38.59 (**a**), 36.71 (**e**); IR (neat, cm^{-1}) 2966 (CH sp^2 stretch), 2901 (CH sp^3 stretch), 1659 (C=O stretch), 1377 (CH₃ antisymmetrical deformation), 1311 (C-N stretch), 686 (CH out-of-plane deformation); HRMS (HRFAB) calcd. for $\text{C}_8\text{H}_{13}\text{NO}_2\text{Li}$ ($\text{M}+\text{Li}$)⁺: 162.1106, found 162.1108 m/z . Please see page 143–144 for ^1H and ^{13}C spectra, respectively.

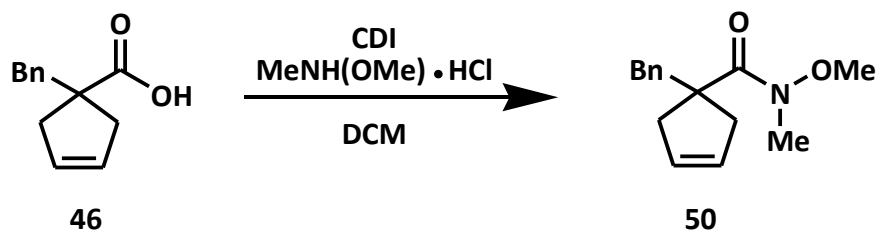




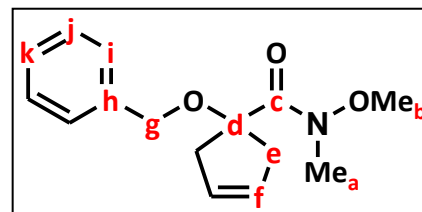
Preparation of 1-methyl-N-phenylcyclopent-3-enecarboxamide. 1-Methylcyclopent-3-enecarboxylic acid (1.8853 g, 14.95 mmol) was dissolved in dichloromethane (75 mL) and cooled to 0 °C. At this temperature was added CDI (2.9079 g, 17.93 mmol) and stirred for 0.5 h. Afterwards, was added *N,O*-dimethylhydroxylamine hydrochloride (3.6440 g, 37.36 mmol). After 16 h, the salts were filtered through cotton and the filtrate was washed with aq. HCl (25 mL, twice) then brine (25 mL, twice) and extracted with dichloromethane. The organic layers were combined and dried over magnesium sulfate. Flash chromatography on silica gel (75:25 hexanes:ethyl acetate) afforded the title compound (1.1124 g, 44%). TLC analysis R_f 0.41 (75:25 hexanes:ethyl acetate); ^1H NMR (300 MHz, CDCl_3) δ 5.61 (2H, s, **f**), 3.69 (3H, s, **b**), 3.20 (3H, s, **a**), 2.95–2.87 (2H, d, $J = 15.0$, **e**), 2.28–2.21 (2H, d, $J = 15.1$, **b**), 1.29 (3H, s, **g**); ^{13}C NMR (75 MHz, CDCl_3) δ 179.41 (**c**), 128.21 (**f**), 60.71 (**b**), 48.96 (**d**), 44.39 (**e**), 33.78 (**a**), 26.07 (**g**); IR (neat, cm^{-1}) 2983 (CH sp^2 stretch), 2924 (CH sp^3 stretch), 1650 (C=O stretch), 1475 (CH₃ antisymmetrical stretch), 1409 (CH₃ symmetrical stretch), 1373 (CH₃ deformation), 1303 (C-N stretch), 731 (CH₂ rocking), 674 (CH out-of-plane deformation); HRMS (HRFAB) calcd. for $\text{C}_9\text{H}_{16}\text{NO}_2$ ($\text{M}+\text{H}$)⁺: 170.1181, found 170.1177 m/z.

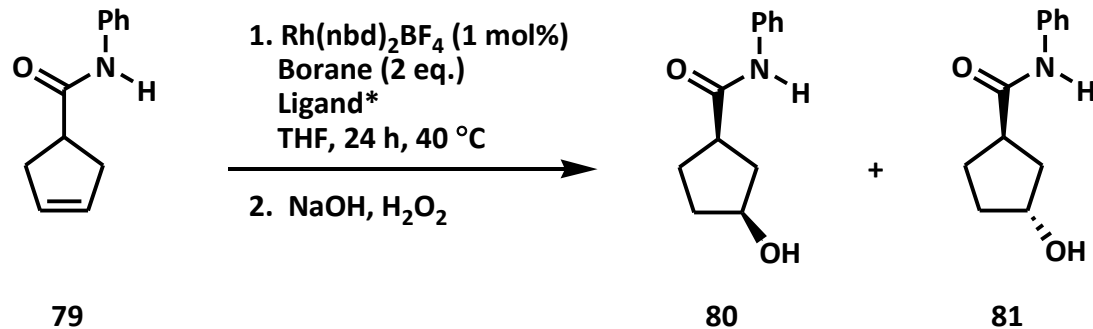
Please see page 145–146 for ^1H and ^{13}C spectra, respectively.



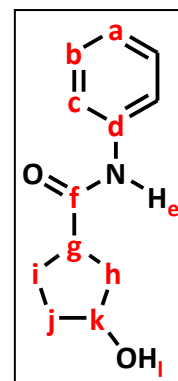


Preparation of 1-benzyl-N-phenylcyclopent-3-enecarboxamide. 1-Benzylcyclopent-3-enecarboxylic acid (1.300 g, 6.43 mmol) was dissolved in dichloromethane (37 mL) and cooled to 0 °C. At this temperature was added CDI (1.2507 g, 7.71 mmol) and stirred for 0.5 h. Afterwards, was added *N,O*-dimethylhydroxylamine hydrochloride (1.5674 g, 16.07 mmol). After 16 h, the salts were filtered through cotton and the filtrate was washed with aq. HCl (25 mL, twice) then brine (25 mL, twice) and extracted with dichloromethane. The organic layers were combined and dried over magnesium sulfate. Flash chromatography on silica gel (75:25 hexanes:ethyl acetate) afforded the title compound (0.6305 g, 40%). TLC analysis R_f 0.44 (75:25 hexanes:ethyl acetate); ^1H NMR (400 MHz, CDCl_3) δ 7.26–7.18 (3H, m, **j**, **k**), 7.11–7.06 (2H, d, $J = 7.7$, **i**), 5.64 (2H, s, **f**), 3.75 (3H, s, **b**), 3.23 (3H, s, **a**), 3.03 (2H, s, **g**), 2.89–2.81 (2H, d, $J = 15.3$, **e**), 2.54–2.45 (2H, d, $J = 15.3$, **e**); ^{13}C NMR (100 MHz, CDCl_3) δ 177.86 (**c**), 138.51 (**h**), 130.13 (**j**), 128.35 (**i**), 128.21 (**k**), 126.60 (**f**), 60.73 (**b**), 54.91 (**d**), 43.12 (**g**), 41.99 (**e**), 33.98 (**a**). Please see page 147–148 for ^1H and ^{13}C spectra, respectively.

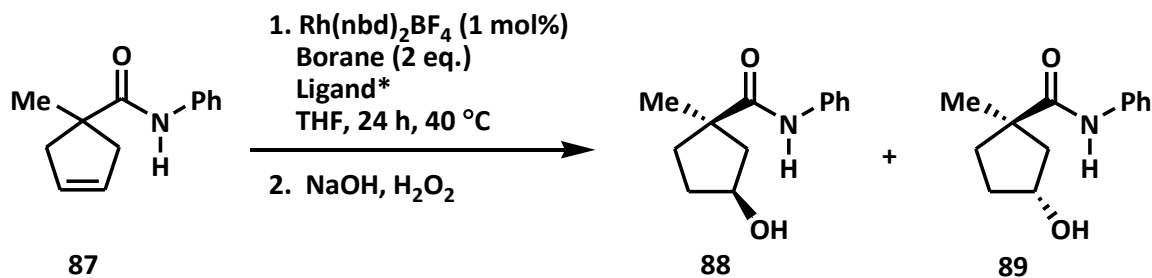




Preparation of 3-hydroxy-N-phenylcyclopentanecarboxamide. In a glove box, a stock solution of $\text{Rh}(\text{nbd})_2\text{BF}_4$ (0.0020 g, $5.35 \mu\text{M}$) was prepared in dry, degassed THF (1 mL). To this was added 1.0 mL of a stock solution of (TADDOL)POPh (0.0078 g, $13.25 \mu\text{M}$) which was prepared in 1.2 mL THF. After 2 h complexation time, the resulting yellow solution was added *N*-phenylcyclopent-3-enecarboxamide (0.0988 g, 0.528 mmol) as a solution in THF (2 mL). To this was added a solution of borane (1.06 mmol) in THF (1 mL). The reaction mixture was heated to $40 \text{ }^\circ\text{C}$ for 24 h. Afterwards, the reaction mixture was cooled to room temperature and quenched by the addition of a methanol (6 mL) followed by 3 *N* NaOH and 30% H_2O_2 (1 mL) and stirred for 2 h. The resulting mixture was extracted with dichloromethane, the combined organic extracts were dried over magnesium sulfate and concentrated under reduced pressure. Flash chromatography on silica (60:40 hexanes:ethyl acetate) afforded the title compound (0.0866 g, 80%):). Chiral HPLC analysis (Chiralcel OD, 80:20 hexanes:isopropanol, flow rate: 0.800) showed peaks at 38 minutes and 42 minutes; TLC analysis R_f 0.39 (60:40 hexanes:ethyl acetate); ^1H NMR (300 MHz, CDCl_3) δ 8.15–8.06 (1H, br d, $J = 5.2$, e), 7.55–7.53

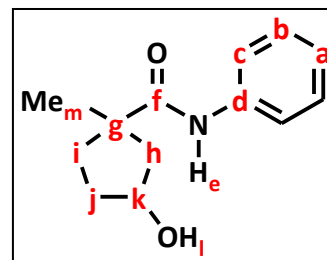


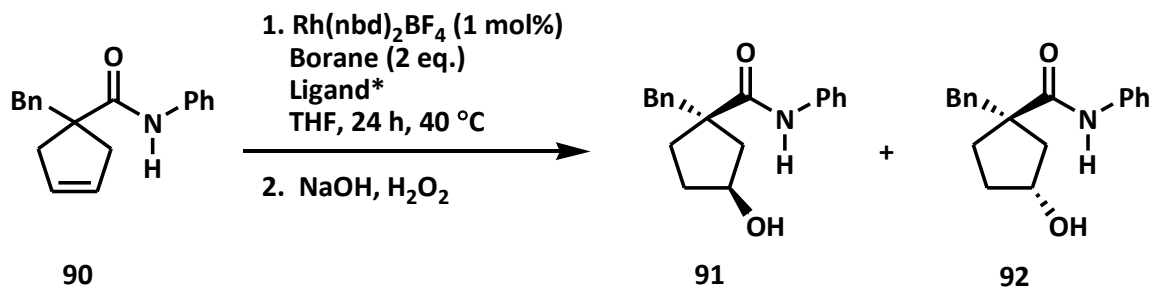
(2H, d, $J = 7.6$, **c**), 7.34–7.29 (2H, dd, $J = 8.3, 7.6$, **b**), 7.11–7.06 (1H, t, $J = 7.4$, **a**), 4.56 (1H, br s, **k**), 2.74 (1H, br s, **l**), 2.57–2.28 (2H, m, **h**), 2.03 (1H, br s, **g**), 1.97–1.84 (2H, m, **i**), 1.82–1.71 (2H, m, **j**); IR (neat, cm^{-1}) 3677 (OH stretch / NH stretch), 2907 (CH sp^2 stretch), 2803 (CH sp^3 stretch), 1728 (C=O stretch), 1663 (aromatic ring stretch), 1597 (N-H bend), 1565, 1389 (C-N stretch), 1238 (C-OH in-plane bend), 1050 (C-OH stretch). Please see page 149 for ^1H NMR spectrum.



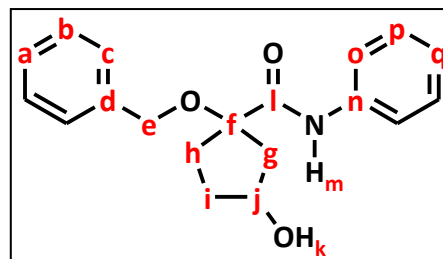
Preparation of 3-hydroxy-1-methyl-N-phenylcyclopentanecarboxamide. In a glove box, a stock solution of Rh(nbd)₂BF₄ (0.0020 g, 5.35 μM) was prepared in dry, degassed THF (1 mL). To this was added 1.0 mL of a stock solution of (TADDOL)POPh (0.0078 g, 13.25 μM) which was prepared in 1.2 mL THF. After 2 h complexation time, the resulting yellow solution was added 1-methyl-N-phenylcyclopent-3-enecarboxamide (0.1062 g, 0.528 mmol) as a solution in THF (2 mL). To this was added a solution of borane (1.06 mmol) in THF (1 mL). The reaction mixture was heated to 40 °C for 24 h. Afterwards, the reaction mixture was cooled to room temperature and quenched by the addition of a methanol (6 mL) followed by 3 N NaOH and 30% H₂O₂ (1 mL) and stirred for 2 h. The resulting mixture was extracted with dichloromethane, the combined organic extracts were dried over magnesium sulfate and concentrated under reduced pressure. Flash chromatography on silica (60:40 hexanes:ethyl acetate) afforded the title compound (0.0891 g, 77%:). Chiral HPLC analysis (Chiralcel OD), 80:20 hexanes:isopropanol, flow rate: 0.700) showed peaks at 18 minutes and 21 minutes; TLC analysis R_f 0.43 (60:40 hexanes:ethyl acetate); ¹H NMR (400 MHz, CDCl₃) δ 7.55–7.49 (2H, dd, *J* = 8.5, 1.0, c), 7.38–7.30 (2H, t, *J* = 8, b), 7.29 (1H, s, e), 7.16–7.08 (1H, tt, *J* = 7.4, 1.1, a), 4.57–4.47 (1H, m, k), 2.69–2.57 (1H, dd, *J* = 14.0, 6.8, h), 2.26–2.18 (1H, m, h), 2.14–

2.03 (1H, m, **j**), 1.90–1.74 (2H, m, **i**), 1.55 (3H, s, **m**), 1.45–1.25 (2H, m, **l, j**); IR (neat, cm^{-1}) 3318 (OH / NH stretch), 2962 (CH sp^2 stretch), 2901 (CH sp^3 stretch), 1663 (C=O stretch), 1536 (C-OH in-plane bend), 1495 (CH_3 antisymmetrical deformation), 1434 (CH₂ antisymmetrical deformation), 1311 (C-N stretch), 657 (C-OH out-of-plane deformation); HRMS (HRCI) calcd. for $\text{C}_{13}\text{H}_{17}\text{NO}_2$ ($\text{M}+\text{H}$)⁺: 220.1338, found 220.1346 m/z. Please see page 150 for ¹H NMR spectrum.

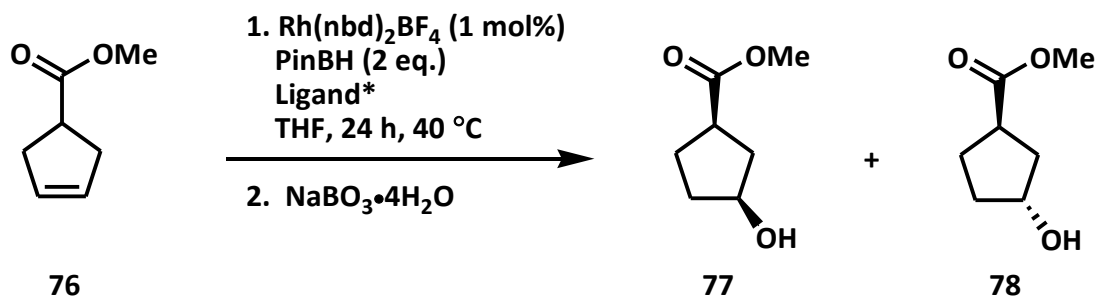




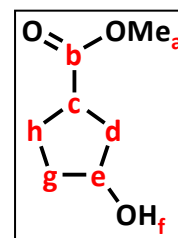
Preparation of 1-benzyl-3-hydroxy-N-phenylcyclopentanecarboxamide. In a glove box, a stock solution of $\text{Rh}(\text{nbd})_2\text{BF}_4$ (0.0020 g, 5.35 μM) was prepared in dry, degassed THF (1 mL). To this was added 1.0 mL of a stock solution of (TADDOL)POPh (0.0078 g, 13.25 μM) which was prepared in 1.2 mL THF. After 2 h complexation time, the resulting yellow solution was added 1-methyl-N-phenylcyclopent-3-enecarboxamide (0.1463 g, 0.528 mmol) as a solution in THF (2 mL). To this was added a solution of borane (1.06 mmol) in THF (1 mL). The reaction mixture was heated to 40 °C for 24 h. Afterwards, the reaction mixture was cooled to room temperature and quenched by the addition of a methanol (6 mL) followed by 3 N NaOH and 30% H_2O_2 (1 mL) and stirred for 2 h. The resulting mixture was extracted with dichloromethane, the combined organic extracts were dried over magnesium sulfate and concentrated under reduced pressure. Flash chromatography on silica (60:40 hexanes:ethyl acetate) afforded the title compound (0.1294 g, 83%:). Chiral HPLC analysis (Chiralcel-OD, 95:5 hexanes:isopropanol , 0.700) showed peaks at 22 minutes and 25 minutes; TLC analysis R_f 0.38 (60:40 hexanes:ethyl acetate); ^1H NMR (300 MHz, CDCl_3) δ 7.33–7.16 (9H, m, **a**, **b**, **c**, **o**, **p**), 7.13–1.07 (1H, m, **q**), 6.72 (1H, br s, **m**),



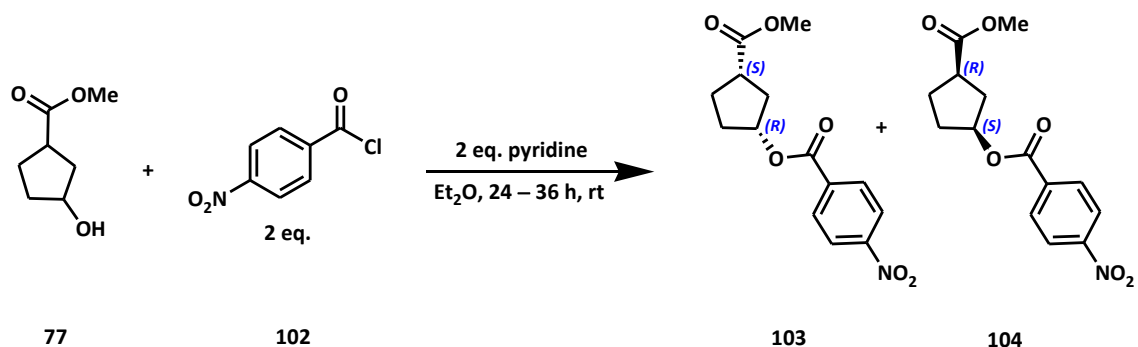
4.57–4.43 (1H, m, **j**), 3.15 (2H, s, **e**), 2.62–2.50 (1H, dd, $J = 13.8, 6.6$, **g**), 2.19–1.72 (6H, m, **g, h, i, k**); IR (neat, cm^{-1}) 3297 (OH / NH stretch), 3019 (CH sp^2 stretch), 2962 (CH sp^3 stretch), 1646 (C=O stretch), 1258 (C-O-C stretch), 1099 (R-C-O stretch), 796 (CH_2 rocking). Please see page 151 for ^1H NMR spectrum.



Preparation of methyl-3-hydroxycyclopentanecarboxylate. In a glove box, a stock solution of $\text{Rh}(\text{nbd})_2\text{BF}_4$ (0.0020 g, 5.35 μM) was prepared in dry, degassed THF (1 mL). To this was added 1.0 mL of a stock solution of (TADDOL)POPh (0.0078 g, 13.25 μM) which was prepared in 1.2 mL THF. After 2 h complexation time, the resulting yellow solution was added methyl-3-enecarboxylate (0.0666 g, 0.528 mmol) as a solution in THF (2 mL). To this was added a solution of pinacolborane (0.16 mL, 1.06 mmol) in THF (1 mL). The reaction mixture was heated to 40 °C for 24 h. Afterwards, the reaction mixture was cooled to room temperature and quenched by the addition of a solution of sodium perborate (0.4062 g, 2.64 mmol) in THF:H₂O (1:1, 4 mL total volume) and vigorously stirred for 4 h. The resulting mixture was extracted with dichloromethane, the combined organic extracts were dried over magnesium sulfate and concentrated under reduced pressure. Flash chromatography on silica (75:25 hexanes:ethyl acetate) afforded the title compound (0.0457 g, 60%): TLC analysis R_f 0.47 (75:25 hexanes:ethyl acetate); ¹H NMR (400 MHz, CDCl₃, 62:38 mixture of diastereomers) δ 4.39–4.30 (1H, m), 4.29–4.20 (1H, m, f), 3.63 (3H, s, a), 3.61 (3H, s, a), 3.05–2.94 (1H, dd, $J = 8.7, 7.8$, c), 2.84–



2.76 (1H, m, **c**), 2.06–1.58 (12H, m, **d, h, g**); IR (neat, cm^{-1}) 3669 (OH stretch), 2991 (CH sp^2 stretch), 2974 (CH sp^3 stretch), 2897 (CH_3 stretch), 1723 (C=O stretch), 1389 (CH_3 symmetrical deformation), 1234 (C-O-C antisymmetrical stretch), 1054 (R-C-O stretch). Please see page 152 for ^1H NMR spectrum.



Preparation of 3-(methoxycarbonyl)cyclopentyl 4-nitrobenzoate. Methyl 3-

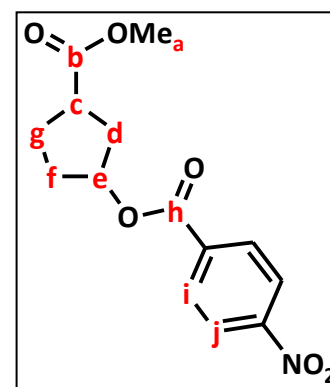
hydroxycyclopentanecarboxylate (0.1083 g, 0.75 mmol) was dissolved in ether (3.75 mL). Was added 4-nitrobenzoyl chloride (0.2788 g, 1.50 mmol) and pyridine (0.12 mL, 1.50 mmol). After 36 h at room temperature, the reaction was quenched with dilute HCl and extracted with ether. The organic layers were combined and dried over magnesium sulfate, filtered and concentrated under reduced pressure. Flash chromatography on silica gel (75:25 hexanes:ethyl acetate) affording the title compound (0.1377 g, 63% yield).

Chiral HPLC analysis (Chiralcel-AD, 98:2 hexanes:isopropanol, 0.96 flow rate) showed peaks at 42, 44, 55, and 64 minutes; TLC analysis R_f 0.52 (75:25 hexanes:ethyl acetate);

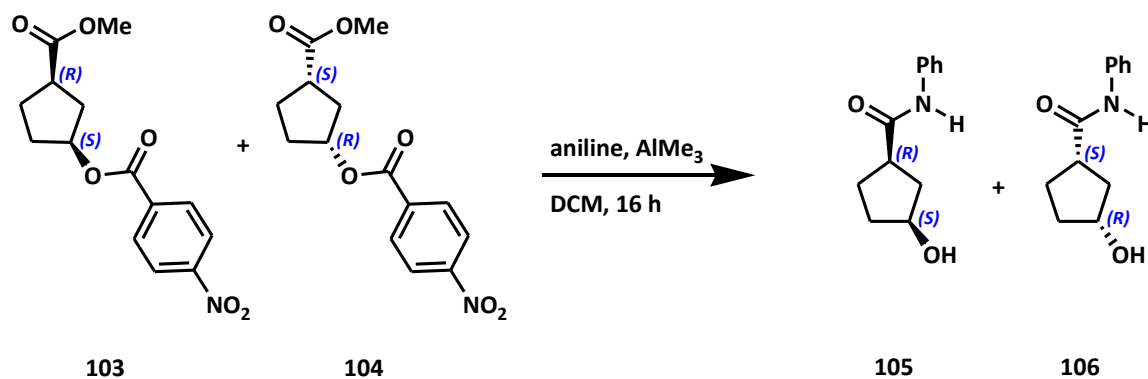
^1H NMR (400 MHz, CDCl_3 , mixture of diastereomers) δ 8.31–8.29 (4H, dt, $J = 8.9, 2.1$, j), 8.20–8.17 (4H, tt, 8.9, 4.2, i), 5.52–5.46 (1H, m, e), 5.43–

5.37 (1H, m, e), 3.68 (3H, s, a), 3.64 (3H, s, a), 3.19–3.08 (1H, m, c), 3.05–2.94 (1H, m, c), 2.41–1.89 (12H, m, d, e, f);

IR (neat, cm^{-1}) 2962 (CH sp^2 stretch), 2902 (CH sp^3 stretch), 1716 (C=O stretch), 1524 (aromatic ring stretching), 1378 (CH_3 antisymmetrical stretch), 1275 (CH_3 symmetrical



stretch), 1258 (C-O-C antisymmetrical stretch), 711 (O-C-O bend). Please see page 153 for ^1H NMR spectrum.



Preparation of 3-hydroxy-*N*-phenylcyclopentanecarboxamide from 3-

(methoxycarbonyl)cyclopentyl 4-nitrobenzoate. Under an atmosphere of nitrogen,

aniline (7 μL , 75.89 μmol) was added to dry dichloromethane. At room temperature, was

added trimethylaluminum (38 μL of a 2 M solution in hexanes, 75.89 μmol). After 15

min, 3-(methoxycarbonyl)cyclopentyl 4-nitrobenzoate (0.0089 g, 30.35 μmol) was added.

After 16 h, the reaction mixture was carefully quenched with dilute HCl and was

extracted with ether. The combined organic extracts were dried over magnesium sulfate.

Preparative plate chromatography on silica (60:40 hexanes:ethyl acetate) afforded the

title compound. Chiral HPLC analysis (Chiralcel-OD, 80:20 hexanes:isopropanol, 0.800

flow rate) showed peaks at 38 minutes and 42 minutes; TLC analysis R_f 0.39 (60:40

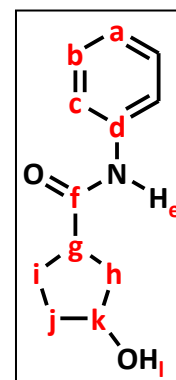
hexanes:ethyl acetate); ^1H NMR (300 MHz, CDCl_3) δ 8.15–8.06 (1H, br

d, $J = 5.2$, e), 7.55–7.53 (2H, d, $J = 7.6$, c), 7.34–7.29 (2H, dd, $J = 8.3$,

7.6, b), 7.11–7.06 (1H, t, $J = 7.4$, a), 4.56 (1H, br s, k), 2.74 (1H, br s, l),

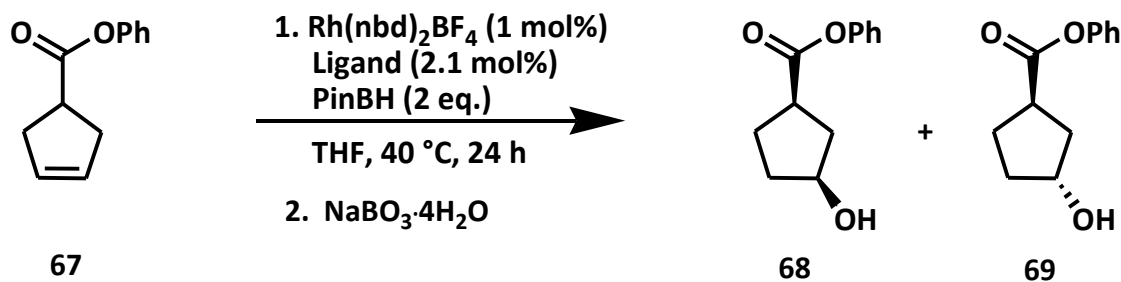
2.57–2.28 (2H, m, h), 2.03 (1H, br s, g), 1.97–1.84 (2H, m, i), 1.82–1.71

(2H, m, j); IR (neat, cm^{-1}) 3677 (OH stretch / NH stretch), 2907 (CH sp^2

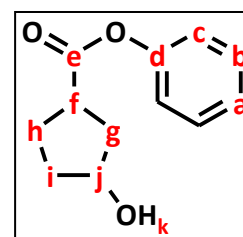


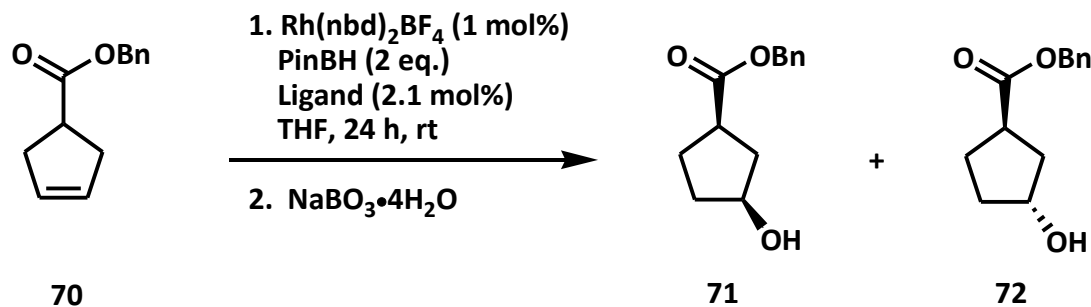
stretch), 2803 (CH sp^3 stretch), 1728 (C=O stretch), 1663 (aromatic ring stretch), 1597 (N-H bend), 1565, 1389 (C-N stretch), 1238 (C-OH in-plane bend), 1050 (C-OH stretch).

Please see page 149 for ^1H NMR spectrum.

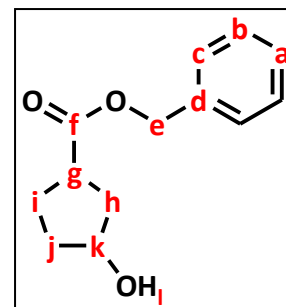


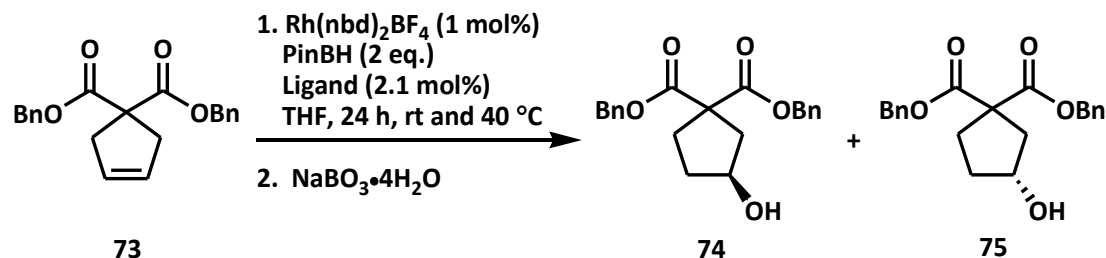
Preparation of phenyl 3-hydroxycyclopentanecarboxylate. In a glove box, a stock solution of $\text{Rh}(\text{nbd})_2\text{BF}_4$ (0.0020 g, 5.35 μM) was prepared in dry, degassed THF (1 mL). To this was added 1.0 mL of a stock solution of (TADDOL)POPh (0.0078 g, 13.25 μM) which was prepared in 1.2 mL THF. After 2 h complexation time, the resulting yellow solution was added phenyl cyclopent-3-enecarboxylate (0.0993 g, 0.528 mmol) as a solution in THF (2 mL). To this was added a solution of borane (1.06 mmol) in THF (1 mL). The reaction mixture was heated to 40 °C for 24 h. Afterwards, the reaction mixture was cooled to room temperature sodium perborate (0.4062 g, 2.64 mmol) in THF:H₂O (1:1, 4 mL total volume) and vigorously stirred for 4 h. The resulting mixture was extracted with dichloromethane; the combined organic extracts were dried over magnesium sulfate and concentrated under reduced pressure. Chiral HPLC analysis (Chiralcel-OD, 95:5 hexanes:isopropanol, 0.700) showed peaks at 47 minutes and 53 minutes; ¹H NMR (400 MHz, CDCl₃) δ 7.41–7.33 (5H, m, **a**, **b**, **c**), 4.49–4.42 and 4.37–4.30 (1H, m, **j**), 3.20–3.07 and 2.99–2.89 (1H, m, **f**), 2.21–1.77 (7H, m, **k**, **g**, **h**, **i**). Please see page 154 for ¹H NMR spectrum.



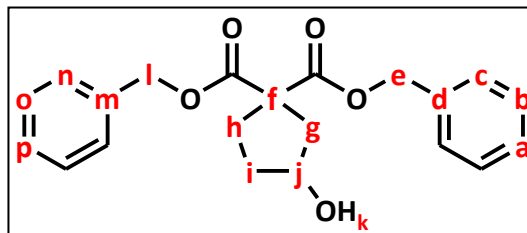


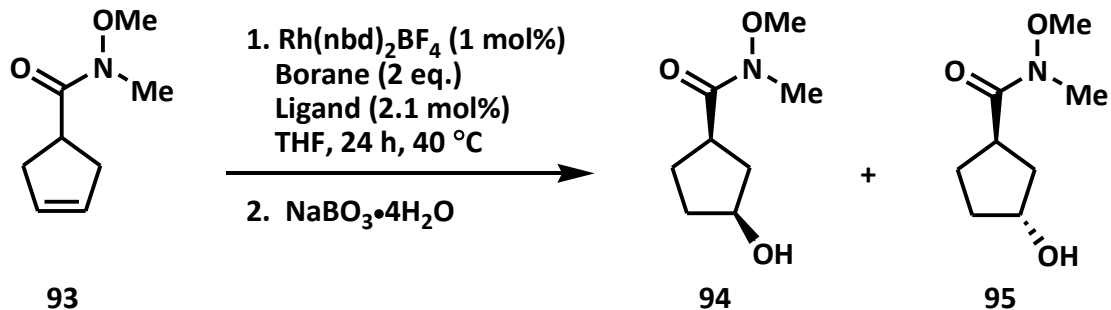
Preparation of benzyl 3-hydroxycyclopentanecarboxylate. In a glove box, a stock solution of $\text{Rh}(\text{nbd})_2\text{BF}_4$ (0.0020 g, 5.35 μM) was prepared in dry, degassed THF (1 mL). To this was added 1.0 mL of a stock solution of (TADDOL)POPh (0.0078 g, 13.25 μM) which was prepared in 1.2 mL THF. After 2 h complexation time, the resulting yellow solution was added benzyl cyclopent-3-enecarboxylate (0.1068 g, 0.528 mmol) as a solution in THF (2 mL). To this was added a solution of borane (1.06 mmol) in THF (1 mL). The reaction mixture was heated to 40 °C for 24 h. Afterwards, the reaction mixture was cooled to room temperature and quenched by the addition of a sodium perborate sodium perborate (0.4062 g, 2.64 mmol) in THF:H₂O (1:1, 4 mL total volume) and vigorously stirred for 4 h. The resulting mixture was extracted with dichloromethane; the combined organic extracts were dried over magnesium sulfate and concentrated under reduced pressure. ¹H NMR (400 MHz, CDCl₃) δ 7.40–7.34 (5H, m, **a**, **b**, **c**), 4.52–4.43 and 4.41–4.30 (1H, br s, **k**), 3.21–3.01 and 3.00–2.89 (1H, m, **g**), 2.19 (2H, s, **e**), 2.15–1.77 (7H, m, **l**, **h**, **i**, **j**). Please see page 155 for ¹H NMR spectrum.





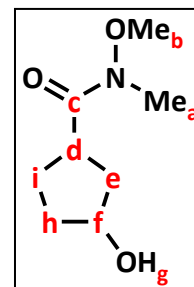
Preparation of dibenzyl 3-hydroxycyclopentanecarboxylate. In a glove box, a stock solution of $\text{Rh}(\text{nbd})_2\text{BF}_4$ (0.0020 g, 5.35 μM) was prepared in dry, degassed THF (1 mL). To this was added 1.0 mL of a stock solution of (TADDOL)POPh (0.0078 g, 13.25 μM) which was prepared in 1.2 mL THF. After 2 h complexation time, the resulting yellow solution was added dibenzyl cyclopent-3-ene-1,1-dicarboxylate (0.1775 g, 0.528 mmol) as a solution in THF (2 mL). To this was added a solution of borane (1.06 mmol) in THF (1 mL). The reaction mixture was heated to 40 °C for 24 h. Afterwards, the reaction mixture was cooled to room temperature and quenched by the addition of a sodium perborate sodium perborate (0.4062 g, 2.64 mmol) in THF:H₂O (1:1, 4 mL total volume) and vigorously stirred for 4 h. The resulting mixture was extracted with dichloromethane, the combined organic extracts were dried over magnesium sulfate and concentrated under reduced pressure. ¹H NMR (400 MHz, CDCl₃) δ 7.37–7.23 (10H, m, **a, b, c, n, o, p**), 5.16 (2H, s, **e**), 5.13 (2H, s, **l**), 4.45–4.38 (1H, br s, **j**), 2.55–2.44 (1H, m, **g**), 2.42–2.38 (2H, d, $J = 4.6$, **h**), 2.34–2.28 (1H, m, **g**), 2.00–1.90 (2H, m, **i**), 1.83–1.75 (1H, **k**). Please see page 156 for ¹H NMR spectrum.



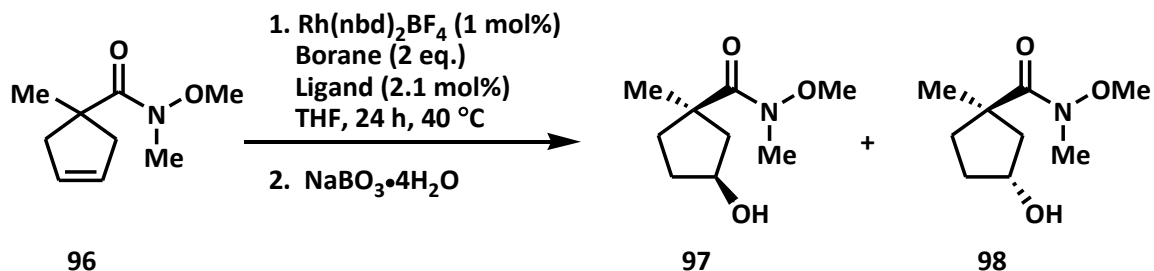


Preparation of 3-hydroxy-N-methoxy-N-methylcyclopentanecarboxamide. In a glove box, a stock solution of $\text{Rh}(\text{nbd})_2\text{BF}_4$ (0.0020 g, 5.35 μM) was prepared in dry, degassed THF (1 mL). To this was added 1.0 mL of a stock solution of (TADDOL)POPh (0.0078 g, 13.25 μM) which was prepared in 1.2 mL THF. After 2 h complexation time, the resulting yellow solution was added *N*-methoxy-*N*-methylcyclopent-3-enecarboxylate (0.0819 g, 0.528 mmol) as a solution in THF (2 mL). To this was added a solution of borane (1.06 mmol) in THF (1 mL). The reaction mixture was heated to 40 °C for 24 h. Afterwards, the reaction mixture was cooled to room temperature and quenched by the addition of a sodium perborate sodium perborate (0.4062 g, 2.64 mmol) in THF:H₂O (1:1, 4 mL total volume) and vigorously stirred for 4 h. The resulting mixture was extracted with dichloromethane; the combined organic extracts were dried over magnesium sulfate and concentrated under reduced pressure.

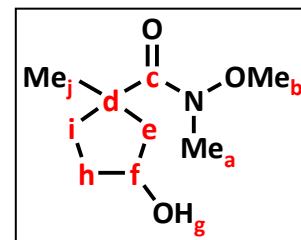
¹H NMR (400 MHz, CDCl₃) δ 4.41 and 4.31 (1H, br s, **f**), 3.75 (3H, s, **b**), 3.73(3H, s, **a**), 3.29–3.15 (2H, m, **d**, **g**), 2.25–1.89 (6H, m, **i**, **h**, **e**).

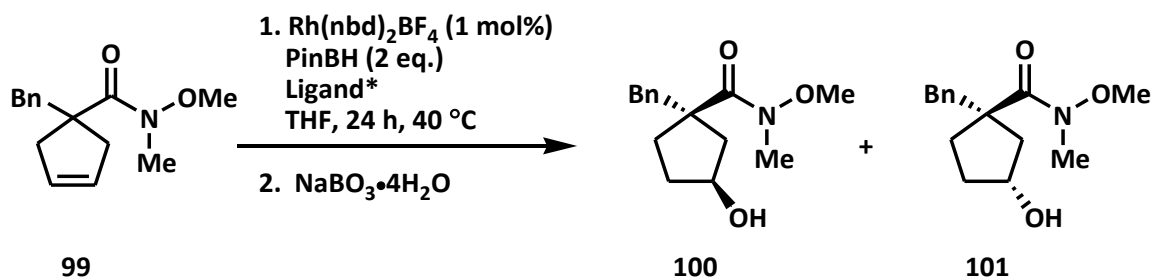


Please see page 157 for ¹H NMR spectrum.



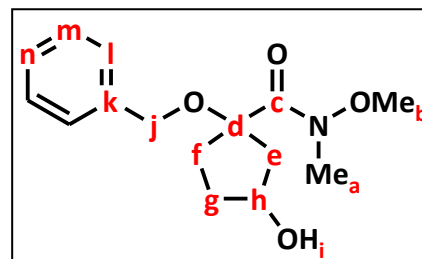
Preparation of 3-hydroxy-*N*,1-dimethoxy-*N*-methylcyclopentanecarboxamide. In a glove box, a stock solution of $\text{Rh}(\text{nbd})_2\text{BF}_4$ (0.0020 g, 5.35 μM) was prepared in dry, degassed THF (1 mL). To this was added 1.0 mL of a stock solution of (TADDOL)POPh (0.0078 g, 13.25 μM) which was prepared in 1.2 mL THF. After 2 h complexation time, the resulting yellow solution was added *N*-methoxy-*N*,1-dimethylcyclopent-3-enecarboxylate (0.0894 g, 0.528 mmol) as a solution in THF (2 mL). To this was added a solution of borane (1.06 mmol) in THF (1 mL). The reaction mixture was heated to 40 °C for 24 h. Afterwards, the reaction mixture was cooled to room temperature and quenched by the addition of a sodium perborate sodium perborate (0.4062 g, 2.64 mmol) in THF:H₂O (1:1, 4 mL total volume) and vigorously stirred for 4 h. The resulting mixture was extracted with dichloromethane; the combined organic extracts were dried over magnesium sulfate and concentrated under reduced pressure. ¹H NMR (400 MHz, CDCl₃) δ 4.58 and 4.30 (1H, br s, **f**), 3.66 (3iH, s, **b**), 3.16 (3H, s, **a**), 2.15 (3H, s, **j**), 1.96–1.49 (7H, m, **e**, **i**, **h**, **g**). Please see page 158 for ¹H NMR spectrum.

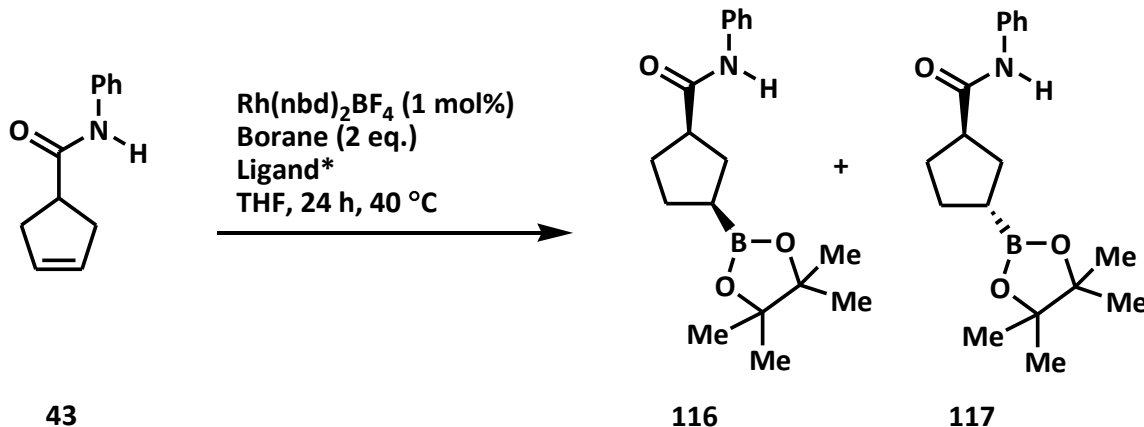




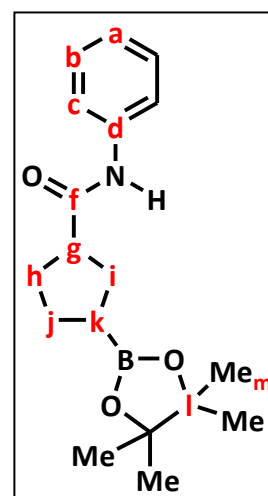
Preparation of 1-benzyl-3-hydroxy-*N*-methoxy-*N*-methylcyclopentanecarboxamide.

In a glove box, a stock solution of $\text{Rh}(\text{nbd})_2\text{BF}_4$ (0.0020 g, 5.35 μM) was prepared in dry, degassed THF (1 mL). To this was added 1.0 mL of a stock solution of (TADDOL)POPh (0.0078 g, 13.25 μM) which was prepared in 1.2 mL THF. After 2 h complexation time, the resulting yellow solution was added 1-benzyl-*N*-methoxy-*N*-methylcyclopent-3-enecarboxylate (0.130 g, 0.528 mmol) as a solution in THF (2 mL). To this was added a solution of borane (1.06 mmol) in THF (1 mL). The reaction mixture was heated to 40 °C for 24 h. Afterwards, the reaction mixture was cooled to room temperature and quenched by the addition of a sodium perborate sodium perborate (0.4062 g, 2.64 mmol) in THF:H₂O (1:1, 4 mL total volume) and vigorously stirred for 4 h. The resulting mixture was extracted with dichloromethane; the combined organic extracts were dried over magnesium sulfate and concentrated under reduced pressure. ¹H NMR (400 MHz, CDCl₃) δ 7.27–7.07 (5H, m, **l**, **m**, **n**), 4.40–4.26 (1H, m, **h**), 3.76 (3H, s, **b**), 3.23 (3H, s, **a**), 2.51–2.31 (2H, **j**), 1.89–1.84 (7H, m, **f**, **e**, **g**, **i**). Please see page 159 for ¹H NMR spectrum.

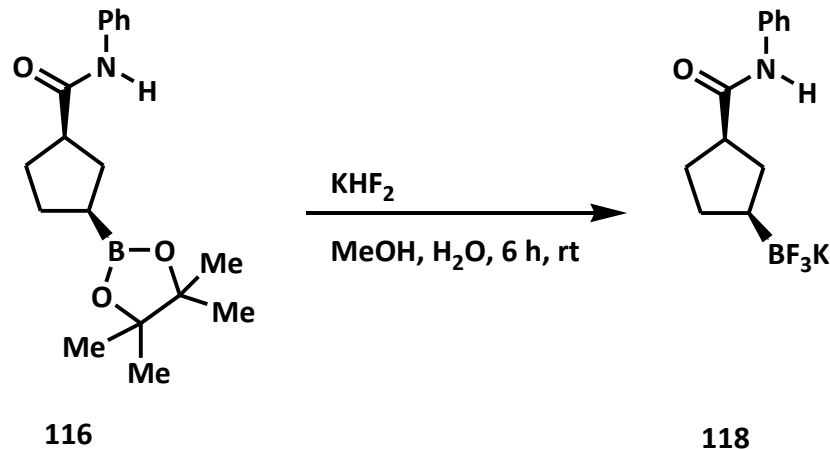




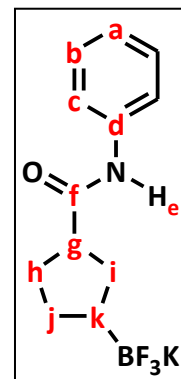
Preparation of 3-(4,4,5,5-tetramethyl-1,3,2-dioxaborolan-2-yl)-*N*-phenylcyclopentane carboxamide. In a glove box, a stock solution of $\text{Rh}(\text{nbd})_2\text{BF}_4$ (0.0020 g, 5.35 μM) was prepared in dry, degassed THF (1 mL). To this was added 1.0 mL of a stock solution of (TADDOL)POPh (0.0078 g, 13.25 μM) which was prepared in 1.2 mL THF. After 2 h complexation time, the resulting yellow solution was added *N*-phenylcyclopent-3-enecarboxamide (0.0988 g, 0.528 mmol) as a solution in THF (2 mL). To this was added a solution of borane (1.06 mmol) in THF (1 mL). The reaction mixture was heated to 40 °C for 24 h. Afterwards, the reaction mixture was concentrated under reduced pressure then extracted with dichloromethane. The combined organic extracts were dried over magnesium sulfate and concentrated under reduced pressure. Flash chromatography on silica (50:50 hexanes:ethyl acetate) afforded the title compound (0.0866 g, 80%):). TLC analysis R_f 0.58 (50:50 hexanes:ethyl acetate); ^1H NMR (300 MHz, CDCl_3) δ 7.59–7.49, (2H, d, $J = 7.8$, **b**), 7.43 (1H, s, **e**), 7.36–7.27 (2H, t, $J = 8.0$, **c**), 7.13–7.04 (1H, t,



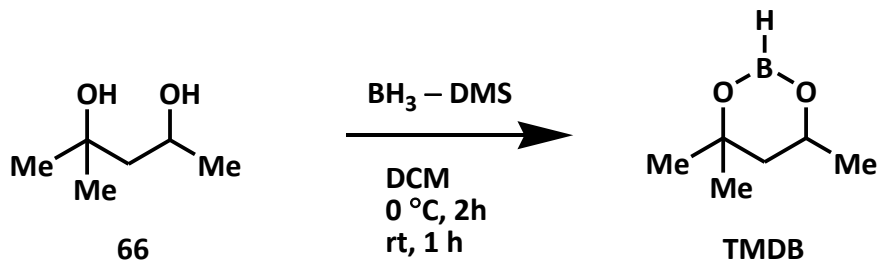
$J = 7.3$, **a**), 2.83–2.69 (1H, quintet, $J = 8.2$, **g**), 2.23–2.09 (1H, m, **k**), 2.03–1.72 (6H, m, **i**, **h**, **j**), 1.25 (12H, s, **m**); ^{13}C NMR (0.75 MHz, CDCl_3) δ 174.56 (**f**), 138.47 (**d**), 129.12 (**b**), 124.16 (**a**), 120.00 (**c**), 83.51 (**l**), 75.25 (**g**), 48.68 (**h**), 33.26 (**i**), 31.53 (**j**), 28.41 (**k**), 24.97 (**m**); IR (neat, cm^{-1}) 3297 (N-H stretch), 2974 (CH sp^2 stretch), 2929 (CH sp^3 stretch), 1663 (C=O stretch), 1605 (C=C stretch), 1536 (N-H bend), 1430 (aromatic ring stretch), 1368 (CH_3 antisymmetrical stretch), 1307 (CH_3 symmetrical stretch), 751 (CH_2 rocking), 666 (C-C=O bend); HRMS (HRFAB) calcd. for $\text{C}_{18}\text{H}_{27}\text{BNO}_3$ ($\text{M}+\text{H}$) $^+$: 316.2084, found 316.2073 m/z . Please see page 160–161 for ^1H and ^{13}C NMR spectra, respectively.



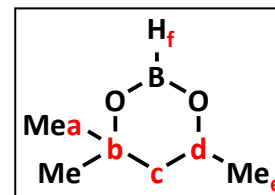
Preparation of potassium 3-*N*-phenylcyclopentancarboxamide trifluoroborate. After dissolving the organoboronate ester (0.2137 g, 0.68 mmol) in methanol (0.75 mL) at room temperature, was added dropwise a saturated aqueous solution of potassium hydrogen fluoride (0.2648 g, 3.39 mmol, 4.52 M). The reaction was allowed to stir at room temperature for 6 h. The solvent was then removed *in vacuo* to afford a mixture of solids that was dried under low pressure for 0.5 h. Extraction of the solid mixture was done with acetone, followed by filtration afforded a solution of the product in acetone. The solution was then reduced under reduced pressure to afford a concentrated acetone solution. Diethylether was added to precipitate the product. After filtration, the product was obtained as a white crystalline solid (0.1555 g, 78% yield): ^1H NMR (300 MHz, CD_3OD) δ 9.64 (1H, s, **e**), 7.61–7.52, (2H, d, $J = 7.7$, **c**), 7.34–7.24 (2H, t, $J = 8.3$, **b**), 7.11–7.02 (1H, t, $J = 7.4$, **a**), 2.80–2.67 (1H, m, **g**), 2.07–1.95, (1H, m, **j**), 1.91–1.80 (2H, m, **h**), 1.77–1.55 (3H, m, **j**, **i**), 0.89 (1H, br s, **k**); ^{19}F NMR (282 MHz, CD_3OD) δ -151.05; IR (neat,



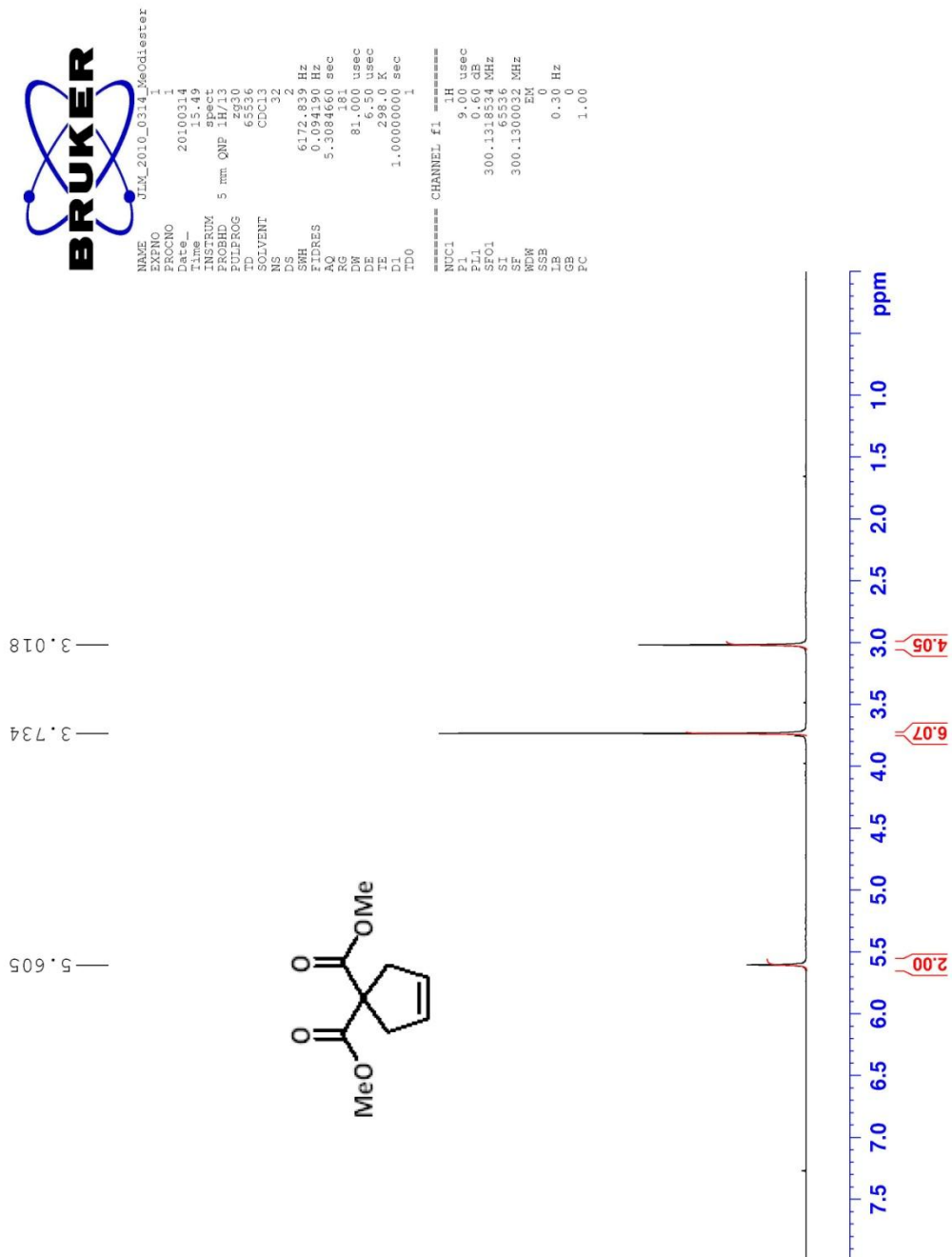
cm⁻¹) 3416 (N-H stretch), 2974 (CH sp² stretch), 2913 (CH sp³ stretch), 2353, 2325, 1671 (C=O stretch), 1385 (C-N stretch), 825 (out-of-plane CH aromatic deformation), 772 (CH₂ rocking). Please see page 162–163 for ¹H and ¹⁹F NMR spectra, respectively.

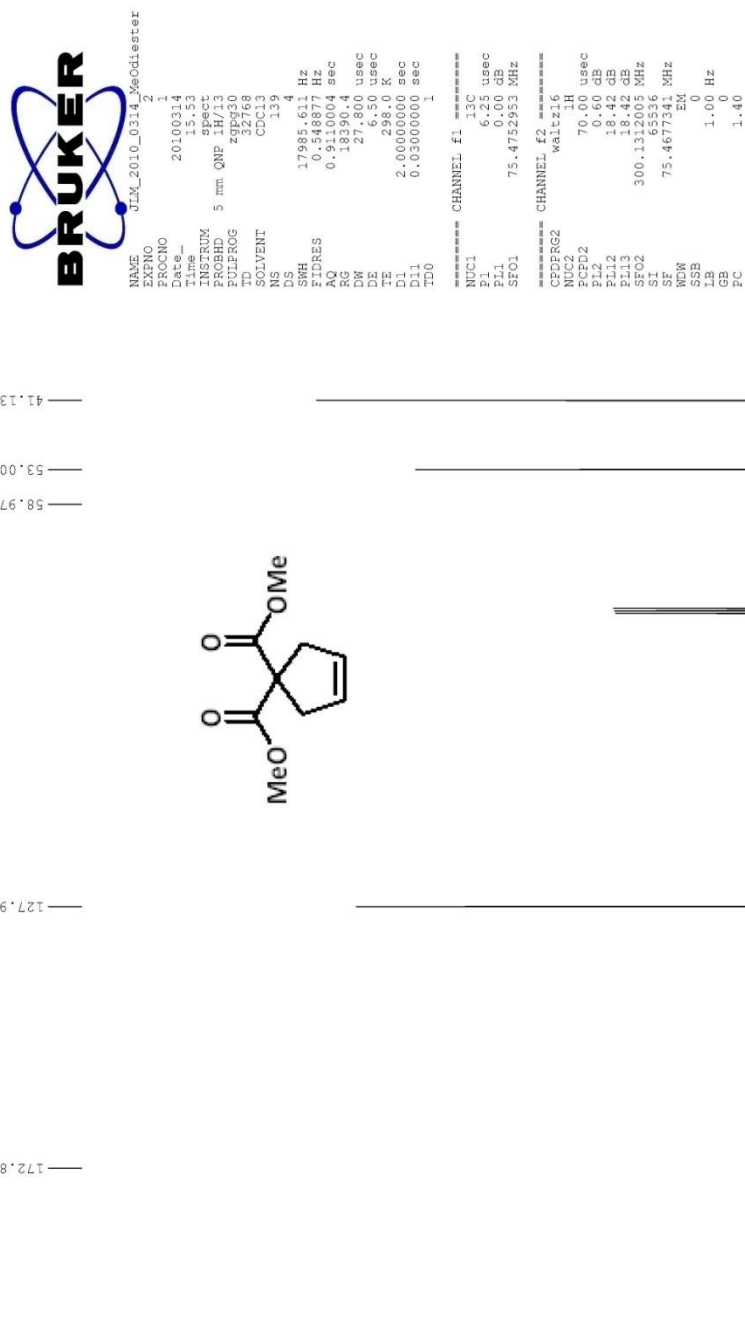


Preparation of TMDB.²⁷ Under an atmosphere of nitrogen, 2-methylpentan-2,4-diol (2.3636 g, 20.00 mmol) was dissolved in dry DCM (10 mL) and cooled to 0 °C. A concentrated solution of BH_3 in DMS (2.0 mL) was added dropwise and stirred at this temperature for 2 h. It was allowed to stir at room temperature for 1 h; after this allotted time the solution was concentrated *in vacuo* for 1 h without added heat. The ^1H NMR is checked for DMS. When DMS no longer remains, the liquid is distilled at 60 torr (50–100 °C) to yield a colorless liquid (1.700 g, 66%): ^1H NMR (400 MHz, CDCl_3) δ 4.26–4.18 (1H, m, **f**), 1.89–1.77 (1H, dq, $J = 14.18, 2.8$, **c**), 1.63–1.50 (1H, t, $J = 13.2$, **c**), 1.33–1.25 (9H, m, **a, e**). Please see page 164 for ^1H NMR spectrum.



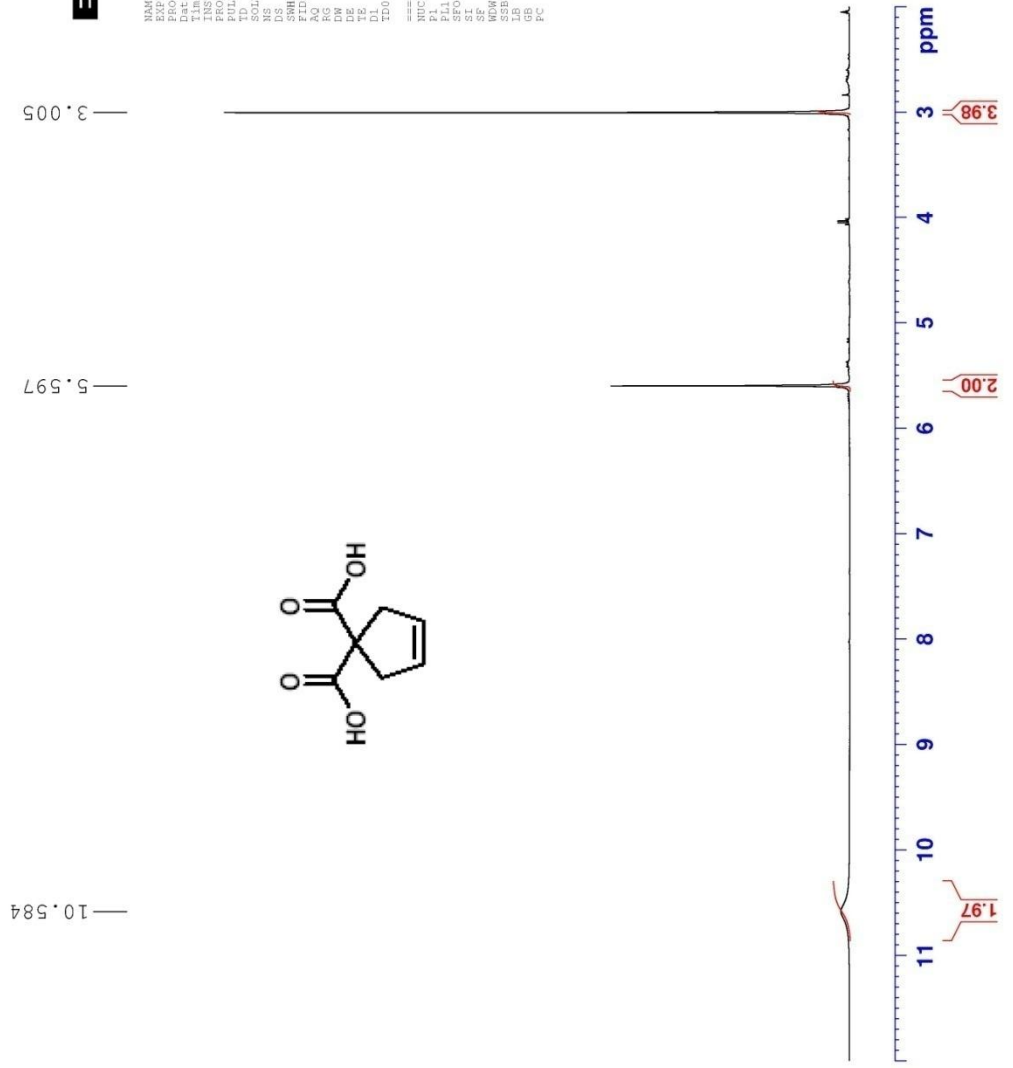
Chapter 15: Spectra Appendix







NAME JTM_2010_0711_discid_acetone_d
PROCNO 1
Date_ 20100711
Time 23:50
INSTRUM 5 mm QNP 1H/13
PROBHD 5 mm QNP 1H/13
PULPROG zgpg30
TD 65536
SOLVENT Acetone
DS 2
SWH 6076.14 Hz
FIDRES 0.73434 Hz
AQ 3.9564243 sec
RG 35.9
IN 60.40 usec
DE 6.50 usec
TE 298.0 K sec
D1 1.00000000 sec
TD0 1
===== CHANNEL f1 =====
NUC1 13C 1H usec
P1 1.00 usec
PL1 -3.50 dB
SFO1 400.1324710 MHz
SI 65536
WDW EM
SSB 0
LB 0.50 Hz
GB 0
PC 1.00



10.584

5.597

3.005

1.97

2.00

3.98



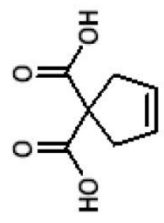
JTM_2010_0711_diacid_acetone_d

NAME
PROCNO
Date_
Time
Time
PROCNO
PROCPRG
PULPROG
TD
SOLVENT
NS
DS
AQ
RG
DE
TE
DI
TD

1
20100711
23.59
1H/13
5 mm QNP 1H/13
zgpg30
65536
Acetone-d6
128
4
29866.8 Hz
299055.8 Hz
1.5664756 sec
20.1024
6.50 usec
298.0 K sec
2.00000000 sec
0.03000000 sec
1

===== CHANNEL F1 =====
NUC1
P1
PL1
SFO1
===== CHANNEL F2 =====
CPDPRG2
NUC2
P2
PL2
PL12
PL13
SI
SF
WDW
SSB
LB
GB
PC

13C
10.00 usec
0.50 dB
100.6282298 MHz
waltz16
1H
70.1H usec
-3.35 dB
13.34 dB
13.08 dB
400.131068 MHz
65536
100.6126774 MHz
EM
0
1.00 Hz
0
1.40

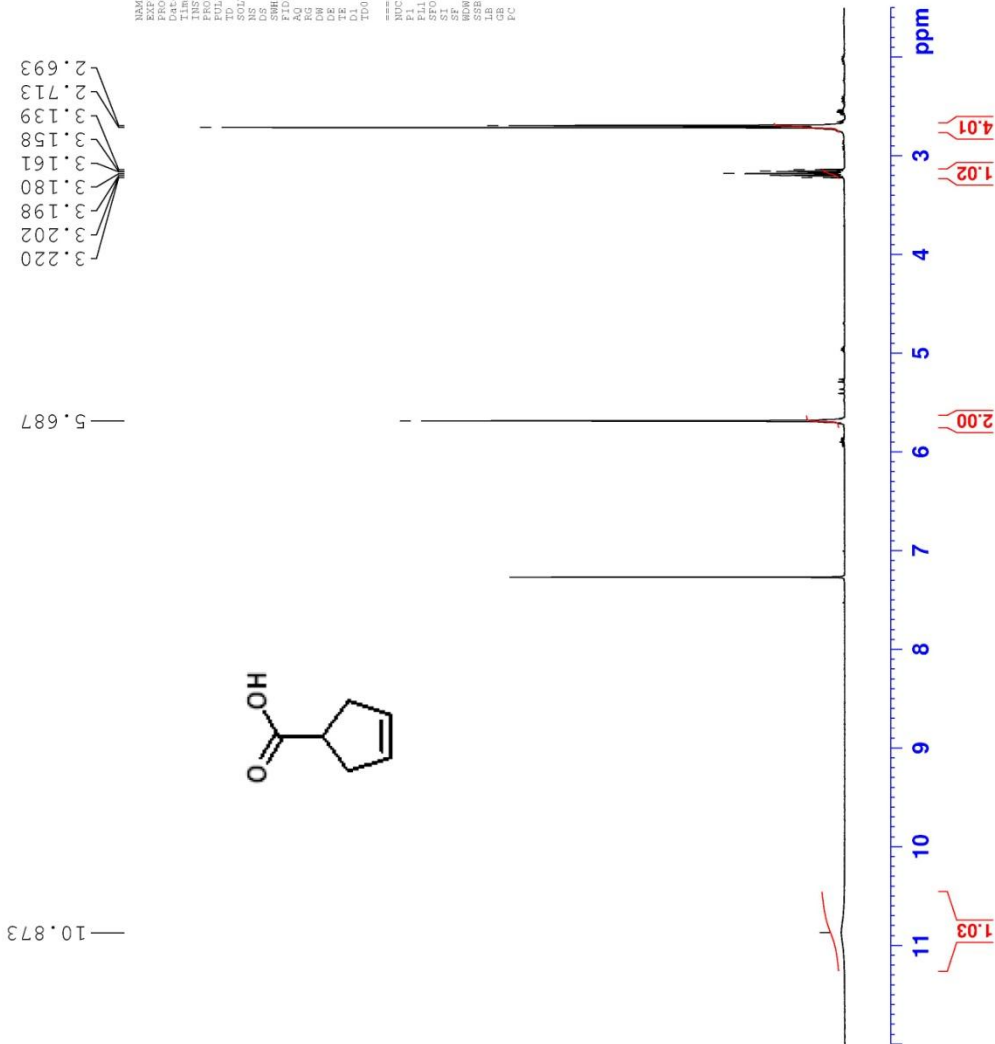
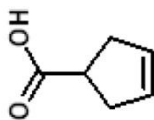




JLM_04109_cyclopentene_monocid

NAME JLM_04109_cyclopentene_monocid
EXPNO 1
PROCNO 1
Time 20090401
Time 18:21
INSTRUM spect
PROBHD 5 mm QNP
PULPROG zgpg30
TD 65536
SOLVENT CDCl3
DS 2
SWH146 Hz
AQ 3.958443 sec
RG 574.7
DE 6.50 usec
TE 296.4 K
TD0 1.0000000 sec
===== CHANNEL f1 =====
NUC1 13C
P1 10.50 usec
PL1 -2.35 dB
SFO1 400.12630 MHz
SF 400.130057 MHz
WDW EM
SSB 0
LB 0.30 Hz
GB 0
PC 1.00

10.873
5.687
3.220
3.202
3.198
3.180
3.161
3.158
3.139
2.713
2.693



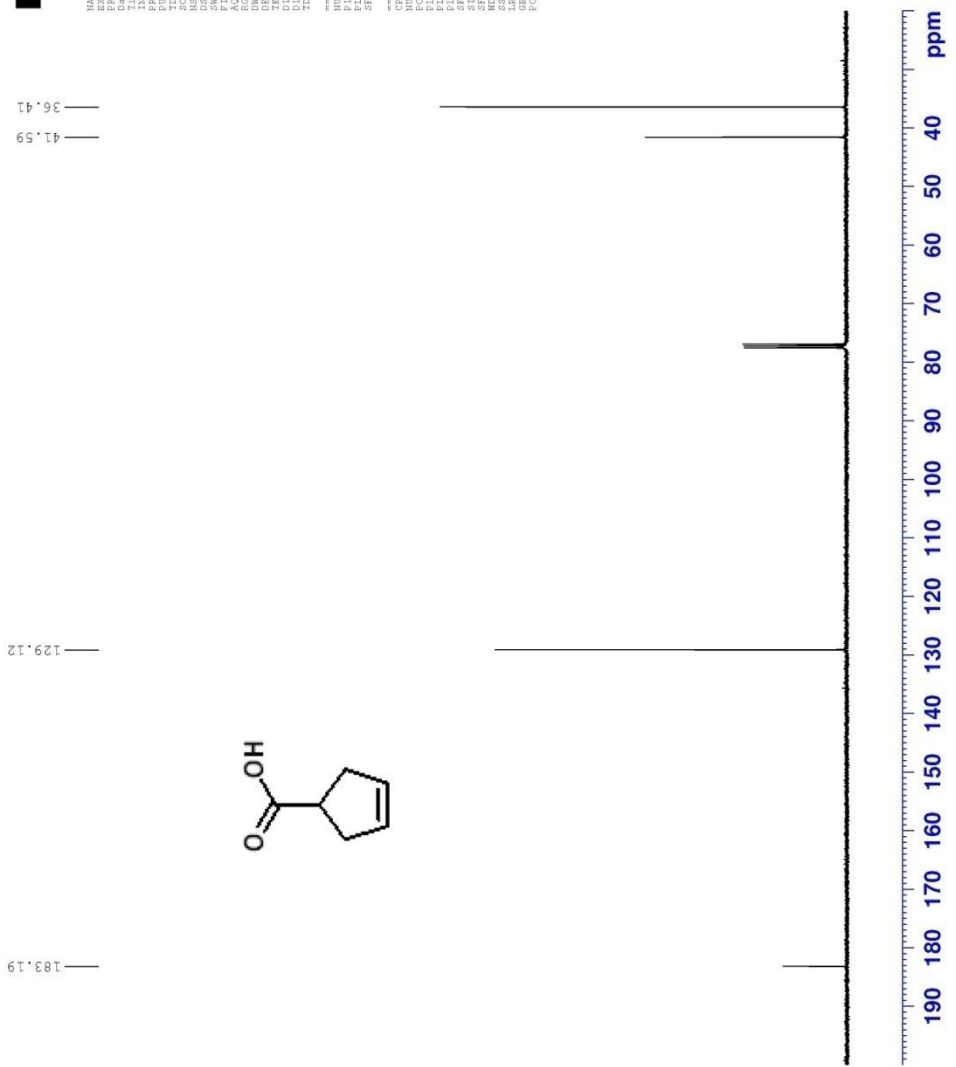
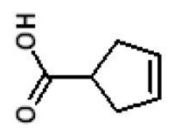


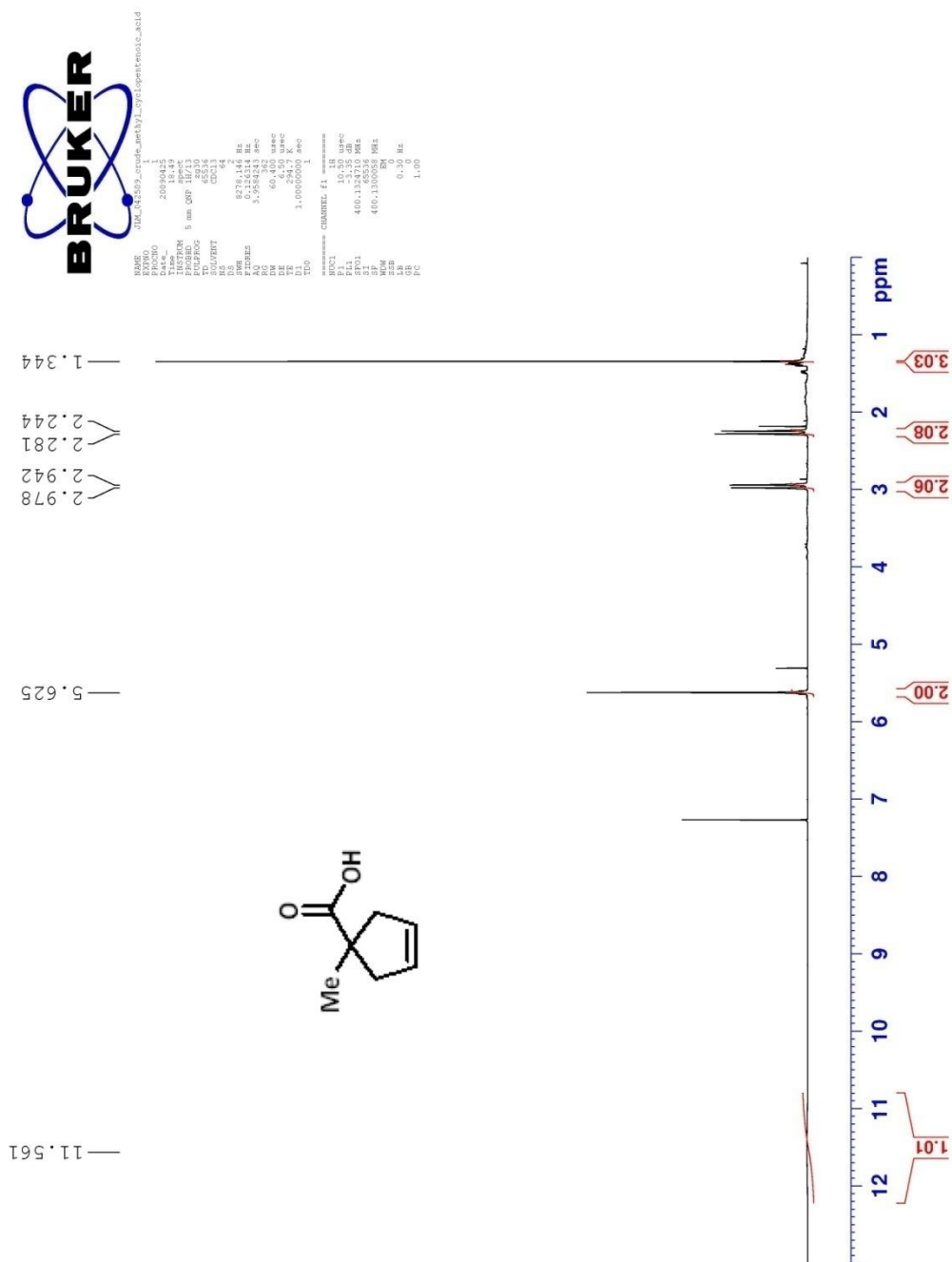
NAME JTM_030933_Cyclopentenolone_acid_dqf1st

PROCNO 1
 F2 20191885
 Time 19.23
 INSTRM spect
 PULPROG zgpg30
 F2 5 mm QNP
 FILLPROG zgpg30
 TD 65536
 SFO1 100.6228238 MHz
 NS 2
 DS 2
 SWH 23380.874 Hz
 FIDRES 0.365918 Hz
 AQ 1.058076 sec
 RG 327.500
 DW 20.850 usec
 DE 1.50 usec
 TE 303.2 K
 D1 2.00000000 sec
 D11 0.03000000 sec
 TRO 1

===== CHANNEL f1 =====
 NUC1 13C
 P1 9.50 usec
 PL1 0.00 dB
 SFO1 100.6228238 MHz

===== CHANNEL f2 =====
 CPDPRG2 waltz16
 P2 70.00 usec
 PL2 -4.00 dB
 PL12 13.82 dB
 PL13 13.82 dB
 SFO2 400.1316005 MHz
 SF 100.6127503 MHz
 SWH 400.1316005 MHz
 LB 1.00 Hz
 GB 0
 PC 1.40

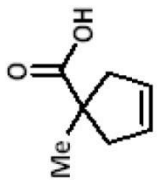
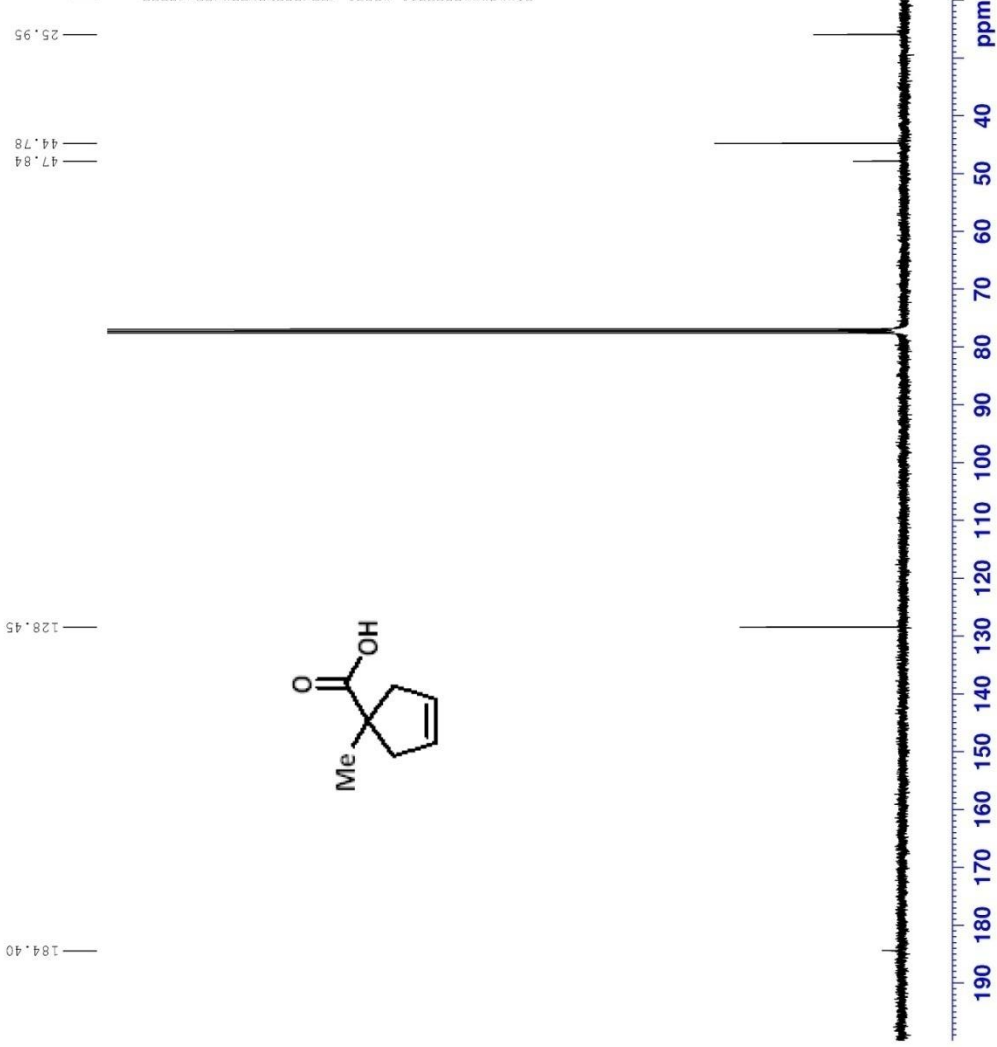






NAME JRL_042509_01c_methy_1_cyclopentenoic_acid

EXPNO 20080425
 F2 - 19.21
 F3 - 19.21
 F4 - 19.21
 F5 - 19.21
 F6 - 19.21
 F7 - 19.21
 F8 - 19.21
 F9 - 19.21
 F10 - 19.21
 F11 - 19.21
 F12 - 19.21
 F13 - 19.21
 F14 - 19.21
 F15 - 19.21
 F16 - 19.21
 F17 - 19.21
 F18 - 19.21
 F19 - 19.21
 F20 - 19.21
 F21 - 19.21
 F22 - 19.21
 F23 - 19.21
 F24 - 19.21
 F25 - 19.21
 F26 - 19.21
 F27 - 19.21
 F28 - 19.21
 F29 - 19.21
 F30 - 19.21
 F31 - 19.21
 F32 - 19.21
 F33 - 19.21
 F34 - 19.21
 F35 - 19.21
 F36 - 19.21
 F37 - 19.21
 F38 - 19.21
 F39 - 19.21
 F40 - 19.21
 F41 - 19.21
 F42 - 19.21
 F43 - 19.21
 F44 - 19.21
 F45 - 19.21
 F46 - 19.21
 F47 - 19.21
 F48 - 19.21
 F49 - 19.21
 F50 - 19.21
 F51 - 19.21
 F52 - 19.21
 F53 - 19.21
 F54 - 19.21
 F55 - 19.21
 F56 - 19.21
 F57 - 19.21
 F58 - 19.21
 F59 - 19.21
 F60 - 19.21
 F61 - 19.21
 F62 - 19.21
 F63 - 19.21
 F64 - 19.21
 F65 - 19.21
 F66 - 19.21
 F67 - 19.21
 F68 - 19.21
 F69 - 19.21
 F70 - 19.21
 F71 - 19.21
 F72 - 19.21
 F73 - 19.21
 F74 - 19.21
 F75 - 19.21
 F76 - 19.21
 F77 - 19.21
 F78 - 19.21
 F79 - 19.21
 F80 - 19.21
 F81 - 19.21
 F82 - 19.21
 F83 - 19.21
 F84 - 19.21
 F85 - 19.21
 F86 - 19.21
 F87 - 19.21
 F88 - 19.21
 F89 - 19.21
 F90 - 19.21
 F91 - 19.21
 F92 - 19.21
 F93 - 19.21
 F94 - 19.21
 F95 - 19.21
 F96 - 19.21
 F97 - 19.21
 F98 - 19.21
 F99 - 19.21
 F100 - 19.21



184.40

128.45

47.84

44.78

25.95

190 180 170 160 150 140 130 120 110 100 90 80 70 60 50 40 ppm



NAME JIM_052909_Bn_COOH_crude

EXPNO 1
 PROCNO 1
 Date_ 20090529
 Time 18:58
 INSTRUM spect
 PROBHD 5 mm Multinucl
 PULPROG zg30
 TD 65536
 SOLVENT CDCl3
 NS 64
 DS 4
 SFO 8278.146 Hz
 FIDRES 0.156314 Hz
 AQ 3.9584243 sec
 RG 128
 DW 60.400 usec
 DE 6.50 usec
 TE 300.2 K
 D1 1.00000000 sec
 TD0 1

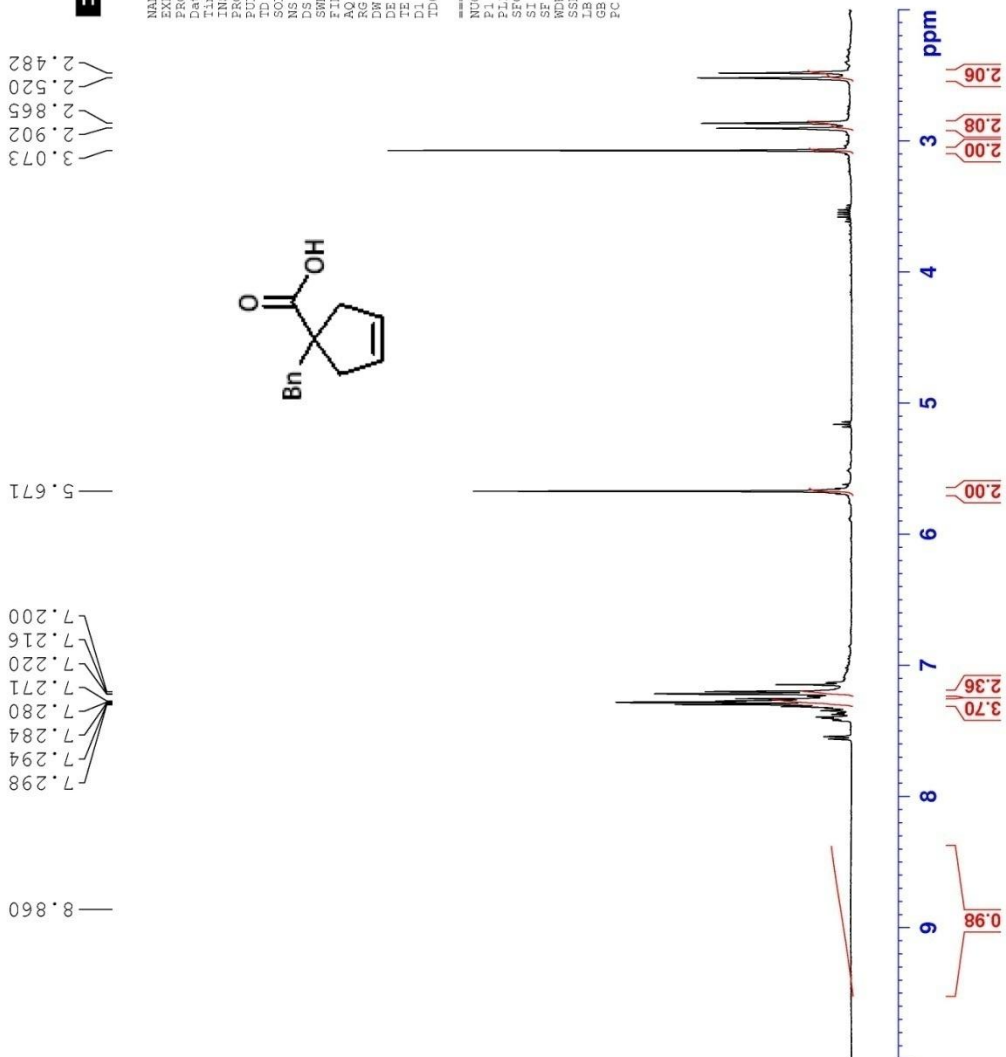
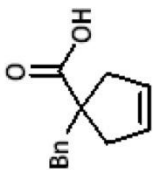
===== CHANNEL f1 =====
 NUC1 1H
 P1 10.50 usec
 PL1 -3.35 dB
 SFO1 400.132410 MHz
 SF 400.130000 MHz
 WDW EM
 SSB 0
 LB 0.30 Hz
 GB 0
 PC 1.00

3.073
 2.902
 2.865
 2.520
 2.482

5.671

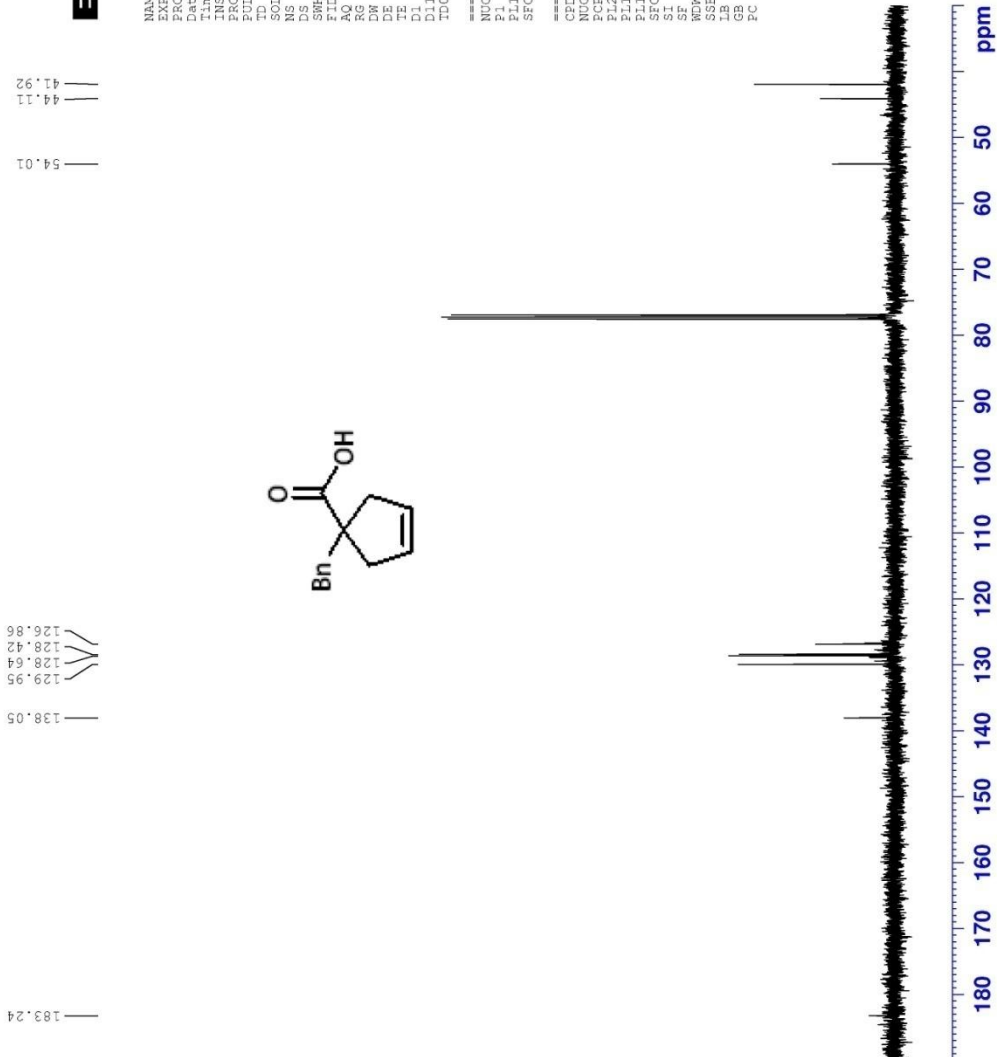
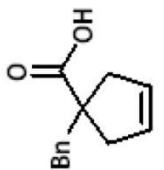
7.298
 7.294
 7.284
 7.280
 7.271
 7.220
 7.216
 7.200

8.860





NAME JILX_052909_Bn_COOH_crude
 EXZNO 2
 PROCNO 1
 Date_ 20090529
 Time_ 19.09
 INSTRUM spect
 PROBHD 5 mm Multinucl
 PULPROG zgpg30
 TD 65536
 SOLVENT CDCl3
 NS 64
 DS 4
 SWH 23980.814 Hz
 FIDRES 0.365918 Hz
 AQ 1.3664756 sec
 RG 5792.6
 DM 20.850 usec
 DE 8.50 usec
 TE 296.2 K
 D1 0.000000 sec
 D11 0.03000000 sec
 TD0 1



===== CHANNEL f1 =====
 NUC1 13C
 P1 10.25 usec
 PL1 0.00 dB
 SF01 100.6228298 MHz
 ===== CHANNEL f2 =====
 CPDPRG2 waltz16
 NUC2 1H
 PCPD2 80.00 usec
 PL2 0.00 dB
 PL12 13.00 dB
 PL14 13.00 dB
 SF02 400.1314005 MHz
 SI 65536
 SF 100.6127492 MHz
 WDW EM
 SSB 0
 LB 1.00 Hz
 GB 0
 FC 1.40



JML_051209_NHPL_cyclopentene

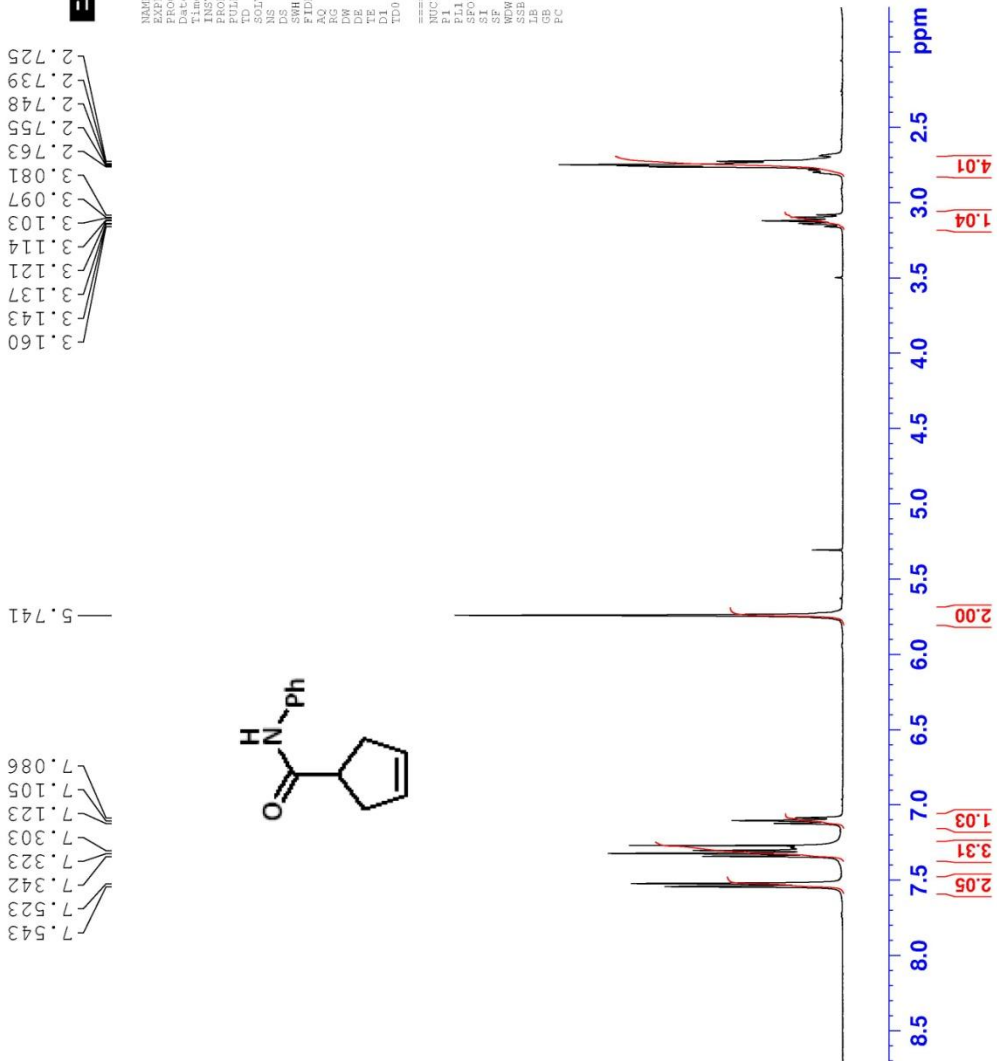
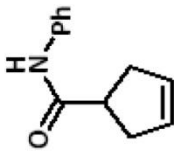
NAME JML_051209_NHPL_cyclopentene
 PROCNO 1
 Date_ 20090512
 Time 12.03
 INSTRUM spect
 PULPROG zgpg30
 TD 65536
 SOLVENT CDCl3
 NS 42
 DS 4
 SWH 8278.146 Hz
 FIDRES 0.126314 Hz
 AQ 3.958423 sec
 RG 655.36
 DW 60.400 usec
 DE 6.50 usec
 TE 294.7 K
 D1 1.00000000 sec
 T00 1

===== CHANNEL F1 =====
 NUC1 1H
 P1 10.00 usec
 PL1 -3.35 dB
 SFO1 400.1324710 MHz
 SI 65536
 SF 400.1300057 MHz
 SWH 8278.146 Hz
 SSB 0
 LB 0.30 Hz
 GB 0
 PC 1.00

3.160
 3.143
 3.137
 3.121
 3.114
 3.103
 3.097
 3.081
 2.763
 2.755
 2.748
 2.739
 2.725

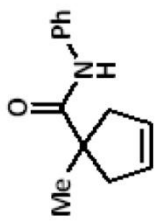
5.741

7.543
 7.523
 7.342
 7.323
 7.303
 7.123
 7.105
 7.086

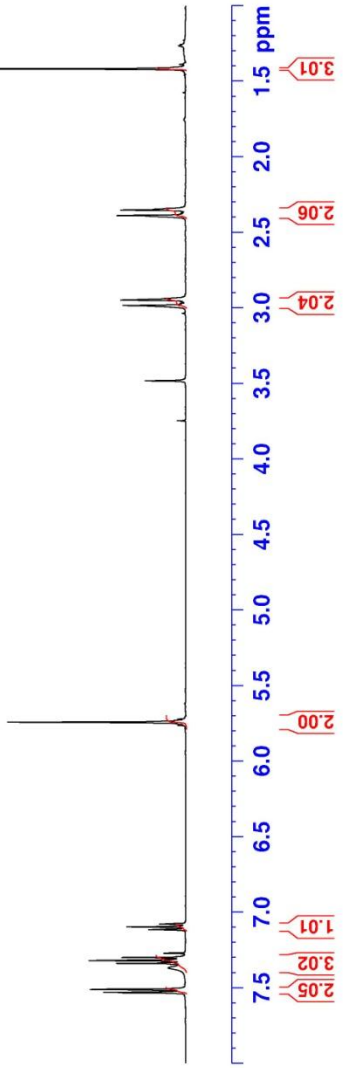




NAME: C14_042609_Me_N(Ph)_Cyclopentene_pure
EXPNO: 1
PROCNO: 1
Date_ 20090526
Time: 23:26
INSTRUM: spect
PROBHD: 5 mm QNP 1H/13
PULPROG: zgpg30
SOLVENT: CDCl3
NS: 16
DS: 4
SWH: 8278.146 Hz
AQ: 0.0561 sec
RG: 327.500 Hz
FIDRES: 0.713 Hz
DE: 6.650 usec
TE: 328.2 K
TD: 1,000,000
SFO: 400.1300054 MHz
AQ: 0.30 Hz
PC: 1.00

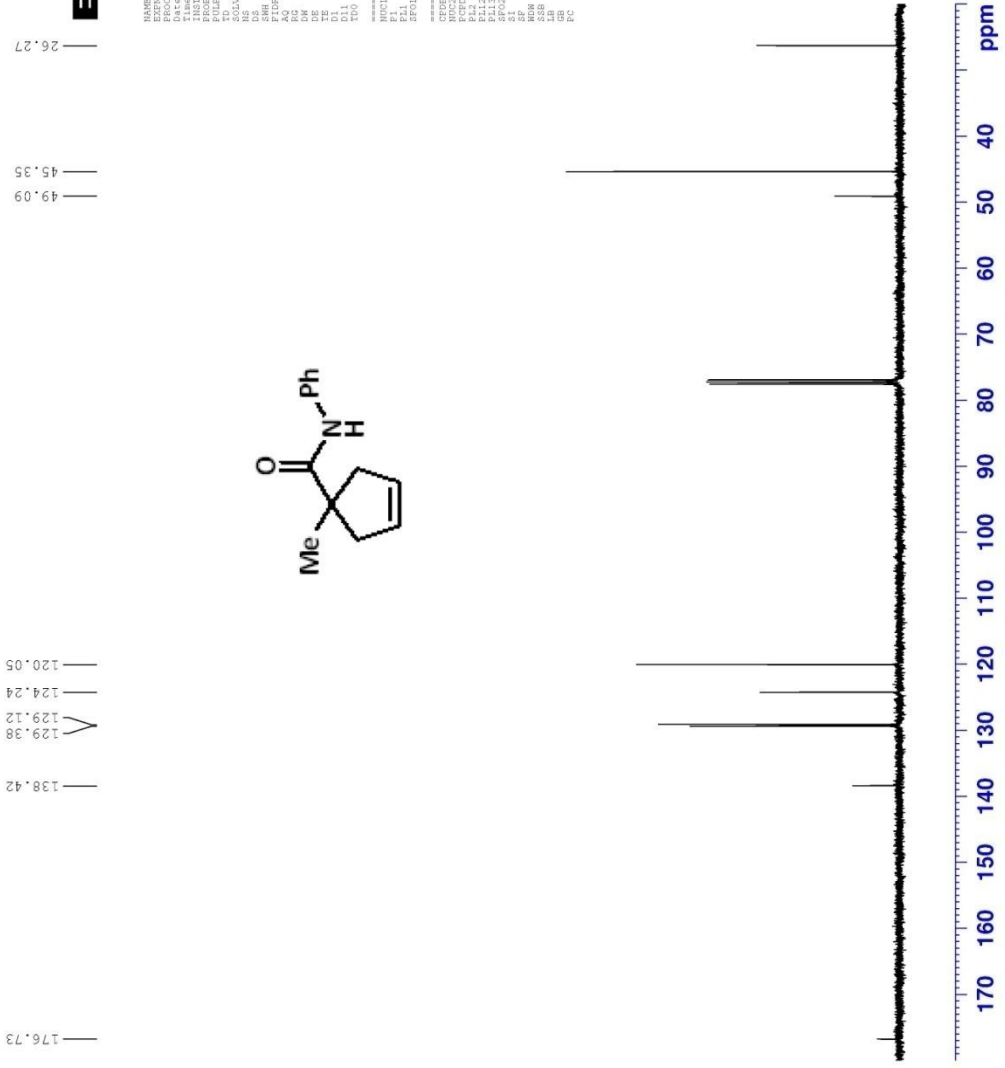
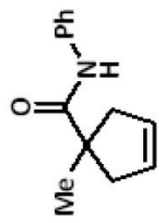


7.509
7.507
7.366
7.337
7.318
7.297
7.115
7.097
7.078
5.742
1.418
2.984
2.949
2.389
2.352





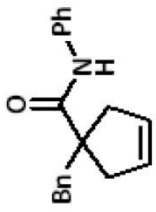
NAME: ULL_042609_Me_2101191_Cyclopentene_101
 EXPNO: 1
 PROCNO: 20009462
 F2 - Date_ Time: 21.30
 F2 - Time: 21.30
 PULPROG: zgpg30
 FILLFACTOR: 5
 SOLVENT: CDCl3
 NS: 102
 DS: 4
 SWH: 23940.814 Hz
 FWHZ: 23940.814 Hz
 AQ: 0.004258 sec
 RG: 1.0266735 Hz
 RB: 2580.3 Hz
 RE: 2.0000000 Hz
 DE: 6.650 usec
 TE: 300.2 K
 DT: 0.0002500 sec
 D1: 0.03000000 sec
 D11: 1.00000000 sec
 D12: 1.00000000 sec
 D13: 1.00000000 sec
 D14: 1.00000000 sec
 D15: 1.00000000 sec
 ===== CHANNEL f1 =====
 NU1: 1
 F1: 9.50 usec
 PC: 1.00 Hz
 LB: 1.40 Hz
 GB: 0.00 Hz
 EB: 0.00 Hz
 FB: 100.0230398 MHz
 ===== CHANNEL f2 =====
 CEFFREQ2: wall1216
 NU2: 1
 F2: 70.00 usec
 PC2: 1.00 Hz
 LB2: -4.00 dB
 GB2: 0.00 Hz
 EB2: 0.00 Hz
 FB2: 121.6230398 MHz
 ===== CHANNEL f3 =====
 SFO3: 400.1316006 MHz
 SF: 100.6127314 MHz
 SWH: 23940.814 Hz
 DS: 4
 SSB: 0.00 Hz
 LB: 1.00 Hz
 GB: 0.00 Hz
 EB: 0.00 Hz
 FB: 1.40 Hz





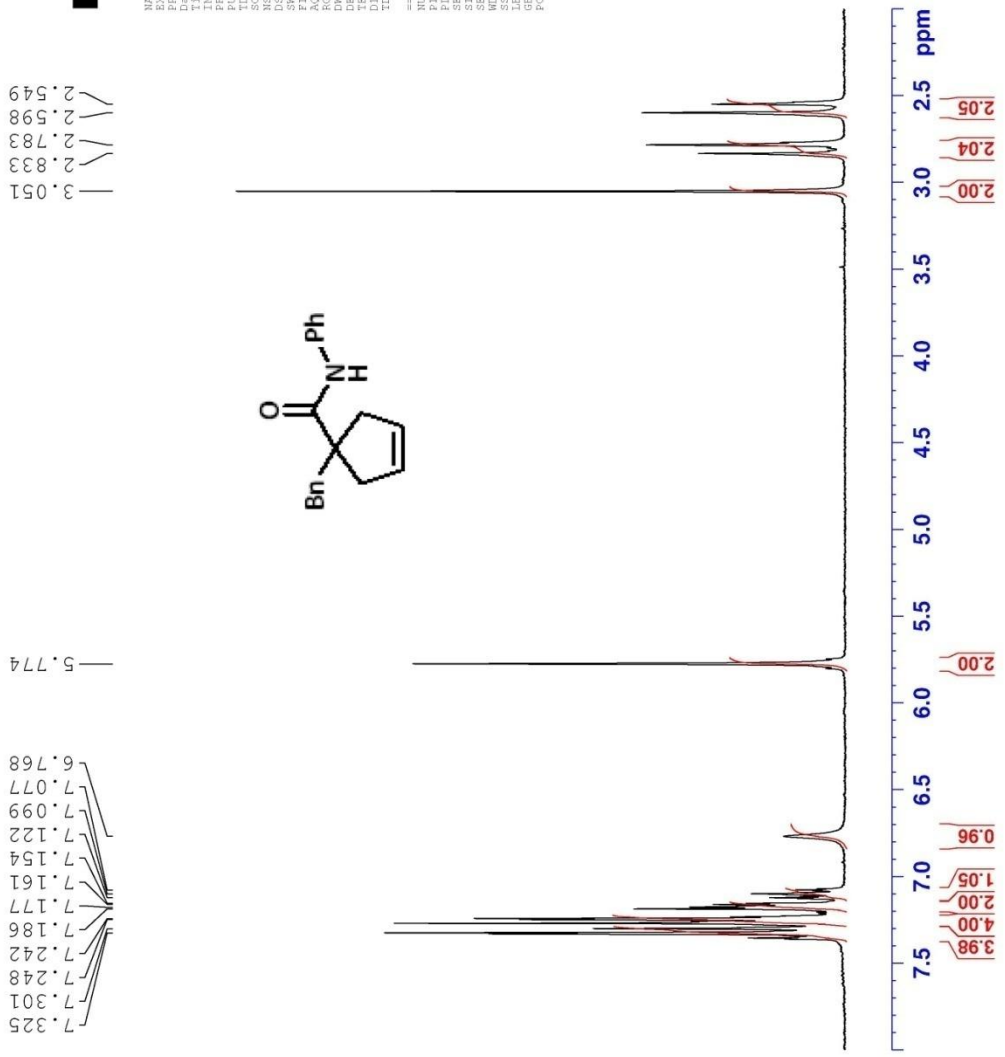
NAME JTM_201_0_0428_Bn_BHPL13C_Char
 PROCNO 1
 Date_ 20100428
 Time 15:09
 INSTRUM spect
 PROCBD 5 mm QNP 1H/13
 PULPROG zgpg30
 TD 65536
 SOLVENT CDCl3
 NS 6016
 DS 2
 SWH 6176.81 Hz
 FIDRES 0.1084130 Hz
 AQ 5.3084660 sec
 RG 812.7
 DE 81.00 usec
 TE 298.0 K sec
 DI 1.0000000 sec
 TDO 1
 ===== CHANNEL f1 =====
 NUC1 13C
 P1 8.00 usec
 PL1 0.00 dB
 SFO1 300.1318534 MHz
 SI 65536
 WDW HANN
 SSB 0
 LB 0
 GB 0
 PC 1.00

3.051
 2.833
 2.783
 2.598
 2.549



5.774

7.325
 7.301
 7.248
 7.242
 7.186
 7.177
 7.161
 7.154
 7.122
 7.099
 7.077
 6.768

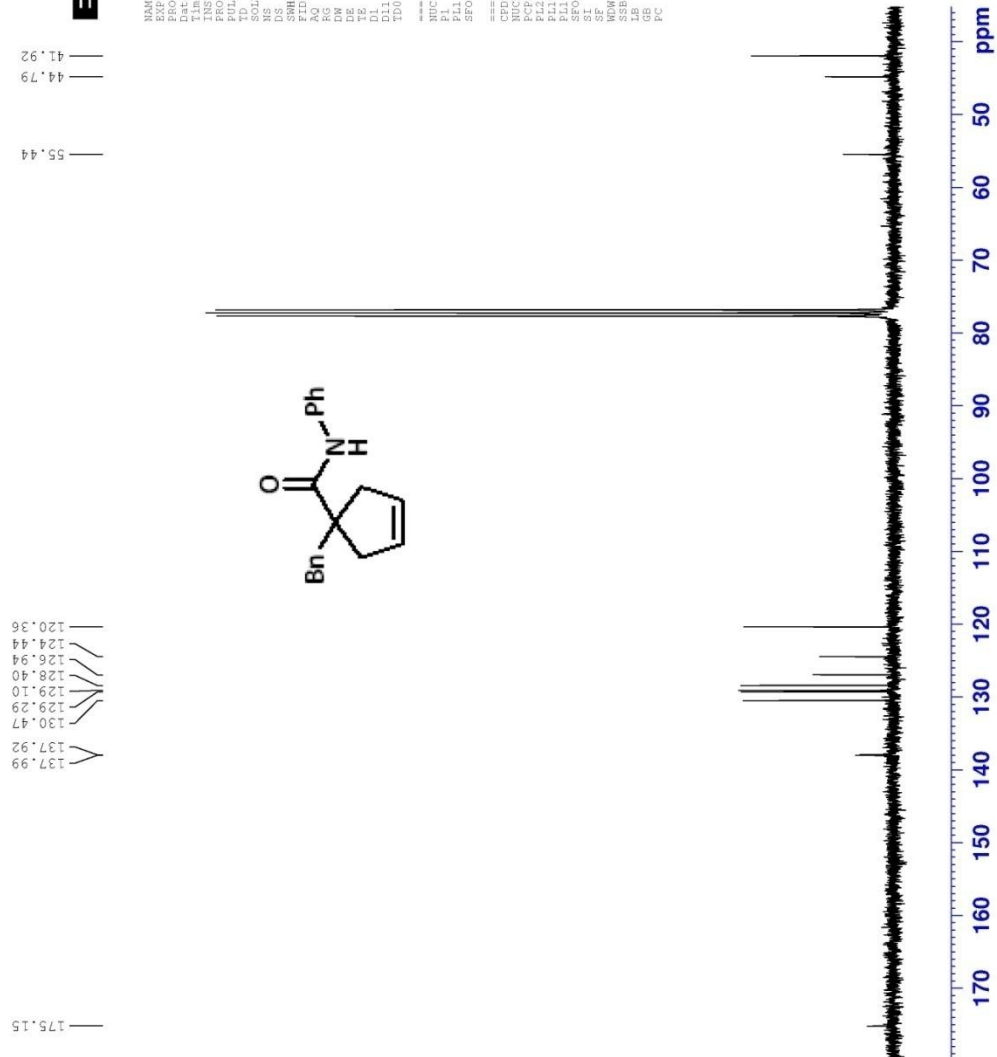
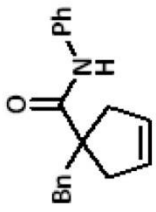


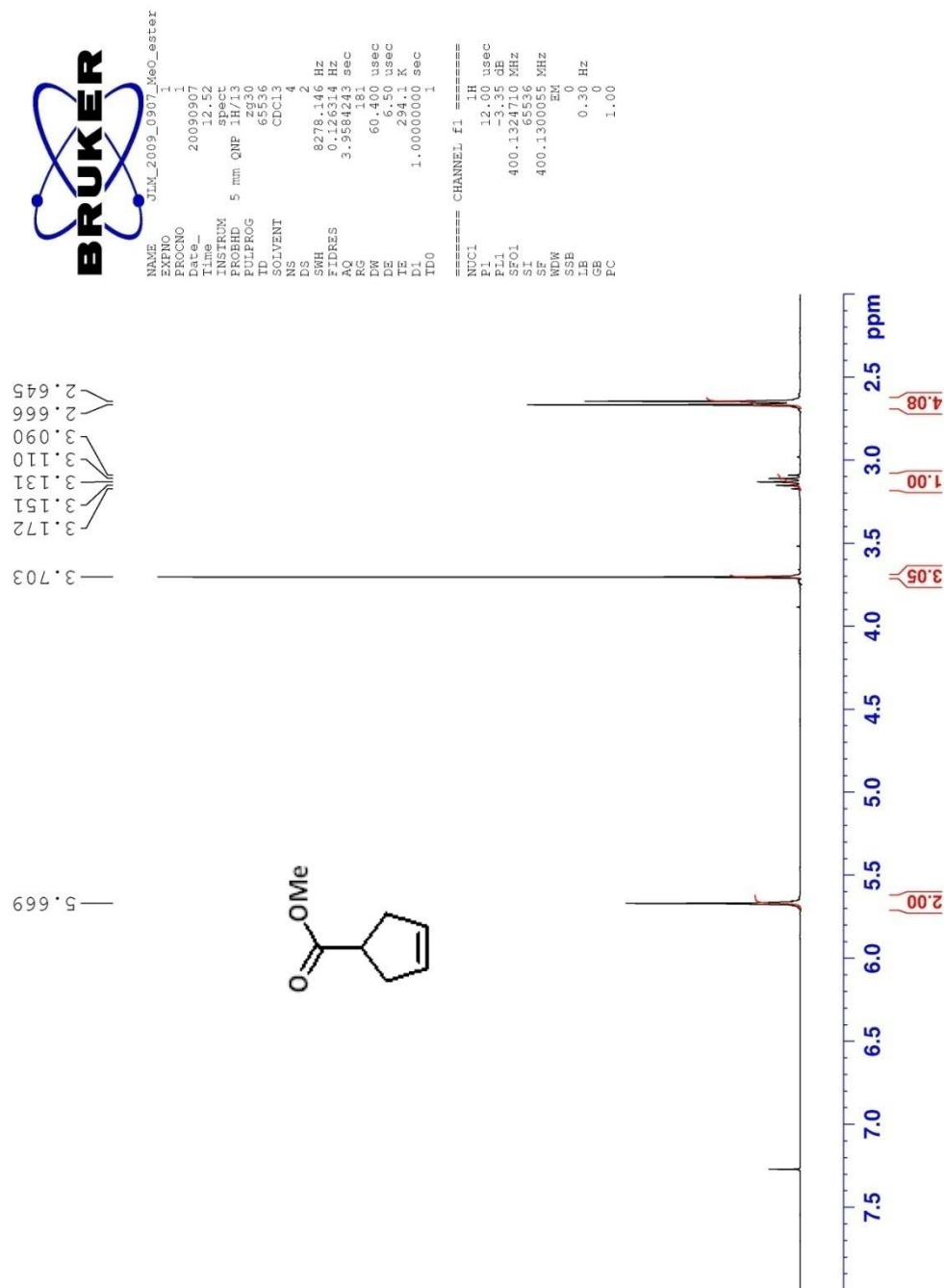
7.5 3.98
 7.0 1.05
 6.5 0.96
 6.0 2.00
 5.5
 5.0
 4.5
 4.0
 3.5
 3.0 2.00
 2.5 2.04
 2.0 2.05



JTM_2010_0428_Bn_BHPL13C_Char

NAME JTM_2010_0428_Bn_BHPL13C_Char
 PROCNO 1
 Date_ 20100428
 Time 15:13
 PULPROG zgpg30
 FREQH0 5 mm QNP 1H/13
 C13 125.76
 SOLVENT CDCl3
 NS 681
 DS 4
 SH 0
 FTRES 0.2546077 Hz
 AQ 0.3110004 sec
 RG 2042.5
 DE 27.6 usec
 TE 298.0 K
 DI 2.0000000 sec
 TD 1
 ===== CHANNEL f1 =====
 NU1 6.25 usec
 PL1 0.00 dB
 SFO1 75.4752553 MHz
 ===== CHANNEL f2 =====
 CPDPRG2 waltz16
 NU2 70.14 usec
 PL2 0.00 dB
 PL12 18.42 dB
 PL13 18.42 dB
 SI 65536
 SF 75.4677325 MHz
 NSW 0
 LB 1.00 Hz
 GB 0
 PC 1.40



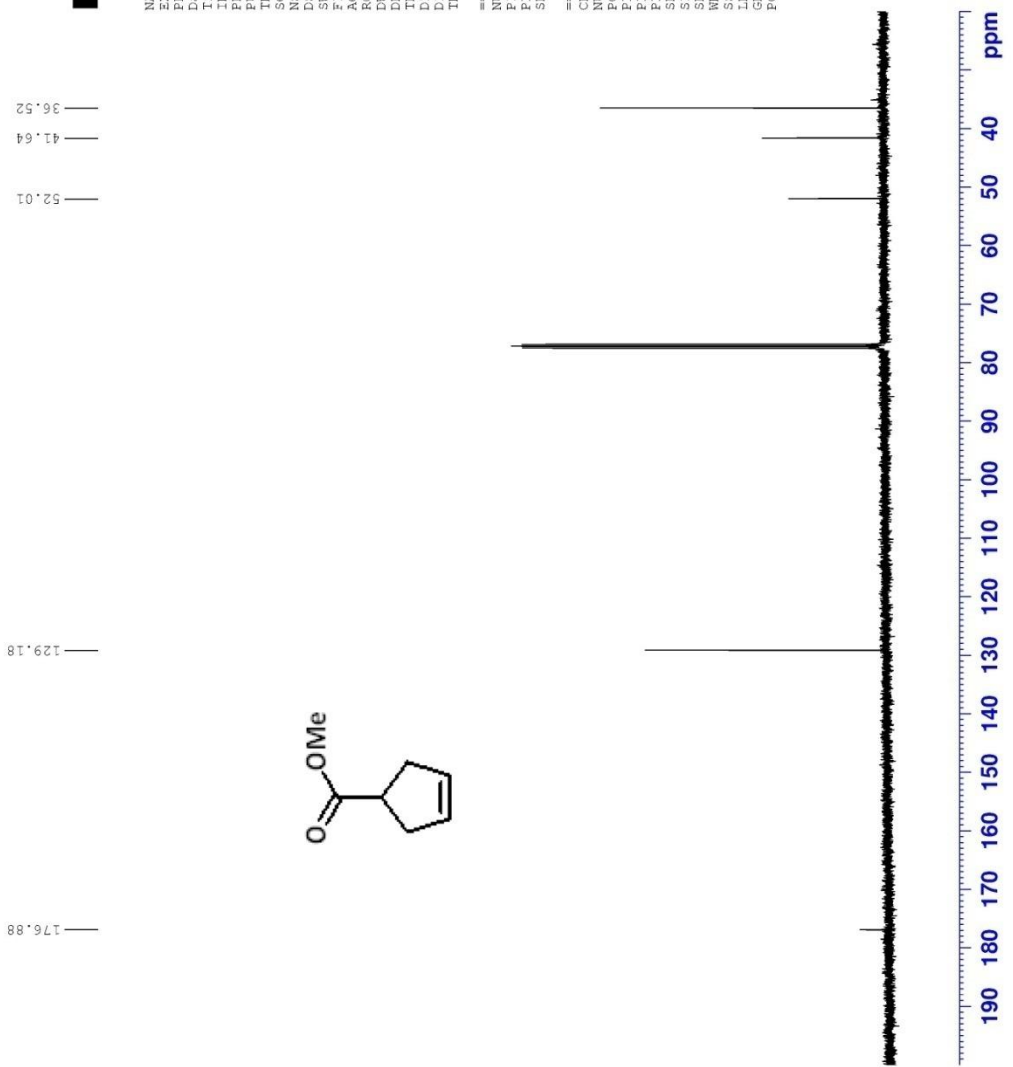
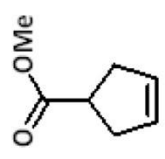




NAME JLM_2009_0907_MeO_ester

EXPNO 1
PROCNO 2
Date_ 20090907
Time 12:57
INSTRUM spect
PROBHD 5 mm QNP 1H/13
PULPROG zgpg30
ID 65536
SOLVENT CDC13
NS 163
DS 4
SWH 23980.814 Hz
FIDRES 0.2669768 Hz
AQ 1.5004756 sec
RG 31149
DM 20.850 usec
DE 6.50 usec
TE 294.8 K
D1 2.00000000 sec
D11 0.03000000 sec
TD0 1

===== CHANNEL f1 =====
NUC1 13C
P1 10.00 usec
PL1 0.00 dB
SF01 100.6228298 MHz
===== CHANNEL f2 =====
CPDPRG2 waltz16
NUC2 1H
PCPD2 70.00 usec
PL2 13.35 dB
PL3 11.97 dB
PL4 11.97 dB
SF02 400.1316005 MHz
SI 65536
SF 100.6127483 MHz
WDW EM
SSB 0
LB 1.00 Hz
GB 0
PC 1.40





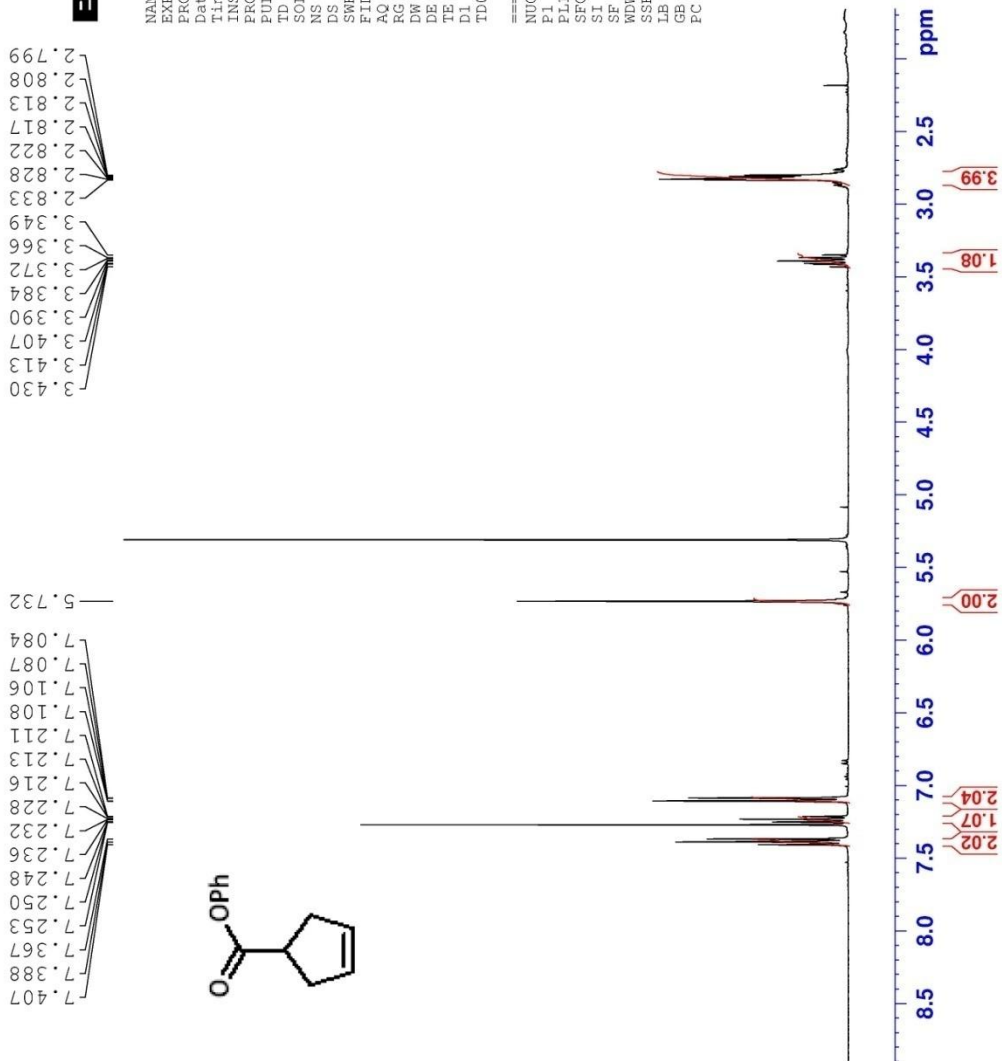
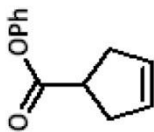
```

NAME JLM_2010_0711_0ph
EXPNO 1
PROCNO 1
Date_ 20100712
Time 1.01
INSTRUM spect
PROBHD 5 mm QNP 1H/13
PULPROG zg30
TD 65536
SOLVENT CDCl3
NS 64
DS 2
SWH 8278.146 Hz
AQ 0.126314 Hz
RG 3.9584243 sec
EG 362
DQ 60.400 usec
DE 6.50 usec
TE 298.0 K
D1 1.00000000 sec
TD0 1

===== CHANNEL f1 =====
NUC1 1H
P1 10.25 usec
PL1 -3.35 dB
SFO1 400.1324710 MHz
SI 65536
SF 400.1300055 MHz
WDW EM
SSB 0
LB 0.30 Hz
GB 0
PC 1.00
    
```

2.799
2.808
2.813
2.817
2.822
2.828
2.833
3.349
3.366
3.372
3.384
3.390
3.407
3.413
3.430

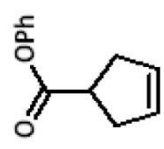
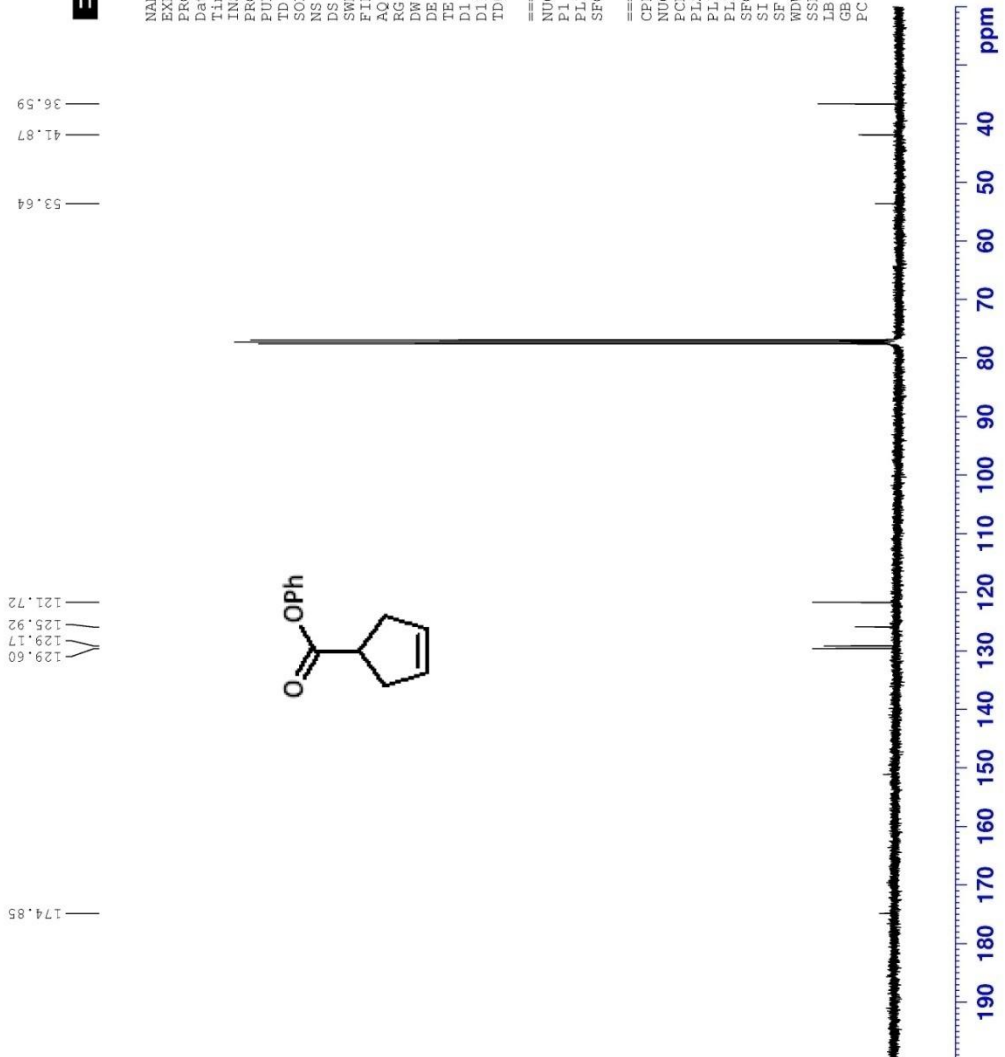
5.732
7.084
7.087
7.106
7.108
7.211
7.213
7.216
7.228
7.232
7.236
7.248
7.250
7.253
7.367
7.388
7.407





NAME JLM_2010_0711_2
 EXPNO 1
 PROCNO 1
 Date_ 20100712
 Time 1.07
 INSTRUM spect
 PROHD 5 mm QNP 1H/13
 PULPROG zgpg30
 TD 65536
 SOLVENT CDCl3
 NS 489
 DS 4
 SWH 23980.814 Hz
 FIDRES 0.365918 Hz
 AQ 1.3664756 sec
 RG 1149.4
 DW 20.850 usec
 DE 650 usec
 TE 298.0 K
 D1 2.00000000 sec
 D11 0.03000000 sec
 TD0 1

===== CHANNEL f1 =====
 NUC1 13C
 P1 10.00 usec
 PL1 0.50 dB
 SF01 100.6228298 MHz
 ===== CHANNEL f2 =====
 CPDPRG2 waltz16
 NUC2 1H
 FCPD2 70.00 usec
 PL2 -3.35 dB
 PL12 13.34 dB
 PL13 13.34 dB
 SF02 400.1316005 MHz
 SI 65536
 SF 100.6127476 MHz
 WDW EM
 SSB 0
 LB 1.00 Hz
 GB 0
 PC 1.40

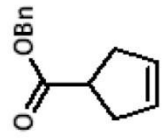




NAME JLM_031409_2yc1cgentene_COObn

PROCNO 2
 Date_ 20090314
 Time 14.48
 PGM 1D
 PULPROG zgpg30
 TD 65536
 SOLVENT CDCl3
 DS 2.04
 SNH 23980.814 Hz
 FIDRES 0.326718 Hz
 RG 2580.3
 DW 20.850 usec
 DE 8.50 usec
 DI 2.0000000 sec
 D11 0.03000000 sec
 TDO 1

===== CHANNEL f1 =====
 NUC1 13C
 P1 9.50 usec
 PL 0.00 dB
 SFO1 100.628298 MHz
 ===== CHANNEL f2 =====
 CPDPRG2 waltz16
 NUC2 1H
 P2 70.00 usec
 PL2 -4.00 dB
 PL1 13.00 dB
 PL3 13.00 dB
 SFO2 400.1316005 MHz
 SI 65536
 SF 100.6127489 MHz
 SSF 0
 SSB 0
 LB 1.00 Hz
 GB 0
 FC 1.40



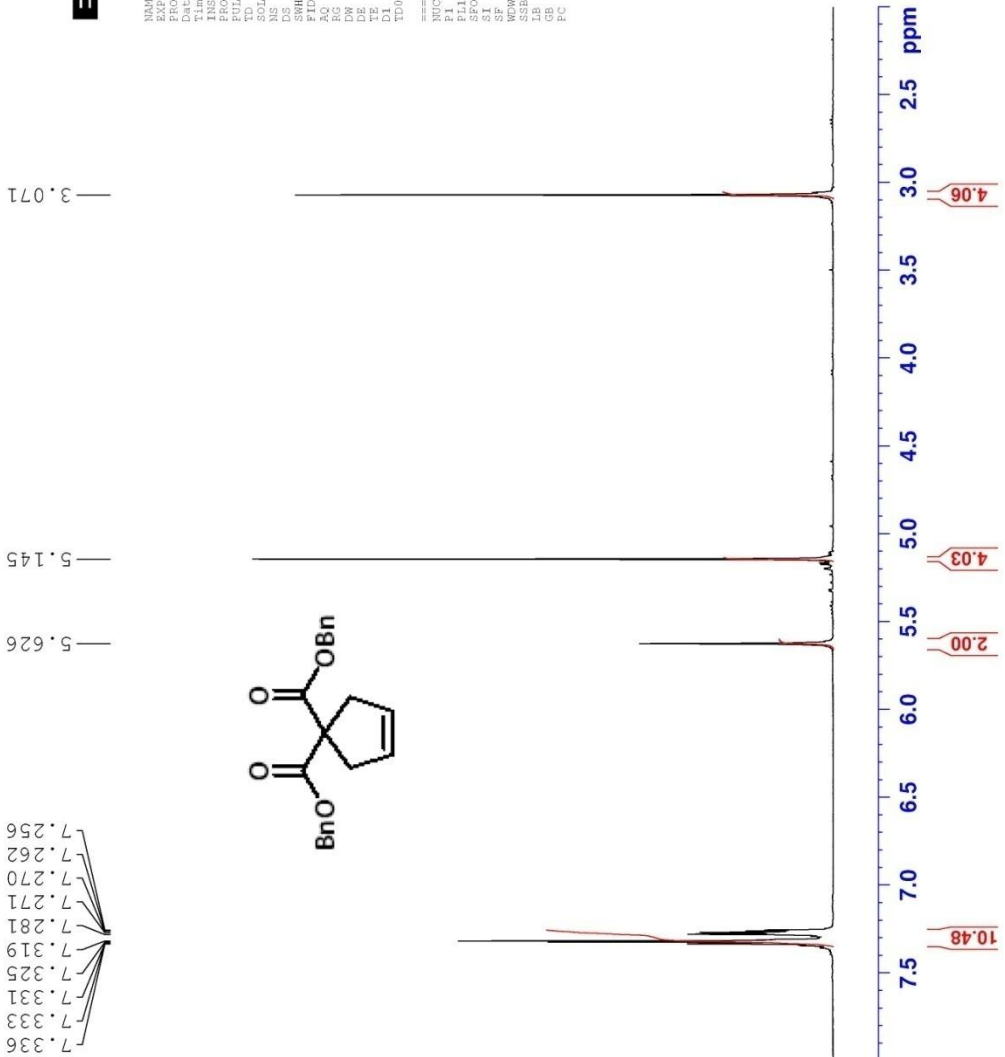
190 180 170 160 150 140 130 120 110 100 90 80 70 60 50 40 ppm



JHM_2010_0711_dibenzylester_

```

NAME_
EXPNO_
PROCNO_ 1
Date_ 20100712
Time_ 1.40
INSTRUM spect
PROBHD 5 mm QNP 1
PULPROG zg30
TD 65536
SOLVENT CDCl3
DS 12
SWH 8278.146 Hz
FIDRES 0.126314 Hz
AQ 3.958243 sec
RG 655.36
DW 60.400 usec
DE 6.50 usec
TE 298.0 K
D1 1.00000000 sec
D0 1
===== CHANNEL f1 =====
NUC1 1H
P1 10.00 usec
PL1 -2.50 dB
SFO1 400.1324710 MHz
SI 65536
SF 400.1300057 MHz
WDW EM
SSB 0
LB 0.30 Hz
GB 0
PC 1.00
    
```

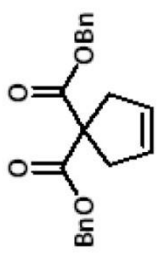
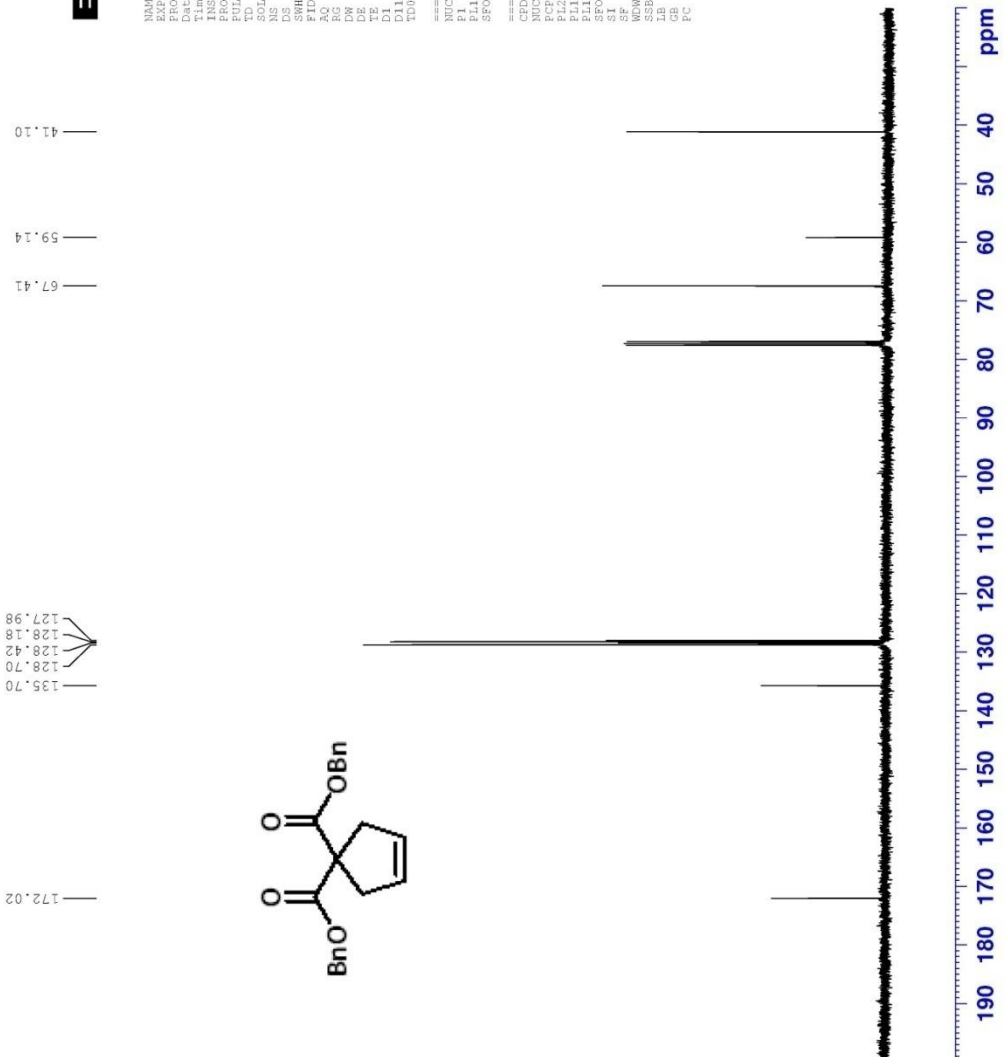




JHM_2010_0711_dibenzylester_

NAME: JHM_2010_0711_dibenzylester_
 PROCNO: 1
 Date_: 20100712
 Time: 1.43
 INSTRUM: spect
 PULPROG: zgpg30
 TD: 65536
 SOLVENT: CDCl3
 NS: 64
 DS: 4
 SWH: 23980.814 Hz
 FIDRES: 0.365918 Hz
 AQ: 1.3664756 sec
 RG: 327.5
 DW: 20.850 usec
 DE: 6.50 usec
 TE: 298.0 K
 D1: 0.000000 sec
 D11: 0.000000 sec
 D12: 0.000000 sec
 D13: 0.000000 sec
 D14: 0.000000 sec
 D15: 0.000000 sec
 D16: 0.000000 sec
 D17: 0.000000 sec
 D18: 0.000000 sec
 D19: 0.000000 sec
 D20: 0.000000 sec
 TD0: 1

===== CHANNEL f1 =====
 NUC1: 13C
 P1: 10.00 usec
 PL1: 0.50 dB
 SFO1: 100.6228298 MHz
 ===== CHANNEL f2 =====
 CPDPRG2: waltz16
 NUC2: 1H
 PCPD2: 70.00 usec
 PL2: 19.00 dB
 PL12: 13.34 dB
 PL13: 13.34 dB
 SFO2: 400.1316005 MHz
 SI: 65536
 SF: 100.6127512 MHz
 WDW: EM
 LB: 0
 GB: 0
 PC: 1.40

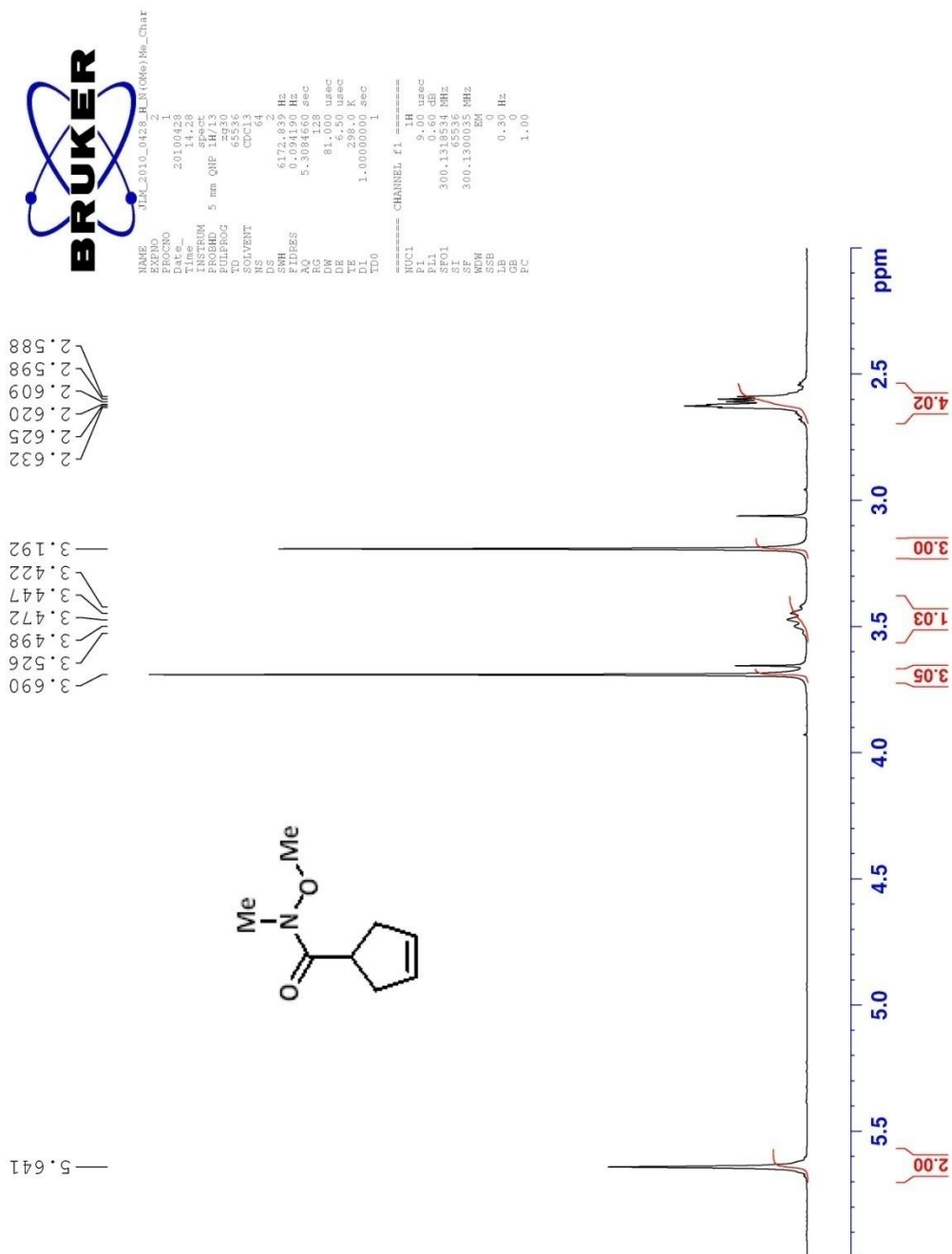


127.98
 128.18
 128.42
 128.70
 135.70

172.02

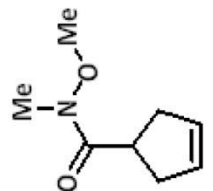
41.10
 59.14
 67.41

190 180 170 160 150 140 130 120 110 100 90 80 70 60 50 40 ppm

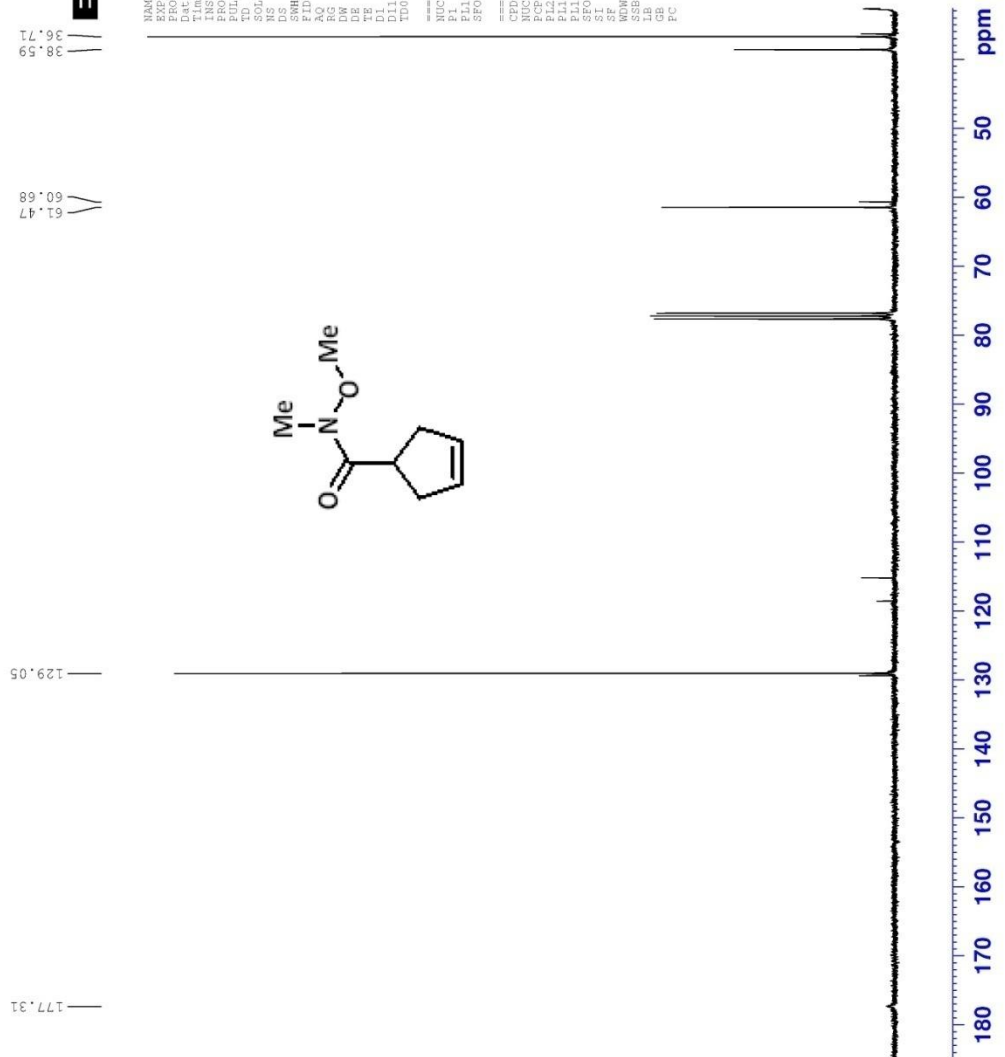




NAME JLM_2010_0428_RLN (006) Me_Char
 PROCNO 3
 Date_ 20100428
 Time 14.37
 PULPROG zgpg30
 SOLVENT CDCl3
 NS 554
 DS 4
 SNH 17985.611 Hz
 FIDRES 0.318007 Hz
 RG 8192
 DW 27.800 usec
 DE 6.50 usec
 DI 0.03000000 sec
 D11 2.00000000 sec
 TD0 1



===== CHANNEL f1 =====
 NUC1 13C
 P1 6.25 usec
 PL1 0.00 dB
 SFO1 75.4775253 MHz
 ===== CHANNEL f2 =====
 CHPROG2 waltz16
 NUC2 1H
 P2 70.00 usec
 PL2 0.60 dB
 PL12 18.42 dB
 PL13 18.42 dB
 SFO2 300.132005 MHz
 SI 65536
 SF 75.4677570 MHz
 SSF 0
 SSB 0
 LB 1.00 Hz
 GB 0
 PC 1.40



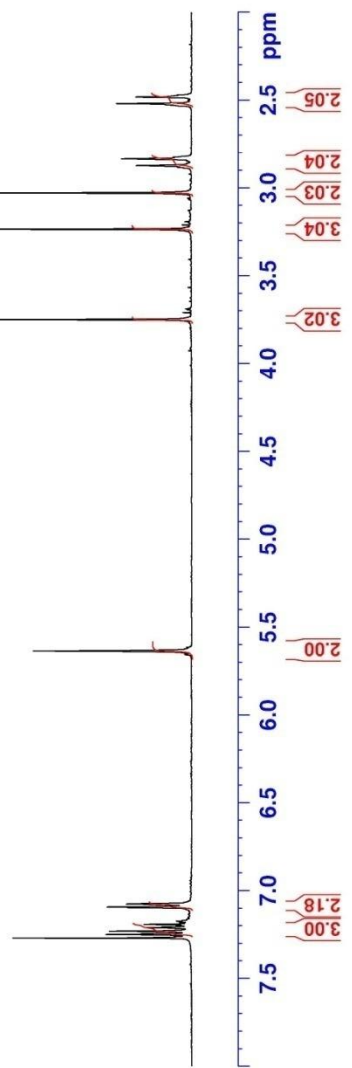
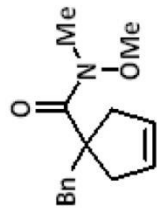
177.31
 129.05
 61.47
 36.71
 ppm



```

NAME JILX_2010_0711_En_weinreb
EXPNO 1
PROCNO 1
PROBHD 5 mm QNP 1H/13
PULPROG zgpg30
SOLVENT CDCl3
NS 64
DS 4
SWH 8278.146 Hz
FIDRES 0.126314 Hz
AQ 3.9584243 sec
RG 362
DM 60.400 usec
DE 8.50 usec
TE 298.0 K
D1 1.00000000 sec
TD0
===== CHANNEL f1 =====
NUC1 1H
P1 10.25 usec
PL1 -2.55 dB
SFO1 400.132450 MHz
SF 400.130055 MHz
WDW EM
SSB 0
LB 0.30 Hz
GB 0
PC 1.00
    
```

7.249
 7.245
 7.234
 7.231
 7.214
 7.210
 7.207
 7.192
 7.093
 7.076
 5.635
 3.748
 3.233
 3.027
 2.871
 2.833
 2.519
 2.481

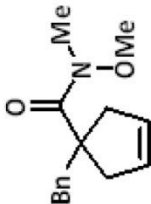
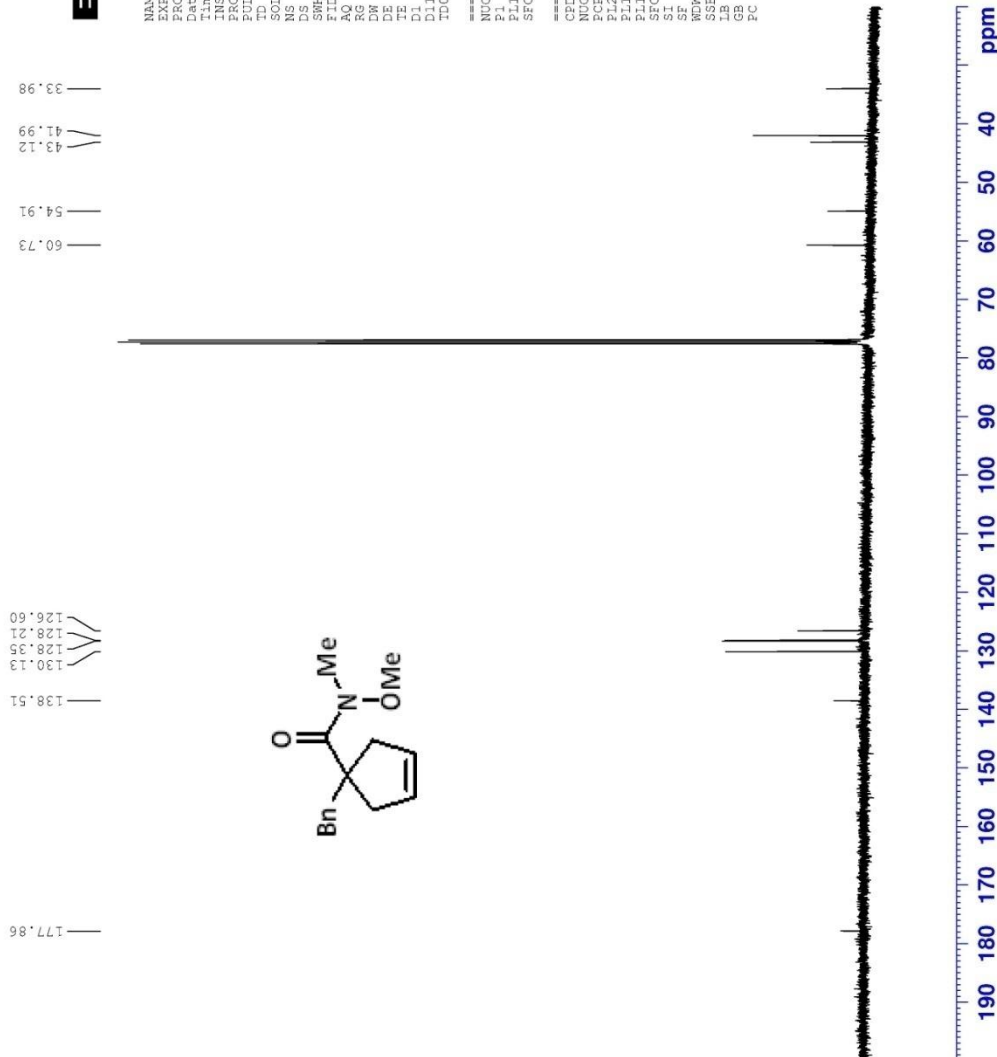




NAME JILX_2010_0711_En_weinreb

EXZNO 2
 PROCNO 1
 Date_ 20100712
 Time_ 0:16
 INSTRUM spect
 PROBHD 5 mm QNP 1H/13
 PULPROG zgpg30
 TD 65536
 SOLVENT CDCl3
 NS 512
 DS 4
 SWH 23980.814 Hz
 FIDRES 0.365918 Hz
 AQ 1.3664756 sec
 RG 812.7
 DM 20.850 usec
 DE 8.50 usec
 TE 296.2 K
 D1 2.00000000 sec
 D11 0.03000000 sec
 TD0 1

===== CHANNEL f1 =====
 NUC1 13C
 P1 10.00 usec
 PL1 0.50 dB
 SFO1 100.6228298 MHz
 ===== CHANNEL f2 =====
 CPDPRG2 waltz16
 NUC2 1H
 P2 70.00 usec
 PL2 -3.35 dB
 PL12 13.34 dB
 PL14 13.34 dB
 SFO2 400.1314005 MHz
 SI 65536
 SF 100.6127480 MHz
 WDW EM
 SSB 0
 LB 1.00 Hz
 GB 0
 EC 1.40

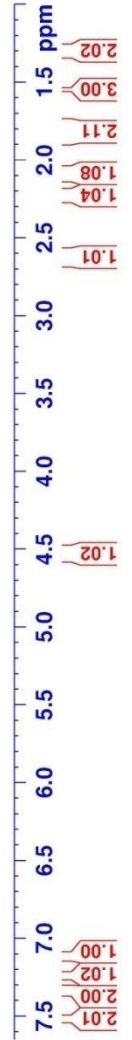
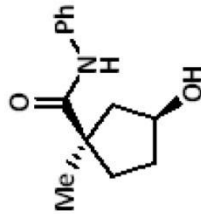




JMK_050209_Me(1H)_Ph_Cyclopentano_Lresc.f3

NAME: JMK_050209_Me(1H)_Ph_Cyclopentano_Lresc.f3
 PROCNO: 20089871
 F1: 13.00
 F2: 19.02
 F3: 19.02
 PULPROG: zgpg30
 TD: 65536
 SFO1: 400.132410 MHz
 SFO2: 400.130057 MHz
 SF: 400.130057 MHz
 AQ: 3.9584243 sec
 DQ: 60.400 usec
 DE: 294.7 usec
 TE: 294.7 K
 DI: 1.00000000 sec
 EQ: 1
 CHANNEL: E1_1H
 P1: 13.00 usec
 SFO1: 400.132410 MHz
 SFO2: 400.130057 MHz
 SF: 400.130057 MHz
 AQ: 3.9584243 sec
 DQ: 60.400 usec
 DE: 294.7 usec
 TE: 294.7 K
 DI: 1.00000000 sec
 EQ: 1

7.527
7.509
7.355
7.336
7.315
7.136
7.117
7.098
4.536
4.531
4.521
4.513
4.506
2.653
2.636
2.618
2.602
2.254
2.240
2.231
2.221
2.209
2.203
2.192
2.112
2.097
2.083
2.077
2.063
2.044
1.889
1.869
1.857
1.851
1.838
1.823
1.813
1.793
1.782
1.766
1.750
1.262



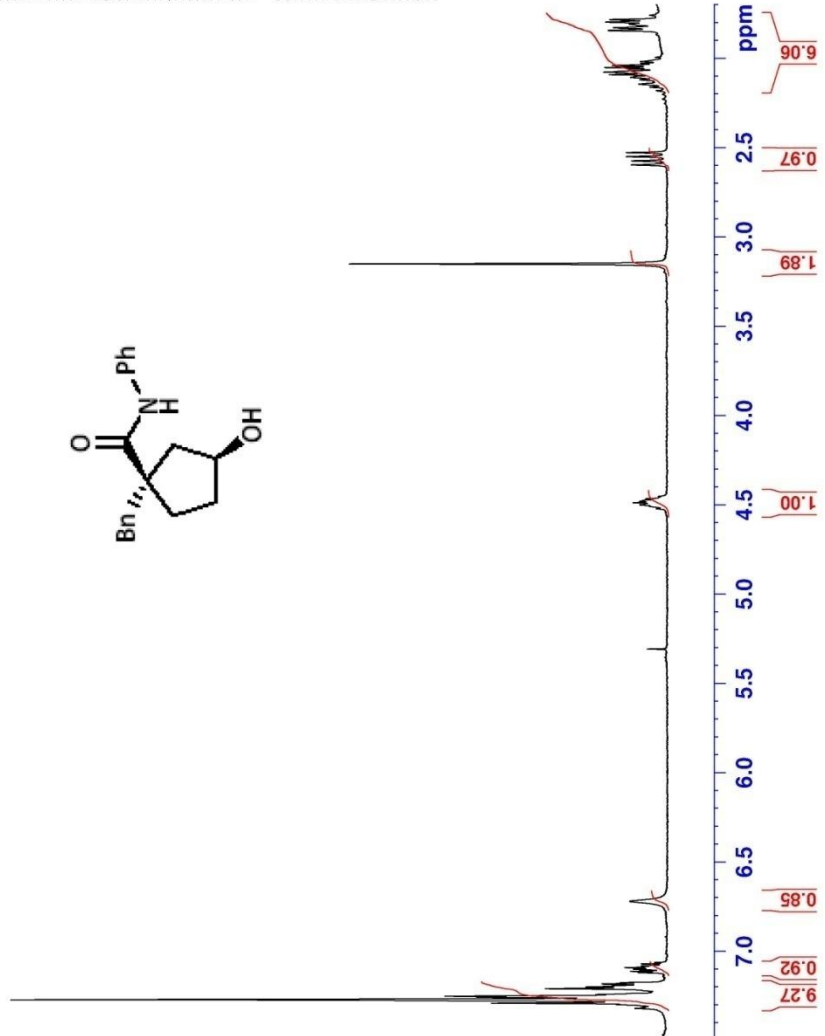
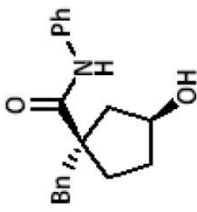


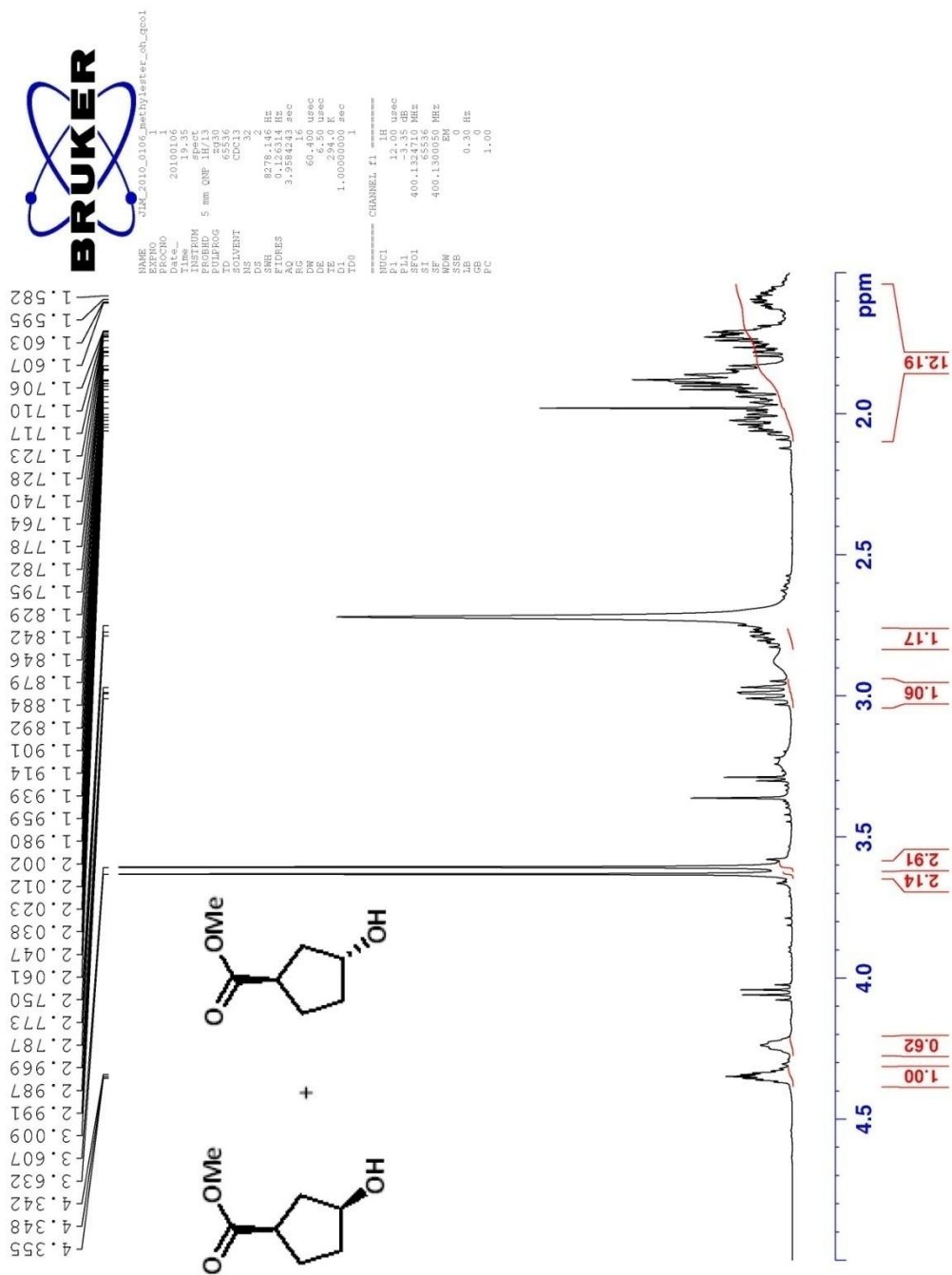
NAME JILX_061809_Br_MHPH_OH_F4

EXZNO 1
 PROCNO 1
 Date_ 20090618
 Time_ 13:30
 INSTRUM spect
 PROBHD 5 mm QNP 1H/13
 PULPROG zgpg30
 TD 65536
 SOLVENT CDCl3
 NS 16
 DS 4
 SWH 6172.839 Hz
 FIDRES 0.094190 Hz
 AQ 5.3084660 sec
 RG 512
 DW 81.000 usec
 DE 6.50 usec
 TE 298.0 K
 D1 1.00 sec
 D11 0.05 sec
 TD0 1.00000000 sec

===== CHANNEL f1 =====
 NUC1 1H
 P1 8.14 usec
 PL1 0.60 dB
 SFO1 300.1318254 MHz
 SF 300.1300031 MHz
 SI EM
 WDW EM
 SSB 0
 LB 0.30 Hz
 GB 0
 FC 1.00

7.290
7.270
7.256
7.250
7.208
7.199
7.193
7.183
7.176
7.121
7.113
7.101
7.092
7.087
7.082
7.072
6.721
4.502
4.489
4.481
4.476
4.467
3.152
2.597
2.575
2.551
2.529
2.145
2.120
2.108
2.102
2.091
2.078
2.061
2.052
2.041
2.029
2.018
1.845
1.829
1.810
1.798
1.784



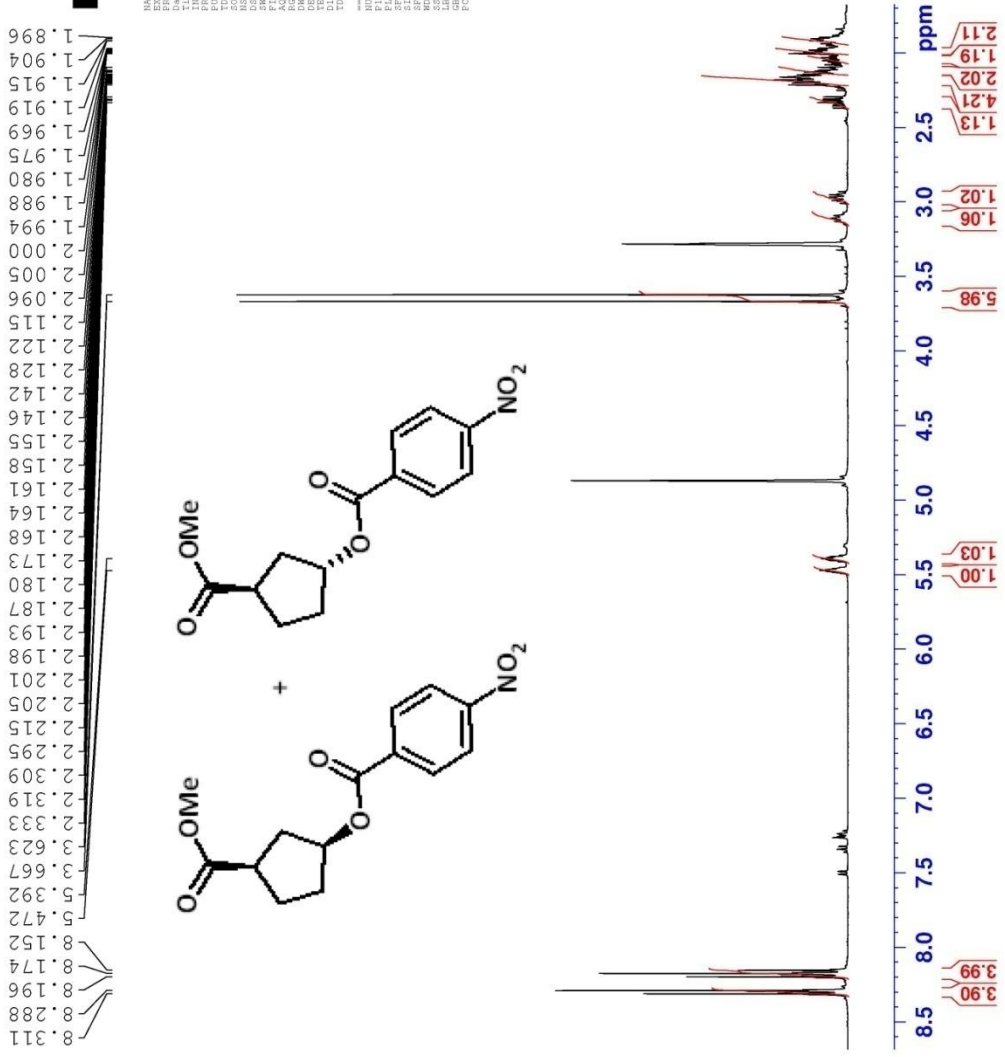




NAME: JDL_2005_1122_1p_ester_nitro_ester_FC_5

EXPNO: 1
 PROCNO: 200911_1
 F2 -> 194.44
 Time: 19:44
 Date_Time: 20051113
 PULPROG: zgpg30
 SFO: 400.1300000 MHz
 5 mm QNP 1H/13
 F2 -> 124.00
 SOLVENT: H2O
 NS: 2
 DS: 4
 SWH: 8278.146 Hz
 FIDRES: 0.3000000 Hz
 AQ: 3.9984441 sec
 RG: 327.500
 DW: 60.400 usec
 DE: 1.0000000 usec
 DB: 6.50 usec
 C1: 0.0000000 usec
 D1: 1.00000000 sec
 TD0: 1

===== CHANNEL f1 =====
 NU1: 13
 P1: 12.00 usec
 PL1: 0.00 dB
 SFO1: 400.1300000 MHz
 SI: 65536 Hz
 SF: 400.1300000 MHz
 WF0: 0.00 Hz
 LB0: 0.00 Hz
 CB: 0
 PC: 1.00



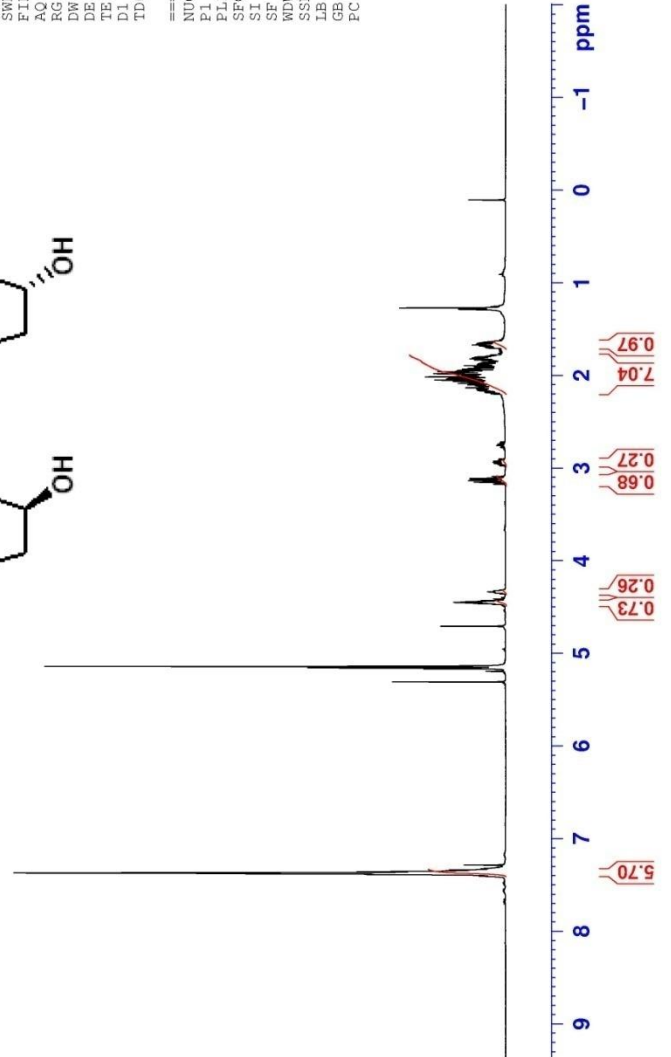
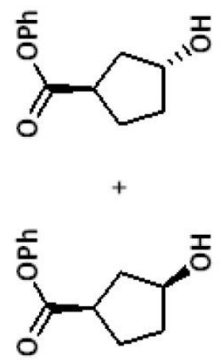


```

NAME JLM_2010_0711
EXPNO 1
PROCNO 1
Date_ 20100712
Time 1.57
INSTRUM spect
PROBHD 5 mm QNP 1H/13
PULPROG zg30
TD 65536
SOLVENT CDC13
NS 64
DS 2
SWH 8278.146 Hz
FIDRES 0.126314 Hz
AQ 3.9584243 sec
RG 320
DE 60.400 usec
TE 298.0 K
D1 1.00000000 sec
TD0 1

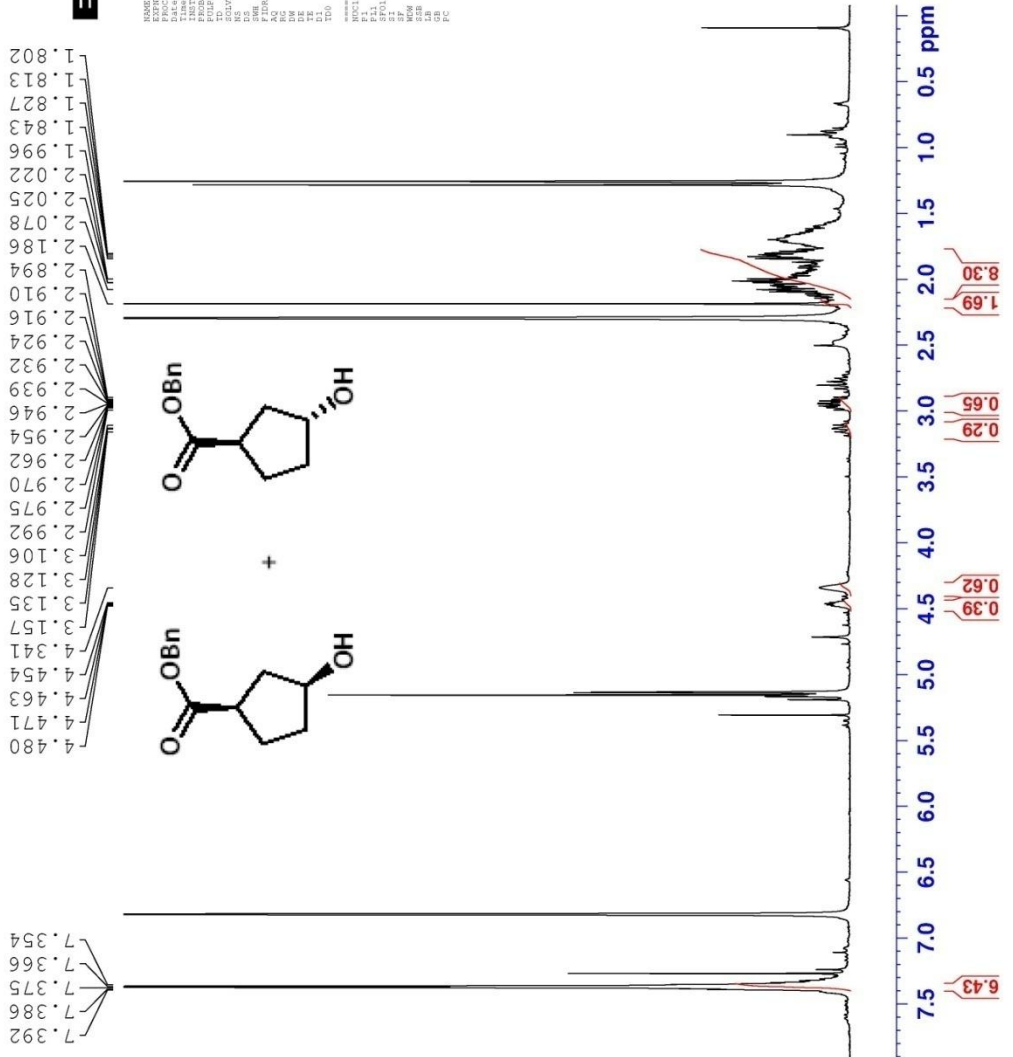
===== CHANNEL f1 =====
NUC1 1H
P1 10.25 usec
PL1 -3.35 dB
SFO1 400.1324710 MHz
SI 65536
SF 400.1300000 MHz
WDW EM
SSB 0
LB 0
GB 0
PC 1.00
    
```

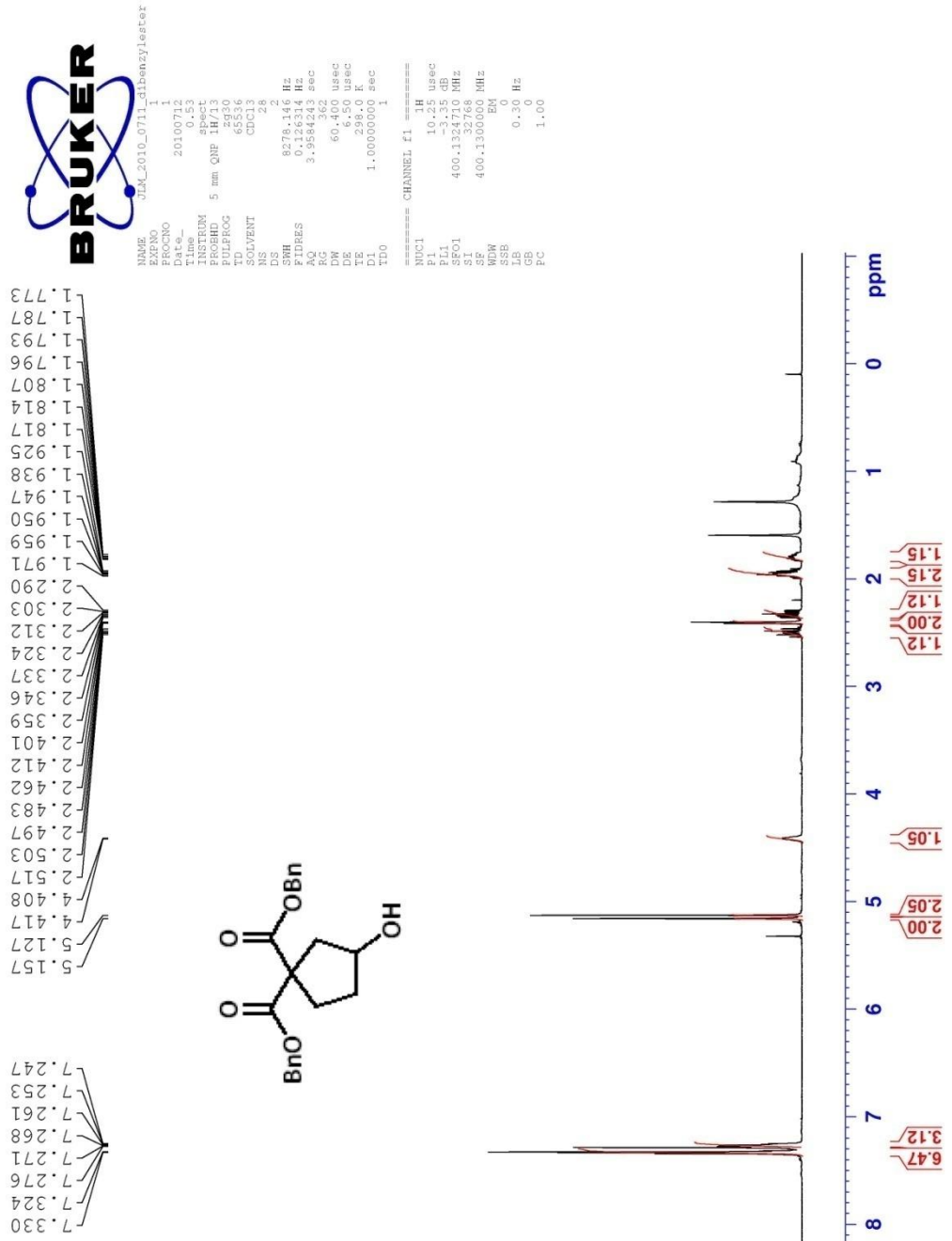
7.386
7.382
7.377
7.370
7.367
7.357
4.462
4.456
4.449
4.443
4.436
4.347
4.342
4.334
4.326
4.322
3.172
3.150
3.133
3.128
3.111
3.106
3.089
2.951
2.939
2.934
2.922
2.062
2.048
2.035
2.027
2.013
1.979
1.974
1.964
1.958
1.682
1.677
1.669
1.665
1.662
1.657





NAME: 31K033002_methylene1_cyclopentanol_screen
 EXPNO: 2
 PROCNO: 20080530
 F2 - Name: 18.44
 F2 - Date_UTC: 18/05/13
 F2 - Time: 11:13
 F2 - File: 45536
 F2 - ID: 45536
 F2 - TD: 65536
 SOLVENT: CDCl3
 DS: 2
 US: 6472.87 Hz
 FIDRES: 0.004150 Hz
 AQ: 5.1000000 sec
 RG: 256
 WC: 256
 FWHM: 0.30 Hz
 SFO: 100.6261250 MHz
 TE: 300.2 K
 DE: 1.0000000 sec
 TD0: 1
 ===== CHANNEL f1 =====
 NU1: 6.14 MHz
 PR1: 0.00
 PL1: 0.00 dB
 SFO1: 100.6261250 MHz
 SI: 32
 SF: 300.1300000 MHz
 WDW: EM
 SSB: 0
 LB: 0.30 Hz
 GB: 0
 CB: 3.00

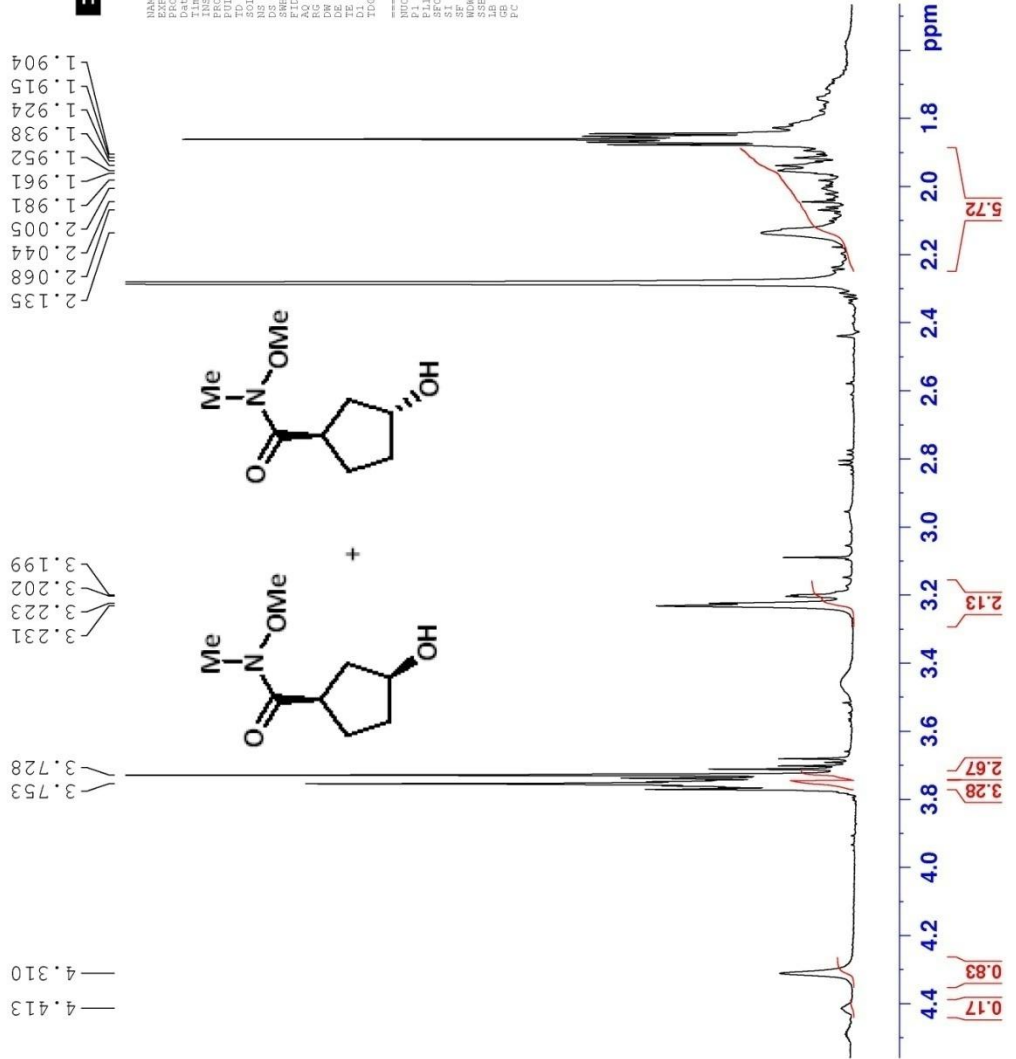


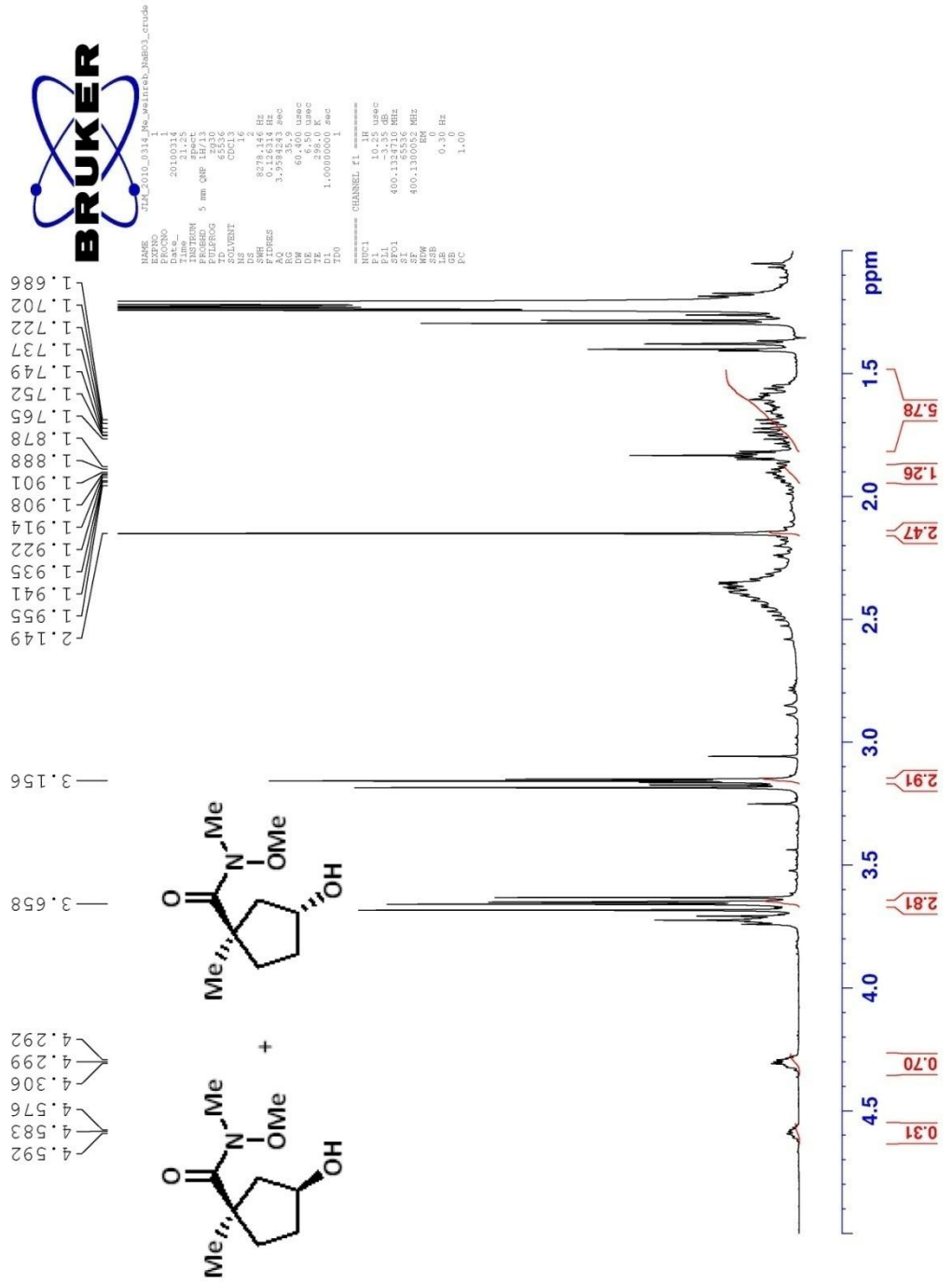




NAME JLM_2010_0315_E_Weinreb_screening

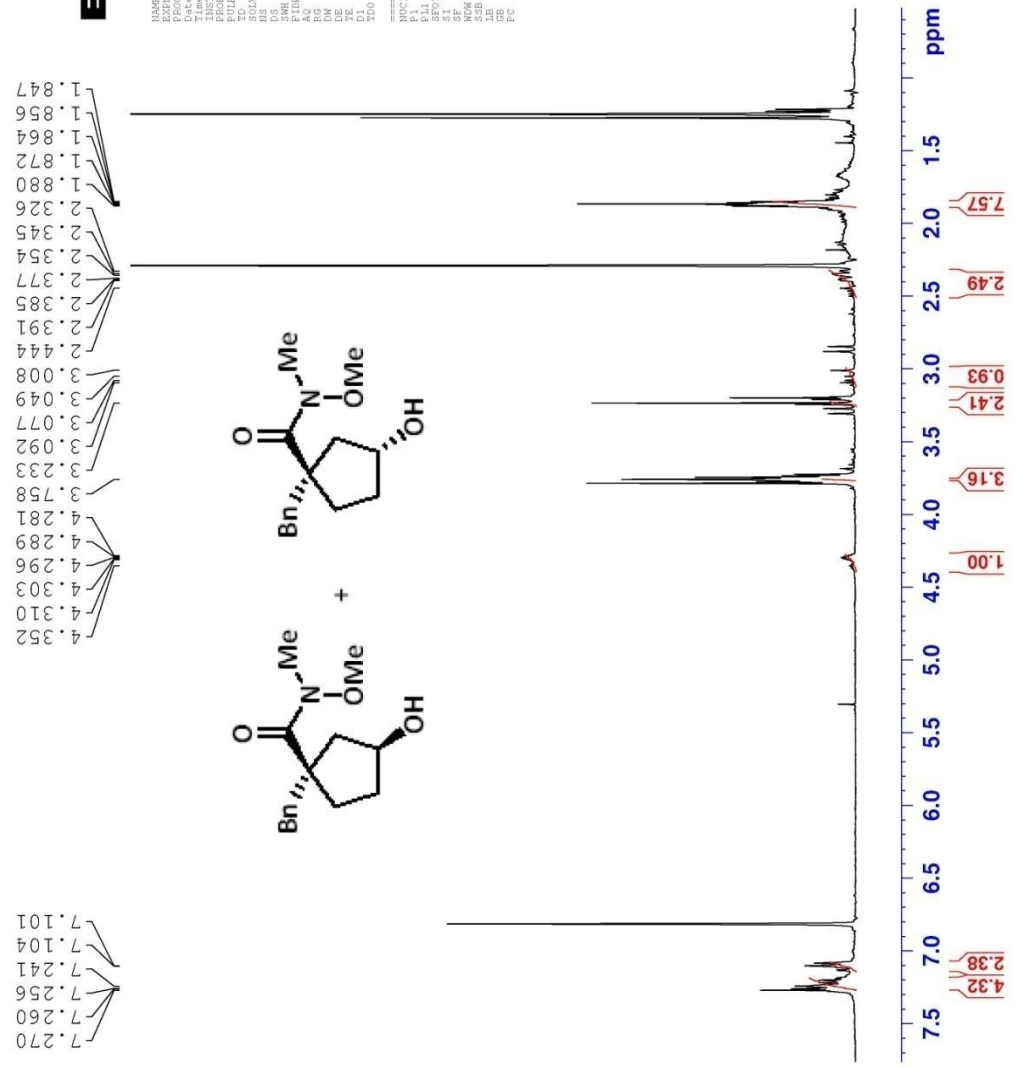
PROCNO 1
 Date_ 20100315
 INSTRUM spect
 PROBRD 5 mm QNP 1H/13
 TOUFRQG 65336
 SOLVENT CDCl3
 DS 4
 SMH 8278.146 Hz
 X10P0ES 3.2586344 Hz
 RG 71.8 Hz
 DR 60.400 usec
 TE 298.0 K
 DI 1.00000000 sec
 200
 CHANNEL F1
 P1 10.25 usec
 PL1 -3.35 dB
 SFO1 400.146300 MHz
 SF 400.130053 MHz
 SWH 500 Hz
 LB 0.30 Hz
 GB 0
 PC 1.00





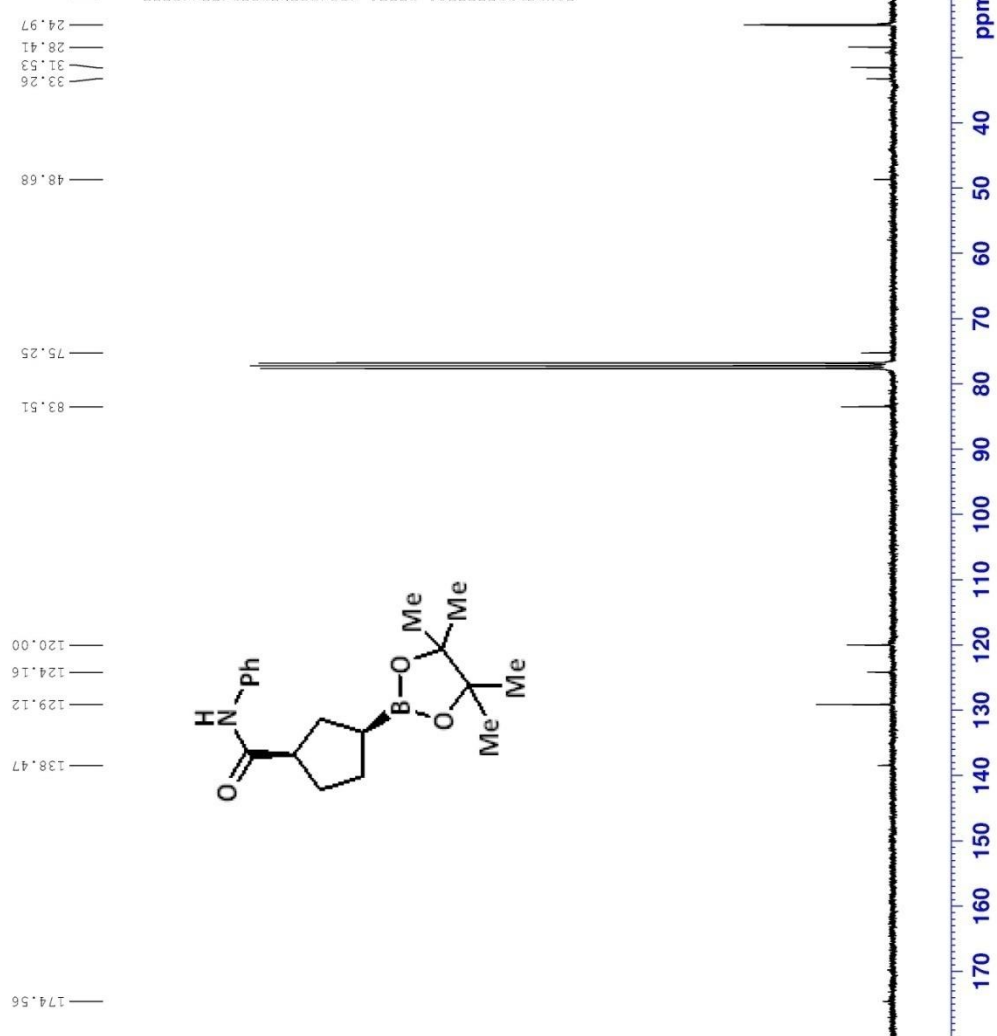


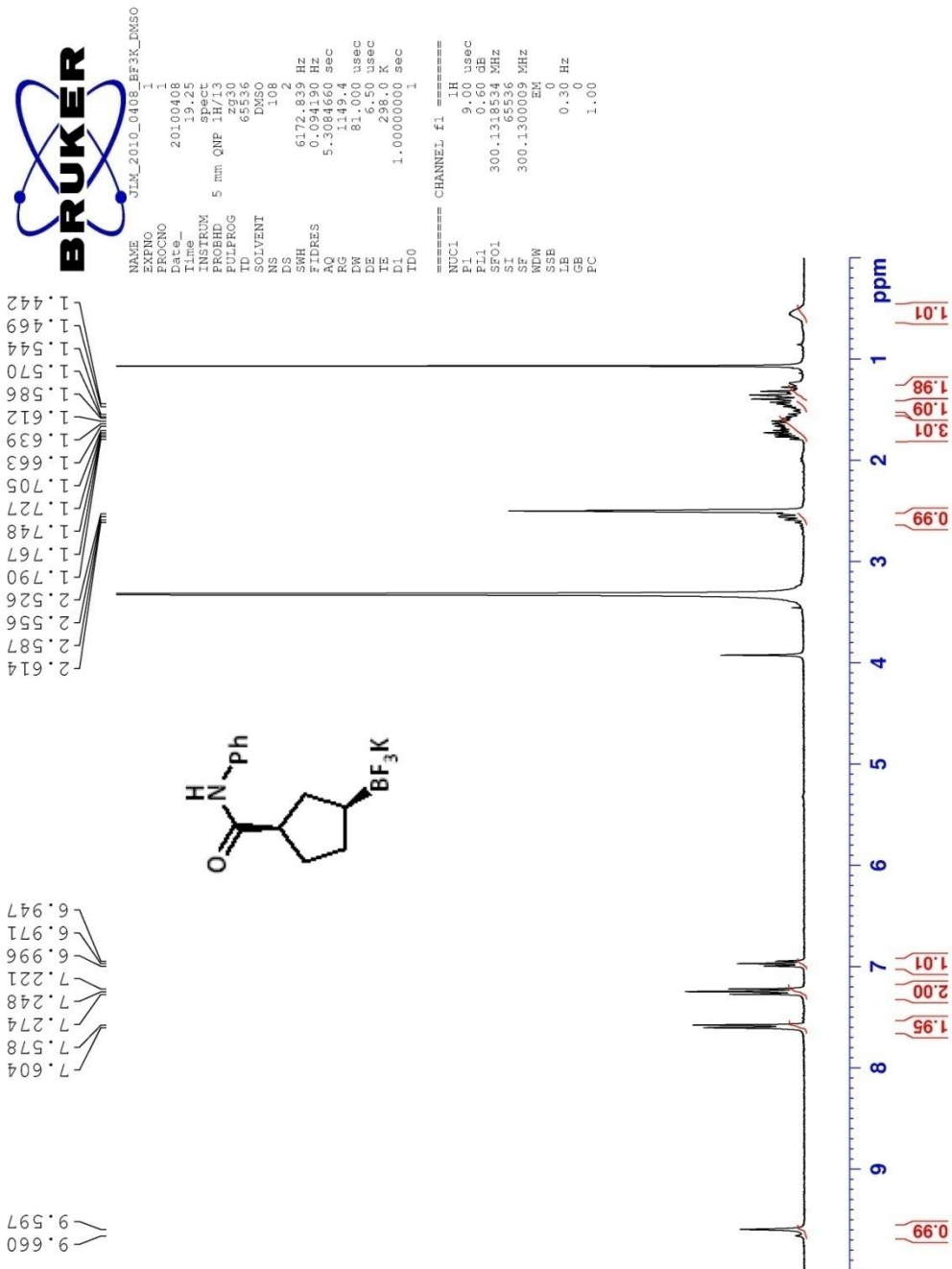
JEM_2010_0315_Bn_weinreb_screening
 NAME JEM_2010_0315_Bn_weinreb_screening
 PROCNO 1
 Date_ 20100216
 INSTRUM spect
 PROBHD 5 mm QNP
 PULPROG zgpg30
 TD 65536
 SOLVENT CDCl3
 DS 1
 SWH 6278.146 Hz
 AQ 3.9584243 sec
 FID 60.128 usec
 DE 6.150 usec
 TE 296.0 K
 TD0 1.00000001 sec
 CHANNEL f1 1H
 NUCL1 1H
 P1 10.25 usec
 SFO1 400.1324710 MHz
 SI 65536
 NUFW 400.1300000 MHz
 SSB 0
 GB 0
 PC 1.00






NAME: UML_010_010_1.mhL_borconatester_char
 PROCNO: 1
 F2: 200.62661
 F1: 12.31
 T1: 200.62661
 PULPROG: zgpg30
 SOLVENT: CDCl3
 NS: 1024
 DS: 4
 SFO: 17945.611 Hz
 AQ: 0.02000000 sec
 RG: 32768
 DE: 6.50 usec
 TE: 300.2 K
 D1: 0.03000000 sec
 D11: 0.03000000 sec
 D12: 0.03000000 sec
 D13: 0.03000000 sec
 D14: 0.03000000 sec
 D15: 0.03000000 sec
 ===== CHANNEL f1 =====
 NU1: 1
 F1: 6.25 usec
 SFO1: 75.475623 MHz
 ===== CHANNEL f2 =====
 CEFFREQ2: waltz16
 P2: 70.00 usec
 P22: 0.60 usec
 P23: 0.60 usec
 P24: 0.60 usec
 P11: 15.42 usec
 P12: 15.42 usec
 SFO2: 300.1312008 MHz
 SF: 75.4677328 MHz
 SWH: 10000 Hz
 LB: 1.00 Hz
 GB: 0 Hz
 PC: 1.40







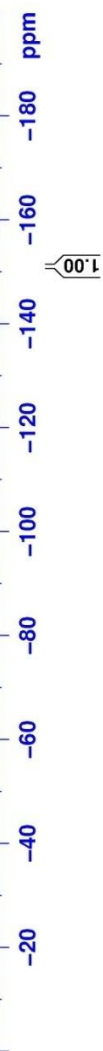
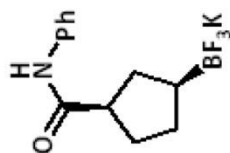
```

NAME JLM_2010_0301_bf3K
EXPNO 3
PROCNO 1
Date_ 20100301
Time 15.46
INSTRUM spect
PROBHD 5 mm QNP 1H/13
PULPROG zgpg1gn
TD 131072
SOLVENT MeOD
NS 47
DS 4
SWH 67567.570 Hz
FIDRES 0.515500 Hz
AQ 0.9699828 sec
RG 812.7
DX 7.400 usec
DE 6.50 usec
TE 298.0 K
D1 1.00000000 sec
TD0 1

===== CHANNEL f1 =====
NUC1 13C
P1 8.63 usec
PL1 0.00 dB
SFO1 282.3761148 MHz
SI 65536
SF 282.4043550 MHz
WDW EM
SSB 0
LB 0.30 Hz
GB 0
PC 1.00

```

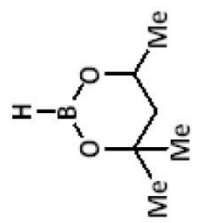
-151.05



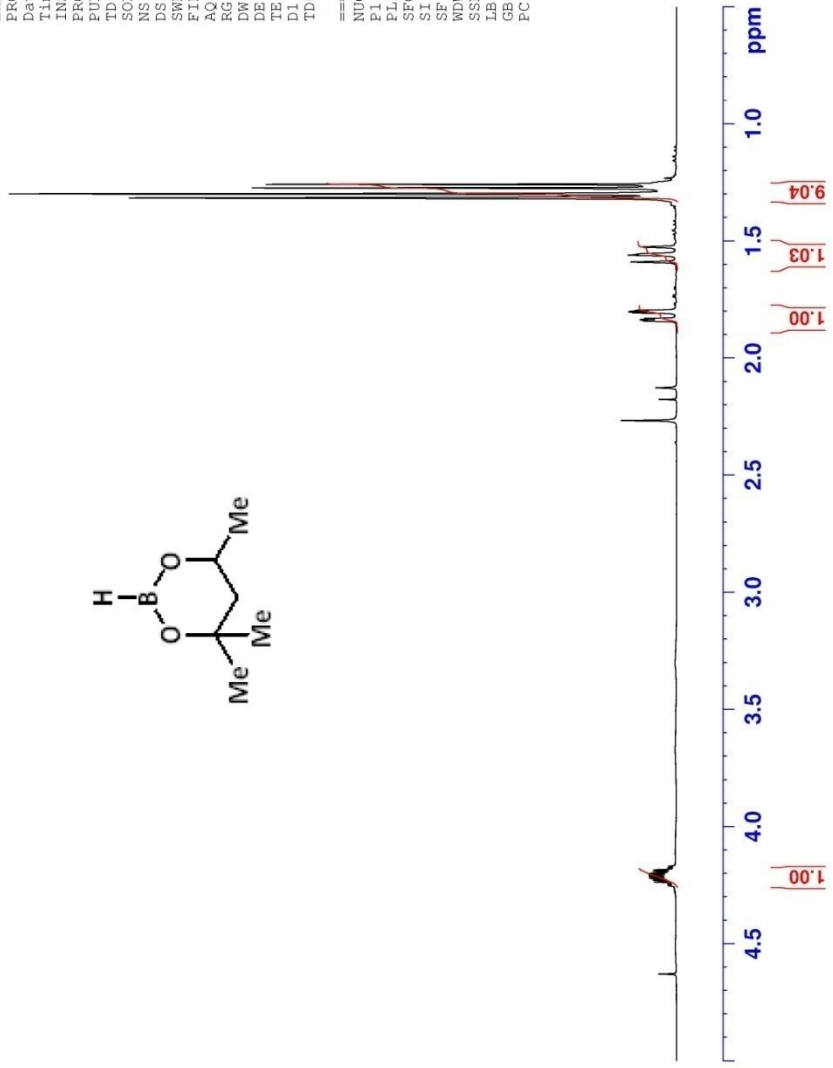


JLM_2009_0711_tmdb
 NAME
 EXPNO 1
 PROCNO 1
 Date_ 20090711
 Time 10.02
 INSTRUM spect
 PROBH 5 mm Multinucl
 PULPROG zg30
 TD 65536
 SOLVENT CDC13
 NS 16
 DS 2
 SWH 8278.146 Hz
 FIDRES 0.126314 Hz
 AQ 3.9584243 sec
 RG 128
 DW 60.400 usec
 DE 6.50 usec
 TE 296.4 K
 D1 1.00000000 sec
 TDO 1
 ===== CHANNEL f1 =====
 NUC1 1H
 P1 12.50 usec
 PL1 -2.50 dB
 SF01 400.1324710 MHz
 SI 65536
 SF 400.1300058 MHz
 WDW EM
 SSB 0
 LB 0.30 Hz
 GB 0
 PC 1.00

1.838
1.835
1.807
1.803
1.800
1.796
1.589
1.560
1.555
1.525
1.316
1.299
1.274
1.258



4.237
4.230
4.222
4.215
4.208
4.201
4.193
4.186



Chapter 16: References

1. McCleverty, J. A.; Meyer, T. J. *Comprehensive Coordination Chemistry II: From Biology to Nanotechnology*; Elsevier: San Diego, 2004.
2. Hayashi, T.; Matsumoto, Y.; Ito, Y. Asymmetric Hydroboration of Styrenes Catalyzed by Cationic Chiral Phosphine-Rhodium(I) Complexes. *Tetrahedron: Asymmetry* **1991**, *2*, 601–612.
3. Fernandez, E.; Maeda, K.; Hooper, M. W.; Brown, J. M. Catalytic Asymmetric Hydroboration / Amination and Alkylamination with Rhodium Complexes of 1,1'-(2-diarylphosphino-1-naphthyl)isoquinoline. *Chem. Eur. J.* **2000**, *6*, 1840–1846.
4. Molander, G. A.; Ito, T. Cross-Coupling Reactions of Potassium Alkyltrifluoroborates with Aryl and 1-Alkenyl Trifluoromethanesulfonates. *Org. Lett.* **2000**, *3*, 393–396.
5. Chen, A. C.; Ren, L.; Crudden, C. M. Catalytic Asymmetric Carbon–Carbon Bond Forming Reactions: Preparation of Optically Enriched 2-Aryl Propionic Acids by a Catalytic Asymmetric Hydroboration–Homologation Sequence. *Chem. Comm.* **1999**, 611–612.
6. Chen, A. C.; Ren, L.; Crudden, C. M. Catalytic Asymmetric Hydrocarboxylation and Hydrohydroxymethylation. A Two-step Approach to the Enantioselective Functionalization of Vinyl Arenes. *J. Org. Chem.* **1999**, *64*, 9704–9710.
7. Guiry, P. J. Expanding the Substrate Scope for Metal-Catalyzed Asymmetric Carbon–Boron Bond Formation. *ChemCatChem* **2009**, *1*, 233–235.
8. Moteki, S. A.; Wu, D.; Chandra, K. L.; Reddy, S.; Takacs, J. M. TADDOL-Derived Phosphites and Phosphoramidites for Efficient Rhodium-Catalyzed Asymmetric Hydroboration. *Org. Lett.* **2006**, *8*, 3097–3100.
9. Männig, D.; Nöth, H. Catalytic Hydroboration with Rhodium Complexes. *Angew. Chem. Int. Ed. Engl.* **1985**, *24*, 878–879.
10. Evans, D. A.; Fu, G. C.; Hoveyda, A. H. Rhodium(I)-Catalyzed Hydroboration of Olefins. The Documentation of Regio- and Stereochemical Control in Cyclic and Acyclic Systems. *J. Am. Chem. Soc.* **1988**, *110*, 6917–6918.
11. Evans, D. A.; Fu, G. C. Amide-Directed, Iridium-Catalyzed Hydroboration of Olefins: Documentation of Regio- and Stereochemical Control in Cyclic and Acyclic Systems. *J. Am. Chem. Soc.* **1991**, *113*, 4042–4043.
12. Smith, S. M.; Thacker, N. C.; Takacs, J. M. Efficient Amide-Directed Catalytic Asymmetric Hydroboration. *J. Am. Chem. Soc.* **2008**, *130*, 3734–3735.
13. Smith, S. M.; Mamma, Y. O. Amide-Directed Asymmetric Hydroboration of Trisubstituted Alkenes. *J. Am. Chem. Soc.* **2010**, *132*, 1740–1741.
14. Rubina, M.; Rubin, M.; Gevorgyan, V. Catalytic Enantioselective Hydroboration of Cyclopropenes. *J. Am. Chem. Soc.* **2003**, *125*, 7198–7199.
15. Shintani, R.; Park, S.; Shirozu, F.; Murakami, M.; Hayashi, T. Palladium-catalyzed Asymmetric Decarboxylative Lactamization of γ -Methylidene- δ -valerolactones with Isocyanates: Conversion of Racemic Lactones to Enantioenriched Lactams. *J. Org. Chem.* **1984**, *49*, 928–931.

16. Deprés, J-P.; Greene, A. E. Improved Selectivity in the Preparation of Some 1,1-difunctionalized 3-Cyclopentenes. High-Yield Synthesis of 3-Cyclopentenecarboxylic Acid. *J. Org. Chem.* **1984**, *49*, 928–931.
17. Evans, D. A.; Fu, G. C.; Anderson, B. A. Mechanistic Study of the Rhodium(I)-Catalyzed Hydroboration Reaction. *J. Am. Chem. Soc.* **1992**, *114*, 6679–6685.
18. Musaev, D.; Mebel, A. M.; Morokuma, K. An ab Initio Molecular Orbital Study of the Mechanism of the Rhodium(I)-Catalyzed Olefin Hydroboration Reaction. *J. Am. Chem. Soc.* **1994**, *116*, 10693–10702.
19. Westcott, S. A.; Taylor, N. J.; Marder, T. B.; Baker, R. T.; Jones, N. J.; Calabrese, J. C. Reaction of Catecholborane with Phosphinorhodium Complexes: Molecular Structures of $[\text{RhHC}](\text{Bcat})[\text{P}(\text{CHMe}_2)_3]_2$ and $[(\text{Me}_2\text{CH})_2\text{PCH}_2]_2\text{Rh}[\eta^6\text{-cat}]\text{Bcat}$ (cat = 1,2- $\text{O}_2\text{C}_6\text{H}_4$). *J. Am. Chem. Soc. Chem. Commun.* **1991**, *5*, 304–305.
20. Vogels, C. M.; Westcott, S. A. Recent Advances in Organic Synthesis Using Transition Metal-Catalyzed Hydroborations. *Curr. Org. Chem.* **2005**, *9*, 687–699.
21. Seebach, D.; Dahinden, R.; Marti, R. E.; Beck, A. K.; Plattner, D. A.; Kühnle, F. N. M. On the Ti-TADDOLate-Catalyzed Diels–Alder Addition of 3-Butenoyl-1,3-oxazolidin-2-one to Cyclopentadiene. General Features of Ti-BINOLate- and Ti-TADDOLate-Mediated Reactions. *J. Org. Chem.* **1995**, *60*, 1788–1799.
22. Brown, H. C.; Chandrasekharan, J. Hydroboration. 65. Relative Reactivities of Representative Alkenes and Alkynes toward Hydroboration by Catecholborane. *J. Org. Chem.* **1983**, *48*, 5080–5082.
23. Burgess, K.; van der Donk, W. A.; Westcott, S. A.; Marder, T. B.; Baker, R. T.; Calabrese, J. C. Reactions of Catecholborane with Wilkinson’s Catalyst: Implications for Transition Metal-Catalyzed Hydroborations of Alkenes. *J. Am. Chem. Soc.* **1992**, *114*, 9350–9359.
24. Crudden, C. M.; Edwards, D. Catalytic Asymmetric Hydroboration: Recent Advances and Applications in Carbon-Carbon Bond-Forming Reactions. *Eur. J. Org. Chem.* **2003**, 4695–4712.
25. Lee, J-E.; Yun, J. Catalytic Asymmetric Boration of Acyclic α,β -Unsaturated Esters and Nitriles. *Angew. Chem. Int. Ed.* **2008**, *47*, 145–147.
26. Kono, H.; Ito, K.; Nagai, Y. Oxidative Addition of 4,4,6-Trimethyl-1,3,2-dioxaborinane and Benzo[1,3,2]dioxaborole to Tris(triphenylphosphine)halorhodium. *Chem. Lett.* **1975**, *10*, 1095–1096.
27. Woods, W. G.; Strong, P. L. 4,4,6-Trimethyl-1,3,2-dioxaborinane. A Stable Dialkoxyborane. *J. Am. Chem. Soc.* **1966**, *88*, 4667–4671.
28. Hodgson, D. M.; Thompson, A. J.; Wadman, S. Carbamate-directed Hydroboration: Enantioselective Synthesis of the Excitatory Amino Acid 1-Aminocyclopentane-1,3-dicarboxylic Acid. *Tetrahedron Lett.* **1998**, *39*, 3357–3358.
29. Tanaka, T.; Hayashi, M. New Approach for Complete Reversal of Enantioselectivity Using a Single Chiral Source. *Synthesis* **2008**, *21*, 3361–3376.
30. Kim, Y. H.; Park, D. H.; Byun, I. S. Stereocontrolled Catalytic Asymmetric Reduction of Ketones with Oxazaborolidines Derived from New Chiral Amino Alcohols. *J. Org. Chem.* **1993**, *58*, 4511–4512.

31. Evans, D. A.; Fu, G. C.; Hoveyda, A. H. Rhodium(I)- and Iridium(I)-Catalyzed Hydroboration Reactions: Scope and Synthetic Applications. *J. Am. Chem. Soc.* **1992**, *114*, 6671–6679.
32. Harrison, K. N.; Marks, T. J. Organolanthanide-Catalyzed Hydroboration of Olefins. *J. Am. Chem. Soc.* **1992**, *114*, 9220–9221.
33. Segarra, A. M.; Daura-Oller, E.; Claver, C.; Poblet, J. M.; Bo, C.; Fernández, E. In Quest of Factors that Control the Enantioselective Catalytic Markovnikov Hydroboration/Oxidation of Vinylarenes. *Chem. Eur. J.* **2004**, *10*, 6456–6467.
34. Westcott, S. A.; Blom, H. P.; Marder, T. B. Nucleophile Promoted Degradation of Catecholborane: Consequences for Transition Metal-Catalyzed Hydroborations. *Inorg. Chem.* **1993**, *32*, 2175–2182.
35. Sivaraman, B.; Aidhen, I.S. The Growing Synthetic Utility of the Weinreb Amide. *Synthesis* **2008**, *23*, 3707–3738.
36. Shigematsu, H.; Matsumoto, T.; Kawauchi, G.; Hirose, Y.; Naemura, K. Horse Liver Alcohol Dehydrogenase-Catalyzed Enantioselective Reduction of Cyclic Ketones: The Effect of the Hydrophobic Side Chain of the Substrate on the Stereoselectivity of the Reaction. *Tetrahedron: Asymmetry* **1995**, *6*, 3001–3008.
37. Dreher, S. D.; Dormer, P. G.; Sandrock, D. L.; Molander, G. A. Efficient Cross-Coupling of Secondary Alkyltrifluoroborates with Aryl Chlorides: Reaction Discovery Using Parallel Microscale Experimentation. *J. Am. Chem. Soc.* **2008**, *130*, 9257–9259.
38. Van den Hoogenband, A.; Lange, J. H. M.; Terpstra, J. W.; Koch, M.; Visser, G. M.; Visser, M.; Korstanje, T. J.; Jastrzebski, J. T. B. Ruphos-Mediated Suzuki Cross-Coupling of Secondary Alkyl Trifluoroborates. *Tetrahedron Lett.* **2008**, *49*, 4122–4124.